THE UNIVERSITY OF CHICAGO

THE GLUTATHIONYLATION OF *YERSINIA PESTIS* LCRV AND ITS EFFECTS ON PLAGUE PATHOGENESIS

A DISSERTATION SUBMITTED TO

THE FACULTY OF THE DIVISION OF THE BIOLOGICAL SCIENCES

AND THE PRITZKER SCHOOL OF MEDICINE

IN CANDIDACY FOR THE DEGREE OF

DOCTOR OF PHILOSOPHY

COMMITTEE ON MICROBIOLOGY

BY

ANTHONY KEITH MITCHELL

CHICAGO, ILLINOIS

AUGUST 2018

TABLE OF CONTENTS

LIST OF FIGURES

PAGE

PAGE

LIST OF TABLES

PAGE

ACKNOWLEDGEMENTS

Many mentors, colleagues, friends, and family members have provided me with invaluable assistance throughout my tenure as a graduate student. I am especially grateful for the enthusiastic supervision, commitment, and generous resources of Dr. Olaf Schneewind. It is often said that the most important phase of any scientific endeavor occurs prior to the start of a single experiment, namely, by asking the right questions. In this respect, as in numerous others, nowhere could I have found a better mentor to guide me to a more comprehensive understanding of the process and methodology that underpins fruitful scientific inquiry. I would also like to express my sincere gratitude to the other members of my Dissertation Committee—Dr. Sean Crosson, Dr. Dominique Missiakas, Dr. Howard Shuman, and Dr. Alexander Chervonsky—for their support and guidance over the past several years; for their beneficial insights and commentary on my research projects; and for sharing their scientific expertise on topics ranging from genetics and biochemistry to immunology and bacterial pathogenesis.

Members of the Schneewind–Missiakas laboratory, both past and present, are likewise deserving of many thanks for their willingness to offer thoughtful scientific advice, to engage in stimulating discussions on any number of subjects, and to provide assistance with, and training in, new experimental techniques. In particular, I would like to thank Dr. Bill Blaylock who not only trained me in the technical and intellectual aspects of experimental microbiology upon my arrival at the laboratory but also exhibited an ongoing passion and dedication to research and teaching that has been a lasting inspiration. I would also like to acknowledge the Pritzker School of Medicine's Growth, Development, and Disabilities Training Program (GDDTP) for providing me with the unique opportunity, as well as the generous financial support, to pursue my PhD studies.

Finally, the *sine qua non* of my graduate school career—and, indeed, throughout my life in general—has been the interminable support and encouragement of my family. From their unconditional love to their endless patience and understanding, I am forever indebted to my parents, Keith and Teresa, as well as to my siblings Traci, Zach, and Drew.

ABSTRACT

Glutathionylation, the formation of reversible mixed disulfides between glutathione and protein cysteine residues, is a posttranslational modification previously observed for intracellular proteins of bacteria. Here we show that *Yersinia pestis* LcrV, a secreted protein capping the type III secretion machine, is glutathionylated at Cys^{273} and that this modification promotes association with host ribosomal protein S3 (RPS3), moderates *Y. pestis* type III effector transport and killing of macrophages, and enhances bubonic plague pathogenesis in mice and rats. Secreted LcrV was purified and analyzed by mass spectrometry to reveal glutathionylation, a modification that is abolished by the codon substitution Cys^{273}Ala in *lcrV*. Moreover, the $lcrV_{C273A}$ mutation enhanced the survival of animals in models of bubonic plague. Investigating the molecular mechanism responsible for these virulence attributes, we identified macrophage RPS3 as a ligand of LcrV, an association that is perturbed by the Cys^{273}Ala substitution. Furthermore, macrophages infected by the $lcrV_{C273A}$ variant displayed accelerated apoptotic death and diminished proinflammatory cytokine release. Deletion of *gshB*, which encodes glutathione synthetase of *Y. pestis*, resulted in undetectable levels of intracellular glutathione, and we used a *Y. pestis* Δ*gshB* mutant to characterize the biochemical pathway of LcrV glutathionylation, establishing that LcrV is modified after its transport to the type III needle via disulfide bond formation with extracellular oxidized glutathione.

Yersinia pestis, the causative agent of plague, has killed large segments of the human population; however, the molecular bases for the extraordinary virulence attributes of this pathogen are not well understood. We show here that LcrV, the cap protein of bacterial type III secretion needles, is modified by host glutathione and that this modification contributes to the high

virulence of *Y. pestis* in mouse and rat models for bubonic plague. These data suggest that *Y. pestis* exploits glutathione in host tissues to activate a virulence strategy, thereby accelerating plague pathogenesis.

CHAPTER I

INTRODUCTION

Glutathione: A Brief Overview

In prokaryotic and eukaryotic cells, the cytoplasm is a reducing environment and protein thiols are maintained in their reduced state by low-molecular-weight (LMW) thiol redox buffers and enzymatic thiol-disulfide oxidoreductases, including the thioredoxin and glutaredoxin systems (Fahey 2013; Van Laer, Hamilton, and Messens 2013). During respiration, cellular metabolism, or host-pathogen interactions, bacteria encounter a variety of highly reactive small molecules—e.g., reactive oxygen species (ROS), reactive nitrogen species (RNS), reactive chlorine species (RCS), reactive sulfur species (RSS), and reactive electrophilic species (RES)—that can induce oxidative stress and potentially damage cellular macromolecules such as proteins, carbohydrates, and nucleic acids (Antelmann and Helmann 2011; Gray, Wholey, and Jakob 2013). Additionally, these reactive species can precipitate a number of unique posttranslational modifications of reactive protein thiols as well as activate or inactivate specific transcription factors that result in the expression of bacterial detoxification pathways. In this respect, LMW thiol redox buffers play a significant role in the detoxification of various reactive species and are often present at millimolar concentrations in the cytoplasm of Gram-negative bacteria (Loi, Rossius, and Antelmann 2015).

The tripeptide glutathione (γ-glutamyl-cysteinyl-glycine [GSH]) is the predominant LWM thiol redox buffer in Gram-negative bacteria as well as in some Gram-positive Firmicutes bacteria, including *Streptococcus agalactiae*, *Listeria monocytogenes*, and *Clostridium acetobutylicum* (Loi, Rossius, and Antelmann 2015). In the Gram-negative bacterium *Escherichia coli*, the *de novo* pathway of GSH biosynthesis occurs in two steps: first, γ-glutamylcysteine ligase (GshA)

catalyzes the formation of γ-glutamylcysteine (γ-Glu-Cys [γ-EC]) from glutamate and cysteine, and second, glutathione synthase (GshB) catalyzes the ligation of glycine to γ-glutamylcysteine to generate GSH (Meister 1995; Anderson 1998). In *S. agalactiae* and *L. monocytogenes*, GSH biosynthesis is carried out by the bifunctional fusion protein GshF, which integrates the catalytic activities of GshA and GshB (Gopal et al. 2005; Janowiak and Griffith 2005). In contrast, *Streptococcus pneumoniae* and *Haemophilus influenza* do not synthesize GSH but encode GSH-uptake mechanisms whereby glutathione is imported from the extracellular environment. Specifically, in *S. pneumoniae*, the ABC transporter binding protein GshT mediates GSH-uptake from the host (Potter, Trappetti, and Paton 2012; Vergauwen et al. 2013), and in *H. influenzae*, glutathione import is mediated by the ABC transporter DppBCDF and requires the periplasmic GSH-binding protein GbpA (Vergauwen et al. 2010). Interestingly, these pathogens utilize host-derived glutathione as a protective mechanism against the host immune defenses (Loi, Rossius, and Antelmann 2015).

In *E. coli*, glutathione is present in the cytoplasm at a concentration of 3.5–6.6 mM, where in addition to its role in maintaining protein thiols in the reduced state, GSH functions as a storage form of cysteine (Masip, Veeravalli, and Georgiou 2006; Fahey 2013). During bacterial growth, or when bacteria are under oxidative stress, GSH is oxidized at its sulfhydryl to glutathione disulfide (GSSG). Due to the cytotoxicity associated with high levels of intracellular GSSG, the NADPH-dependent enzyme glutathione reductase (Gor) catalyzes the conversion of GSSG to its reduced state (GSH), thereby maintaining a high cytoplasmic GSH/GSSG ratio that ranges from 30:1 to 100:1 (Hwang, Lodish, and Sinskey 1995; Van Laer, Hamilton, and Messens 2013). The various detoxification functions of glutathione have been extensively studied in Δ*gshA* and Δ*gshB* mutant *E. coli* strains. These studies have illuminated the crucial physiological roles played by

glutathione in maintaining intracellular redox balance, detoxifying chlorine compounds and methylglyoxal, regulating intracellular potassium levels, and protecting the cell against acidic, oxidative, and osmotic environmental stresses (Masip, Veeravalli, and Georgiou 2006). In particular, the biochemical mechanism for bacterial detoxification of xenobiotics, electrophiles, and antibiotics by GSH occurs either spontaneously by *S*-conjugation or by the catalytic activity of an intracellular glutathione *S*-transferase (GST) (Fahey 2013). Moreover, the primary pathway for methylglyoxal detoxification in *E. coli* is the GSH-dependent glyoxalase pathway whereby resistance to methylglyoxal is linked to the activation of potassium efflux, which in turn leads to cytoplasmic acidification and thus limits the interaction of methylglyoxal with bacterial DNA (Loi, Rossius, and Antelmann 2015).

Although the detoxification functions of GSH have long been understood as a mechanism for maintaining cytoplasmic redox balance, it was only recently that glutathione was shown to contribute to the virulence of pathogenic bacteria. In *S. pneumoniae*, for instance, a study demonstrated that the glutathione reductase Gor and the GSH-importer GshT were required for oxidative stress protection and metal ion resistance. Further, when analyzed in a mouse model of pneumococcal infection, Δ*gshT* mutant *S. pneumoniae* was attenuated for colonization and invasion relative to the wild-type strain (Potter, Trappetti, and Paton 2012). In *S. pneumoniae*, therefore, glutathione protects against the host immune defenses and contributes to bacterial fitness.

Glutathione has also been shown to play a significant role in the pathogenesis of *L. monocytogenes*, a facultative intracellular pathogen that can synthesize GSH via its GshF fusion protein as well as import GSH from its host (Gopal et al. 2005). A recent study reported that Δ*gshF* mutant *L. monocytogenes* was two-fold less virulent compared to wild-type bacteria in a mouse

model of infection. Moreover, *in vitro* assays demonstrated that the Δ*gshF* mutant was more sensitive to oxidative stress, possessed lower levels of ActA, and formed smaller plaques in tissue culture assays used to measure cell-to-cell spread by the bacterium (Reniere et al. 2015). Significantly, ActA—an actin assembly-inducing protein that is under the control of the master virulence regulator PrfA—is responsible for propelling *L. monocytogenes* through host cells (Freitag, Port, and Miner 2009). Reniere and colleagues (2015) revealed that the activation of PrfA was mediated by its allosteric binding to both bacterial and host-derived GSH, and that the attenuated virulence of Δ*gshF* mutant *L. monocytogenes* resulted from a lack of PrfA activation. Intriguingly, it was also shown that *S*-glutathionylation, which involves the covalent addition of GSH to protein cysteine residues, did not contribute to PrfA activation (Reniere et al. 2015). Thus, in *L. monocytogenes*, glutathione functions as a signaling molecule to activate virulence gene expression.

Another recent study elucidated the contributions of glutathione to the virulence of the gastrointestinal pathogen *Salmonella enterica* serovar Typhimurium (*S.* Typhimurium). In particular, it was shown that GSH antagonized the bacteriostatic activity of RNS *in vivo*, and that Δ*gshA* mutant *S.* Typhimurium was more sensitive to ROS and RNS than the wild-type strain. When analyzed in an acute model of salmonellosis using mice expressing the wild-type NRAMP1^{R} allele, which is linked to high nitric oxide (NO) production by macrophages, the Δ*gshA* and Δ*gshB* mutants were attenuated in virulence relative to wild-type *S.* Typhimurium. Moreover, using the same mouse model, GSH was shown to protect against ROS and RNS produced by the NADPH phagocyte oxidase and the inducible nitric oxide synthase (iNOS) (Song et al. 2013). Glutathione thus enhances *S.* Typhimurium fitness by protecting against oxidative and nitrosative stresses encountered by the bacterium in the course of host infection.

Taken together, these studies on the pathogenic bacteria *S. pneumoniae*, *L. monocytogenes*, and *S.* Typhimurium highlight the significance of glutathione in the control of virulence functions, the expression of virulence factors, and the optimization of pathogen fitness during *in vivo* infections. Perhaps the most intriguing possibility, as revealed for *L. monocytogenes*, is that glutathione could play a similar role in other bacterial pathogens, namely, by regulating the activation, or perhaps the deactivation, of virulence gene expression via redox control of virulence gene regulators.

The Regulatory Potential of Protein Glutathionylation

Under conditions of oxidative stress, glutathione forms reversible mixed disulfides with specific protein cysteine residues in a posttranslational modification that is termed protein glutathionylation (or *S*-glutathionylation). Although the mechanisms involved in protein glutathionylation are numerous, they nevertheless share the common requirement for a protein cysteine thiol to be converted to a reactive cysteine oxidation intermediate, for example, a sulphenic acid or *S*-nitrosyl or sulphenylchloride intermediate. In eukaryotes, protein glutathionylation has emerged as a major redox-regulatory mechanism that controls the activity of redox sensing transcription factors and protects active site cysteine residues against potentially irreversible oxidation to sulfonic acids (Dalle-Donne et al. 2009). Furthermore, glutathionylation has been demonstrated to control numerous physiological processes—such as cellular growth and differentiation, cell cycle progression, and apoptosis—and has also been implicated in the pathogenesis of neurodegenerative and cardiovascular diseases (Klatt and Lamas 2000; Ghezzi 2005; Dalle-Donne et al. 2007; Dalle-Donne et al. 2009; Ghezzi 2013). To function as a redox-regulatory mechanism, protein glutathionylation must meet the following criteria: (1) reversibility;

(2) specificity to active site cysteine residue; (3) change in protein function/activity; and (4) induction by reactive species (Dalle-Donne et al. 2009).

In contrast to the many known physiological functions of protein glutathionylation in eukaryotes, much less is understood about the extent and impact of this posttranslational modification in prokaryotes. In *E. coli*, for example, glutathionylation has only been shown to function as a redox-regulatory mechanism for a few intracellular proteins. Specifically, the oxidative stress regulator OxyR is activated by glutathionylation *in vitro* (Kim et al. 2002), whereas the activities of glyceraldehyde 3-phosphate dehydrogenase (Gap), methionine synthase (MetE), and PAPS reductase (PpaC) are inhibited by the glutathionylation of specific protein cysteine residues (Lillig et al. 2003; Hondorp and Matthews 2004; Brandes, Schmitt, and Jakob 2009). Protein glutathionylation has also been demonstrated in other Gram-negative bacteria, including *S.* Typhimurium, *Neisseria meningitidis*, *Pseudoalteromonas haloplanktis*, and *Synechocystis* sp. PCC6803. In each of these bacterial species, as with *E. coli*, a redox-regulatory role for glutathionylation was strictly limited to intracellular proteins (Loi, Rossius, and Antelmann 2015). To date, there has not been a surface or extracellular bacterial secreted protein that has been shown to be modified by glutathionylation.

Yersinia pestis and Human Disease

Y. pestis is a Gram-negative coccobacillus and the etiologic agent of bubonic, pneumonic, and septicemic plague. The genus *Yersinia* is a member of the family Enterobacteriaceae and consists of eleven species, including three that are pathogenic in humans: *Y. pestis*, *Y. enterocolitica,* and *Y. pseudotuberculosis*. While *Y. enterocolitica* and *Y. pseudotuberculosis* are food-borne enteric pathogens that cause a self-limiting gastrointestinal illness in

immunocompetent adults (Perry and Fetherston 1997; Cornelis et al. 1998; Lee and Schneewind 1999), *Y. pestis* is transmitted by fleabite, direct contact, gastrointestinal uptake, or inhalation of aerosolized droplets and causes a severe, acute, and rapidly progressive febrile illness with significant mortality rates (Slack 1989; Perry and Fetherston 1997). *Y. pestis* survives in sylvatic animal reservoirs, primarily in rodents, but has achieved a near-global distribution in many different animal and flea hosts (Gage and Kosoy 2005). Historically, epizootic plague outbreaks in rodents has triggered flea-borne transmission of *Y. pestis* into human populations with devastating consequences (Perry and Fetherston 1997).

Bubonic plague, the most common manifestation of the disease in humans, results from the introduction of *Y. pestis* into the dermal layer of the skin via the bite of an infected flea (Brubaker 1991); however, it is also possible, albeit rare, for an infected flea to cause primary septicemic plague if its bite happens to deposit the bacteria directly into a dermal blood vessel (Perry and Fetherston 1997; Cornelis et al. 1998; Prentice and Rahalison 2007). Using the host lymphatic system to traffic from the dermis to the regional draining lymph node (dLN), *Y. pestis* replicates within the confines of this preferred niche at such a staggering pace that, at only 48 hours post-fleabite, the number of plague bacteria in the dLN has increased by a factor of approximately 2×10^5 relative to the initial dermal inoculum (Gonzalez et al. 2015). It is a combination of this massive bacterial proliferation, the associated host inflammatory responses, and *Y. pestis*-mediated destruction of immune cells and lymph node tissues that ultimately gives rise to the pathognomonic "bubo," an acutely swollen and painful lymph node (Inglesby et al. 2000). The continual replication of plague bacilli, as well as the increasingly severe degradation of the lymph node's native cellular architecture, eventually allows *Y. pestis* to escape into the bloodstream—a bacteremia that is termed secondary septicemic plague—and thus provides for rapid bacterial

spread and invasion of peripheral organs (Perry and Fetherston 1997; Sebbane et al. 2005). This progression from localized to systemic plague disease is associated with a mortality rate of approximately 90% (Comer et al. 2010). Secondary pneumonic plague, a highly lethal and contagious air-borne form of the disease, develops from hematogenous dissemination of *Y. pestis* into the lungs during bubonic or septicemic plague (Pechous et al. 2016). Primary pneumonic plague, which is acquired by direct inhalation of aerosolized droplets containing *Y. pestis*, is the rarest form of the disease. Although it is nearly 100% fatal if left untreated, pneumonic plague presents with the onset of mild "flu-like" symptoms—and, in some cases, the presence of a low fever and/or gastrointestinal complaints—but rapidly progresses to a severe and ultimately lethal pneumonia (Inglesby et al. 2010; Pechous et al. 2016).

Y. pestis is considered the single most virulent bacterial pathogen as well as a weapon of mass destruction (Inglesby et al. 2000; Inglesby, Grossman, and O'Toole 2001). Indeed, as a result of its fulminant spread and very high mortality, *Y. pestis* has killed more people worldwide than any other infectious disease agent (Slack 1989). The notoriety of *Y. pestis* stems in no small part from its association with three high-mortality pandemics in human history: first, the Justinian Plague (AD 541 to 544) that spread from Central Asia across the Mediterranean basin into Europe, with attributable population losses of 50–60% in afflicted regions; second, the Medieval "Black Death" (AD 1347 to 1351) that emerged from plague foci in East Asia and spread along trade routes to Europe, where the disease killed 30–40% of the population; and third, the Asian Plague Pandemic (AD 1855 to 1959) that originated in China before disseminating via transoceanic shipping routes to all inhabited continents and ultimately resulted in more than 40 million deaths (Girard and Robic 1942; Perry and Fetherston 1997; Inglesby et al. 2000; Benedictow 2004; Little 2007). During the course of these pandemics, wherever *Y. pestis* became established in the local

rodent population—a process whose outcome is determined by a variety of climatic and ecological factors (Gage and Kosoy 2005)—subsequent outbreaks of plague disease occurred in regular cycles for up to several centuries (Perry and Fetherston 1997; Benedictow 2004; Little 2007; Spyrou et al. 2016; Harper 2017).

Historians estimate that, remarkably, plague pandemics and epidemics were responsible for eliminating three-quarters of the worldwide human population (Bos et al. 2011). Today, *Y. pestis* remains a significant health concern as small plague epidemics continue throughout the world, with approximately 4,000 human plague cases reported annually (Schrag and Wiener 1995; Perry and Fetherston 1997; Cornelis 2000; Stenseth et al. 2008). Plague remains endemic in the United States, as well, with about twenty cases reported each year (Inglesby et al. 2000). The Centers for Disease Control and Prevention (CDC) classifies *Y. pestis* as a Category A (Tier-1) select agent on account of its ubiquitous distribution in zoonotic reservoirs and insect vectors, the ease of pathogen preparation for aerosol dissemination, the high fatality rate of pneumonic plague disease and its potential for secondary spread, and the pathogen's bioweapon history (Perry and Fetherston 1997; Inglesby et al. 2000; Ligon 2006; Prentice and Rahalison 2007). While antibiotic treatment is available for *Y. pestis* infections, it must be administered within a relatively narrow therapeutic window, and antibiotic resistant strains of *Y. pestis* have been reported (Prentice and Rahalison 2007; Ivanov et al. 2008).

The Asian Plague Pandemic was halted through widespread administration of the live-attenuated plague vaccine EV76 (Girard and Robic 1942; Girard 1955; Russell et al. 1995). However, a subsequent clinical trial in the United States revealed that *Y. pestis* EV76 immunization resulted in severe side effects and even plague disease (Meyer 1970), which can occur in individuals with elevated iron levels or hemochromatosis (Frank, Schneewind, and Shieh 2011;

Quenee et al. 2012). Due to these safety concerns, the EV76 vaccine has not received licensure for clinical use as a plague vaccine in the United States (Meyer 1970). Although considerable effort continues to be directed toward the development of a safe and efficacious plague vaccine for humans, an FDA approved product is not currently available, albeit that a number of candidate vaccines are currently in clinical trials (Quenee and Schneewind 2009).

The *Y. pestis* Type III Secretion System

A unifying feature of pathogenic *Yersinia* species is their use of a virulence plasmid-encoded type III secretion system (T3SS) to evade phagocytic killing during host infection (Perry et al. 1986; Rosqvist, Bölin, and Wolf-Watz 1988; Cornelis et al. 1998). Although it was first described in *Yersinia*, type III secretion (T3S) is a conserved virulence strategy that is employed by a number of Gram-negative pathogens for the transport of virulence factors from the bacterial cytosol across the plasma membrane of targeted eukaryotic cells (Rosqvist, Magnusson, and Wolf-Watz 1994; Lee 1997; Hueck 1998; Galán and Collmer 1999). The T3S machine, which is evolutionarily related to the bacterial flagellum (Yip et al. 2005), has been described as a secretion device that promotes self-assembly of a complex protein conduit between bacteria and host cells (Galán and Wolf-Watz 2006). The T3SS is composed of at least twenty distinct proteins that assemble into three major parts: (1) a basal body that spans both the inner and outer bacterial membranes; (2) a polymerized needle filament that protrudes from the basal body into the extracellular environment; and (3) a tip complex that is exported to the distal end of the needle filament (Cornelis 2006; Matteï et al. 2011).

In *Y. pestis*, the numerous Ysc (*Yersinia* secretion) components required to assemble a functional T3S machine are encoded on a 70-kb virulence plasmid (pCD1), which also harbors the

genes that encode the needle filament protein (YscF), the needle cap protein (LcrV), and a panoply of secreted type III effectors, known as Yops (*Yersinia* outer proteins) (Michiels et al. 1991; Allaoui, Schulte, and Cornelis 1995; Cornelis et al. 1998). The essential virulence strategy of type III secretion is tightly regulated in *Y. pestis* by two environmental signals, namely, temperature and extracellular calcium concentration. First, the temperature shift associated with *Y. pestis* transmission from its flea vector (18–30°C) to a mammalian host (37°C) triggers the expression of LcrF—the master transcriptional activator of pCD1-encoded type III genes—and, consequently, to a massive upregulation in the synthesis and assembly of T3S machines (Yother, Chamness, and Goguen 1985; Hoe and Goguen 1993; Schwiesow et al. 2015). Second, establishment of the *Y. pestis* type III conduit into a host cell is associated with a perceived drop in calcium levels—owing to the more than 100-fold difference between the concentration of calcium ions in extracellular fluids (1.2 mM) and within cells (<10 μM)—that activates the T3SS for injection of Yop effectors into the host cell (Pollack, Straley, and Klempner 1986; Lee, Mazmanian, and Schneewind 2001). Possibly due to the extensive energy requirements of type III secretion, *Y. pestis* exhibits a low-calcium response (LCR) phenotype, which is defined as bacterial growth restriction during active type III secretion (Kupferberg and Higuchi 1958; Goguen, Yother, and Straley 1984). Further, suppression of the LCR under secretion-permissive conditions is indicative of *Y. pestis* inability to activate the type III pathway and also associated with a loss of virulence in animal models of plague disease (Yother and Goguen 1985; Skryzpek and Straley 1993, 1995).

Assembly of the *Yersinia* T3SS, which is also called the injectisome, requires the protein products of more than twenty genes (Cheng and Schneewind 2000; Cornelis 2006) and proceeds in a tightly regulated, stepwise fashion (Kimbrough and Miller 2000; Deane et al. 2010). The formation of the T3SS begins with the basal body, which is composed of a protein scaffold, an

export apparatus, an ATPase complex, and a cytoplasmic ring (C-ring). The scaffold of the basal body is formed by three membrane proteins—YscC, YscD, and YscJ—that are translocated via the Sec pathway and assembled to generate a structure with rotational symmetry in the bacterial envelope (Michiels et al. 1991; Blocker et al. 2001; Marlovits et al. 2004; Galán and Wolf-Watz 2006). Specifically, basal body formation begins with the oligomerization of YscC, which forms the outer membrane ring and extends deeply into the periplasm (Koster et al. 1997; Diepold et al. 2010). After the outer membrane ring is formed, a ring of YscD is assembled into the inner membrane and is thought to bind YscC, thereby connecting the inner and outer membrane rings (Diepold et al. 2010; Ross and Plano 2011). YscD then recruits the lipoprotein YscJ, which oligomerizes on the periplasmic face of the inner membrane to complete the inner membrane ring (Diepold et al. 2010). The ATPase complex—composed of YscK, YscL, and YscN—assembles on the cytosolic face of the basal body. YscN, an ATPase related to the F1-ATP synthase, is necessary for the export of type III substrates by the T3SS; YscL functions as a negative regulator of ATPase activity; and the function of YscK is as yet unknown (Blaylock et al. 2006). The C-ring of the basal body is comprised of YscQ, which colocalizes with YscC in the membrane and associates with the ATPase complex (Jackson and Plano 2000; Diepold et al. 2010). Assembling independently of the scaffold proteins, the export apparatus—which is composed of the integral membrane proteins YscR, YscS, YscT, YscU, and YscV—forms the export channel across the inner membrane and is believed to recognize type III substrates (Sorg et al. 2007; Diepold, Wiesand, and Cornelis 2011). Following its assembly, the export apparatus is recruited to YscJ in the inner membrane ring of the scaffold (Diepold, Wiesand, and Cornelis 2011). With the joining of the protein scaffold, the ATPase–C-ring complex, and the export apparatus, the basal body is fully assembled and capable of exporting type III secretion substrates (Diepold et al. 2010).

Proteins secreted by *Y. pestis* are loosely classified as early, middle, or late substrates, depending on the stage of type III secretion at which they are required (Riordan and Schneewind 2008). In this model, then, substrate selection is an ordered process that, following assembly of the T3SS basal body, begins with the recognition and export of early substrates—such as YscI, YscF, and YscP—that are required for needle assembly. The YscI protein forms a rod-like structure within the center of the basal body (Kimbrough and Miller 2000; Marlovits et al. 2004), which is required for needle stability and may function as a platform for the initiation of needle polymerization (Marlovits et al. 2006; Wood, Jin, and Lloyd 2008). The needle protein YscF is then secreted through the YscI rod (Diepold et al. 2012), and the polymerization of YscF generates a hollow needle structure that extends approximately 42 nm from the bacterial surface (Hoiczyk and Blobel 2001; Journet et al. 2003). YscP is secreted during YscF polymerization and functions as a "molecular ruler" by regulating the length of the type III needle (Stainier et al. 2000; Journet et al. 2003), as proper needle length is important for efficient translocation of Yop effectors into a targeted host cell (Mota et al. 2005). Once the needle has reached the appropriate length, YscP interacts with YscU in the export apparatus to mediate a substrate specificity switch that allows the T3SS to export middle and late substrates (Sorg et al. 2007; Riordan and Schneewind 2008).

Following needle assembly, the T3SS exports three translocator proteins—LcrV, YopB, and YopD—that comprise the middle substrates. LcrV is secreted and polymerizes at the distal end of the YscF needle to form a pentameric needle tip complex (Mueller et al. 2005). Upon host cell contact, the LcrV tip complex is thought to act as a platform for insertion of the pore-forming proteins, YopB and YopD, into the host cell membrane (Håkansson et al. 1993; Håkansson et al. 1996; Sorg, Miller, and Schneewind 2005; Mueller, Broz, and Cornelis 2008). Once activated by low-calcium signals associated with the extension of the *Y. pestis* type III conduit into the host

cell, the T3SS exports late substrates—the effector proteins YopE, YopH, YopM, YpkA, YopJ, YopQ, and YopT—directly into the host cell cytoplasm (Pollack, Straley, and Klempner 1986; Michiels et al. 1990; Lee, Mazmanian, and Schneewind 2001; Cornelis 2006; Mueller, Broz, and Cornelis 2008). To evade host immune defenses during plague pathogenesis, *Y. pestis* targets immune cells for injection of Yop effectors, which inhibit actin polymerization, prevent phagocytosis, suppress proinflammatory cytokine release, and produce cytotoxic effects (Rosqvist, Bölin, and Wolf-Watz 1988; Rosqvist, Magnusson, and Wolf-Watz 1994; Nakajima, Motin, and Brubaker 1995; Black and Bliska 1997; Marketon et al. 2005).

LcrV: The Swiss Army Knife of *Y. pestis* Virulence Factors

The type III secretion substrate LcrV (low-calcium response V antigen) is a dynamic, multifunctional virulence factor that is absolutely required for *Y. pestis* pathogenesis (Burrows 1956, 1957; Perry et al. 1986). In the bacterial cytoplasm, LcrV plays a regulatory role in Yop secretion that is mediated by its association with LcrG, a negative regulator of the type III pathway. In response to the appropriate signals, LcrV stimulates type III secretion by binding to LcrG, thereby titrating its capacity to repress secretion. Further, this cytoplasmic association between LcrV and LcrG is required for the secretion of LcrV (Nilles et al. 1997; Matson and Nilles 2001; DeBord, Lee, and Schneewind 2001).

Following needle assembly, but prior to host cell contact, LcrV is secreted and caps the distal end of the YscF needle as a homopentameric ring-like structure (Mueller et al. 2005). The location and stoichiometry of the LcrV cap was revealed by electron microscopy experiments with *Y. enterocolitica* needle complexes sheered from the bacterial surface (Mueller et al. 2005; Mueller, Broz, and Cornelis 2008). LcrV is also required for *Y. pestis* translocation of Yop

effectors into host cells (Pettersson et al. 1999; Lee, Tam, and Schneewind 2000). Specifically, upon contact of the capped needle with host cell membranes, LcrV interacts with YopB and YopD to form the translocation pore, a YopB-YopD complex embedded in the eukaryotic plasma membrane that extends the type III conduit into the targeted host cell (Broz et al. 2007; Mueller, Broz, and Cornelis 2008). In addition to its secretion and capping of the type III needle, LcrV is secreted into the extracellular milieu where it exerts immunosuppressive effects on host immune cells owing to its activation of Toll-like receptor 2/6 (TLR2/6) and Jun N-terminal protein kinase 2 (JNK2) signaling pathways, thereby repressing the proinflammatory cytokines tumor necrosis factor alpha (TNF-α) and interferon gamma (INF-γ) and promoting the release of interleukin-10 (IL-10) (Nakajima and Brubaker 1993; Nakajima, Motin, and Brubaker 1995; DePaolo et al. 2008).

The Development of a Plague Protective Subunit Vaccine

The potential for unimaginable devastation resulting from the use of *Y. pestis* as a bioweapon, as well as the possibility of naturally occurring plague epidemics or pandemics, have long provided an impetus for the development of a plague protective vaccine (Inglesby et al. 2000; Inglesby, Grossman, and O'Toole 2001). To this end, recent research efforts have focused on the development of a soluble subunit vaccine containing one or more plague protective antigens (Quenee and Schneewind 2009). In this respect, antibodies against two protective antigens, LcrV and F1, are known to confer immunity against plague (Baker et al. 1952; Burrows 1956). Plague protective immunity is based on B-cell mediated antibody responses (Williamson et al. 1999), and LcrV- or F1-specific antibodies interfere with *Y. pestis* type III injection of host cells (Quenee et al. 2009). Located on the 100-kb pFra (pMT1) plasmid of *Y. pestis*, the *caf1* structural gene encodes

F1 (Caf1) pilin subunits that are assembled into pili which, at 37°C, form a dense antiphagocytic capsule surrounding the bacterium (Baker et al. 1952; Du, Rosqvist, and Forsberg 2002; Zavialov et al. 2003). Although F1 subunit vaccines elicit protective immunity (Baker et al. 1952; Andrews et al. 1996), *caf1* is not essential for the pathogenesis of pneumonic plague in mice, rats, guinea pigs, and nonhuman primates (Friedlander et al. 1995; Quenee et al. 2008; Anderson et al. 2009). Significantly, a Δ*caf1* mutant *Y. pestis* strain was isolated from a fatal case of human plague (Winter, Cherry, and Moody 1960), suggesting that F1 pili may likewise be dispensable for plague pathogenesis in humans. Furthermore, *Y. pestis caf1A*::IS*1541* escape variants, which arise spontaneously due to IS*1541* transposition into the structural gene for the outer membrane usher protein (Caf1A) required for F1 pilus assembly, break through the protection generated by F1 subunit vaccines and cause fulminant plague disease (Quenee et al. 2008; Cornelius et al. 2009). Thus, the F1 pilin protein cannot be used as the sole antigen in a plague subunit vaccine.

Unlike the genetic determinants for the F1 capsular antigen, which are dispensable for disease establishment and targeted by *Y. pestis* escape variants, the *lcrV* gene is absolutely essential for plague pathogenesis (Perry et al. 1986), and escape variants to LcrV subunit vaccines have not been isolated (Miller et al. 2012). Indeed, when used as a purified subunit vaccine, LcrV generates humoral immune responses that are protective against bubonic or pneumonic plague challenge in every animal model examined (Quenee and Schneewind 2009; Quenee et al. 2011). Although the molecular mechanism whereby protective antibodies against LcrV neutralize the type III pathway is not fully understood, electron microscopy studies suggest that LcrV antibodies can bind to the pentameric ring structure of LcrV at the tip of the type III needle (Mueller et al. 2005). On this basis, it has been suggested that LcrV-specific antibodies disrupt dynamic changes required for *Y. pestis* type III injection, for example, by preventing the needle tip complex from opening for

subsequent translocation of Yop effectors or by precluding the formation of a functional translocation pore by interfering with physical associations between LcrV and its translocation partners YopB and YopD (Quenee and Schneewind 2009; Miller et al. 2012).

CHAPTER II

GLUTATHIONYLATION OF *YERSINIA PESTIS* LCRV AND ITS EFFECTS ON PLAGUE PATHOGENESIS

The material presented in this Chapter previously appeared as an article in the journal *mBio*; it is reprinted here by permission of the publisher. The original citation is as follows:

> Anthony Mitchell, Christina Tam, Derek Elli, Thomas Charlton, Patrick Osei-Owusu, Farbod Fazlollahi, Kym F. Faull, and Olaf Schneewind. 2017. "Glutathionylation of *Yersinia pestis* LcrV and Its Effects on Plague Pathogenesis." *mBio* 8 (3): e0064-17. https://doi.org/10.1128/mBio.00646-17.

The author contributions are as follows: A.M., C.T., K.F.F., and O.S. conceived the project. A.M., C.T., D.E., F.F., K.F.F., and O.S. purified and analyzed $LcrV_{S228}$. A.M., C.T., and D.E. characterized *Y. pestis* type III secretion and effector injection. C.T., D.E., T.C., P.O.-O., and O.S. performed animal experiments and quantified serum antibody titers. A.M. conducted HPLC experiments, characterized *Y. pestis* growth in sheep blood and serum, and analyzed genome sequence data. A.M., C.T., K.F.F., and O.S. wrote the paper.

ABSTRACT

Glutathionylation, the formation of reversible mixed disulfides between glutathione and protein cysteine residues, is a posttranslational modification previously observed for intracellular proteins of bacteria. Here we show that *Yersinia pestis* LcrV, a secreted protein capping the type III secretion machine, is glutathionylated at Cys^{273} and that this modification promotes association with host ribosomal protein S3 (RPS3), moderates *Y. pestis* type III effector transport and killing

of macrophages, and enhances bubonic plague pathogenesis in mice and rats. Secreted LcrV was purified and analyzed by mass spectrometry to reveal glutathionylation, a modification that is abolished by the codon substitution $Cys^{273}Ala$ in *lcrV*. Moreover, the $lcrV_{C273A}$ mutation enhanced the survival of animals in models of bubonic plague. Investigating the molecular mechanism responsible for these virulence attributes, we identified macrophage RPS3 as a ligand of LcrV, an association that is perturbed by the $Cys^{273}Ala$ substitution. Furthermore, macrophages infected by the $lcrV_{C273A}$ variant displayed accelerated apoptotic death and diminished proinflammatory cytokine release. Deletion of *gshB*, which encodes glutathione synthetase of *Y. pestis*, resulted in undetectable levels of intracellular glutathione, and we used a *Y. pestis* Δ*gshB* mutant to characterize the biochemical pathway of LcrV glutathionylation, establishing that LcrV is modified after its transport to the type III needle via disulfide bond formation with extracellular oxidized glutathione.

IMPORTANCE

Yersinia pestis, the causative agent of plague, has killed large segments of the human population; however, the molecular bases for the extraordinary virulence attributes of this pathogen are not well understood. We show here that LcrV, the cap protein of bacterial type III secretion needles, is modified by host glutathione and that this modification contributes to the high virulence of *Y. pestis* in mouse and rat models for bubonic plague. These data suggest that *Y. pestis* exploits glutathione in host tissues to activate a virulence strategy, thereby accelerating plague pathogenesis.

INTRODUCTION

Glutathione, the predominant low-molecular-weight (LMW) peptide thiol present in all mitochondrial eukaryotes and nearly all Gram-negative bacteria, exists as a redox couple between its reduced (GSH) and oxidized (GSSG) forms and plays a pivotal role in many physiological processes (Masip, Veeravalli, and Georgiou 2006). In *Escherichia coli*, glutathione maintains the proper oxidation state of protein thiols, regulates intracellular potassium levels, detoxifies methylglyoxal and halogenated compounds, and protects bacteria against acidic, oxidative, and osmotic stresses (Loi, Rossius, and Antelmann 2015). Protein glutathionylation, a posttranslational modification whereby the sulfhydryl of glutathione forms a reversible mixed disulfide with protein cysteine residues, is increased during oxidative stress and protects reactive protein thiols from potentially irreversible oxidation (Dalle-Donne et al. 2009). Glutathione in body fluids of vertebrates has been shown to impact the pathogenesis of bacterial infections by regulating the expression of microbial virulence functions or by protecting against oxidative and nitrosative stresses (Potter, Trappetti, and Paton 2012; Song et al. 2013; Reniere et al. 2015). A role for extracellular glutathione in modifying the surface of bacterial pathogens has heretofore not been described.

Yersinia pestis, the etiologic agent of plague, has killed more people worldwide than any other infectious agent (Slack 1989). This bacterium employs a specialized type III secretion system to evade and neutralize the immune responses of its mammalian hosts (Marketon et al. 2005). Particularly significant in this respect is the multifunctional virulence factor LcrV, the plague protective antigen and needle cap protein of the *Yersinia* type III secretion machine (Burrows 1956; Mueller et al. 2005). LcrV is essential for plague pathogenesis (Perry et al. 1986) as the polypeptide enables the transport of *Yersinia* effector proteins (Yops) across the eukaryotic plasma

membrane, where they exert cytotoxic and immunomodulatory effects within host immune cells (Lee, Tam, and Schneewind 2000). Here we report that *Y. pestis* LcrV is glutathionylated at cysteine residue 273 and that this modification impacts the pathogenesis of plague infections.

RESULTS

LcrV, the Cap Protein of *Y. pestis* Type III Secretion Machines, Is Glutathionylated at Cys^{273}

$LcrV_{S228}$ carries a Strep-tag insertion at amino acid 228 that does not affect its function (Ligtenberg et al. 2013). $LcrV_{S228}$ was purified from the culture supernatant of *Y. pestis* KLD29 Δ*lcrV*(pKG48), and the recombinant form of $LcrV_{S228}$ ($rLcrV_{S228}$) was purified from extracts of *E. coli* DH5α(pKG48). Both proteins were analyzed by combined liquid chromatography-electrospray ionization mass spectrometry (LC-ESI-MS) to reveal average masses of 38,594.4 Da ($LcrV_{S228}$) and 38,284.9 Da ($rLcrV_{S228}$) (Fig. 1*A* and Fig. 2*A* and *B*). *Y. pestis* $LcrV_{S228}$ was 309.5 Da heavier than *E. coli* $rLcrV_{S228}$ and 314.2 Da heavier than the calculated mass for the 334-amino-acid protein with the initiator methionine (38,280.22 Da). Edman degradation of *Y. pestis* $LcrV_{S228}$ released N-terminal amino acids with the sequence NH_2-MIRA-CO_2H, identical to the predicted protein sequence (Perry et al. 1986) (Fig. 2*C*). To locate the site of the modification, reverse-phase-purified *Y. pestis* $LcrV_{S228}$ and *E. coli* $rLcrV_{S228}$ were treated with trypsin, and overlapping cleavage maps from LC-ESI-MS data were compared (Table 1). These experiments identified peptide 270-284 (NH_2-DNNELSHFATTCSDK-CO_2H) as the site of the modification in *Y. pestis* $LcrV_{S228}$ because its measured monoisotopic mass (1,985.79 Da) was 305.08 Da heavier than that obtained for $rLcrV_{S228}$ (1,680.71 Da), which is in close agreement with the calculated mass for the predicted peptide (1,680.70 Da) (Table 1). Collisionally induced dissociation of the 1,985.79-Da $LcrV_{S228}$ peptide generated fragment ions that identified Cys^{273} as

the site of modification (Table 2). Treatment with dithiothreitol (DTT), a disulfide reductant, collapsed the average mass of *Y. pestis* $LcrV_{S228}$ to match the mass of $rLcrV_{S228}$, which was unaffected by DTT treatment (Fig. 1*B*). DTT treatment of the *Y. pestis* $LcrV_{S228}$ tryptic digest resulted in disappearance of the 1,985.79-Da signal, with appearance of a peptide with molecular mass of 1,680.71 Da, which on the basis of high-performance liquid chromatography (HPLC) retention time and molecular mass was indistinguishable from the corresponding $rLcrV_{S228}$ peptide (Fig. 1*B*). On the basis of mass concordance, these data suggest that Cys^{273} of *Y. pestis* $LcrV_{S228}$ forms a disulfide with glutathione (calculated residue monoisotopic mass of 305.07 Da). Confirming this conclusion, *Y. pestis* $LcrV_{S228}$, but not *E. coli* $rLcrV_{S228}$, was recognized by an antibody specific for glutathione (Fig. 1*C*).

lcrV$_{C273A}$ Accelerates *Y. pestis* Killing of Macrophages and Increases Type III Injection of Effectors into Neutrophils

Unlike wild-type (WT) *Y. pestis* (KIM D27), the Δ*lcrV* mutant (KLD29) did not secrete YopE via the type III pathway (Fig. 3*A*). The *lcrV*$_{C273A}$ mutation did not impact type III secretion of YopE or LcrV in either low-calcium-induced broth cultures or during *Yersinia* infection of HeLa tissue cell cultures (Fig. 3*A* and Fig. 4*A* and *B*). We wondered whether *Y. pestis* KIM D27 Δ*pgm*, a non-pigmented plague strain (Brubaker 1969) and parent of the *Y. pestis* KLD29 Δ*lcrV* variant (Ligtenberg et al. 2013), secretes glutathionylated LcrV. Because the glutathione-specific antibody, due to its low affinity (Gao et al. 2009), failed to detect LcrV in *Y. pestis* extracts, we used glutathione *S*-transferase (GST)-Sepharose as bait for enrichment of glutathionylated LcrV. Culture supernatants of *Y. pestis* KIM D27 and AM6 *lcrV*$_{C273A}$ were subjected to GST-Sepharose affinity chromatography, and the eluate was analyzed with LcrV-specific antibody to reveal that

wild-type LcrV, but not $LcrV_{C273A}$, was selectively retained (Fig. 3*B*). Thus, *Y. pestis* KIM D27 LcrV is glutathionylated similarly to $LcrV_{S228}$.

We investigated the impact of LcrV glutathionylation on *Y. pestis* infection of host immune cells. Following infection of human neutrophils, *Y. pestis* effector injection was measured by the conversion of the CCF2-AM fluorophore (green) to its YopM-Bla-cleaved chromophore (blue) (Marketon et al. 2005), which occurred to a greater extent with *Y. pestis* AM6 relative to *Y. pestis* KIM D27 (Fig. 3*C* and *D*). During infection of murine J774.A1 macrophages, *Y. pestis* effector secretion triggers apoptotic cell death as well as a low level of pyroptotic cell death, and overall cytotoxicity can be quantified by enumerating propidium iodide (PI)-positive cells (Miller et al. 2012). *Y. pestis* AM6-mediated killing of J774.A1 macrophages occurred with significantly increased kinetics compared to *Y. pestis* KIM D27 (Fig. 3*E* and *F*). Prior work has demonstrated that, during *in vivo* pathogenesis as well as *ex vivo* infection of splenocytes, *Y. pestis* selectively targets neutrophils, macrophages, and dendritic cells for injection of Yops in order to evade and eliminate the innate immune responses of its mammalian host (Marketon et al. 2005; Pechous et al. 2013). For this reason, our observation that glutathionylated LcrV impedes *Y. pestis* type III injection of Yop effectors and the killing of innate immune cells suggests that this modification could play a role in mediating *Y. pestis* target cell preference during bacterial pathogenesis.

Glutathionylated LcrV is Associated with Enhanced Virulence in Rodent Models of Bubonic Plague

To examine whether the glutathionylation of LcrV impacts bubonic plague pathogenesis, we introduced the $lcrV_{C273A}$ mutation into *Y. pestis* CO92 pgm^+ *lcrV*, a pigmented plague strain isolated from a fatal case of human plague in Colorado (Doll et al. 1994), resulting in the

generation of *Y. pestis* TD1 pgm^+ $lcrV_{C273A}$. Genome sequencing confirmed that apart from the Cys^{273}Ala codon substitution in *lcrV*, *Y. pestis* CO92 and TD1 were genetically identical. *Y. pestis* CO92 and TD1 catalyzed type III secretion of LcrV and YopE at similar rates (Fig. 4*C* and *D*). GST-Sepharose affinity chromatography detected the glutathionylation of LcrV secreted by *Y. pestis* CO92 but not by the $lcrV_{C273A}$ variant *Y. pestis* TD1 (Fig. 4*E*).

Nonenzootic mammalian hosts are highly susceptible to *Y. pestis* infection, a disease process that can be modeled by subcutaneous challenge of laboratory mice (cohorts of 6- to 8-week-old female BALB/c mice [$n = 20$]). Whereas the Δ*lcrV* mutant is avirulent in this model, *Y. pestis* CO92 causes lethal bubonic plague at a 50% lethal dose (LD_{50}) of 1 to 5 bacteria (Quenee et al. 2008). When analyzed in BALB/c mice by subcutaneous inoculation of 20 CFU *Y. pestis* CO92 or TD1, all mice succumbed to lethal plague disease by 11 days postchallenge (Fig. 5*A*). Nevertheless, mice infected by *Y. pestis* TD1 were slow to exhibit the characteristic features of plague disease (ruffled fur and hunched posture), and the median time to death of *Y. pestis* TD1-infected mice was delayed by 2.5 days relative to that of mice infected with *Y. pestis* CO92 (Fig. 5*A*). Animals were euthanized after exhibiting the symptoms of terminal plague disease: laterally recumbent and lethargic with rapid respiration. We examined *Y. pestis* colonization and dissemination in moribund BALB/c mice that were euthanized between 4 and 7 days postinfection. At the terminal stage of disease, the bacterial loads in the regional lymph node and spleen were similar for all *Y. pestis*-infected mice (Fig. 6*A*).

Bubonic plague pathogenesis was also examined in Brown Norway rats (*Rattus norvegicus*), an enzootic species that is moderately resistant to challenge with *Y. pestis* CO92, which causes bubonic disease in rats at an LD_{50} of 1,000 to 5,000 CFU (Chen and Meyer 1974). Cohorts of 6-week-old female *Rattus norvegicus* animals ($n = 15$) were infected by subcutaneous

injection into the left inguinal fold with 500 CFU *Y. pestis* CO92 or TD1. Whereas only 13% (2/15) of the rats survived bubonic plague infection with *Y. pestis* CO92, 53% (8/15) of infected rats survived the *Y. pestis* TD1 challenge (Fig. 5*B*). Bubonic plague-infected rats ($n = 5$) were also euthanized at 3 days postchallenge to monitor disease progression. Compared to *Y. pestis* CO92-infected rats, rats infected with *Y. pestis* TD1 displayed a reduction in the kinetics of replication in the regional lymph node (4.4×10^7 CFU CO92 versus 1.5×10^5 CFU TD1; $P = 0.24$) as well as in the kinetics of dissemination to the spleen (3.2×10^8 CFU CO92 versus 1.4×10^6 CFU TD1; $P = 0.75$); due to the small cohort size of rats surviving *Y. pestis* CO92 challenge, the observed differences were not statistically significant (Fig. 6*B*).

Rats euthanized between 4 and 7 days postchallenge were analyzed for disease progression. At the terminal stage of bubonic plague disease, *Y. pestis* CO92 and TD1 had replicated to similar levels in the regional lymph node as well as the spleen (Fig. 6*C*). Rats that survived bubonic plague infection for 14 days were euthanized and necropsied. All survivors of *Y. pestis* CO92 and TD1 challenge lacked detectable levels of plague bacteria in their spleens, nor was there a statistically significant difference in the number of viable plague bacteria in the regional lymph nodes of surviving animals (1.2×10^7 CFU CO92 versus 1.0×10^2 CFU TD1; $P = 0.67$) (Fig. 6*D*). Moreover, no difference in antibody titers against LcrV or capsular fraction 1 (F1), the predominant plague antigen, was detectable in serum from *Y. pestis* CO92- and TD1-infected animals (Fig. 6*E* and *F*). Together these data indicate that a single amino acid substitution ($Cys^{273}Ala$) associated with loss of LcrV glutathionylation increases the survival of bubonic plague-infected rats.

Serine Substitution at LcrV Residue 273

The plague pathogen evolved in the rodent population of China (Achtman et al. 1999), where isolates are still scattered over multiple phylogenetic branches (Morelli et al. 2010; Bos et al. 2012). The pCD1-encoded type III secretion machine and its *lcrV* gene are conserved among all members of this clade, albeit that a polymorphism substituting LcrV $Cys^{273}Ser$ is found in some isolates of the *Y. pestis* biovar *microtus*, which does not cause plague in humans (Zhou et al. 2004), and in the *Y. pestis* biovar *pestoides* Angola isolate (Chain et al. 2006) (Fig. 7*A*). A previous study reported that the $lcrV_{C273S}$ polymorphism impacts the oligomerization of LcrV and represents one out of four highly variable regions of LcrV that are unique to nonepidemic strains of *Y. pestis* (Anisimov et al. 2010). Since the $lcrV_{C273A}$ mutation was associated with attenuated virulence in animal models of bubonic plague, we asked whether the $lcrV_{C273S}$ mutation causes a similar phenotype when introduced into modern plague strains. The codon substitution $Cys^{273}Ser$ was introduced into the *lcrV* alleles of *Y. pestis* KIM D27 and *Y. pestis* CO92 to generate *Y. pestis* AM15 Δ*pgm* $lcrV_{C273S}$ and *Y. pestis* DE1 pgm^{+} $lcrV_{C273S}$, respectively. *Y. pestis* KIM D27 *lcrV* and AM15 $lcrV_{C273S}$ catalyzed type III secretion of YopE and LcrV into the extracellular medium at similar rates (Fig. 7*B* and *C*). LcrV secreted by *Y. pestis* AM15 was not retained during GST-Sepharose affinity chromatography, suggesting that Ser^{273} was not modified with glutathione (Fig. 7*D*). To validate this conjecture, $LcrV_{S228\,C273S}$ was affinity purified from the culture supernatant of *Y. pestis* KLD29 Δ*lcrV*(pAM199) (Fig. 7*E*). When analyzed by matrix-assisted laser desorption ionization–time of flight mass spectrometry (MALDI-TOF MS) along with recombinant $rLcrV_{S228\,C273S}$ purified from *E. coli* DH5α(pAM199) lysates, we observed *m*/*z* 38,261.34 for $LcrV_{S228\,C273S}$ and *m*/*z* 38,286.09 for $rLcrV_{S228\,C273S}$ (Fig. 7*E* and Table 4). These measurements approximate the calculated mass for unmodified $LcrV_{S228\,C273S}$ (38,264.16 Da),

suggesting that $LcrV_{S228\,C273S}$ is not posttranslationally modified with glutathione (Table 4). Following infection of human neutrophils, *Y. pestis* AM15(pYopM-Bla), compared to *Y. pestis* KIM D27(pYopM-Bla), caused a small but statistically insignificant increase in the conversion of CCF2-AM fluorophore to the YopM-Bla-cleaved chromophore (blue) (Fig. 7*F* and *G*). *Y. pestis* CO92 *lcrV* and *Y. pestis* DE1 $lcrV_{C273S}$ exported type III effectors into the extracellular milieu at similar levels (Fig. 7*H* and *I*). When analyzed in a mouse model of bubonic plague following subcutaneous inoculation of 20 CFU, all *Y. pestis* CO92- or DE1-infected animals succumbed to lethal plague disease. Similar to mice infected with *Y. pestis* TD1 $lcrV_{C273A}$, *Y. pestis* DE1 $lcrV_{C273S}$ infection caused a delay in time to death (Fig. 7*J*). Taken together, these data suggest that the codon 273 polymorphism ($lcrV_{C273S}$) observed in *Y. pestis* biovar *pestoides* and *microtus* isolates (Anisimov et al. 2010) prevents LcrV glutathionylation and affects bubonic plague pathogenesis.

Decreased LcrV-RPS3 Association Is Correlated with Increased Macrophage Apoptosis and Diminished Cytokine Release

Earlier work demonstrated that YopJ, a type III effector injected into host immune cells, functions as an acetyltransferase that inhibits NF-κB and mitogen-activated protein kinase (MAPK) signaling, triggers caspase-1 activation and interleukin-1β (IL-1β) and IL-18 secretion, and also promotes target cell death in *Y. pestis*-infected macrophages (Mukherjee et al. 2006; Zheng et al. 2011). Furthermore, *yopJ* has been shown to be dispensable for bubonic plague pathogenesis in *Y. pestis*-infected Brown Norway rats (Lemaître et al. 2006). Since loss of LcrV glutathionylation attenuated plague pathogenesis, we asked whether *yopJ* was required for or contributed to increased cytotoxicity *in vitro* by generating an in-frame *yopJ* deletion strain by allelic exchange with *Y. pestis* AM6. Significantly, the $lcrV_{C273A}$-mediated increase in macrophage

cell death during *Y. pestis* infection did not require *yopJ*, as *Y. pestis* AM29 *lcrV*$_{C273A}$ Δ*yopJ* also promoted increased macrophage cytotoxicity compared with *Y. pestis* KIM D27 (Fig. 8*A* and Fig. 9*A*).

To investigate the molecular mechanism for LcrV-mediated killing of immune cells, we purified LcrV$_{S228}$ via affinity chromatography from *Y. pestis*-infected J774.A1 macrophages and used mass spectrometry to identify proteins separated by Coomassie-stained SDS-PAGE (Fig. 8*B* and Table 3). Infection of macrophages with *Y. pestis* KLD29 expressing LcrV$_{S228}$ (pKG48), but not with *Y. pestis* KLD29 expressing wild-type LcrV (pNM77), led to purification of LcrV$_{S228}$ and ribosomal protein S3 (RPS3), a component of the eukaryotic 40S ribosomal subunit and a regulator of DNA repair, apoptosis, and innate immune responses (Gao and Hardwidge 2011) (Fig. 8*B* and *C* and Table 3). Strikingly, analysis of J774.A1 macrophages infected with *Y. pestis* KLD29 expressing LcrV$_{S228\ C273A}$ (pAM128) revealed that copurification of RPS3 with LcrV$_{S228\ C273A}$ was diminished (Fig. 8*C* and *D*). Earlier work has shown that pathogenic *E. coli* effectors, injected into immune cells by type III secretion machines, target RPS3 to inhibit host immune defenses by modulating RPS3/NF-*κ*B-mediated signaling and proinflammatory responses (Gao and Hardwidge 2011; Wan et al. 2011; Hodgson et al. 2015). We wondered whether the differential association between RPS3 and LcrV variants that was observed for *Y. pestis*-infected macrophages influences host inflammatory responses. The impact of LcrV glutathionylation on host inflammatory responses in *Y. pestis*-infected J774.A1 macrophages undergoing apoptotic or pyroptotic cell death was assessed by quantifying the caspase 1/11-induced cytokines IL-1β and IL-18 (LaRock and Cookson 2012). Compared to *Y. pestis* KLD29 expressing wild-type LcrV (pNM77) or LcrV$_{S228}$ (pKG48), *Y. pestis* KLD29 expressing LcrV$_{S228\ C273A}$ (pAM128) caused a significant increase in nonpyroptotic cell death of J774.A1 macrophages, as suggested by reduced

levels of IL-1β and IL-18 cytokine release (Fig. 8*E* and *F*). Thus, the association of LcrV with RPS3 may be involved in regulating macrophage cell death during *Y. pestis* infection and, reciprocally, perturbation of the RPS3 association with LcrV in *Y. pestis*-infected macrophages may be responsible for the decrease in disease severity as well as the increase in apoptotic cell death observed for the $lcrV_{C273A}$ variants (Fig. 3*F*, Fig. 5*A* and *B*, and Fig. 8*D*).

LcrV Is Modified via Disulfide Formation with Extracellular Glutathione

In *E. coli*, a Gram-negative enterobacterium and relative of *Y. pestis*, the tripeptide glutathione (γ-glutamyl-cysteinyl-glycine [GSH]) can be synthesized through two pathways. The *de novo* GSH biosynthetic pathway is a two-step process catalyzed by the ATP-dependent enzymes γ-glutamylcysteine synthetase (GshA) and glutathione synthetase (GshB), whereby glutamate (Glu [E]) and cysteine (Cys [C]) are first ligated by GshA to form γ-glutamylcysteine (γ-EC), which is then conjugated to glycine by GshB to generate GSH (Hopkins 1921; Quastel, Stewart, and Tunnicliffe 1923) (Fig. 10*A*). An alternate pathway for GSH synthesis was characterized in a Δ*gshA* mutant strain of *E. coli* and involves the first enzyme of the proline biosynthetic pathway, γ-glutamyl kinase (ProB), catalyzing the conversion of glutamate to γ-glutamyl phosphate, which in a condensation reaction with cysteine, generates γ-glutamylcysteine that is subsequently ligated to glycine by GshB to form GSH (Veeravalli et al. 2011) (Fig. 10*A*). Glutathione is oxidized at its sulfhydryl to generate glutathione disulfide (GSSG), which, in turn, is reduced by the NADPH-dependent enzyme glutathione reductase (Gor) in order to maintain a high GSH/GSSG ratio in the bacterial cytoplasm (Rall and Lehninger 1952) (Fig. 10*A*).

We asked whether LcrV glutathionylation occurs in the *Y. pestis* cytoplasm via thiol-disulfide exchange with GSSG or a mixed disulfide prior to its secretion and capping of the type

III needle complex. As GshB is required for both the *de novo* and compensatory pathways of GSH synthesis, we generated an in-frame Δ*gshB* deletion strain by allelic exchange with *Y. pestis* KLD29. We hypothesized that Δ*gshB* mutant *Y. pestis* would be unable to synthesize glutathione and thereby preclude cytoplasmic, but not extracellular, glutathionylation of LcrV. When analyzed for type III secretion in Luria-Bertani (LB) broth, a rich medium that contains glutathione (Fig. 9*B*), *Y. pestis* KLD29 Δ*lcrV*(pKG48) and *Y. pestis* AM43 Δ*lcrV* Δ*gshB*(pKG48) exhibited calcium-regulated secretion of $LcrV_{S228}$ and YopE (Fig. 10*B* and Fig. 9*C*). To assess glutathionylation of LcrV secreted by *Y. pestis* during growth in LB broth, $LcrV_{S228}$ was affinity purified from *Y. pestis* KLD29(pKG48) and *Y. pestis* AM43(pKG48) and analyzed by MALDI-TOF MS to reveal *m*/*z* 38,583.10 and 38,592.16, respectively, which approximate the calculated mass for glutathionylated $LcrV_{S228}$ (38,585.54 Da) (Fig. 10*C* and Table 4). Compared to the *m*/*z* of $rLcrV_{S228}$ purified from *E. coli* DH5α(pKG48) grown in LB broth (38,271.66), these data suggest that $LcrV_{S228}$ secreted by Δ*gshB* mutant *Y. pestis* is glutathionylated. Confirming this result, DTT treatment collapsed the measured masses of *Y. pestis* $LcrV_{S228}$ to match the mass of $rLcrV_{S228}$, which was unaffected by DTT treatment (Table 4). These data establish that $LcrV_{S228}$ secreted by Δ*gshB* mutant *Y. pestis* during growth in LB broth is modified with glutathione.

Following growth at 37°C in thoroughly modified Higuchi's (TMH) medium, a chemically defined minimal medium that lacks glutathione (Fig. 9*B*), *Y. pestis* KLD29(pKG48) and *Y. pestis* AM43(pKG48) exhibited calcium-regulated export of $LcrV_{S228}$ and YopE at similar rates (Fig. 10*D* and Fig. 9*D*). To investigate whether the Δ*gshB* mutation was sufficient to abolish bacterial glutathione synthesis, *Y. pestis* KLD29 and AM43 were propagated to stationary phase in TMH medium, and nonprotein thiols were acid extracted, reduced by treatment with tris(2-carboxyethyl)phosphine (TCEP), derivatized with the thiol-specific reagent

monobromobimane (mBBr), and analyzed by high-performance liquid chromatography (HPLC) for the total abundance of cysteine, glutathione, and γ-glutamylcysteine in cell extracts. Compared to *Y. pestis* KLD29, the HPLC chromatogram of *Y. pestis* AM43 revealed an undetectable level of glutathione alongside a significant accumulation of its biosynthetic precursor, γ-glutamylcysteine (Fig. 10*E*). We infer from these data two conclusions. First, the glutathionylation of LcrV occurs after the protein is exported from the *Y. pestis* cytoplasm to cap the type III needle complex, and second, the molecular mechanism underpinning LcrV glutathionylation is thiol-disulfide exchange with oxidized glutathione in the extracellular milieu.

Glutathione Promotes *Y. pestis* Growth in Mammalian Blood and Heat-Inactivated Serum

The survival of *Y. pestis* in the blood of its mammalian host—as occurs during its initial trafficking from the site of fleabite inoculation to the regional lymph node and, more significantly, during its systemic hematogenous dissemination to colonize distal host tissues—is essential for bubonic plague pathogenesis (Sebbane et al. 2005). Recent studies of pathogenic bacteria identified mutations that, either by abolishing *de novo* glutathione synthesis or abrogating bacterial import of host-derived glutathione, result in attenuated virulence in animal models of infection and/or impaired survival in vertebrate blood (Loi, Rossius, and Antelmann 2015). Glutathione has also been shown to play a significant role in bacterial pathogenesis by functioning as a thiol redox buffer that enables blood-borne pathogens to rapidly acclimate to the high osmolality and oxidative stresses inherent to animal blood (Song et al. 2013). For these reasons, we investigated whether the $lcrV_{C273A}$ and Δ*gshB* mutations impact *Y. pestis* survival in defibrinated sheep blood by enumerating the mean fold change in viable CFU following 18 h of growth at 37°C. Unlike *Y. pestis* KIM D27 *lcrV* (1,034-fold increase in CFU), *Y. pestis* KLD29 Δ*lcrV* (954-fold increase),

or *Y. pestis* AM6 *lcrV*$_{C273A}$ (636-fold increase), the CFU of *Y. pestis* AM43 Δ*lcrV* Δ*gshB* increased only 216-fold (Fig. 10*F*). Animal blood contains immune cells and factors facilitating complement-mediated cell lysis. To determine whether these antimicrobial properties of blood account for the diminished replication of Δ*gshB* mutants, *Y. pestis* survival was assayed in heat-inactivated sheep serum. Compared to the increase in viable CFU observed for *Y. pestis* KIM D27 (980-fold), *Y. pestis* KLD29 (832-fold), and *Y. pestis* AM6 (342-fold) following 18 h of growth at 37°C, growth in heat-inactivated sheep serum was diminished for *Y. pestis* AM43 (64-fold increase in CFU) (Fig. 10*F*). This result suggests that neither immune cells nor the complement system of defibrinated sheep blood is responsible for the observed growth defects of *lcrV*$_{C273A}$ or Δ*gshB* variant *Y. pestis* strains. As Δ*gshB* mutant *Y. pestis* exhibited a pronounced growth defect in both blood and heat-inactivated serum, we presume that the Δ*gshB* mutation may also attenuate the pathogenesis of *Y. pestis* in animal models of bubonic plague.

DISCUSSION

Although *Y. pestis* LcrV has been the subject of intensive study for decades, a complete understanding of its multifaceted contributions to plague pathogenesis continues to evolve. Here we demonstrate that LcrV is modified by host-derived glutathione following its export to the tip of the type III secretion machine. LcrV glutathionylation moderates the rate of *Y. pestis* type III effector injection into immune cells and enhances *Y. pestis* virulence in mouse and rat models of bubonic plague. We arrived at these conclusions when comparing the phenotypes of wild-type (Cys^{273}) and *lcrV* mutant (Ala^{273}) strains, where the amino acid side chains of LcrV residue 273 both display hydrophobic properties (methylene-sulfhydryl in cysteine and methyl in alanine); however, alanine, in contrast to cysteine, cannot be glutathionylated. On the other hand, the

lcrV Ser^{273} mutant, in which the methylene-hydroxyl side chain at residue 273 exerts a polar character, displayed weaker phenotypes in both *Y. pestis* type III injection and plague virulence assays. We presume that the side chain of LcrV residue 273 occupies a critical position that may directly affect the type III injection of *Y. pestis* effectors. LcrV glutathionylation promotes also the association of LcrV with host RPS3 and suppresses the apoptotic killing of *Y. pestis*-infected macrophages. We think it is likely that the abundance of glutathione and the strong oxidizing environment in mammalian blood promote Cys^{273} glutathionylation. It is, however, not clear whether LcrV glutathionylation is impacted during *Y. pestis* type III injection of effectors into immune cells, as the disulfide of LcrV glutathione may be exposed to the reducing environment of the host cell cytoplasm. LcrV glutathionylation promotes necroptotic cell death and IL-1β and IL-18 secretion, triggering inflammatory responses to plague infection that presumably enable *Y. pestis* to rapidly kill large numbers of immune cells via the type III mechanism or to disseminate with immune cells through host tissues. These activities of glutathionylated LcrV are correlated with its association with RPS3, a protein that resides in the cytoplasm of host cells. We presume that LcrV may gain access to RPS3 via the *Y. pestis* type III mechanism; however, the molecular details for these events are not known. In the absence of LcrV glutathionylation, *Y. pestis* injects larger amounts of effectors into immune cells, an alteration that is associated with increased apoptotic cell death and diminished secretion of IL-1β and IL-18. This reduction in host inflammatory responses may delay *Y. pestis* type III-mediated killing of immune cells and the distribution of plague bacteria in host tissues, thereby attenuating *Y. pestis* virulence in animal models of plague pathogenesis. Intriguingly, the site of LcrV glutathionylation is located in a domain that is also known to modulate host immune responses by stimulating IL-10 release (Overheim et al. 2005). To the best of our knowledge, LcrV glutathionylation represents the first

report of a bacterial secreted virulence factor that is modified by glutathione. We wondered whether other virulence factors, whether secreted by *Y. pestis* or other bacterial pathogens, may likewise be modified by host-derived glutathione and contribute to the pathogenesis of infectious diseases. The *lcrV* genes of two related pathogens, *Yersinia pseudotuberculosis* and *Yersinia enterocolitica*, also carry a cysteine codon at position 273. In contrast, the genes for needle cap proteins in the type III pathways of many other bacterial pathogens are not endowed with cysteine codons. Thus, glutathionylation of the type III secretion needle cap protein may be unique to *Yersinia* spp. and not a universal attribute of pathogenic bacteria.

MATERIALS AND METHODS

Ethical Conduct

Experiments with blood from human volunteers were performed with protocols that had been reviewed, approved, and supervised by the University of Chicago's Institutional Review Board (IRB). Animal research was performed in accordance with institutional guidelines following experimental protocol review, approval, and supervision by the Institutional Biosafety Committee and the Institutional Animal Care and Use Committee at the University of Chicago to ensure ethical conduct and humane treatment of experimental animals.

Biosafety, Biosecurity, and Personnel Reliability

Experiments with *Y. pestis* were performed in biosafety level 3 (BSL-3)/animal BSL-3 (ABSL-3) containment at the Howard Taylor Ricketts Laboratory (HTRL), a facility in which all University of Chicago select agent research is conducted. The University of Chicago Select Agent Program is approved and routinely inspected by both the Institutional Biosafety Committee and

Centers for Disease Control and Prevention (CDC) officials. All entry and exit activities to the HTRL are access controlled, with its BSL-3 and ABSL-3 facilities protected by multiple layers of control. Personnel wear personal protective equipment and powered air-purifying respirators for high efficiency particulate air (HEPA) filtration of breathing air. Experimental work with *Y. pestis* and plague-infected animals is performed in class II biosafety cabinets within BSL-3/ABSL-3 laboratories. Personnel working with *Y. pestis* are enrolled in the University of Chicago Tier 1 Select Agent Personnel Reliability Program. These staff members have received Federal Select Agent security clearance, have passed the required University of Chicago background and reference checks, and are subject to ongoing suitability assessments. All University of Chicago Select Agent research staff signed a *Select Agent Code of Conduct* and received pre-access laboratory training for work with *Y. pestis*; furthermore, annual refresher training in biosafety, biosecurity, biosurety as well as blood-borne pathogens and chemical hygiene are mandatory for personnel working with virulent *Y. pestis*. HTRL staff and Responsible Officials sustain emergency response plans and conduct annual drills involving emergency first responders to minimize biological risks and ensure personnel safety. Pathogens are stored in locked containment under constant security monitoring. The HTRL is in compliance with federal regulations for work on Tier 1 Select Agents and meets or exceeds the standards outlined in *Biosafety in Microbiological and Biomedical Laboratories* (Chosewood and Wilson 2009).

Dual-Use Research of Concern

This manuscript was analyzed for dual-use research of concern (DURC): i.e., the description of mutations that may increase the virulence of natural isolates of *Y. pestis* or affect their ability to cause fulminant plague or epizootic outbreaks in rats or other host species. The

analysis was reviewed by the University of Chicago's Institutional Biosafety Committee DURC Task Force (DTF). DTF agreed with the investigators' assessment that the findings presented in this manuscript do not present DURC potential in that the mutations characterized herein actually attenuate *Y. pestis* virulence. Specifically, the data presented shows that, in *Y. pestis*, mutations precluding the posttranslational modification (glutathionylation of Cys^{273}) of LcrV—the cap protein of type III secretion needles and plague protective antigen—attenuate bacterial pathogenesis *in vivo*. The DURC analyses were also reviewed by the funding agency, the National Institute of Allergy and Infectious Diseases, which approved the manuscript for publication.

Bacterial Strains, Plasmids, and Growth Conditions

The strains and plasmids used in this study are listed in Table 5. *Y. pestis* KIM D27 (Δ*pgm*) is a non-pigmented variant attenuated for plague pathogenesis (Brubaker 1969), and *Y. pestis* CO92 (pgm^+) is a fully virulent plague isolate representative of the currently disseminating American clone (Doll et al. 1994). Overnight cultures of *Y. pestis* KIM D27 and its derivatives, as well as *Y. pestis* CO92 and its derivatives, were propagated at 26°C in heart infusion broth (HIB), M9-Casamino Acids (M9-Ca) minimal medium, or thoroughly modified Higuchi's (TMH) medium, as described previously (Brubaker 1969; Higuchi 1970; DeBord et al. 2006; Ligtenberg et al. 2013). To propagate bacteria on solid medium, *Y. pestis* KIM strains and *Y. pestis* CO92 strains were incubated at 26°C on heart infusion agar (HIA) or HIA supplemented with 0.01% Congo Red, respectively. The *E. coli* strains DH5α and S17-1 were propagated at 37°C in Luria-Bertani (LB) broth or agar. When necessary, the growth medium was supplemented with ampicillin (100 μg/ml), kanamycin (50 μg/ml), or chloramphenicol (20 μg/ml) for plasmid

maintenance. Standard methods for transformation of plasmids into *E. coli* and *Y. pestis* were employed.

Strain and Plasmid Construction

The primers used in this study are listed in Table 6. The *Y. pestis* KIM D27 derivative KLD29 (Δ*lcrV*) (Marketon et al. 2005) and the *Y. pestis* CO92 derivative LQ1 (Δ*lcrV*) (Quenee et al. 2008) have been described previously. The $lcrV_{C273A}$ mutant strains, AM6 and TD1, were generated via allelic exchange in *Y. pestis* KIM D27 and *Y. pestis* CO92, respectively. Using primers P141 for and P141 rev, the pCD1 virulence plasmid of *Y. pestis* KIM D27 served as the template for PCR amplification of a 2-kb fragment centered at codon $lcrV_{C273}$. The resulting PCR product and the suicide vector pLC28 (Cheng, Anderson, and Schneewind 1997) were each digested with XbaI and BamHI and then ligated together to generate the recombinant plasmid, pLC28-lcrV$_{C273}$, which was transformed into *E. coli* mating strain S17.1 λpir^{+} (de Lorenzo et al. 1993). The QuikChange Lightning site-directed mutagenesis kit (Agilent) was used to introduce the codon substitution LcrV Cys^{273}Ala into pLC28-lcrV$_{C273}$ using the primers P140 for and P140 rev. The resulting plasmid, pAM105, was transformed into *Y. pestis* KIM D27, single-crossover events were selected by plating bacteria on HIA supplemented with 20 μg/ml chloramphenicol, and resolution of replication-defective plasmid cointegrates was achieved by streaking bacteria on HIA supplemented with 5% sucrose as counter-selection for *sacB* (Blomfield et al. 1991). PCR and DNA sequencing of chloramphenicol-sensitive and sucrose-resistant colonies was used to confirm the generation of *Y. pestis* AM6 ($lcrV_{C273A}$). To construct *Y. pestis* strain TD1, pAM105 served as a template for PCR amplification of its 2-kb insert containing the desired $lcrV_{C273A}$ substitution using the primers P142 for and P142 rev. The resulting PCR product

and the suicide vector pCVD442 (Donnenberg and Kaper 1991) were each digested with SacI and SalI and then ligated together to generate the recombinant plasmid, pCVD442-lcrV$_{C273A}$. After pCVD442-lcrV$_{C273A}$ was electroporated into *Y. pestis* CO92, single-crossover events were selected by plating bacteria on HIA supplemented with 50 μg/ml ampicillin, with resolution of replication-defective plasmid cointegrates achieved by streaking bacteria on HIA supplemented with 5% sucrose. Ampicillin-sensitive and sucrose-resistant colonies were screened by PCR and DNA sequencing to confirm the generation of *Y. pestis* TD1 (*lcrV$_{C273A}$*). A similar genetic approach was used to generate the *lcrV$_{C273S}$* variant *Y. pestis* strains. Briefly, the codon substitution LcrV Cys^{273}Ser was introduced into pCVD442-lcrV$_{C273A}$ by site-directed mutagenesis using the primers P190 for and P190 rev. The resulting plasmid, pAM155, was transformed into *Y. pestis* KIM D27 and *Y. pestis* CO92, and application of the allelic exchange procedure led to the generation of *Y. pestis* strains AM15 (*lcrV$_{C273S}$*) and DE1 (*lcrV$_{C273S}$*), respectfully.

An in-frame deletion of *yopJ* was introduced by allelic exchange into *Y. pestis* KIM D27 and *Y. pestis* AM6, resulting in strains AM27 and AM29, respectively. Using the pCD1 virulence plasmid as template, a 1.3-kb fragment upstream of *yopJ* was PCR amplified using the primers P227 for and P227 rev, and a 1.5-kb fragment downstream of *yopJ* was PCR amplified using the primers P228 for and P228 rev. The resulting upstream and downstream PCR fragments were double-digested with SacI and HindIII or HindIII and SalI, respectively, and inserted into pCVD442, which had been previously digested with SacI and SalI, to generate the recombinant plasmid, pAM178. Following the electroporation of pAM178 into *Y. pestis* KIM D27 and AM6, the allelic exchange approach was employed as before to generate *Y. pestis* strains AM27 (Δ*yopJ*) and AM29 (*lcrV$_{C273A}$*, Δ*yopJ*), respectively.

A clean deletion of *gshB* was engineered in *Y. pestis* KLD29 via allelic exchange. Using genomic DNA isolated from *Y. pestis* KIM D27 as template, a 1.5-kb fragment upstream of *gshB* was PCR amplified using the primers P296 for and P296 rev, and a 1.3-kb fragment downstream of *gshB* was PCR amplified using the primers P297 for and P297 rev. After digesting the upstream PCR fragment with SacI and BamHI, the downstream PCR fragment with BamHI and SalI, and pCVD442 with SacI and SalI, the restriction enzyme-digested inserts and vector were combined in a triple-ligation reaction. The resulting plasmid, pAM196, was electroporated into *Y. pestis* KLD29, and the allelic exchange approach was used to generate *Y. pestis* AM43 (Δ*lcrV*, Δ*gshB*).

The plasmids pNM77 (wild-type *lcrV*) (Miller et al. 2012), pKG48 ($lcrV_{S228}$) (Ligtenberg et al. 2013), and pYopM-Bla (pMM83) and pGST-Bla (pMM91) (Marketon et al. 2005) have been described previously. For the construction of plasmid pAM128 ($lcrV_{S228\ C273A}$), the Cys^{273}Ala codon substitution was introduced by PCR mutagenesis into the $lcrV_{S228}$ allele carried by pKG48 using the primers P140 for and P140 rev. The same site-directed mutagenesis approach was employed to generate plasmid pAM199 ($lcrV_{S228\ C273S}$) using the primers P190 for and P190 rev. All plasmid constructs were verified by PCR and DNA sequencing.

Genome Sequencing and Analysis of *Y. pestis* Strains

Genomic DNA was extracted from *Y. pestis* strains CO92 *lcrV*, TD1 $lcrV_{C273A}$, and DE1 $lcrV_{C273S}$ using the Wizard Genomic DNA purification kit (Promega). The Next Generation Sequencing Core at Argonne National Laboratory (Lemont, IL) used the extracted genomic DNA to generate TruSeq libraries (average insert size, 400 to 500 bp) that were sequenced on an Illumina MISeq System (250 by 250 bp, paired-end reads). The FASTQ formatted files of raw genomic sequencing data were analyzed with Geneious R9.0 (www.geneious.com, Biomatters Ltd.,

Auckland, New Zealand) (Kearse et al. 2012). The sequencing reads of each *Y. pestis* strain were trimmed for quality using the "Trim Ends" feature with the following parameters: 5% error probability limit; Q >30; and trim 5′ and 3′ ends. The trimmed reads were paired and then mapped to the NCBI Reference Sequences for *Y. pestis* CO92 (RefSeq: NC_003143.1, NC_003131.1, NC_003134.1, and NC_003132.1), using the Geneious Reference Assembler's "Custom Sensitivity" option to run 5 iterations with the following parameters: 2% maximum mismatches; 1% allowed gaps per read (maximum size of 3); 50 bp minimum overlap (95% overlap identity); word length of 18 (ignore words repeated >12 times); and a maximum ambiguity of 4. The assembled genomes of *Y. pestis* CO92, TD1, and DE1 were analyzed for single nucleotide polymorphisms (SNPs), insertions/deletions (InDels), and structural variations using the "Find Variations/SNPs" feature with the following parameters: Coverage >5 and Variant Frequency >70%. Compared with *Y. pestis* CO92, *Y. pestis* TD1 and *Y. pestis* DE1 carried the $lcrV_{C273A}$ and $lcrV_{C273S}$ mutations, respectively, without additional mutations affecting the coding sequence of proteins.

Purification of LcrV$_{S228}$ from *Y. pestis* and *E. coli*

To purify LcrV$_{S228}$ secreted by *Y. pestis* KLD29(pKG48), overnight cultures were diluted 1:20 into 4 liters of HIB, grown for 2 h at 26°C, supplemented with 5 mM $CaCl_2$ and 1 mM isopropyl-β-D-thiogalactopyranoside (IPTG), and propagated at 37°C for 3 h. Bacteria were sedimented by centrifugation at 8,500 × *g* for 7 min, and the supernatant was filtered through a 0.22-μm-pore membrane (Millipore). Proteins were precipitated with 60% ammonium sulfate and overnight incubation at 4°C. Protein precipitate was sedimented by centrifugation at 12,500 × *g* for 15 min, suspended in 16 ml of column buffer (150 mM NaCl, 50 mM Tris-HCl [pH 7.0]),

dialyzed twice against 4 liters of column buffer using SpectroPore Dialysis Membrane (molecular weight cutoff [MWCO], 6,000 to 8,000), and subjected to affinity chromatography using 2 ml of preequilibrated 50% (vol/vol) Strep-Tactin–Sepharose (IBA BioTAGnology). The column was washed four times with 15 ml of column buffer, and bound proteins were eluted in four 1-ml fractions with 2.5 mM desthiobiotin in column buffer.

Recombinant $LcrV_{S228}$ ($rLcrV_{S228}$) was purified from cell extracts of *E. coli* DH5α (Hanahan 1983) as previously described (Ligtenberg et al. 2013). In brief, overnight *E. coli* DH5α(pKG48) cultures were diluted 1:20 into 1 liter of LB broth, grown for 2 h at 37°C, supplemented with 1 mM IPTG, and propagated at 37°C for 3 h. Bacteria were sedimented at 8,500 × *g* for 7 min, suspended in 20 ml of column buffer, and stored overnight at −20°C. The bacterial cells were thawed on the following day and lysed in a French press at 15,000 lb/in^2. The crude lysate was centrifuged at 30,000 × *g* for 30 min, and the supernatant was subjected to Strep-Tactin–Sepharose affinity chromatography, as described above.

To analyze $LcrV_{S228}$ purified from *Y. pestis* and *E. coli*, eluate fractions were examined by Coomassie-stained SDS-PAGE. Samples were also subjected to native PAGE, electrotransferred to polyvinylidene difluoride (PVDF) membranes, and immunoblotted with anti-GSH antibodies (Virogen). For Edman degradation, *Y. pestis* $LcrV_{S228}$ was separated by SDS-PAGE, electrotransferred to a PVDF membrane, and detected by Coomassie staining. After washing the Coomassie-stained PVDF membrane with HPLC-grade H_2O, the protein band corresponding to $LcrV_{S228}$ was carefully excised using a clean scalpel. Edman degradation was performed by Alphalyse, Inc. (Palo Alto, CA) using an ABI Procise 494 sequencer.

Mass Spectrometry

Combined liquid chromatography-electrospray ionization mass spectrometry with fraction collection (LC-ESI-MS^+) was used to analyze $LcrV_{S228}$ purified from *Y. pestis* culture supernatants and *E. coli* cell extracts. Sample volumes—typically 400 to 1,000 μl, each containing 0.4 to 0.6 mg protein/ml in 50 mM Tris-HCl (pH 7.0)–150 mM NaCl buffer—were dried in a vacuum concentrator and redissolved in water (250 to 1,000 μl), and aliquots (typically 250 μl) were loaded onto a polymeric reverse-phase column (Agilent PLRP-S; 300-Å pore size, 5-μm particle size, 2.1- by 150-mm), equilibrated in solvent A (water-formic acid, 100/0.1 [vol/vol]), and eluted (100 μl/min) with a linearly increasing concentration of solvent B (acetonitrile-isopropanol-formic acid, 50/50/0.1 [vol/vol/vol]: min/% B, 0/5, 5/5, 45/90, 50/5, and 60/5). The column effluent was passed through a stream splitter, with a proportion (approximately 50%) directed to a fraction collector (1 min/fraction) and the remainder to an Ionspray source connected to a triple-quadrupole mass spectrometer (ABI Sciex API III^+) scanning in the positive-ion MS mode from *m/z* 500 to 1,850 (step size, 0.3 Da; dwell, 1 ms; 4.82 s/scan; orifice, 90 V). Multiple injections of the same samples were collected into the same fraction collector tubes. For disulfide reduction, protein samples were treated with 6 M guanidine-HCl containing 300 mM dithiothreitol (DTT) for 60 min at room temperature prior to injection onto the liquid chromatograph. Data were collected using software supplied by the instrument's manufacturer (Tune 2.5-FPU) and were interrogated using MacSpec (version 3.3) for molecular mass calculations from multiply charged ion clusters and BioMultiView (version 1.3.1) for display of the deconvoluted spectra. Protein and peptide molecular weight calculations from known amino acid sequences were made online with ExPASy (http://www.expasy.org/proteomics) using the Compute Pi/MW subroutine.

For trypsin digestion, proteins of interest were pooled in preweighed glass test tubes and taken to dryness in a vacuum concentrator. An estimation of the protein content of each dried sample was made from the increased mass of the tube after drying. Dried samples were dissolved in 50 mM ammonium bicarbonate, and aliquots (4.34 nmol) were treated with sequencing-grade trypsin (Promega [50 pmol]) in a total volume of 150 µl of 50 mM ammonium bicarbonate at 37°C for 15 h.

The tryptic digests were processed by LC-ESI-MS^+ as described above, with minor modifications. Specifically, aliquots (100 µl) were injected onto the same polymeric reverse-phase column (Agilent PLRP-S; 300-Å pore size, 5-µm particle size, 2.1- by 150-mm), equilibrated in solvent C (water-formic acid-trifluoroacetic acid, 100/0.05/0.05 [vol/vol/vol]), and eluted (100 µl/min) with a linearly increasing concentration of solvent D (acetonitrile-formic acid-trifluoroacetic acid, 100/0.05/0.05 [vol/vol/vol]: min/% D, 0/5, 5/5, 45/90, 50/5, and 60/5). The column effluent was passed through a stream splitter, with a proportion (approximately 50%) directed to a fraction collector (1 min/fraction) and the remainder to an Ionspray source connected to a triple-quadrupole mass spectrometer (ABI Sciex API III^+) scanning in the positive-ion MS mode from *m/z* 500 to 1,850 (step size, 0.3 Da; dwell, 1 ms; 4.82 s/scan; orifice, 70 V). Multiple injections of the same samples were collected into the same fraction collector tubes. Data were collected using software supplied by the instrument's manufacturer (Tune 2.5-FPU) and interrogated using MacSpec (version 3.3) for molecular mass calculations from multiply charged ion clusters. Predicted tryptic maps from known amino acid sequences were made online with ExPASy (http://www.expasy.org/proteomics) using the PeptideMass subroutine.

The tryptic digests were also processed by high resolution mass spectrometry. Aliquots (2 to 10 µl) were injected onto a Phenomenex Kinetex C_{18} column (100-Å pore size, 1.7-µm

particle size, 150- by 2.1-mm), equilibrated in solvent A, and eluted (100 µl/min) with a linearly increasing concentration of solvent B (min/% B, 0/3, 2.5/3, 62.5/80, 65/3, and 80/3). The column effluent was directed to an Agilent Jet Stream source connected to a hybrid quadrupole time-of-flight mass spectrometer (Agilent 6550 iFunnel QTOF) scanning in the positive-ion data-dependent mode (*m/z* 200 to 2,500 for MS and *m/z* 100 to 2,000 for tandem MS [MS/MS]; 4 spectra/s; MS/MS on multiply charged precursors of intensity >/1000 counts excluded after one cycle; fragmentor, 380 V; collision energy automatically adjusted by instrument manufacturer-supplied software). Data were interrogated using MassHunter software. To reduce disulfide bonds, trypsin-digested samples were treated with 143 mM DTT in 50 mM ammonium bicarbonate at 37°C for 60 min. For the prediction of peptide fragmentation patterns (displays of b and y ions) from a known amino acid sequence, the MS-Product subroutine at Protein Prospector was used (http://prospector.ucsf.edu).

For MALDI-TOF MS analysis, Strep-tagged LcrV was purified from *Y. pestis* supernatants ($LcrV_{S228}$, $LcrV_{S228\ C273S}$) or *E. coli* extracts ($rLcrV_{S228}$, $rLcrV_{S228\ C273S}$) by Strep-Tactin–Sepharose affinity chromatography as described above, with the following modifications: (1) overnight *Y. pestis* cultures were propagated in LB broth at 26°C, and, on the following day, diluted 1:20 into 6 liters of fresh LB broth; and (2) 50 mM ammonium bicarbonate was used as the column buffer for all *Y. pestis* and *E. coli* purifications. $LcrV_{S228}$ and $LcrV_{S228\ C273S}$ purified from *Y. pestis* and *E. coli* strains were concentrated prior to analysis by matrix-assisted laser desorption ionization–time of flight mass spectrometry (MALDI-TOF MS). For each purification, eluate fractions were examined by Coomassie-stained SDS-PAGE, and selected fractions containing the protein of interest were pooled in Eppendorf tubes and taken to dryness in a vacuum concentrator at 30°C. The dried sample was washed twice with 500 µl of HPLC-grade H_2O, suspended in 30 µl

of HPLC-grade H_2O, and incubated overnight at 4°C. The concentrated sample was then stored at −20°C. Samples, either treated with DTT or left untreated, were spotted undiluted with sinapinic acid onto a MALDI plate and subjected to MALDI-TOF MS using an Autoflex Speed Bruker MALDI instrument in linear mode (10- to 60-kDa range), with myoglobin as a calibration standard (2,000 shots/s at 95% intensity). Integrated data processing software (Bruker) was used to determine the molecular weight of each sample.

GST-Sepharose Purification of LcrV Secreted by *Y. pestis*

Overnight *Y. pestis* cultures were diluted 1:20 into 60 ml of M9-Ca minimal medium, incubated at 26°C for 2 h, and then incubated at 37°C for 3 h to induce type III secretion. Bacteria were sedimented by centrifugation at 7,500 × *g* for 10 min, and 50 ml of supernatant was filtered (0.22-μm-pore membrane). Protein in the filtrate was concentrated in an Amicon Ultra-15 centrifugal device (MWCO, 10,000) by serial centrifugations at 3,000 × *g* for 10 min and then washed twice with 14 ml of GST-tag column buffer (140 mM NaCl, 40 mM phosphate buffer [pH 7.3]). After the second wash, the concentrated sample was transferred to an Eppendorf tube containing 100 μl of preequilibrated 50% (vol/vol) GST-Sepharose (Pierce); the final reaction volume was brought to 1 ml by the addition of GST-tag column buffer. Following overnight incubation at 4°C on a rotating shaker, the sample was centrifuged at 5,000 × *g* for 5 min. The supernatant was discarded, and the sedimented GST-Sepharose was washed with 1 ml of GST-tag column buffer. After four washes, the GST-Sepharose was suspended in 60 μl of 2× reducing SDS-PAGE sample buffer to elute bound proteins. Samples were boiled at 100°C for 5 min, centrifuged at 15,000 × *g* for 5 min, and analyzed by SDS-PAGE and immunoblotting with LcrV-specific antisera.

Type III Secretion and F1 Assembly Assays

Assays for *Y. pestis* type III secretion of Yops into the culture medium, as well as measurements for *Y. pestis* F1 pilus assembly, were performed as previously described (Quenee et al. 2008; Miller et al. 2012). Briefly, to monitor type III secretion of bacterial effectors during growth at 37°C in medium lacking calcium ions, *Y. pestis* overnight cultures were diluted 1:20 into 4 ml of M9-Ca minimal medium, TMH medium, or LB broth, which, as a rich medium, required supplementation with 20 mM $MgCl_2$ and 20 mM magnesium oxalate to chelate exogenous calcium ions. To assess calcium-regulated type III secretion by *Y. pestis* strains, the growth media were supplemented with 5 mM $CaCl_2$. Cultures were incubated at 26°C for 2 h and then shifted to 37°C for 3 h to induce type III secretion; when appropriate, cultures were supplemented with 1 mM IPTG prior to the temperature shift in order to induce the expression of plasmid-borne *lcrV* alleles. At the conclusion of the 37°C incubation, culture aliquots (1.4 ml) were centrifuged at 15,000 × *g* and separated into supernatant and pellet fractions. Proteins in both fractions were precipitated with 5% trichloroacetic acid (TCA), washed with ice-cold acetone, and dried overnight at room temperature. Proteins were solubilized in 2× reducing SDS-PAGE sample buffer, separated by 15% SDS-PAGE, transferred to PVDF membranes, and analyzed by immunoblotting with rabbit antibodies. Densitometric analysis was performed on triplicate type III secretion assays in order to compare the secretion of type III substrates (LcrV and YopE) between *Y. pestis* strains. The intensities of immunoreactive signals corresponding to the supernatant (S) and pellet (P) fractions were quantified by densitometry using ImageJ (version v1.51h), and the percent secretion of each type III substrate was calculated as follows: $[(S) / (S + P)] \times 100$.

To assay for F1 pilus assembly, *Y. pestis* strains were inoculated into 4 ml of HIB supplemented with 5 mM $CaCl_2$ and grown for 12 h at 37°C. Culture aliquots were centrifuged

and fractionated as described above, and samples were analyzed by SDS-PAGE and immunoblotting with rabbit antisera raised against purified recombinant F1 (Cornelius et al. 2009).

HeLa Cell Cytotoxicity Assay

HeLa cells (ATCC# CCL-2) were maintained in Dulbecco's modified Eagle's medium (DMEM) supplemented with 10% fetal bovine serum (FBS) and 1% GlutaMAX (Invitrogen) at 37°C in the presence of 5% CO_2. One day prior to *Y. pestis* infection, 10^5 HeLa cells were seeded into each well of 24-well tissue culture dishes containing 1 ml of fresh growth media. One hour prior to infection, the HeLa cell monolayers were washed once with phosphate-buffered saline (PBS) and covered with 1 ml of DMEM. Overnight *Y. pestis* cultures were diluted 1:20 into 4 ml of HIB, propagated at 26°C for 2 h, and added at a multiplicity of infection (MOI) of 10 to the HeLa cells. After 3 h of infection at 37°C with 5% CO_2, the HeLa cells were washed once with PBS and fixed overnight at 4°C with 3.7% formaldehyde in PBS. On the following day, fixation was quenched with 0.1 M glycine in PBS for 5 min at room temperature. The HeLa cells were washed once with PBS, permeabilized with 0.1% Triton X-100 in PBS for 30 min at 4°C, washed three times with PBS, and blocked for 20 min at room temperature with PBS containing 5% nonfat dried milk and 0.05% Tween-20. Filamentous actin was then labelled with 3 units (99 nM) of rhodamine-conjugated phalloidin (Invitrogen) for 20 min at room temperature in the dark. The HeLa cells were washed three times with PBS and visualized by differential interference contrast (DIC) imaging and fluorescence microscopy using an Olympus IX81 inverted microscope. Rhodamine visualization was achieved using excitation at 591 nm and emission at 608 nm (Miller et al. 2012).

Macrophage Killing Assay

Murine J774.A1 macrophages were maintained in DMEM supplemented with 10% FBS and 1% GlutaMAX at 37°C with 5% CO_2. For J774.A1 macrophage infection experiments, 10^5 cells were seeded on the day prior to infection into each well of 24-well tissue culture dishes containing 1 ml of fresh growth media. One hour prior to *Y. pestis* infection, the macrophage monolayers were washed once with PBS and covered with 1 ml of DMEM. Overnight *Y. pestis* cultures were diluted 1:20 into 4 ml of HIB, propagated at 26°C for 2 h and then at 37°C for 1 h, added at an MOI of 5 to the J774.A1 cells, and incubated at 37°C with 5% CO_2 for variable lengths of time. Following *Y. pestis* infection, the J774.A1 cells were washed once with PBS and stained with 2 μg/ml propidium iodide (Sigma) and 15 μg/ml Hoechst 33342 (Life Technologies, Inc.) for 10 min at room temperature. Macrophages were washed twice with PBS, fixed with 3.7% formaldehyde in PBS for 10 min at room temperature, washed once with PBS, and then visualized by fluorescence microscopy using an Olympus IX81 inverted microscope. All J774.A1 macrophage infections were performed in triplicate in order to compare the kinetics of *Y. pestis*-mediated macrophage killing between different bacterial strains; for each macrophage infection, the total numbers of live and dead macrophages were enumerated for three randomly selected fields of view.

***Y. pestis* Type III Injection of Human Neutrophils**

To measure *Y. pestis* translocation of Yop effectors into primary neutrophils, 40 ml of Na_2EDTA-anticoagulated venous blood drawn from healthy human volunteers was layered 1:1 (vol/vol) onto PolymorphPrep (Axis-Shield, Oslo, Norway) and centrifuged at 500 × *g* for 35 min at 20°C. The neutrophil-containing band was carefully removed, mixed 1:1 (vol/vol) with

0.5× Hank's balanced saline solution (HBSS), and centrifuged at 350 × *g* for 10 min. Sedimented neutrophils were suspended in 10 ml HBSS, centrifuged at 350 × *g* for 10 min, suspended in 2 ml of red blood cell lysis buffer (Roche), and incubated at room temperature for 2 min. Samples were centrifuged at 250 × *g* for 5 min, and neutrophils were washed in 10 ml HBSS and suspended in 2 ml of RPMI 1640 (Cellgro 10-040-CV) supplemented with 2% (vol/vol) human serum albumin (HSA). Neutrophil viability (>95%) and purity (>97%) were determined by Trypan blue exclusion and Wright/Giemsa staining, respectively, with at least 400 cells counted per assay.

Overnight *Y. pestis* cultures were diluted 1:40 into 4 ml of fresh HIB supplemented with 20 μg/ml chloramphenicol, incubated for 1.5 h at 26°C to reach the mid-exponential phase, and then incubated for 1.5 h at 37°C to induce the *Yersinia* type III secretion system. Human neutrophils were suspended in Eppendorf tubes at a density of 5.5×10^5 cells in 500 μl of growth medium (RPMI 1640 supplemented with 2% [vol/vol] HSA). Neutrophils were infected for 3 h (37°C, 5% CO_2) at an MOI of 10 with *Y. pestis* strains expressing either YopM-Bla (pMM83) or, as a negative control, GST-Bla (pMM91) in a final volume of 600 μl growth medium. At the conclusion of the infection, polymorphonuclear leukocytes (PMNs) were sedimented by centrifugation at 1,500 × *g* for 3 min and suspended in 100 μl of growth medium supplemented with 50 μg/ml kanamycin to abrogate *Y. pestis* growth and type III injection. Neutrophils were stained with 1× CCF2-AM (Invitrogen) for 1 h at room temperature in the dark. Cells were collected by centrifugation at 1,500 × *g* for 3 min, washed once with 500 μl HBSS, and suspended in 500 μl of HBSS Flow (1× HBSS, 0.5 mM EDTA, 25 mM HEPES, 2% bovine serum albumin [BSA] [pH 7.4]). Samples were kept on ice and shielded from light until flow cytometry analysis. To discriminate between live and dead cells, propidium iodide (PI) was added to each sample at a final concentration of 0.5 μg/ml immediately prior to fluorescence-activated cell sorter (FACS)

analysis. A BD FACSCanto flow cytometer (BD Biosciences, CA) was used to analyze at least 10,000 cells per sample, and data were analyzed using FlowJo (v10.0.7) and Prism 6 (GraphPad Software, Inc.). Samples were first gated with forward and side scatter for the population of singlet PMNs and subsequently gated for live cells by negative PI selection. PI-negative cells were then analyzed for blue fluorescence indicative of *Y. pestis* type III injection of YopM-Bla. Uninfected neutrophils were used to determine the background level of blue fluorescence.

Purification of LcrV$_{S228}$ from *Y. pestis*-Infected Macrophages

Murine J774.A1 macrophages were propagated to confluence in 225-cm^2 tissue culture flasks with 40 ml of DMEM supplemented with 10% FBS and 1% GlutaMAX. On the day of infection, the macrophage monolayers were washed once with PBS and covered with 40 ml of DMEM supplemented with 1 mM IPTG. Overnight *Y. pestis* p*lcrV$_{S228}$* cultures were diluted 1:20 into 20 ml of HIB and grown at 26°C for 2 h. After 1 mM IPTG supplementation, cultures were propagated at 37°C for 1 h. Bacteria were added at an MOI of 10 to the J774.A1 macrophages. After 3 h of infection at 37°C with 5% CO_2, the tissue culture media were decanted and retained for cytokine analysis; the macrophages were then collected by suspension in 20 ml of column buffer (150 mM NaCl, 50 mM Tris-HCl [pH 7.0]). Macrophage samples were freeze-thawed twice at −80°C, lysed in a French press at 15,000 lb/in^2, and centrifuged at 30,000 × *g* for 30 min. The supernatant was subjected to affinity chromatography using 2 ml of preequilibrated 50% (vol/vol) Strep-Tactin–Sepharose. The columns were washed twice with 15 ml of column buffer, and bound proteins were eluted in four 0.5-ml fractions with 5 mM desthiobiotin in column buffer.

Eluate fractions were analyzed by silver- and Coomassie-stained SDS-PAGE. Proteins copurifying with LcrV$_{S228}$ were excised from the gel and then identified by the Taplin Biological

Mass Spectrometry Facility (Harvard Medical School), which subjected each excised protein band to in-gel proteolysis and analyzed the resulting mixture of tryptic peptides by microcapillary liquid chromatography–tandem mass spectrometry (LC-MS/MS) using Orbitrap mass spectrometers (Thermo Scientific). Samples were also examined by SDS-PAGE and immunoblotting with antibodies specific for LcrV, RPS3 (Abcam, Inc.), and actin (Sigma); where indicated, the intensities of immunoreactive signals from triplicate affinity purification experiments were quantified by densitometry using ImageJ (version v1.49t).

For cytokine analysis of tissue culture media, samples were freeze-thawed twice at −80°C, centrifuged at 30,000 × *g* for 30 min to pellet insoluble material, and the supernatant was transferred to a new conical tube. Using commercially available enzyme-linked immunosorbent assay (ELISA) kits (eBioscience), the concentrations of IL-1β and IL-18 in the tissue culture media overlying *Y. pestis*-infected J774.A1 macrophages were determined according to the manufacturer's protocols.

Animal Experiments

BALB/c mice (6- to 8-week-old females) and Brown Norway rats (6-week-old females) were purchased from Charles River Laboratories, Inc. For the bubonic plague experiments in mice and rats, *Y. pestis* strains were propagated overnight in HIB at 26°C, and, on the day of infection, the bacteria were washed and diluted in sterile PBS to the required concentration. Viable CFUs were enumerated on HIA-Congo Red plates to verify the infectious dose. BALB/c mice (n = 15 or 20, as indicated) and Brown Norway rats (n = 15) were infected by subcutaneous injection into the left inguinal fold with 100 µl of a PBS suspension containing *Y. pestis* CO92, TD1, or DE1 at a dose of 20 CFU (mice) or 500 CFU (rats), as previously described (Quenee al. 2011). Plague-

infected animals were observed for morbidity and mortality over a course of 14 days. At 72 h postchallenge in rats, or when animals (mice and rats) were deemed moribund—laterally recumbent and lethargic with rapid respiration—the animals were euthanized by compressed CO_2 inhalation. At day 14 postinfection, Brown Norway rats that survived the initial challenge were euthanized as detailed above. Cardiac puncture was performed to obtain sera for analysis of IgG antibody titers. Draining lymph nodes and spleens were removed during necropsy and analyzed for bacterial load by CFU enumeration.

ELISA Analysis of IgG Antibody Titers

Immune sera obtained from Brown Norway rats was assayed by ELISA for the concentration of LcrV- and F1-specific IgG antibodies, as described previously (Overheim et al. 2005). Briefly, 96-well ELISA plates (Nunc) were coated with purified recombinant antigen (rLcrV or rF1) at 1 μg/ml in carbonate buffer and incubated overnight at 4°C. After two washes with PBST (PBS supplemented with 0.05% [vol/vol] Tween-20), the wells were blocked for 1 h at room temperature with 200 μl of blocking buffer (PBS supplemented with 1% [vol/vol] BSA) and then washed twice with PBST. Rat sera samples were serially diluted in blocking buffer, added in triplicate (100 μl per well) to the washed plates, and incubated for 2 h at room temperature. Following three washes with PBST, 100 μl of the horseradish peroxidase (HRP)-conjugated anti-rat IgG secondary antibody (diluted at 1:10,000 in blocking buffer) was added to the wells, and the plates were incubated for 1 h at room temperature. After three washes with PBST, the samples were developed using a 3,3′,5,5′-tetramethylbenzidine (TMB) substrate reagent kit (Pierce) according to the manufacturer's instructions. The absorbance at 450 nm (A_{450}) was measured using

an ELISA plate reader, and half-maximal titers were derived via determination of the 4-Parameter (4P) logistic curve using Prism 6 (GraphPad Software, Inc.).

HPLC Analysis of Thiol-mBBr Derivatives

All chemicals used in the extraction, derivatization, and analysis of low-molecular-weight (LMW) thiols by high-performance liquid chromatography (HPLC) were of the highest purity available. Diethylenetriaminepentaacetic acid (DTPA), trifluoroacetic acid (TFA), 3-[4-(2-hydroxyethyl)piperazinyl]propanesulfonic acid (HEPPS), *N*-acetylcysteine (NAC), methanesulfonic acid (MSA), glutathione, γ-glutamylcysteine, and cysteine were purchased from Sigma (St. Louis, MO). Tris(2-carboxyethyl)phosphine (TCEP), monobromobimane (mBBr), HPLC-grade acetonitrile, and HPLC-grade H_2O were purchased from Thermo Fisher Scientific (Waltham, MA).

Y. pestis strains were propagated overnight at 26°C in TMH medium, washed once and subcultured into 4 ml of fresh TMH medium at an initial optical density at 600 nm (OD_{600}) of 0.5, and then grown for 5 h at 26°C to reach the stationary phase. After transferring 1 ml of stationary-phase culture to a preweighed Eppendorf tube, *Y. pestis* cells (~200 mg) were sedimented by centrifugation at 7,500 × *g* for 5 min and washed once with 1 ml of 1× PBS. Nonprotein thiols were then acid extracted from *Y. pestis* samples using an assay adapted from the methods of previous studies (Minocha et al. 1994; Sneller et al. 2000). The washed bacterial cells were suspended in 1 ml of extraction buffer (6.3 mM DTPA, 0.1% [vol/vol] TFA) and subjected to three rounds of freeze-thawing, wherein the sample was first frozen at −20°C for 3 h and then thawed at room temperature for 1 h. After the final freeze-thaw cycle, the sample was centrifuged at 15,000 × *g* for 10 min to sediment cellular debris. The supernatant was transferred to a new

Eppendorf tube and stored at −80°C, and the pellet was dried using a vacuum concentrator at 30°C. The dry weight of the cell pellet was used to normalize the abundance of LMW thiols present in the corresponding supernatant fraction. A similar approach was used to analyze LMW thiol abundance in *Y. pestis* growth media (LB broth and TMH medium). Specifically, 1 ml of extraction buffer was added to an Eppendorf tube containing 250 µl of growth medium, and the sample was subjected to three freeze-thaw cycles as described above. After the sample was centrifuged at 15,000 × *g* for 10 min to pellet any insoluble material, the supernatant was immediately collected, transferred to another Eppendorf tube, and stored at −80°C.

The assay for mBBr derivatization of LMW thiols was adapted from prior studies (Rijstenbil and Wijnholds 1996; Sneller et al. 2000; Minocha et al. 2008). A set of thiol standard mixtures—with cysteine, glutathione, and γ-glutamylcysteine combined at equimolar concentrations of 1 µM, 5 µM, 10 µM, 25 µM, and 50 µM—were prepared in a final volume of 250 µl extraction buffer. For mBBr derivatization, 615 µl of HEPPS buffer (200 mM HEPPS, 6.3 mM DTPA [pH 8.2]) was mixed in an Eppendorf tube with 25 µl of 20 mM TCEP, a nonthiol disulfide reductant. To this mixture, 250 µl of a thiol standard mixture or sample extract was added, followed by the addition of 10 µl of 0.5 mM NAC, which served as an internal control. After preincubation of this reaction mixture in a heat block at 45°C for 10 min, derivatization was carried out by adding 10 µl of 50 mM mBBr and incubating the samples in a heat block at 45°C for 30 min in the dark. The reaction was terminated by the addition of 100 µl of 1 M MSA, and samples were passed through 0.45-µm-pore nylon syringe filters (Pall-Gelman Labs) and stored at −20°C.

HPLC analysis of thiol-mBBr derivatives was performed over a 250- by 4.6-mm Thermo Scientific Hypersil Gold column with a 5-µm particle-size guard column (Thermo Scientific). The column temperature was maintained at 40°C, and the injection volume was 10 µl. Separation of

LMW thiol-mBBr adducts was achieved by using a linear gradient in which the mobile phase was supplemented with 0.1% TFA. The gradient was derived from buffer A (water, 10% acetonitrile, 0.1% TFA) and buffer B (acetonitrile, 0.1% TFA), with a continuous flow rate of 1 ml per min and the following parameters: 0 to 5 min, 0% buffer B; 5 to 16.2 min, linear gradient from 0 to 10.6% buffer B; 16.2 to 29.8 min, linear gradient from 10.6 to 21.1% buffer B; 29.9 to 39.9 min, 100% buffer B; 40 to 45 min, 0% buffer B. The elution profile was monitored by fluorescence, using an excitation wavelength of 394 nm and an emission wavelength of 490 nm. Data were acquired and processed by Shimadzu LCsolution software (version 1.24 SP1). HPLC chromatogram peaks corresponding to the mBBr adducts of glutathione, γ-glutamylcysteine, and cysteine were assigned on the basis of retention time by comparison to the known thiol standards. All HPLC analyses were conducted using a Shimadzu Prominence LC-20A series system (Shimadzu, Kyoto, Japan).

Y. pestis Survival in Vertebrate Blood and Serum

Defibrinated sheep blood and sheep serum were purchased from Hemostat Laboratories. For heat inactivation, serum bottles were placed in a 56°C water bath for 30 min, with constant swirling to ensure uniform heating of the serum, and then removed and allowed to cool slowly to room temperature. Assays for *Y. pestis* growth in sheep blood or heat-inactivated serum were adapted from a previous study (Minato et al. 2013). In brief, *Y. pestis* strains were propagated overnight in 4 ml of LB broth at 26°C. After 0.5 ml of *Y. pestis* overnight culture was centrifuged at 7,500 × *g* for 5 min, the sedimented bacteria were washed once with 1 ml of 1× PBS and then suspended in 1 ml of 1× PBS. After dilution of the bacterial suspension at 1:20 in 1× PBS, its OD_{600} was measured in order to calculate the volume required to inoculate 10^5 CFU of the bacterial

suspension into 4 ml of sheep blood or serum. Cultures were incubated for 18 h at 37°C. To enumerate the fold change in viable *Y. pestis* cells over 18 h of growth, CFU counts were determined both pre- and postincubation by serially diluting sheep blood or sheep serum cultures and plating on LB agar.

Statistics

Statistical analysis was performed using Prism 6 (GraphPad Software, Inc.). For *in vitro* experiments, the two-tailed unpaired Student's *t* test was used to compare differences between two groups, and one-way analysis of variance (ANOVA) with Tukey's multiple-comparison posttest was used to compare differences between more than two groups. For *in vivo* experiments, differences between two groups were analyzed using either the Mann-Whitney *U* test (CFU) or the two-tailed unpaired Student's *t* test (serum IgG titers). Survival analysis of *Y. pestis*-infected animals was performed using the Gehan-Breslow-Wilcoxon test. A P value of <0.05 was determined to be statistically significant.

ACKNOWLEDGEMENTS

We thank Owen Demke for experimental assistance and members of our laboratories for critical comments and discussion.

This project has been supported by funds from the National Institute of Allergy and Infectious Diseases, National Institutes of Health, Department of Health and Human Services, under awards U19 AI107792, RO1AI042797, and S10RR023718.

CHAPTER III

CONCLUSION

The results of this study clearly demonstrate that *Y. pestis* LcrV, the plague protective antigen and needle cap protein of type III secretion machines (Burrows 1956; Mueller et al. 2005), is glutathionylated at Cys^{273} following its secretion to the distal end of the type III needle. Significantly, this is the first report of a bacterial secreted virulence factor that is posttranslationally modified with host-derived glutathione. The codon substitution $Cys^{273}Ala$, which precludes LcrV glutathionylation, increased *Y. pestis* type III injection and killing of innate immune cells and enhanced the survival of mice and rats in models of bubonic plague disease. Macrophages infected by the $lcrV_{C273A}$ mutant displayed accelerated apoptotic death and diminished proinflammatory cytokine release. While investigating the molecular mechanism underpinning these virulence attributes, LcrV was shown to associate with the intracellular macrophage protein RPS3, a known regulator of apoptosis and innate inflammatory responses (Gao and Hardwidge 2011), and this association was perturbed by the $Cys^{273}Ala$ substitution in *lcrV*. Furthermore, LcrV glutathionylation promoted the release of inflammatory cytokines by *Y. pestis*-infected macrophages and enhanced bubonic plague pathogenesis in mice and rats. Taken together, these data establish LcrV glutathionylation as a novel modification that alters the functionality of this essential virulence factor.

LcrV of *Y. pestis* is, at present, the only extracellular bacterial secreted protein that is known to be glutathionylated. For this reason, it will be essential to determine in future research whether the glutathionylation of *Y. pestis* type III secretion substrates is restricted to LcrV or, alternatively, whether this posttranslational modification involves other type III secretion

substrates with cysteine sulfhydryl moieties, such as YopB, YopE, YopM, and YopN. To address this question, the gene encoding each Yop will be cloned into a low-copy-number plasmid engineered to express the type III secretion substrate under the control of the IPTG-inducible *tac* promoter. Guided by the known or predicted three-dimensional structure of the Yop, the eight-residue Strep tag will be inserted into the protein by site-directed PCR mutagenesis at a location where the tag is unlikely to interfere with the protein's structure or function. After transforming this plasmid into *Y. pestis*, the Strep-tagged Yop will be purified by Strep-Tactin–Sepharose affinity chromatography from the culture supernatant of *Y. pestis* following several hours of growth in secretion-permissive conditions. To determine whether the Strep-tagged Yop is glutathionylated, the purified protein will be mass measured by combined liquid chromatography-electrospray ionization mass spectrometry (LC-ESI-MS); glutathionylation sites—i.e., peptides with a measured mass that is approximately 305 Da (the calculated mass of glutathione) greater than predicted—will be identified in tryptic peptides via LC-ESI-MS and then positioned via tandem mass spectrometry (MS/MS). Analysis of these data will reveal whether the cysteine moieties of other type III secretion substrates are, like LcrV, modified with glutathione.

This was the first study to identify host RPS3 as a ligand for LcrV during *Y. pestis* infection of murine J774.A1 macrophages. This association was more pronounced for wild-type LcrV than its non-glutathionylated $LcrV_{C273A}$ variant, with increased LcrV-RPS3 association corresponding to less apoptotic cell death and more proinflammatory cytokine release by *Y. pestis*-infected macrophages. RPS3 of J774.A1 cells, a macrophage cell line derived from *Mus muscularis*, harbors a total of three cysteine residues, thereby raising the possibility that disulfide formation between LcrV and RPS3 might play a role in mediating the association between these two proteins. The finding that $LcrV_{C273A}$ copurified with RPS3, albeit to a significantly lesser extent than wild-

type LcrV, rules out disulfide formation as a necessary condition for LcrV-RPS3 association; nevertheless, it is possible that the capacity for LcrV to form a disulfide bond may have contributed to the differential association between RPS3 and LcrV variants that was observed for *Y. pestis*-infected macrophages.

Protein glutathionylation, which can proceed spontaneously or enzymatically, is promoted by oxidative or nitrosative stress but also occurs in unstressed cells. The reverse reaction, protein deglutathionylation, frequently occurs following exposure of the disulfide modification to a reducing environment (Dalle-Donne et al. 2007; Dalle-Donne et al. 2009). In this study, the biochemical pathway of LcrV glutathionylation was characterized as proceeding via spontaneous thiol-disulfide exchange between LcrV residue Cys^{273} and extracellular oxidized glutathione (GSSG). During *Y. pestis* growth in laboratory broth, LcrV is both secreted into the culture medium and assembled into type III needle complexes (Lee, Tam, and Schneewind 2000; Mueller et al. 2005). During *Y. pestis* infection of tissue culture cells, however, LcrV is not found in the extracellular medium, but instead remains associated with bacteria that adhere to tissue culture cells; the precise location of LcrV under these conditions is not known. While type III injection of LcrV into the cytoplasm of tissue culture cells has never been demonstrated, LcrV is known to be involved in the translocation of Yop effectors, namely, in the establishment of a conduit between type III needles and the eukaryotic cytoplasm (Pettersson et al. 1999; Lee, Tam, and Schneewind 2000). Perhaps LcrV, as it fulfills its physiological role at the needle tip in penetrating the host cell membrane, is in a location that is accessible to RPS3. Since the host cell cytoplasm is a reducing environment, it seems plausible that the disulfide bond linking LcrV and glutathione may be attacked by other thiol-containing compounds. Nevertheless, since the interface between *Y. pestis* and the immune cell targeted for type III injection is dominated by highly reactive small molecules

that collectively induce oxidative stress (Luebke and Giedroc 2015), it seems equally plausible that the disulfide modification at Cys^{273} of LcrV may not be perturbed. For this reason, future work will need to address the oxidation state of LcrV residue Cys^{273} in macrophages and determine whether any additional modifications may influence the association between LcrV and RPS3.

Although the codon substitutions Cys^{273}Ala and Cys^{273}Ser abolished LcrV glutathionylation without affecting the secretion of LcrV or Yop effectors, the presence of a serine residue at LcrV position 273 had a dramatically lesser impact on *Y. pestis* type III injection and bubonic plague virulence assays. While the $lcrV_{C273A}$ mutation enhanced type III injection of Yop effectors into *Y. pestis*-infected neutrophils, there was not a measurable difference in Yop translocation between wild-type and $lcrV_{C273S}$ mutant *Y. pestis*. Although the $lcrV_{C273A}$ and $lcrV_{C273S}$ mutants were attenuated in virulence relative to wild-type (WT) *Y. pestis* when analyzed separately in a murine model of bubonic plague disease, there was a striking difference between the delay in median time to death associated with each *lcrV* mutation: $lcrV_{C273A}$ vs. WT, 2.5 days, and $lcrV_{C273S}$ vs. WT, 9 hours. Nevertheless, the key observation was that both codon substitutions in *lcrV* attenuated *Y. pestis* virulence in rodent models of bubonic plague disease, thereby indicating that the sulfhydryl-containing residue Cys^{273} plays an important role in plague pathogenesis.

To gain a better understanding of how the chemical nature of the side chains at residue 273 impact LcrV function, the full suite of *in vitro* and *in vivo* assays that were used to characterize the $lcrV_{C273A}$ mutant will need to be applied to $lcrV_{C273S}$ mutant *Y. pestis*. It will be crucial to establish, for example, whether the $lcrV_{C273S}$ mutation promotes apoptotic cell death with rapidly increased kinetics in *Y. pestis*-infected J774.A1 macrophages, as was observed for the $lcrV_{C273A}$ mutant relative to wild-type *Y. pestis*. Similarly, it will be critical to determine whether—and, if so, to

what degree—$LcrV_{C273S}$ associates with RPS3 in *Y. pestis*-infected macrophages; moreover, the tissue culture media overlying the infected macrophages will be analyzed by ELISA for the concentration of proinflammatory cytokines (IL-18 and IL-1β). Analysis of these data will indicate whether the $lcrV_{C273S}$ mutation is associated with a shift from necroptotic to apoptotic death of *Y. pestis*-infected immune cells, as was observed for the $lcrV_{C273A}$ mutation. Finally, the virulence of $lcrV_{C273S}$ mutant *Y. pestis* will be assessed using a rat model of bubonic plague pathogenesis. Although the most pronounced virulence defect associated with the $lcrV_{C273A}$ mutation was measured in Brown Norway rats, where a delay in median time to death as well as increased survival were observed, there was also a significant delay in the median time to death of BALB/c mice infected by the $lcrV_{C273A}$ mutant. Since BALB/c mice, unlike wild rodents, are highly susceptible to plague infection, it was for economic reasons—such as the costs of animal acquisition and ABSL-3 maintenance—that we only examined the virulence of $lcrV_{C273S}$ mutant *Y. pestis* in BALB/c mice. For this reason, it will be essential to investigate whether the $lcrV_{C273S}$ mutation is associated with a more pronounced virulence defect during *Y. pestis* infection of Brown Norway rats.

The results of this study undoubtedly highlight the process whereby naturally occurring polymorphisms—such as the polymorphism substituting LcrV $Cys^{273}Ser$ found in some isolates of *Y. pestis* biovar Microtus, which does not cause plague in humans—play a major role in the adaptation of *Y. pestis* to new and diverse environments wherein its mammalian hosts and insect vectors exhibit widely varying susceptibility to plague bacilli (Perry and Fetherston 1997; Anisimov et al. 2004; Zhou et al. 2004; Chain et al. 2006). Unlike the codon 273 polymorphism ($lcrV_{C273S}$) observed in *Y. pestis* biovar Microtus isolates, the presence of a cysteine residue at LcrV position 273 is a conserved feature among all human pathogenic and epidemic *Y. pestis* strains

(Anisimov et al. 2010; Sawa, Katoh, and Yasumoto 2014). Thus, glutathionylation may represent a mechanism whereby LcrV is posttranslationally modified in order to regulate its function; this hypothesis, if correct, may also explain the evolutionary pressure for epidemic *Y. pestis* strains to retain the only cysteine residue in this essential virulence factor. The proposal of glutathionylation as a mechanism for regulating and retaining a highly conserved cysteine residue of an essential virulence factor is supported by the recent work of Portman and colleagues (2017). This study reports that the essential virulence factor listeriolysin O (LLO)—a pore-forming protein secreted by the facultative intracellular pathogen *L. monocytogenes* that facilitates bacterial escape from a phagocytic vacuole into the host cell cytoplasm (Portnoy, Jacks, and Hinrichs 1988; Schnupf and Portnoy 2007)—is rendered fully inactive by glutathionylation at Cys^{484}, which is the only cysteine residue in a conserved C-terminal undecapeptide that mediates LLO membrane binding (Tweten, Hotze, and Wade 2015; Portman et al. 2017). Furthermore, the codon substitution $Cys^{484}Ala$, which abolishes LLO glutathionylation, does not impact *in vitro* infections of bone marrow-derived macrophages and yet significantly attenuates *L. monocytogenes* virulence when analyzed in a competitive murine infection model (Portman et al. 2017).

APPENDIX A

LCRV MUTANTS THAT ABOLISH *YERSINIA* TYPE III INJECTISOME FUNCTION

The material presented in this Appendix previously appeared as an article in the *Journal of Bacteriology*; it is reprinted here by permission of the publisher. The original citation is as follows:

Katherine Given Ligtenberg, Nathan C. Miller, Anthony Mitchell, Gregory V. Plano, and Olaf Schneewind. 2013. "LcrV Mutants That Abolish *Yersinia* Type III Injectisome Function." *Journal of Bacteriology* 195 (4): 777–87. https://doi.org/10.1128/JB.02021-12.

The author contributions are as follows: K.G.L., N.C.M., and A.M. contributed equally to this article. K.G.L., N.C.M., A.M., and O.S. conceived the project. A.M. performed the genetic screen to isolate *Y. pestis lcrV* mutants with the dominant negative low-calcium response (LCR^-) phenotype. K.G.L. and A.M. conducted LCR growth assays for *Y. pestis* strains. K.G.L. and N.C.M. performed affinity chromatography experiments and characterized type III secretion and effector injection for *Yersinia* strains expressing Strep-tagged LcrV variants. K.G.L. imaged type III needle complexes by transmission electron microscopy. G.V.P. provided *yscF* mutant *Y. pestis* strains. K.G.L., N.C.M., A.M., G.V.P., and O.S. wrote the paper.

ABSTRACT

LcrV, the type III needle cap protein of pathogenic *Yersinia*, has been proposed to function as a tether between YscF, the needle protein, and YopB-YopD to constitute the injectisome, a conduit for the translocation of effector proteins into host cells. Further, insertion of LcrV-capped needles from a calcium-rich environment into host cells may trigger the low-calcium signal for effector translocation. Here, we used a genetic approach to test the hypothesis that the needle cap

responds to the low-calcium signal by promoting injectisome assembly. Growth restriction of *Yersinia pestis* in the absence of calcium (low-calcium response [LCR^+] phenotype) was exploited to isolate dominant negative *lcrV* alleles with missense mutations in its amber stop codon (*lcrV*$_{*327}$). The addition of at least four amino acids or the eight-residue Strep tag to the C terminus was sufficient to generate an LCR^- phenotype, with variant LcrV capping type III needles that cannot assemble the YopD injectisome component. The C-terminal Strep tag appears buried within the cap structure, blocking effector transport even in *Y. pestis yscF* variants that are otherwise calcium blind, a constitutive type III secretion phenotype. Thus, LcrV$_{*327}$ mutants arrest the needle cap in a state in which it cannot respond to the low-calcium signal with either injectisome assembly or the activation of type III secretion. Insertion of the Strep tag at other positions of LcrV produced variants with wild-type LCR^+, LCR^-, or dominant negative LCR^- phenotypes, thereby allowing us to identify discrete sites within LcrV as essential for its attributes as a secretion substrate, needle cap, and injectisome assembly factor.

INTRODUCTION

Three pathogenic *Yersinia* species—*Yersinia enterocolitica*, *Yersinia pseudotuberculosis*, and *Yersinia pestis*—employ a virulence plasmid-encoded type III secretion machine to establish disease (Perry et al. 1986; Rosqvist, Bölin, and Wolf-Watz 1988; Cornelis et al. 1998). The key function of type III secretion machines during the pathogenesis of *Yersinia* infections is the transport of effectors (YopE, YopH, YopM, YopO, YopP [J], YopT, and YopQ) into host cells, thereby enabling bacterial escape from innate immune responses (Rosqvist, Magnusson, and Wolf-Watz 1994; Cornelis 2002). Assembly of the *Yersinia* type III secretion machine involves 23 different protein components encoded by *ysc* genes (Yop secretion), which catalyze the

successive secretions of early, middle, and late (effector) substrates (Cornelis 2006; Sorg, Blaylock, and Schneewind 2006). During the initial assembly stage of the *Yersinia* type III machine, a protein transport channel with a central conduit is formed across the bacterial inner and outer membranes (Galán and Wolf-Watz 2006). The type III machine promotes self-assembly of its basal membrane components and secretion of its inner rod (YscI) and needle (YscF) extensions (Hoiczyk and Blobel 2001; Diepold et al. 2012), followed by the transport of middle substrates to cap the needle (LcrV, YopD) (Mueller et al. 2005). Contact of capped needles with host cells is thought to promote the assembly of the injectisome in host cell membranes (YopB, YopD) (Sorg, Miller, and Schneewind 2005; Mueller, Broz, and Cornelis 2008). Establishment of a *Yersinia* type III conduit into host cells is associated with a decrease in calcium ions: the concentration of calcium ions is 1.2 mM in extracellular fluids and <10 μM within cells (Pollack, Straley, and Klempner 1986). Reception of this signal activates the *Yersinia* type III pathway for the translocation of effectors into host cells (Pollack, Straley, and Klempner 1986; Lee, Mazmanian, and Schneewind 2001).

Electron microscopy experiments with *Y. enterocolitica* needle complexes revealed the LcrV cap (Mueller et al. 2005). Like *Y. pestis yscF* mutants, *lcrV* variants are unable to complete the type III conduit into host cells and cannot activate the pathway even when calcium ions are chelated (Perry et al. 1986; Nilles, Fields, and Straley 1998; Lee, Tam, and Schneewind 2000). A different phenotype has been observed for *yopB* and *yopD*; *Yersinia* mutants lacking *yopB* or *yopD* respond to the low-calcium signal with type III secretion, yet these variants are unable to direct effectors into host cells (Håkansson et al. 1993; Håkansson et al. 1996). When extracellular calcium ions are removed, wild-type *Y. pestis* cannot form colonies on laboratory media at 37°C (low-calcium response [LCR^+] phenotype) (Goguen, Yother, and Straley 1984); however, this

growth restriction is abolished when *yscF* or *lcrV* is deleted (LCR$^-$) (Perry et al. 1986; Torruellas et al. 2005). In contrast, *Y. pestis* calcium-blind mutants secrete effectors even in the presence of extracellular calcium ions and cannot form colonies at 37°C (temperature sensitive for growth [*ts*] phenotype) (Yother and Goguen 1985). Torruellas and colleagues (2005) isolated *yscF* variants with calcium-blind *ts* phenotypes. These YscF mutants harbor single amino acid substitutions of negatively charged aspartic acid residues with neutral amino acids, suggesting that the association of aspartyl with calcium ions may enable the needle protein to act as a calcium sensor (Torruellas et al. 2005). The LCR pathway also involves factors in the *Y. pestis* cytoplasm. For example, LcrG and LcrE (YopN) are required for the *Y. pestis* blockade of effector secretion in the presence of calcium, as *lcrG* and *lcrE* mutants also display calcium-blind *ts* phenotypes (Yother and Goguen 1985; Skryzpek and Straley 1993, 1995). LcrG binds LcrV in the bacterial cytoplasm, and this association is required for LcrV secretion (Nilles et al. 1997; Lee, Tam, and Schneewind 2000).

LcrV, but not any other component of the type III pathway, is the plague protective antigen; antibodies that bind LcrV prevent *Y. pestis* translocation of effectors into host cells (Burrows 1956; DeBord et al. 2006). Although wild-type LcrV could not be crystallized, the structure of a variant (K40A/D41A/K42A) was revealed by X-ray crystallography (Derewenda et al. 2004). Of note, the N and C termini of LcrV (residues 23 to 27 and 323 to 326), Y^{90}, and two internal loops (residues 49 to 63 and 260 to 275) were not visible in the electron density map (Derewenda et al. 2004). $LcrV_{K40A/D41A/K42A}$ assumed an overall dumbbell-shaped structure with a central coiled coil connecting two globular folds (Derewenda et al. 2004). This structure was modeled into high-resolution electron microscopy images of the LcrV needle cap, which suggest an atomic model for a pentameric LcrV ring (Mueller, Broz, and Cornelis 2008). The functional relevance of the proposed structure is, however, not clear. The LcrV residues involved in forming a central conduit,

in associating with the needle protein (YscF), or in forming the injectisome (YopB and YopD) are not yet known. Furthermore, although the aforementioned hypothesis proposes a dynamic role for LcrV in capping type III needles and in promoting injectisome assembly, experimental proof for this conjecture is still missing. Here, we used genetic as well as molecular biology approaches to address these questions.

MATERIALS AND METHODS

Bacterial Strains and Plasmids

Y. pestis strain KIM D27 (wild type) (Brubaker 1969) and the Δ*lcrV* mutant (KLD29) (DeBord et al. 2006) were grown in heart infusion broth (HIB), M9-Casamino Acids (M9-Ca) minimal medium, or thoroughly modified Higuchi's (TMH) medium (Brubaker 1969; Higuchi 1970; DeBord et al. 2006). *Y. enterocolitica* strain W22703 (wild type) (Cornelis and Colson 1975) and the Δ*lcrV* mutant (CT1) (Lee, Tam, and Schneewind 2000) were grown in tryptic soy broth (TSB) or M9-Ca medium, as indicated. Chloramphenicol was added to *Y. enterocolitica* (30 μg/ml) or *Y. pestis* (10 μg/ml) cultures for plasmid retention. For PCR mutagenesis experiments, determination of the low-calcium response (LCR) was performed on solid medium by plating *Y. pestis* cultures onto tryptose blood agar (TBA) plates containing 20 mM $MgCl_2$, 20 mM sodium oxalate, and 1 mM isopropyl-β-D-thiogalactopyranoside (IPTG). Duplicate plates were inoculated with transformants and incubated at 26°C or 37°C for 48 h and then scored for their LCR.

The construction of plasmids p$lcrV_{W22703}$ (pNM142) and p$lcrV_{D27}$ (pNM77) has been described previously (Miller et al. 2012). PCR mutagenesis of p$lcrV_{D27}$ (harboring *Y. pestis* KIM D27 *lcrV*) was performed with the GeneMorph II EZClone domain mutagenesis kit (Agilent)

using primers complementary to the vector backbone at positions approximately 60 bp outside the *lcrV* coding region: 5′-TGCGCCGACATCATAACGGTTC-3′ (pHSG lcrV 5′) and 5′-TCTGCC TCCCAGAGCCTGATA-3′ (pHSG lcrV 3′). Plasmids carrying the LcrV-Strep alleles of *Y. enterocolitica* were generated with the QuikChange Lightning site-directed mutagenesis kit (Agilent) with reverse complementary primers containing the Strep tag sequence (5′-TGGTCTCATCCTCAATTTGAGAAG-3′), and plasmids harboring the sequential C-terminal additions of the Strep tag amino acid residues to $LcrV_{D27}$ (p*lcrV*$_{+1}$, p*lcrV*$_{+2}$, p*lcrV*$_{+3}$, p*lcrV*$_{+4}$, p*lcrV*$_{+5}$, p*lcrV*$_{+6}$, p*lcrV*$_{+7}$) were assembled in a similar manner. Standard methods for transformation of the plasmids into *Y. pestis* were employed.

LCR Growth Assay

To determine the bacterial growth phenotypes in the presence and absence of calcium, overnight cultures of *Y. pestis* were diluted 1:40 into 4 ml of TMH medium and incubated for 2 h at 26°C, at which time 200-µl aliquots of each sample were added in triplicate to a sterile 96-well flat-bottom growth plate (wells were supplemented in advance, where necessary, by the addition of $CaCl_2$ and IPTG to final concentrations of 2.5 mM and 1 mM, respectively). Bacterial growth at 37°C was recorded by a plate reader over a period of 12 h by measuring the optical density at 600 nm (OD_{600}) for shaking cultures containing TMH medium alone or TMH medium supplemented with 2.5 mM $CaCl_2$.

***Yersinia* Type III Secretion**

To monitor secretion into the extracellular environment, *Y. pestis* and *Y. enterocolitica* overnight cultures were diluted 40-fold into 4 ml M9-Ca medium or TSB supplemented with

5 mM EGTA, respectively, incubated at 26°C for 2 h, and then shifted to 37°C for 3 h to induce type III secretion. When appropriate, IPTG was added to a final concentration of 1 mM to induce the expression of plasmid-borne *lcrV* alleles. Cultures were fractionated and analyzed for type III secretion as described previously (Cheng, Anderson, and Schneewind 1997). To screen for *Yersinia* type III translocation of effectors, overnight cultures of *Y. pestis* and *Y. enterocolitica* were diluted 1:40 into 4 ml HIB or TSB, respectively, and incubated for 2 h at 26°C. Bacteria were added at a multiplicity of infection (MOI) of 10 to HeLa cell monolayers of about 2×10^5 cells that had been seeded a day earlier. After 3 h of infection at 37°C, cells were fixed with 3.7% formaldehyde for 20 min, quenched with 0.1 M glycine for 5 min, washed with phosphate-buffered saline (PBS), permeabilized with 0.1% Triton X-100 for 30 min at 4°C, washed three times with PBS, and blocked with 5% nonfat dried milk in PBS for 20 min at room temperature. Filamentous actin was then labeled with 3 units of rhodamine-conjugated phalloidin (99 nM) for 20 min. After the labeling solution was removed, the cells were washed three times with PBS and visualized by phase-contrast imaging and fluorescence microscopy using a Nikon TE-2000 inverted microscope (Miller et al. 2012).

Purification of LcrV from *Yersinia* Extracts

To assay for cytosolic protein-protein interactions, 50 ml of overnight cultures of *Y. pestis* or *Y. enterocolitica* was inoculated into 1 liter of HIB supplemented with 20 mM $MgCl_2$ and 20 mM sodium oxalate or TSB supplemented with 5 mM EGTA, respectively. Cultures were incubated at 26°C for 2 h and then grown at 37°C for another 3 h. IPTG, at a final concentration of 1 mM, was added prior to the temperature shift to induce expression of plasmid-borne LcrV. Bacteria were sedimented by centrifugation at 7,500 × *g* for 10 min, suspended in 20 ml of column

buffer (100 mM Tris-HCl, 150 mM NaCl [pH 7.5]), and left at –20°C overnight. The cells were thawed the following day and French pressed twice at 15,000 lb/in^2. The crude lysate was centrifuged twice at 8,000 × *g* for 15 min, and the supernatant (load) was subjected to chromatography on 1.5 ml of Strep-Tactin–Sepharose (IBA BioTAGnology). The column was washed with 30 ml of column buffer, and the proteins were eluted with column buffer with 2.5 mM desthiobiotin. Samples were analyzed by 15% SDS-PAGE, Coomassie staining, or immunoblotting with rabbit antisera raised against purified recombinant *Yersinia* proteins or mouse monoclonal antibody directed against the Strep tag.

Purification and Visualization of Type III Needles

Needle purification was carried out by inoculation of a 50-ml overnight culture of *Y. enterocolitica* into 1 liter of M9-Ca medium, which was incubated at 26ºC for 2 h and then grown at 37°C for 3 h. LcrV expression was induced by the addition of 1 mM IPTG prior to incubation at 37°C. Bacteria were sedimented by centrifugation at 2,700 × *g* for 10 min and suspended in 40 ml of 1 M Tris-HCl (pH 7.5). Needles on the bacterial surface were mechanically sheared by vortexing samples for 5 min. Bacteria were again sedimented by centrifugation at 8,000 × *g* for 10 min, and the needle containing shearate was passed through a 0.45-μm cellulose acetate membrane filter (Whatman). Needles were sedimented by ultracentrifugation at 45,000 × *g* for 30 min. The needle sediment was suspended in 20 mM Tris-HCl (pH 7.5) and examined by either immunoblotting or electron microscopy. For electron microscopy, all samples were placed on a carbon-coated copper grid and stained with 1% uranyl acetate before viewing on a Tecnai F30 electron microscope at 300 kV.

RESULTS

Mutations in *lcrV* with a Dominant Negative LCR$^-$ Phenotype in *Y. pestis*

Y. pestis $lcrV_{D27}$ was subjected to PCR mutagenesis, introducing mutations at frequencies ranging from 1 to 10 lesions per kilobase. Mutated plasmids were purified and transformed into wild-type *Y. pestis* strain KIM D27. Transformants were spread on agar with chelated calcium ions and incubated for 2 days at 37°C in the presence of 1 mM IPTG to induce the expression of plasmid-borne *lcrV*. Under these conditions, *Y. pestis* variants that lost the ability to secrete effectors formed colonies (Goguen, Yother, and Straley 1984); these colonies were isolated, and the plasmids were purified and transformed again into *Y. pestis* KIM D27. Transformants that retained the LCR$^-$ phenotype on calcium-chelated agar supplemented with 1 mM IPTG were analyzed by DNA sequencing of plasmid-borne *lcrV*. Eighty-seven independent mutants were isolated, 18 of which harbored missense mutations in codon 327 (UGA amber stop), extending the $lcrV_{D27}$ reading frame by 22 codons (Fig. A1*A*). Specifically, we identified 6 CGA (Arg), 2 GGA (Gly), 3 UGG (Trp), 2 UGU (Cys), 4 UUA (Lys), and 1 UCA (Ser) codon variants. The remaining mutants that answered the selection were stop or frameshift mutations at various locations throughout the *lcrV* gene.

Y. pestis KIM D27 strains harboring plasmids expressing wild-type $lcrV_{D27}$ (p$lcrV_{D27}$) or the amber codon suppressors (p$lcrV_{*327R}$ and p$lcrV_{*327W}$) were grown in liquid media at 37°C for 12 h under secretion-permissive (TMH medium) or secretion-nonpermissive conditions (TMH medium supplemented with 2.5 mM $CaCl_2$) (Fig. A1*B*). In contrast to the plasmid expressing $lcrV_{D27}$, p$lcrV_{*327R}$ and p$lcrV_{*327W}$ enabled IPTG-induced *Y. pestis* cultures to grow at 37°C in the absence of calcium ions (LCR$^-$) (Fig. A1*B*). As controls, *Y. pestis* KIM D27 without plasmid was LCR$^+$, whereas p$yopN_{F234S}$ resulted in the expected dominant negative LCR$^-$ phenotype

(Ferracci et al. 2005) (Fig. A1*B*). Deletion of the *lcrV* gene on pCD1 from *Y. pestis* KIM D27 also caused an LCR$^-$ phenotype, as the Δ*lcrV* mutant strain (KLD29) continued to grow at 37°C in the absence of calcium; this defect was complemented by the transformation of KLD29 with p$lcrV_{D27}$ (Fig. A1*B*).

Y. pestis strains were grown in liquid media for 2 h at 26°C and then shifted to 37°C for 3 h to induce type III secretion. The cultures were centrifuged to separate the extracellular medium with the supernatant from the bacterial sediment. Proteins in both fractions were analyzed by immunoblotting with rabbit antisera raised against purified LcrV, YopE, or RNA polymerase subunit A (RpoA) (Table A1). *Y. pestis* strain KIM D27 (p$lcrV_{D27}$) secreted LcrV and YopE into the extracellular medium, whereas RpoA was found only in the bacterial sediment. As expected, the Δ*lcrV* mutant did not express LcrV and failed to secrete YopE, which was again complemented by p$lcrV_{D27}$ (Table A1). *Y. pestis* KIM D27 harboring p$lcrV_{*327R}$ or p$lcrV_{*327W}$ failed to secrete YopE yet retained the ability to secrete mutant LcrV$_{*327R}$ and LcrV$_{*327W}$, albeit at reduced abundance (Table A1). Together, these data indicate that the IPTG-inducible expression of $lcrV_{*327R}$ and $lcrV_{*327W}$ causes a dominant negative LCR$^-$ phenotype in *Y. pestis* strain KIM D27. This is attributable to a type III secretion block of $lcrV_{*327R}$ and $lcrV_{*327W}$ mutants for effector Yops, whereas the secretion of LcrV was reduced but not blocked.

C-Terminal Extensions of LcrV Block the *Y. pestis* Type III Pathway

We wondered whether the LCR$^-$ phenotype of the $lcrV_{*327R}$ and $lcrV_{*327W}$ mutants critically depended on the 22 codons downstream of their stop codon suppressors. To test this, we extended the $lcrV_{D27}$ open reading frame by insertions of random single amino acid codons immediately prior to codon 327 (UGA). The resulting variants were expressed from plasmids via IPTG

induction of the lac_{UV5} promoter. Expression of *lcrV* alleles with one (p$lcrV_{+1}$), two (p$lcrV_{+2}$), or three codon insertions (p$lcrV_{+3}$) did not affect bacterial growth; however, *lcrV* alleles with four (p$lcrV_{+4}$), five (p$lcrV_{+5}$), six (p$lcrV_{+6}$), or seven (p$lcrV_{+7}$) codon insertions abolished the LCR of *Y. pestis* strain KIM D27 (Fig. A2). These data indicate that the mere extension of *Y. pestis* LcrV by four or more residues at its C-terminal end is sufficient to impose a dominant negative blockade on the type III pathway.

Strep Tag Insertions into *Y. enterocolitica* LcrV

Earlier work revealed that LcrV caps the tip of *Y. enterocolitica* needles (Mueller et al. 2005). As details regarding *Y. pestis* needles and their LcrV caps have not yet been revealed (Blaylock, Berube, and Schneewind 2010), we sought to examine the cap structure and other functional attributes of *lcrV* alleles in *Y. enterocolitica* W22703 (Cornelis and Colson 1975; Cornelis et al. 1998). $LcrV_{W22703}$ is three residues shorter than $LcrV_{D27}$; however, the two molecules are 96% identical (Fig. A3*A*). To generate a C-terminal extension of $LcrV_{W22703}$, we appended the eight-residue Strep tag to the C-terminal end of the polypeptide chain by inserting the corresponding eight codons immediately upstream of the $lcrV_{W22703}$ stop codon (p$lcrV_{S324}$). Furthermore, we wondered whether Strep tag insertions at other sites also cause a dominant negative type III secretion (LCR) phenotype, and we selected $LcrV_{W22703}$ positions 1, 20, 55, 170, 228, and 270 for insertions. The relative positions of these insertions in the three-dimensional structure of $LcrV_{K40A/D41A/K42A}$ and their corresponding phenotypes are summarized in Fig. A3*B*. Plasmids expressing $lcrV_{W22703}$ or its variants via the lac_{UV5} promoter were transformed into *Y. enterocolitica* CT1, the Δ*lcrV* variant of W22703. In contrast to *Y. pestis,* where the deletion of *lcrV* abolished the LCR and type III secretion, *Y. enterocolitica* CT1 (Δ*lcrV*) remains competent

for both YopE expression and type III secretion (Fig. A3*C*) (Lee, Tam, and Schneewind 2000). Of note, LcrG, the cytoplasmic chaperone of LcrV, is expressed at very low abundance in the *lcrV* mutant strain (Fig. A3*C*) (Lee, Tam, and Schneewind 2000). Transformation of *Y. enterocolitica* CT1 with p*lcrV*$_{W22703}$ restored the expression of both LcrV$_{W22703}$ and LcrG and enabled the secretion of LcrV$_{W22703}$ (Fig. A3*C*). Similar phenotypes were observed with p*lcrV*$_{S1}$, p*lcrV*$_{S20}$, p*lcrV*$_{S55}$, p*lcrV*$_{S170}$, and p*lcrV*$_{S228}$. The p*lcrV*$_{S270}$ plasmid did not restore the expression of LcrG, and LcrV$_{S270}$ was not secreted into the extracellular medium. Plasmid p*lcrV*$_{S324}$ restored the expression of LcrG, and only very small amounts of LcrV$_{S324}$ were secreted into the extracellular medium (Fig. A3*C*).

To analyze the binding of LcrV mutants to LcrG, extracts of *Y. enterocolitica* CT1 harboring *lcrV* plasmids were subjected to affinity chromatography on Strep-Tactin–Sepharose. Cleared lysate (L) and eluate (E) were analyzed by Coomassie blue-stained SDS-PAGE and immunoblotting (Fig. A4). LcrV$_{S1}$, LcrV$_{S20}$, LcrV$_{S55}$, LcrV$_{S228}$, and LcrV$_{S324}$ were isolated by affinity chromatography and purified together with LcrG (Fig. A4). LcrV$_{S170}$ did not bind Strep-Tactin resin, and the Strep tag was only poorly recognized by a specific monoclonal antibody (Fig. A4). We therefore conclude that the Strep tag of LcrV$_{S170}$ may be buried within the polypeptide and inaccessible to either antibody or Strep-Tactin. LcrV$_{S270}$ was purified from *Yersinia* lysate; however, this protein cannot copurify with LcrG, as the chaperone is not expressed by *Y. enterocolitica* CT1 harboring p*lcrV*$_{S270}$ (Fig. A4). Thus, with the exception of LcrV$_{S270}$, all other variants do bind to their LcrG chaperone.

To assess the functions of *lcrV* alleles in needle cap assembly and injectisome functions, we measured *Y. enterocolitica* effector translocation into tissue culture cells. HeLa cells were infected with *Y. enterocolitica* CT1 expressing mutant *lcrV*. Phase-contrast microscopy and

fluorescence microscopy images of phalloidin-stained tissue cultures were used to reveal actin filament rearrangements and cell rounding as measures for *Yersinia* type III translocation of effectors (Rosqvist, Magnusson, and Wolf-Watz 1994) (Fig. A5). Of note, p*lcrV*$_{S1}$, p*lcrV*$_{S20}$, p*lcrV*$_{S55}$, and p*lcrV*$_{S228}$ enabled *Y. enterocolitica* CT1 (Δ*lcrV*) to inject effectors, whereas p*lcrV*$_{S170}$, p*lcrV*$_{S270}$, and p*lcrV*$_{S324}$ did not (Fig. A5). When transformed into wild-type *Y. enterocolitica* W22703, only p*lcrV*$_{S324}$ caused a dominant negative effect on type III effector translocation, while p*lcrV*$_{S1}$, p*lcrV*$_{S20}$, p*lcrV*$_{S55}$, p*lcrV*$_{S170}$, p*lcrV*$_{S228}$, and p*lcrV*$_{S270}$ had no effect (Fig. A5). These data indicate that the C-terminal extension of LcrV$_{W22703}$ in *Y. enterocolitica lcrV*$_{S324}$ blocked the type III secretion pathway similarly to *lcrV*$_{*327W}$, *lcrV*$_{*327R}$, and *lcrV*$_{S324}$ in *Y. pestis*. Further, Strep tag insertions at positions 170 and 270 abolished the ability of LcrV$_{S170}$ and LcrV$_{S270}$ to assemble the type III injectisome and translocate effectors. For LcrV$_{S270}$, this is attributable to a defect in binding and stabilizing LcrG, which results in a defect in the type III secretion of LcrV$_{S270}$.

LcrV$_{S228}$ and LcrV$_{S324}$ Cap *Y. enterocolitica* Type III Needles

We sought to determine whether LcrV$_{S324}$ can cap type III needle structures. *Y. enterocolitica* CT1 (Δ*lcrV*) without plasmid or with p*lcrV*$_{W22703}$, p*lcrV*$_{S228}$, or p*lcrV*$_{S324}$ was sheared to remove type III secretion needles, which were subsequently sedimented by ultracentrifugation. Electron microscopy experiments revealed the absence of a cap structure on *Y. enterocolitica* Δ*lcrV* needles (Fig. A6*A*). Plasmids p*lcrV*$_{W22703}$, p*lcrV*$_{S228}$, as well as p*lcrV*$_{S324}$, restored the assembly of the LcrV cap on YscF needles (Fig. A6*A*). To examine whether capped needles also copurify with the injectisome component YopD, needle preparations were subjected to immunoblotting (Olsson et al. 2004; Mueller et al. 2005). As expected, needles derived from *Yersinia* with p*lcrV*$_{W22703}$ or p*lcrV*$_{S228}$ were assembled from YscF, YopD, and LcrV, whereas

needle preparations from the Δ*lcrV* mutant harbored YscF, very little YopD, and no LcrV. In contrast, needles from *Y. enterocolitica* Δ*lcrV* (p*lcrV*$_{S324}$) were assembled from YscF and LcrV$_{S324}$; however, the structures lacked YopD (Fig. A6*B*). Taken together, these data suggest that LcrV$_{S324}$ can indeed cap the type III needle. In contrast to wild-type LcrV or LcrV$_{S228}$, LcrV$_{S324}$-capped needles lack YopD, which may explain the effector translocation defect of the *lcrV*$_{S324}$ mutant strain. Electron microscopy experiments have not yet positioned YopD within the capped-needle complex. The finding that LcrV$_{S228}$-capped needles, but not the nonfunctional LcrV$_{S324}$ cap, associate with YopD provides evidence for a model whereby specific interactions between YscF, LcrV, and YopD promote the formation of capped needles that eventually progress toward injectisome assembly.

Phenotypes of Strep-Tagged LcrV Expressed in *Y. pestis*

Subtle differences between the type III pathways of *Y. enterocolitica* and *Y. pestis* have been reported (Ramamurthi and Schneewind 2002). First, *Y. pestis*, but not *Y. enterocolitica*, displays an LCR phenotype (Goguen, Yother, and Straley 1984; Cornelis, Vanootegem, and Sluiters 1987). Thus, low-calcium-induced activation of type III secretion in *Y. enterocolitica* does not lead to complete growth restriction even though large amounts of effectors are secreted into the extracellular medium (Michiels et al. 1990). Second, even though *lcrG* and *lcrV* encode nearly identical products in pathogenic *Yersinia*, mutations in these genes cause different phenotypes. Deletion of *Y. pestis lcrG* causes a calcium-blind phenotype, whereas deletion of *lcrV* results in an LCR$^-$ phenotype, whereby the type III secretion of effectors is abolished even when bacteria are incubated in the absence of calcium (Skryzpek and Straley 1993, 1995). In contrast, the deletion of *Y. enterocolitica lcrV* does not abrogate low-calcium-induced type III secretion of effectors

(Lee, Tam, and Schneewind 2000). These differences cannot be explained by the amino acid polymorphisms of *lcrV* products, as the expression of $lcrV_{W22703}$ in *Y. pestis* or $lcrV_{D27}$ in *Y. enterocolitica* results in wild-type phenotypes (Miller et al. 2012). The deletion of *Y. enterocolitica lcrG* causes a class I secretion phenotype (Anderson et al. 2002); although *Y. enterocolitica lcrG* mutants continue to grow, the variants secrete all effectors in both the presence and absence of calcium (Lee, Tam, and Schneewind 2000; DeBord, Lee, and Schneewind 2001).

To test whether *lcrV* alleles isolated here displayed different phenotypes in *Y. enterocolitica* and *Y. pestis*, plasmids p$lcrV_{S1}$, p$lcrV_{S20}$, p$lcrV_{S55}$, p$lcrV_{S170}$, p$lcrV_{S228}$, p$lcrV_{S270}$, and p$lcrV_{S324}$ were also transformed into *Y. pestis* strains KIM D27 and KLD29 (Δ*lcrV*). When analyzed for growth in the presence or absence of calcium, plasmids p$lcrV_{S1}$, p$lcrV_{S170}$, and p$lcrV_{S228}$ restored the LCR^- phenotype of *Y. pestis* strain KLD29 (Δ*lcrV*) to LCR^+, whereas p$lcrV_{S20}$, p$lcrV_{S55}$, p$lcrV_{S270}$, and p$lcrV_{S324}$ did not (Fig. A7). Further, p$lcrV_{S1}$, p$lcrV_{S170}$, and p$lcrV_{S228}$ complemented the type III secretion defect of the Δ*lcrV* mutant, whereas p$lcrV_{S270}$ and p$lcrV_{S324}$ blocked the secretion of both YopE and $LcrV_{S270}$ or $LcrV_{S324}$ (Table A2). Two *lcrV* plasmids produced different phenotypes in *Y. pestis* and *Y. enterocolitica*. Plasmids p$lcrV_{S20}$ and p$lcrV_{S55}$ caused a dominant negative LCR^- and effector translocation phenotype in *Y. pestis* (Fig. A7) and reduced the type III secretion of YopE (Table A2). In contrast, p$lcrV_{S20}$ and p$lcrV_{S55}$ complemented the type III secretion and effector translocation defects of the *Y. enterocolitica lcrV* mutant. In comparison with p$lcrV_{S20}$ and p$lcrV_{S55}$, p$lcrV_{S324}$ caused a stronger LCR^- phenotype in *Y. pestis* strain KIM D27 and abolished the type III secretion of YopE, similar to the effects of $lcrV_{*327W}$ and $lcrV_{*327R}$ (Tables A1 and A2).

As with data obtained with *Y. enterocolitica*, affinity chromatography of Strep-tagged LcrV on Strep-Tactin resin revealed the copurification of $LcrV_{S1}$, $LcrV_{S20}$, $LcrV_{S55}$, $LcrV_{S228}$, and $LcrV_{S324}$ with LcrG (Fig. A8*A* and *B*). As LcrG is not expressed in *Y. pestis* KLD29 (p$lcrV_{S270}$), $LcrV_{S270}$ did not copurify with LcrG. GST-LcrG was purified from the cytoplasm of *Escherichia coli* using affinity chromatography on glutathione-Sepharose (Lee, Tam, and Schneewind 2000). GST-LcrG binding to $LcrV_{S228}$, $LcrV_{S170}$, or $LcrV_{S270}$ was analyzed via chromatography of *Yersinia* lysates and immunoblotting; GST-LcrG retained $LcrV_{S228}$ and $LcrV_{S170}$ but not $LcrV_{S270}$ (Fig. A8*C*). As a control, YopB harboring a Strep tag at the N terminus was not retained during GST-LcrG chromatography (Fig. A8*C*). These data indicate that LcrV binding is required for LcrG expression. Presumably, LcrG that is not bound to LcrV is rendered unstable and may be degraded by *Yersinia*.

When analyzed for the type III injection of effectors into HeLa cells, *Y. pestis* strain KIM D27 with or without p$lcrV_{W22703}$ caused actin cable rearrangements and cell rounding (Fig. A9). Plasmids p$lcrV_{S1}$ and p$lcrV_{S228}$ did not affect the ability of *Y. pestis* KIM D27 type III machines to translocate effectors, whereas p$lcrV_{S170}$, p$lcrV_{S270}$, and p$lcrV_{S324}$ caused a dominant negative blockade of the *Y. pestis* type III pathway (Fig. A9). Of note, we observed an intermediate type III effector translocation phenotype for p$lcrV_{S20}$ and p$lcrV_{S55}$ (Fig. A9). When transformed into *Y. pestis* strain KLD29 (Δ*lcrV*), p$lcrV_{W22703}$, p$lcrV_{S1}$, and p$lcrV_{S228}$ complemented the type III injection phenotype, whereas p$lcrV_{S170}$, p$lcrV_{S270}$, and p$lcrV_{S324}$ did not. In contrast to *Y. enterocolitica*, expression of $lcrV_{S20}$ or $lcrV_{S55}$ in the *Y. pestis* Δ*lcrV* mutant did not restore function for the type III pathway (Fig. A9).

LcrV$_{S324}$ Blocks the Calcium-Blind Phenotype of *Y. pestis yscF* Needle Mutants

Earlier work revealed that *Y. pestis* YP517 *yscF*$_{D28A}$, *yscF*$_{D46A}$, and *yscF*$_{D28A,D46A}$ mutants display a calcium-blind growth phenotype and secrete effectors constitutively when bacteria are grown at 37°C (Torruellas et al. 2005). IPTG-induced expression of *lcrV*$_{S324}$ blocked the calcium-blind phenotype of *yscF*$_{D28A}$, *yscF*$_{D46A}$, and *yscF*$_{D28A,D46A}$ mutants, imposing an LCR$^-$ blockade on the type III pathway (Fig. A10 and Table A3). As a control, the expression of *lcrV*$_{S324}$ did not affect the growth of *yscF*$_{D77A}$ LCR$^-$ mutants. When we analyzed for type III secretion, we found that the expression of *lcrV*$_{S324}$ blocked the secretion of YopH in *yscF*$_{D28A}$, *yscF*$_{D46A}$, and *yscF*$_{D28A,D46A}$ mutants but did not restore the ability of the *yscF*$_{D77A}$ variant to secrete YopH (Table A3).

DISCUSSION

LcrV is the protective antigen of *Y. pestis*, and subunit vaccines that raise high-titer antibodies against this polypeptide confer protection against bubonic and pneumonic plague in mice, rats, guinea pigs, rabbits, cynomolgus macaques, and African Green monkeys (Burrows 1956; Quenee et al. 2011). Both *in vitro* and *in vivo* studies have indicated that LcrV antibodies block *Y. pestis* type III translocation of effectors into immune cells (DeBord et al. 2006; Miller et al. 2012). Studies with *Yersinia lcrV*, *yopB*, and *yopD* mutants suggest that these type III secretion substrates are each required for the translocation of effectors into host cells (Håkansson et al. 1993; Håkansson et al. 1996; Lee, Tam, and Schneewind 2000). Electron microscopy and biochemistry experiments revealed that the YscF needle of *Y. enterocolitica* is capped by LcrV and perhaps by YopD (Mueller et al. 2005). Contact of the needle with host cell membranes is thought to trigger the formation of the injectisome, a YopB-YopD complex that establishes a conduit across the plasma membrane of host cells (Broz et al. 2007; Mueller, Broz, and Cornelis 2008). Appreciation

of the molecular details and the mechanistic features of this model is necessary in order to understand why some, but certainly not all, antibodies against LcrV block effector translocation by the *Y. pestis* type III machine (Quenee et al. 2010; Miller et al. 2012). We reported recently that the ability of LcrV antibodies to block *Y. pestis* effector translocation does not extend to *Y. enterocolitica* type III machines and that the observed differences are not based on the amino acid polymorphisms in $LcrV_{W22703}$ and $LcrV_{D27}$ (Miller et al. 2012). These observations suggest that type III machines in *Y. pestis* and *Y. enterocolitica* have evolved discrete differences in injectisome assembly. Here, we used a genetic approach to initiate the analysis of LcrV features essential for injectisome assembly and effector translocation.

Exploiting *Y. pestis* LCR growth restriction, we isolated dominant negative *lcrV* mutants and observed that these variants harbored missense mutations in the amber codon at position 327, which extended the *lcrV* open reading frame by 22 codons. Neither the identity of the amino acids in the C-terminal extension nor its length appears to be critical for the type III blockade, as four or more residues with seemingly random sequences caused the same dominant negative LCR^{-} phenotype as the 22-residue extension. We achieved a similar effect by adding a C-terminal Strep tag to *Y. enterocolitica* strain W22703 and expressing $lcrV_{S324}$ in *Y. pestis*. The $LcrV_{S324}$ protein assembles as a cap on *Y. enterocolitica* YscF needles; however, the $LcrV_{S324}$-capped needles are not competent for effector translocation into HeLa cells. Unlike wild-type LcrV, $LcrV_{S324}$ needles lack YopD, suggesting that the C-terminal extension of LcrV may block the assembly of the injectisome. This assembly process appears to occur within the cap structure, as wild-type needles do not bind YopD antibodies and YopD antibodies cannot block effector translocation (Benner et al. 1999; Ivanov et al. 2008). Further, needles capped by $LcrV_{S324}$ do not bind Strep-Tactin resin or Strep tag-specific antibodies, and these needles lack the YopD component of the injectisome.

We propose a model whereby the LcrV cap of the type III needle not only interacts with YscF but also contributes to the recruitment of YopD into the injectisome.

YscF, the needle protein, is thought to function as a calcium sensor and may bind calcium ions via aspartyls 28 and 46 (Torruellas et al. 2005). *Y. pestis* type III machines harboring $YscF_{D28A,D46A}$ are calcium blind and secrete effectors even in the presence of millimolar concentrations of calcium ions, presumably because the mutant needle complexes assume the conformation of a fully activated type III pathway (Torruellas et al. 2005). The experiments illustrated in Fig. A10 demonstrate that the expression of $lcrV_{S324}$ in *Y. pestis* $yscF_{D28A,D46A}$ results in a dominant negative LCR^- phenotype and in the complete blockage of type III secretion. We surmise that $LcrV_{S324}$ is able to cap $YscF_{D28A,D46A}$ needles and lock the secretion machine in a conformation representing an inactive assembly intermediate. Such a model allows us to derive several predictions. First, $lcrV_{S324}$ may exert a dominant negative phenotype for other calcium-blind mutants capable of $LcrV_{S324}$ secretion, which may include the *yopN*, *tyeA*, *sycN*, and *yscB* mutants but not the *lcrG* mutant, which is required for LcrV secretion. Further, the contact sites between YscF and LcrV may be identified by the use of a suppressor screen for $yscF_{D28A,D46A}$ mutants, devised to restore the calcium-blind phenotype of strains also expressing wild-type *lcrV*. Lastly, the C-terminal end of LcrV may interact directly with YopD during the assemblies of the needle cap and injectisome. Of note, cap assembly does not require YopD (Mueller et al. 2005); however, without YopD (or YopB), the cap cannot advance to generate an injectisome for effector translocation (Håkansson et al. 1993).

We noted phenotypic similarities but also differences for Strep-tagged LcrV mutants expressed in *Y. enterocolitica* or *Y. pestis*. $LcrV_{S270}$ and $LcrV_{S324}$ did not complement the Δ*lcrV* phenotype in *Y. enterocolitica* or in *Y. pestis*. Further, $LcrV_{S324}$ displayed a dominant negative

LCR$^-$ phenotype as well as a block in effector translocation in both *Y. enterocolitica* and *Y. pestis*. LcrV$_{S270}$ did not bind to LcrG, and the mutant protein was not a substrate for type III secretion. The *lcrV$_{S170}$* allele complemented the LCR$^-$ phenotype of the *Y. pestis* Δ*lcrV* mutant and enabled type III secretion of YopE and LcrV$_{S170}$. Nevertheless, *lcrV$_{S170}$* failed to restore effector translocation in both *Y. pestis* and *Y. enterocolitica* Δ*lcrV* mutants. Although LcrV$_{S170}$ did not bind to Strep-Tactin resin, the mutant copurified with GST-LcrG. Taken together, these data suggest that LcrV$_{S170}$, similarly to LcrV$_{S324}$, may assemble into a needle cap that is defective for injectisome assembly. In contrast, LcrV$_{S270}$ cannot bind LcrG and appears not to be secreted by *Yersinia*. These results are in agreement with earlier work identifying residues 277, 289, and 292 as sites of 5-residue linker insertions that abolished the association between mutant LcrV and LcrG (Hamad and Nilles 2007). Finally, LcrV$_{S20}$ and LcrV$_{S55}$ are secreted by Δ*lcrV* mutant *Y. pestis* and *Y. enterocolitica*. In *Y. enterocolitica*, *lcrV$_{S20}$* and *lcrV$_{S55}$* restore YopE secretion and effector translocation, whereas in *Y. pestis*, *lcrV$_{S20}$* and *lcrV$_{S55}$* cause a dominant negative LCR$^-$ phenotype and a block in effector translocation. These data suggest that LcrV$_{S20}$ and LcrV$_{S55}$ form a functional needle cap in *Y. enterocolitica*. In contrast, LcrV$_{S20}$ and LcrV$_{S55}$ needle cap assembly may occur in *Y. pestis*; however, if formed, these caps cannot respond to the low-calcium signal or activate effector translocation. Of note, the alleles *lcrV$_{S20}$* and *lcrV$_{S55}$* enabled us to identify for the first time LcrV mutants that exert different phenotypes when expressed in *Y. enterocolitica* and *Y. pestis*. Thus, these mutants may be useful in elucidating the subtle differences between *Y. enterocolitica* and *Y. pestis* type III machines.

Sato and colleagues (2011) performed linker-scanning mutagenesis of *pcrV*, encoding the cap protein of *Pseudomonas aeruginosa* type III needles. Of note, PcrV and LcrV are 37% identical and 67% similar at the amino acid level, and the two proteins are presumed to assemble

into structures with similar functions (Broz et al. 2007; Sato and Frank 2011). The insertion of a 19-residue linker at position 119 (D^{151}), 120 (S^{152}), 131 (L^{153}), 134 (E^{156}), 138 (L^{160}), or 279 (F^{308}) of PcrV abolished effector translocation in *P. aeruginosa* (in parentheses are the corresponding residues of the $LcrV_{W22703}$ orthologue) (Sato et al. 2011). The linker insertions map to helices α7 and α12 of LcrV, and the insertions likely interfere with the binding of mutant PcrV to PcrG, the LcrG orthologue in *P. aeruginosa* (Lee et al. 2010; Sato et al. 2011).

ACKNOWLEDGEMENTS

We thank members of our laboratory for critical comments and discussion. We also thank Antoni Hendrickx for guidance with transmission electron microscopy experiments.

This work was supported by a grant (AI42797) from the National Institute of Allergy and Infectious Diseases (NIAID), Infectious Diseases Branch (to O.S.). K.G.L. was a trainee of the Graduate Training in Growth and Development program at the University of Chicago (grant HD009007). The authors acknowledge membership within and support from the Region V "Great Lakes" Regional Center of Excellence in Biodefense and Emerging Infectious Diseases Consortium (NIH Award 1-U54-AI-057153).

APPENDIX B

YFBA, A *YERSINIA PESTIS* REGULATOR REQUIRED FOR COLONIZATION AND BIOFILM FORMATION IN THE GUT OF CAT FLEAS

The material presented in this Appendix previously appeared as an article in the *Journal of Bacteriology*; it is reprinted here by permission of the publisher. The original citation is as follows:

Christina Tam, Owen Demke, Timothy Hermanas, Anthony Mitchell, Antoni P. A. Hendrickx, and Olaf Schneewind. 2014. "YfbA, a *Yersinia pestis* Regulator Required for Colonization and Biofilm Formation in the Gut of Cat Fleas." *Journal of Bacteriology* 196 (6): 1165–73. https://doi.org/10.1128/JB.01187-13.

The author contributions are as follows: C.T., O.D., T.H., A.M., and O.S. conceived the project. T.H. and A.M. generated a library of more than 7,500 transposon mutants with mapped insertional mini-Tn*5* lesions in the genome of *Y. pestis* CO92(ΔpCD1). C.T., O.D., and T.H. performed flea infection experiments and *in vitro* biofilm assays. A.P.A.H. imaged flea digestive tracts by scanning electron microscopy. C.T., O.D., T.H., A.M., and O.S. wrote the paper.

ABSTRACT

For transmission to new hosts, *Yersinia pestis*, the causative agent of plague, replicates as biofilm in the foregut of fleas that feed on plague-infected animals or humans. *Y. pestis* biofilm formation has been studied in the rat flea; however, little is known about the cat flea, a species that may bridge zoonotic and anthroponotic plague cycles. Here, we show that *Y. pestis* infects and replicates as a biofilm in the foregut of cat fleas in a manner requiring *hmsFR*, two determinants for extracellular biofilm matrix. Examining a library of transposon insertion mutants, we identified

the LysR-type transcriptional regulator YfbA, which is essential for *Y. pestis* colonization and biofilm formation in cat fleas.

INTRODUCTION

Yersinia pestis is the causative agent of plague (Yersin 1894), a frequently lethal disease that affects many mammalian species, including humans (Gage and Kosoy 2005). Plague is transmitted by fleas, which are infected during blood meals and may be colonized via a gastrointestinal biofilm (Simond 1898; Bacot and Martin 1914). Transmission of *Y. pestis* occurs when newly infected (early-phase transmission) or colonized (regurgitative transmission) insects feed on new hosts (Vetter et al. 2010; Hinnebusch 2012). Several different rodents are enzootic reservoir hosts for the plague pathogen (Gage and Kosoy 2005). Historically, epizootic outbreaks in certain rodent species have triggered flea-borne transmission of plague into human populations with devastating consequences (Eisen and Gage 2012). Examples are the Justinian plague (541 to 767), the Black Death (1346 to the 18th century), and the Asian pandemics (1850 to 1935) (Pollitzer 1951).

Genetic analysis revealed that *Y. pestis* is a monomorphic clone of its more diverse parental species, the human gastrointestinal pathogen *Yersinia pseudotuberculosis* (Achtman et al. 1999). Evolution of *Y. pestis* occurred >2,600 years ago in the rodent population of China; here, *Y. pestis* isolates are still scattered over four phylogenetic branches, biovars Orientalis, Medievalis, Antiqua, and Pestoides (Anisimov, Lindler, and Pier 2004; Morelli et al. 2010). The *Y. pestis* genome encompasses 4,012 chromosomal genes, including 149 pseudogenes and three plasmids (Parkhill et al. 2001). The pCD1 plasmid encodes the type III secretion machine for delivery of effector proteins (Yops) from the bacterium into immune cells of mammalian hosts

(Cornelis et al. 1998; Marketon et al. 2005). pFra harbors genes for the expression and assembly of capsular fraction antigen F1, a surface (pilus) organelle, and the murine toxin (Ymt), which contribute to regurgitative transmission and *Y. pestis* persistence in the flea vector (Hinnebusch et al. 2002; Sebbane et al. 2009). pPCP1 encodes the Pla surface protease, which is dispensable for *Y. pestis* survival in the flea but contributes to its escape from mammalian innate immune responses (Sodeinde et al. 1992; Hinnebusch, Fischer, and Schwan 1998). Although the functions of many genes on the three virulence plasmids have been revealed, little is known about chromosomal determinants for the unique life cycle of *Y. pestis* (Perry and Fetherston 1997).

The relevance of the oriental rat flea, *Xenopsylla cheopis*, to the transmission of plague is well established (Hinnebusch 2012). After feeding on infected blood, the flea digestive tract is eventually blocked by massive *Y. pestis* replication at the proventriculus and midgut (Bacot and Martin 1914). Since *X. cheopis* and several other flea species (for example, *Ctenocephalides felis*) are intermittent feeders, starvation causes these species to increase their feeding behavior, which is associated with transmission of *Y. pestis* to new hosts (Hinnebusch 2012). The *Y. pestis hms* locus is required for rat flea colonization, biofilm formation, intestinal blockade, and regurgitative transmission (Hinnebusch 2012); the locus comprises a four-gene operon (*hmsHFRS*) for the synthesis of poly-(β1-6)-*N*-acetylglucosamine (PNAG), an extracellular matrix polymer of *Y. pestis* biofilms (Perry, Pendrak, and Schuetze 1990; Erickson et al. 2008). Acquisition of the *hms* locus predates the evolutionary divergence of *Y. pestis* from *Y. pseudotuberculosis* (Chain et al. 2004). However, *Y. pseudotuberculosis*, but not *Y. pestis*, expresses *nghA*, which encodes a PNAG hydrolase that is thought to interfere with biofilm formation in the flea gut (Erickson et al. 2006; Erickson et al. 2008). Of note, *Y. pseudotuberculosis* infection of fleas triggers intestinal toxicity and diarrhea in *X. cheopis* (Erickson et al. 2007). Further, the *rcsA* gene, which encodes a

negative regulator for the diguanylate cyclase (HmsT) of *Y. pseudotuberculosis*, contains a 30-bp internal duplication in *Y. pestis*, rendering *rcsA* nonfunctional (Sun, Hinnebusch, and Darby 2008; Sun et al. 2012). Nevertheless, the signaling molecule cyclic di-GMP is required for *Y. pestis* PNAG synthesis and biofilm formation in the flea foregut, but not for the pathogenesis of plague disease in mammalian hosts (Bobrov et al. 2011; Sun et al. 2011). A positive transcriptional regulator for *Y. pestis* flea colonization and biofilm formation in the foregut has thus far not been identified (Hinnebusch 2012).

C. felis, the cat flea, has been investigated as a vector for plague transmission in Africa, China, and the United States (Gage et al. 2000; Eisen and Gage 2012). The host range of *C. felis* encompasses domesticated animals, household pets, squirrels, rats, and mice, as well as humans (Eisen et al. 2008). This flea species has been studied for the attribute of bridging zoonotic and anthroponotic plague cycles (Eisen et al. 2008; Graham et al. 2013). *C. felis* is a common infestation of dogs, which are infected by *Y. pestis* and seroconvert to produce F1-specific antibodies but rarely develop fatal disease (Orloski and Eidson 1995; Salkeld and Stapp 2006). Dog infestation with infected *C. felis* is associated with flea contamination of human dwellings and transmission, as documented in Uganda, China, and the United States (Kilonzo et al. 2006; Gould et al. 2008; Yin et al. 2011). Earlier work revealed the ability of *C. felis* to produce early-phase transmission of *Y. pestis* to mammalian hosts (Eisen et al. 2008). This work left unresolved whether *Y. pestis* forms persistent biofilms in *C. felis* and by what mechanism such colonization may occur.

MATERIALS AND METHODS

Bacterial Strains and Growth Conditions

Y. pestis CO92(ΔpCD1) and its mutants were grown on heart infusion agar (HIA) at 26°C and stored frozen in 5% monosodium glutamate-5% bovine serum albumin (BSA). When necessary, mutant strains were grown on selective medium containing ampicillin (100 μg/ml), kanamycin (50 μg/ml), or chloramphenicol (30 μg/ml). Where indicated, *Y. pestis* CO92(ΔpCD1) and its mutants were electroporated with plasmid pEGFP (Clontech, Palo Alto, CA).

Y. pestis Transposon Mutagenesis

To generate mini-Tn*5* transposon mutants, 50 ml of heart infusion broth (HIB) was inoculated with *Y. pestis* CO92(ΔpCD1) and grown at 26°C overnight. The following day, the cells were chilled on ice, sedimented by centrifugation, washed twice with ice-cold sterile water, and suspended at a density of 9×10^9 CFU ml^{-1} for electroporation. One microliter of purified transposase complex of the EZ-Tn*5* (Kan-2) transposon kit (Epicentre, Madison, WI) was added to 100 μl bacterial suspension and pulsed at 1,800 V, 100 Ω, 25 μF. *Y. pestis* organisms were diluted in 1 ml HIB, incubated for 4 h at 26°C, spread on HIA with kanamycin, and finally grown at 26°C for 48 h. Individual colonies were picked, propagated in HIB by overnight growth, and subjected to freezing and isolation of genomic DNA. To identify the positions of Tn*5* insertions, the genomic DNA was digested with HhaI and circularized by ligation with T4 DNA ligase. Transposon insertions were PCR amplified with primers provided with the transposon kit and submitted for DNA sequencing. DNA sequences were BLAST analyzed against the *Y. pestis* CO92 genome sequence to identify the insertion site, and gene-specific primers were designed to confirm insertion in the open reading frame (Altschul et al. 1990; Parkhill et al. 2001).

Infection of Cat Fleas with *Y. pestis*

Mixed-sex adult *C. felis* fleas were obtained from the Elward II Laboratory (Soquel, CA), separated into 50 to 100 fleas per acrylic cage, and housed in an artificial feeding system at 25°C and 75% humidity (Wade and Georgi 1988). The fleas were starved for 48 h prior to infection and fed on defibrinated sheep's blood (Hemostat, Dixon, CA) containing *Y. pestis* CO92(ΔpCD1) or its variants for 5 h at 37°C. After the initial infectious feeding period, the unfed fleas (identifiable by lack of fresh blood in the midgut and corresponding increase in body size) were removed and the remaining fleas were sustained on daily blood meals with 5 ml sheep's blood for the remainder of the study.

For infection, *Y. pestis* strains were spread on a Congo Red-heart infusion agar plate and grown at 26°C for 48 h to confirm pigmentation status. A single colony was picked, inoculated into HIB, and grown for 12 h at 26°C. The following day, the optical density was measured and the bacterial load was calculated using a conversion factor of 2.7×10^8 CFU for absorbance at 600 nm (A_{600}). Bacterial cultures were sedimented by centrifugation at 17,090 × *g* for 10 min, suspended in 1 ml of phosphate-buffered saline (PBS), and added to 4 ml of prewarmed 37°C sterile sheep's blood (1×10^8 to 1×10^{10} CFU ml^{-1}). Control cohorts of uninfected fleas were fed on 4 ml of sterile sheep's blood diluted with 1 ml PBS.

Enumeration of *Y. pestis* Organisms in Infected Fleas

Infected fleas were frozen at −80°C, surface sterilized with 70% ethanol, and placed into 2-ml vials with 6 to 8 sterile 2.3-mm steel beads (Biospec Products) and 200 μl of HIB. The fleas were mechanically disrupted using agitation in a Bead Beater (Biospec Products) for 45 s at 4.0 m/s. The vials were briefly centrifuged, and the liquid supernatant was removed, serially

diluted in PBS, spread on HIA plates, and grown at 26°C for 48 to 72 h prior to enumeration of colonies.

Flea Dissection and Microscopy

Fleas were anesthetized by chilling at −20°C for 5 min and then placed into a drop of PBS for dissection. The fleas were decapitated by prying the upper thorax and head off using two U-100 insulin syringes. The digestive tract was withdrawn from the abdomen by gently pulling on the proventriculus with fine tweezers. For microscopic imaging of the digestive tract, the flea guts were placed on a glass carrier with a drop of PBS, and coverslips were placed on top. Bright-field microscopic images were captured with a charge-coupled-device (CCD) camera using an Olympus IX81 microscope. Fluorescent images were acquired using a Leica SP5 Tandem Scanner Spectral 2-Photon confocal microscope. Images were acquired with the red Texas red (594-nm) and green green fluorescent protein (GFP) (488-nm) fluorescence channels. Images were merged using ImageJ software (NIH).

Scanning Electron Microscopy

Flea digestive tracts were isolated and fixed in 2% glutaraldehyde in PBS overnight, and then the proventriculus was cut open using a surgical scalpel. Samples were serially dehydrated by consecutive incubations in 25% and 50% ethanol-PBS, 75% and 90% ethanol-water, and 100% ethanol (twice, each step for 5 min), followed by 50% ethanol-hexamethyldisilazane (HMDS) (15 min) and 100% HMDS (20 min), which was allowed to evaporate in the final wash. After overnight evaporation of HMDS at room temperature, the samples were mounted onto specimen mounts (Ted Pella, Inc., Redding, CA) and coated with 80% Pt-20% Pd to 11 nm using

a Cressington 208HR Sputter Coater at 20 mA prior to examination with a Fei Nova NanoSEM 200 scanning electron microscope (FEI Co., Hillsboro, OR) at a distance of 5 mm.

Construction of Complementation Plasmids

The *Y. pestis* CO92(ΔpCD1) transposon mutants were complemented with plasmids expressing a wild-type copy of each gene. To generate p*yfbA*, a 1,097-bp DNA fragment containing the 191-bp upstream and 906-bp coding regions of *yfbA* from wild-type CO92(ΔpCD1) was amplified by PCR using the specific primers 5′ AAACATATGCTCCTGATG CCATCATTAATCAATTGCAGTACAG and 3′ AAAGGATCCTCACCGTTCATCCAATTG GCTGAAG. This PCR fragment was subcloned into the 5′ NdeI and 3′ BamHI sites of pMCSG7 (Amp), a high-copy-number pET vector. p2458 was generated by PCR amplification of a 1,182-bp DNA fragment from wild-type CO92(ΔpCD1) of *ypo2458* consisting of the 201-bp upstream and 981-bp coding regions of *ypo2458* using the specific primers 5′ AAACATATG ATTTTCATCACCGGGTCCTGTGAGG and 3′ AAAGGATCCCTAAAGCACAGCCGGTAG AGGTTTG. This DNA was subcloned into the 5′ NdeI and 3′ BamHI sites of pMCSG7.

To generate pP_{tac}-*yfbA*, *yfbA* was amplified using the specific primers 5′ AAAACATAT GCACGATCTCAATGATCTCTATTACTACGCAGAAGTTGTAG and 3′ AAAGGATCCTCA CCGTTCATCCAATTGGCTGAAG. This DNA fragment was cloned into the 5′ NdeI and 3′ BamHI sites of a pHSG575 derivative (Takeshita et al. 1987; Anderson and Schneewind 1997) to express *yfbA* under the control of the *tac* promoter.

Each complementing plasmid was confirmed by DNA sequencing. p*yfbA* or pP_{tac}-*yfbA* was introduced into CO92(ΔpCD1) *yfbA*::Tn*5* by electroporation. CO92(ΔpCD1) *ypo2458*::Tn*5* and

wild-type CO92(ΔpCD1) were transformed with p2458 and the pMCSG7 empty vector, respectively, via electroporation. The presence of the complementing plasmids in the mutant strains was confirmed by PCR.

In Vitro Biofilm Analysis

Strains were grown overnight in HIB supplemented with the relevant antibiotics, 4 mM $CaCl_2$, and 4 mM $MgCl_2$. The following day, the cultures were subcultured to an A_{600} of 0.02, and 10 replicates of 200 µl each were plated in treated Costar polystyrene 96-well plates in HIB supplemented with 4 mM $CaCl_2$ and 4 mM $MgCl_2$ with 1 mM IPTG (isopropyl-β-D-thiogalactopyranoside) added to the pP_{tac}-*yfbA* culture. A row of medium-only wells was used as a control for background absorbance. The plates were incubated at 26°C with shaking at 250 rpm for 24 h. Planktonic cells were removed, and the wells were washed two times with H_2O and stained for 15 min with crystal violet (0.02%). The stain was removed, the wells were washed four times with H_2O, and the bound crystal violet was solubilized with an 80% ethanol-20% acetone solution. Absorbance was measured at 600 nm using a Synergy HT plate reader (Biotek), and the average absorbance from the medium-only control wells was subtracted from the recorded absorbances to obtain the final measurements.

Fluorescence Microscopy of *Y. pestis* Biofilms

Y. pestis biofilms were grown on 18-mm round glass coverslips pretreated with 1 µg/ml human fibronectin (Sigma) in Costar 12-well polystyrene plates. The wells were washed two times with PBS before adding 400 µl of *Y. pestis* CO92(ΔpCD1) or its *yfbA*::Tn*5* variant to an A_{600} of 0.02. The plates were incubated at 26°C for 24 h with shaking at 250 rpm. Glass coverslips were

washed twice with PBS and stained with 5 μM Syto9 (Invitrogen) at room temperature for 20 min. The coverslips were washed twice and fixed with 4% formalin before washing, drying, and mounting on glass slides with 1 μl SlowFade Gold (Invitrogen). Fluorescent images of biofilms were acquired in the green GFP channel (488 nm) on an Olympus IX81 microscope using a 40× objective and captured with a CCD camera.

RESULTS

Y. pestis Infection and Colonization of *C. felis*

Mixed-sex adult *C. felis* fleas (n = 50 to 100 fleas) were isolated in acrylic cages at 25°C and starved for 48 h prior to feeding on defibrinated sheep's blood mixed with 1×10^8 CFU ml^{-1} *Y. pestis* CO92(ΔpCD1) or its variants. Blood samples were maintained for 5 h at 37°C in a humidified feeding chamber (artificial dog) during feeding (Noden et al. 1998). The fleas were subsequently fed daily on defibrinated sheep's blood without added bacteria and analyzed for *Y. pestis* colonization. To determine the *Y. pestis* load in the gut, flea homogenates were spread on agar plates and the bacteria were enumerated. These studies revealed that the flea guts harbored 1.47×10^2 CFU *Y. pestis* CO92 1 h after the end of feeding (Fig. B1*A*). Between 24 h and 3 days postinfection, *Y. pestis* was able to replicate inside the fleas (Fig. B1*A*). At day 7 after feeding, the bacterial load increased to 2.89×10^4 CFU (Fig. B1*A*). Increases in the bacterial load were correlated with decreased flea survival. By day 14, more than 60% of the infected flea population succumbed to *Y. pestis* infection (Fig. B1*C*). Approximately half of all infected cat fleas (49%) were not colonized by wild-type *Y. pestis* CO92(ΔpCD1) (see below). The *Y. pestis*(ΔpCD1, Δ*hmsF*) mutant lacks the (β1-6)-*N*-acetylglucosamine deacetylase (HmsF) required for functional assembly of PNAG and biofilm formation (Forman et al. 2006). When the *Y. pestis hmsF* mutant

was used for infection of *C. felis*, 1.5×10^2 CFU were isolated 1 h after feeding, similar to wild-type *Y. pestis* (Fig. B1*A*). This observation indicates that both wild-type and *hmsF* mutant *Y. pestis* CO92 infect cat fleas, in agreement with the recent report that *C. felis* is capable of early-phase plague transmission between mammalian hosts (Vetter et al. 2010). Nevertheless, the *hmsF* mutant did not replicate in the flea gut and did not affect the survival of infected *C. felis* compared to mock-infected insects (Fig. B1*C*).

Y. pestis Forms a Biofilm in the Proventriculus of *C. felis*

Y. pestis-infected or mock-infected cat fleas were immobilized and viewed by light microscopy (Fig. B2). While the guts of mock-infected fleas could be discerned as a red (hemin-colored) contour within the flea body, the gut of *Y. pestis* CO92(ΔpCD1)-infected fleas appeared as dark-brown-stained material (Fig. B2*A* and *B*). The latter was difficult to discern against the pigmented chitin bodies of the insects. To analyze the flea gut, insects were decapitated, the intestines were removed, and the proventriculus and midgut were viewed by microscopy (Fig. B2*C* to *E*). In uninfected fleas, the esophagus and proventriculus could be discerned by their characteristic shape and dense structure, respectively (Fig. B2*C*). The midgut of cat fleas presented as an amorphous, bag-like structure connected to the proventriculus, which was filled with granular, light-brown-pigmented material (Fig. B2*C*). Immediately following *Y. pestis* infection, the esophagus, proventriculus, and midgut of cat fleas were not affected compared to uninfected *C. felis*. On day 3, dark-brown pigment was detected on the proventriculus of *Y. pestis*-infected fleas (Fig. B2*D*). By day 14, most of the midgut was filled with the dark-brown pigmented material (Fig. B2*E*). In *X. cheopis*, this pigmented material was previously shown to represent *Y. pestis* biofilm (Jarrett et al. 2004).

To discern whether the dark-brown-pigmented material in the proventriculus and midgut of cat fleas indeed represented *Y. pestis* biofilms, wild-type and *hmsF* mutant strains were transformed with pEGFP, a plasmid providing for constitutive expression of GFP. Following infection of fleas with wild-type or *hmsF* mutant *Y. pestis* CO92(ΔpCD1, pEGFP), the fleas were dissected, and their intestines were examined by fluorescence microscopy. *C. felis* displayed GFP fluorescence in the proventriculus on day 3 for wild-type- but not *hmsF* mutant-infected insects (Fig. B3*A* to *F*). On day 7, GFP fluorescence had expanded into large aggregates in the proventriculus and midgut of fleas infected with wild-type *Y. pestis* (Fig. B3*G* to *I*). *C. felis* infected with the *hmsF* mutant harbored only weak GFP fluorescence signals in the flea midgut (Fig. B3*A* to *C*).

To obtain further evidence for the formation of biofilms in the proventriculus of cat fleas, we analyzed the foregut of mock- or *Y. pestis*-infected *C. felis* by scanning electron microscopy. Individual bacteria, as well as large clumps of bacterial masses, could be detected at the tip and along the spines of the proventriculus of infected *C. felis* (Fig. B3*J*). The spines in the proventriculus of uninfected *C. felis* were not associated with bacterial deposits (Fig. B3*K*). Taken together, these data indicate that wild-type *Y. pestis* forms a biofilm on the proventriculus and in the midgut of infected *C. felis*. Biofilm formation likely requires the production of PNAG, as *hmsF* mutant *Y. pestis* cannot persistently colonize cat fleas or assemble as bacterial aggregates within an extracellular matrix (Fig. B1*B*). In contrast, wild-type *Y. pestis* formed massive intestinal biofilms in up to 60% of infected fleas (Fig. B1*B*).

The *Y. pestis* Mutant Is Defective for *In Vitro* Biofilm Formation

We sought to identify other genes required for *Y. pestis* replication in *C. felis*. Assuming that genes required for bacterial biofilm growth *in vitro* may also be required for flea colonization, a library of mutants with insertional mini-Tn*5* lesions in the genome of *Y. pestis*(ΔpCD1) was generated and screened for defects in *in vitro* biofilm formation. As reported earlier, *Y. pestis*(ΔpCD1) forms biofilms during stationary growth at 26°C, which can be detected and quantified by crystal violet staining and A_{600} (Kirillina et al. 2004). As controls, *Y. pestis* CO92(ΔpCD1) formed a robust biofilm, whereas the *hmsR*::Tn*5* mutant, which catalyzes the polymerization of poly-β(1-6)-*N*-acetylglucosamine in the cytoplasmic membrane (Gerke et al. 1998; Forman et al. 2006), did not (Fig. B4*A*). *hms* mutants, such as an *hmsR*::Tn*5* mutant, were also detected via a nonpigmentation phenotype when grown at 26°C on Congo Red agar plates (Fig. B4*E*); Congo Red staining identifies PNAG, the *Y. pestis* exopolysaccharide (Kirillina et al. 2004) (Fig. B4*D*). The *Y. pestis* mutant with an insertional lesion in *ypo2150*, here designated *yfbA* (Y*ersinia pestis f*lea *b*iofilm regulator *A*), failed to form biofilms when grown as static *in vitro* cultures, similar to the *hmsR* variant (Fig. B4*A*). This defect could also be visualized with fluorescence microscopy of Syto9-stained static cultures, comparing wild-type and *yfbA* mutant biofilms (Fig. B4*B* and *C*). The biofilm defect of the *yfbA* mutant could be complemented in *trans* with plasmid-borne expression of wild-type *yfbA* (p*yfbA*) or IPTG-induced expression from the P_{tac} promoter (pP_{tac}-*yfbA*) (Fig. B4*A*). Of note, the *Y. pestis yfbA*::Tn*5* mutant formed red colonies on Congo Red agar plates, indicating that the gene and its product are not required for the biosynthesis of PNAG (Fig. B4*E* to *G*). Tn*5* insertions in two other genes, *ypo2458* and *ypo3682*, also caused a reduction of *in vitro* biofilm formation, although the phenotype was not as pronounced as in *yfbA* and *hmsR* mutant *Y. pestis* (Fig. B4*A*).

yfbA Is Required for *Y. pestis* Colonization of *C. felis*

yfbA, ypo2458, and *ypo3682* encode LysR-type transcriptional regulators (LTTRs) (Henikoff et al. 1988; Parkhill et al. 2001). Earlier work by Vadyvaloo and colleagues (2010) and Sebbane and colleagues (2006) examined the expression of *Y. pestis* KIM (Medievalis) genes with microarray studies using *in vitro* growth at 26°C and 37°C, as well as in the gut of *X. cheopis* fleas or rat bubos. This work revealed the expression of *yfbA* (*y2171*)*, ypo2458* (*y1731*), and *ypo3682* (*y0181*) in the flea gut but not in rat bubos (Vadyvaloo et al. 2010). LTTRs encompass an N-terminal DNA-binding helix-turn-helix motif and a C-terminal coinducer binding domain (Maddocks and Oyston 2008). LTTRs dimerize and bind DNA, thereby increasing the affinity of RNA polymerase for specific promoters. Their transcriptional activity can be restricted to either individual genes or many dozens of different genes (Maddocks and Oyston 2008).

We wondered whether *yfbA, ypo2458*, or *ypo3682* is required for *Y. pestis* colonization of *C. felis*. Fourteen days after infection, cat fleas were homogenized and analyzed for their bacterial loads. Compared to fleas infected with wild-type *Y. pestis*, the *yfbA* mutant displayed a reduced bacterial load ($P < 0.0001$) in the flea gut (Fig. B5*A*). This defect was complemented by plasmid-borne expression of *yfbA* (p*yfbA*) (Fig. B5*A*). Whereas 51% of infected cat fleas were colonized with wild-type *Y. pestis*, only 8% of infected fleas were colonized with the *yfbA* mutant (Fig. B5*B*). This colonization defect was in part restored by the plasmid-borne expression of *yfbA* (p*yfbA*) (Fig. B5*B*). As expected, the *hmsR* mutant was also defective in colonizing cat fleas (Fig. B5*A* and *B*). *Y. pestis ypo2458* or *ypo3682* encodes other members of the LTTR family of transcriptional regulators (Parkhill et al. 2001). Similar to *yfbA* (*ypo2150*), *Y. pestis ypo2458* or *ypo3682* is preferentially expressed in the gut of *Y. pestis* KIM-infected *X. cheopis* (Vadyvaloo et al. 2010). Though *Y. pestis ypo2458* and *ypo3682* mutants showed a reduction in biofilm formation

in an *in vitro* assay, these mutants did not display defects in the colonization of the intestines of infected cat fleas (Fig. B5*A* and *B*).

yfbA Is Required for *Y. pestis* Biofilm Formation in Infected *C. felis*

To examine the ability of the *Y. pestis yfbA* mutant to form biofilms in the proventriculus, infected cat fleas were examined by microscopy (Fig. B6). Compared to fleas infected with wild-type *Y. pestis* CO92(ΔpCD1) (42% biofilm formation), only 6% of *C. felis* fleas infected with the *yfbA* mutant harbored biofilms (Fig. B5*C*). This defect was in part complemented in *Y. pestis yfbA*(p*yfbA*) (Fig. B5*C*). As a control, the *hmsR* mutant did not form biofilms in any of the infected fleas (Fig. B5*C*). Representative images of infected flea guts and biofilm formation are shown in Fig. B6.

DISCUSSION

Y. pestis infects many mammalian species, including humans, and remains endemic as a zoonotic pathogen in African, North and South American, and Asian countries (Gage and Kosoy 2005). Although *Y. pestis* causes pandemic disease outbreaks in humans and remains a public health threat, plague is primarily a disease of rodents and their fleas. Rodent species are highly variable in their susceptibilities, ranging from enzootic species with high-level prolonged resistance to plague, e.g., the great gerbil (*Rhombomys opimus*) in Kazakhstan, to epizootic, highly susceptible species (black-tailed prairie dog) (Davis et al. 2004; Webb et al. 2006). Plague transmission cycles were modeled, and infected off-host fleas, where *Y. pestis* can survive for more than a year (Bazanova and Maevskii 1996), are thought to play important roles in maintaining enzootic cycles (Buhnerkempe et al. 2011). Off-host questing fleas may become infected and

transmit plague to new hosts, which may precipitate epizootic outbreaks from on-host fleas that transiently maintain high infectious loads of *Y. pestis* through repeated infectious feeds (Buhnerkempe et al. 2011). Early-phase transmission by fleas can drive plague dynamics at the population level; however, late-phase regurgitative transmission also contributes to plague persistence and outbreaks (Bacot and Martin 1914; Eisen et al. 2006; Buhnerkempe et al. 2011; Eisen and Gage 2012; Hinnebusch 2012).

C. felis, the cat flea, is one of the most abundant and widespread flea species (Eisen et al. 2008). Cat fleas are capable of being infected with *Y. pestis* and promoting early-phase transmission of plague disease between animals and perhaps also animals and humans (Eisen et al. 2008). *C. felis* has been investigated as a vector for plague transmission in Africa, China, and the United States (Gage et al. 2000; Eisen and Gage 2012). Cat fleas feed on domesticated animals, household pets, squirrels, rats, and mice, as well as humans (Eisen et al. 2008). Cat fleas can also be categorized by their behavior in leaving their hosts after feeding and remaining on the floors of animal burrows or human dwellings, where they could serve as an off-host vector for plague transmission (Graham et al. 2013). Although cat fleas promote early-phase transmission of *Y. pestis,* a specific mechanism or gene required for cat flea colonization or transmission of plague was heretofore not known (Eisen et al. 2008). Here, we show that *Y. pestis* colonizes cat fleas and forms biofilms in its proventriculus and midgut, which may contribute to the accelerated mortality of infected fleas. Using a library of *Y. pestis* CO92(ΔpCD1) mutants with insertional Tn*5* lesions and screening for *in vitro* biofilm defects, we identified three genes whose expression is required for efficient biofilm growth: *ypo2150*, *ypo2458*, and *ypo3682*. All three genes encode LTTRs, and *Y. pestis* KIM5 microarray studies revealed that these genes are expressed in the gastrointestinal tract of infected *X. cheopis* fleas (Vadyvaloo et al. 2010). However, when examined for their

contribution to *Y. pestis* colonization and biofilm formation in the intestinal tract of cat fleas, only *ypo2150*, but not *ypo2458* and *ypo3682*, was required. We have designated *ypo2150 yfbA* (Y*ersinia pestis f*lea *b*iofilm *A*), as the gene appears to contribute to efficient colonization and biofilm formation by *Y. pestis* in cat fleas. It seems plausible that *yfbA* may control the expression of a still unidentified biofilm or colonization factor. Similar phenotypes have been reported for two regulatory factors, PhoP (a two-component response regulator) and Hfq (a bacterial RNA binding protein), when studying biofilm formation in the rat flea (Rempe, Hinz, and Vadyvaloo 2012; Rebeil et al. 2013).

Y. pestis biofilm formation in the intestinal tract of *X. cheopis* is dependent on the *hmsHFRS* genes and production of PNAG, an extracellular polysaccharide (Hinnebusch 2012). In some fleas, biofilm formation leads to blockage of the gut. Blocked or partially blocked fleas accumulate blood meals in the esophagus and may regurgitate blood mixed with biofilm material during feeding; this may contribute to the transmission of *Y. pestis* to new hosts (Bacot and Martin 1914; Hinnebusch 2012). Work over the past 2 decades identified several genetic traits of *Y. pestis* that are required for either colonization or biofilm formation and blockage of the intestinal tract of *X. cheopis*, including the *ymt*, *hfq*, *gmhA*, and *rcs* genes, as well as genes involved in the synthesis and regulation of the second messenger cyclic di-GMP. The contributions of two diguanylate cyclase genes (*hmsT* and *hmsD*), as well as *hmsP*, which encodes a cyclic di-GMP phosphodiesterase, and of the Rcs phosphorelay system are to the regulation of PNAG production (Kirillina et al. 2004; Bobrov et al. 2011; Sun et al. 2011; Sun et al. 2012). However, the contributions of *ymt*, *hfq*, and *gmhA* genes cannot be explained as regulators of *hmsHFRS*. Hfq is a cytoplasmic protein that binds many different small RNAs and controls their stability and regulatory attributes (Koo et al. 2011; De Lay, Schu, and Gottesman 2013). *Y. pestis hfq* is

expressed both in the mammalian host and in flea intestines (Lemaître et al. 2006; Vadyvaloo et al. 2010); however, a specific RNA(s) that supports bacterial adaptation to the flea gut is not yet known (Rempe, Hinz, and Vadyvaloo 2012). *Y. pestis ymt* encodes cytoplasmic phospholipase D, which is not required for laboratory growth or the pathogenesis of plague in mice (Hinnebusch et al. 2002). *Y. pestis ymt* mutants are eliminated from the flea gut and assume a spheroplast-like morphology, suggesting that phospholipase D may be responsible for neutralizing a toxic compound in flea intestines (Hinnebusch 2003). Finally, *gmhA*, encoding a phosphoheptose isomerase, is thought to promote lipopolysaccharide (LPS) biosynthesis, and a *gmhA* mutant cannot effectively block the proventriculus of infected fleas (Darby et al. 2005).

Douglas and Wheeler (1943) studied the capacity of *C. felis* to become infected with *Y. pestis* and to transmit plague from infected guinea pigs or mice to healthy animals. This work suggested that cat fleas may become infected but are not blocked following *Y. pestis* infection (Douglas and Wheeler 1943). While infected *C. felis* fleas were capable of early-phase transmission with mass-infected fleas, two trials with small numbers of fleas (either 6 or 8 *C. felis* fleas) did not show transmission of *Y. pestis*, suggesting that cat fleas have low transmission potential (Wheeler and Douglas 1945). Using an artificial feeding system with defribrinated sheep's blood, we show here that about 50% of infected *C. felis* fleas are colonized and eventually blocked, which was associated with diminished survival of colonized fleas. We have not examined blocked *C. felis* for its ability to transmit *Y. pestis* to mammalian hosts. If one considers the abundance and global distribution of *C. felis* and its propensity as a questing, off-host species to feed on domesticated animals, rodents, and humans, a more thorough investigation of cat fleas as a vector for early-phase and late-phase transmission of plague seems warranted. The foundation

for such studies is provided here, as we demonstrate both early-phase colonization and late-phase biofilm formation in *Y. pestis*-infected cat fleas.

ACKNOWLEDGEMENTS

We thank Lauriane Quenee, Bill Blaylock, and members of our laboratory for experimental assistance, critical comments, and discussion.

This project has been funded in whole or in part with Federal funds from the National Institute of Allergy and Infectious Diseases, National Institutes of Health, Department of Health and Human Services, under grant/contract no. U19 AI107792 and RO1AI042797. We acknowledge membership of and support from the Region V Great Lakes Regional Center of Excellence in Biodefense and Emerging Infectious Diseases Consortium (NIH award 1-U54-AI-057153).

APPENDIX C

FIGURES

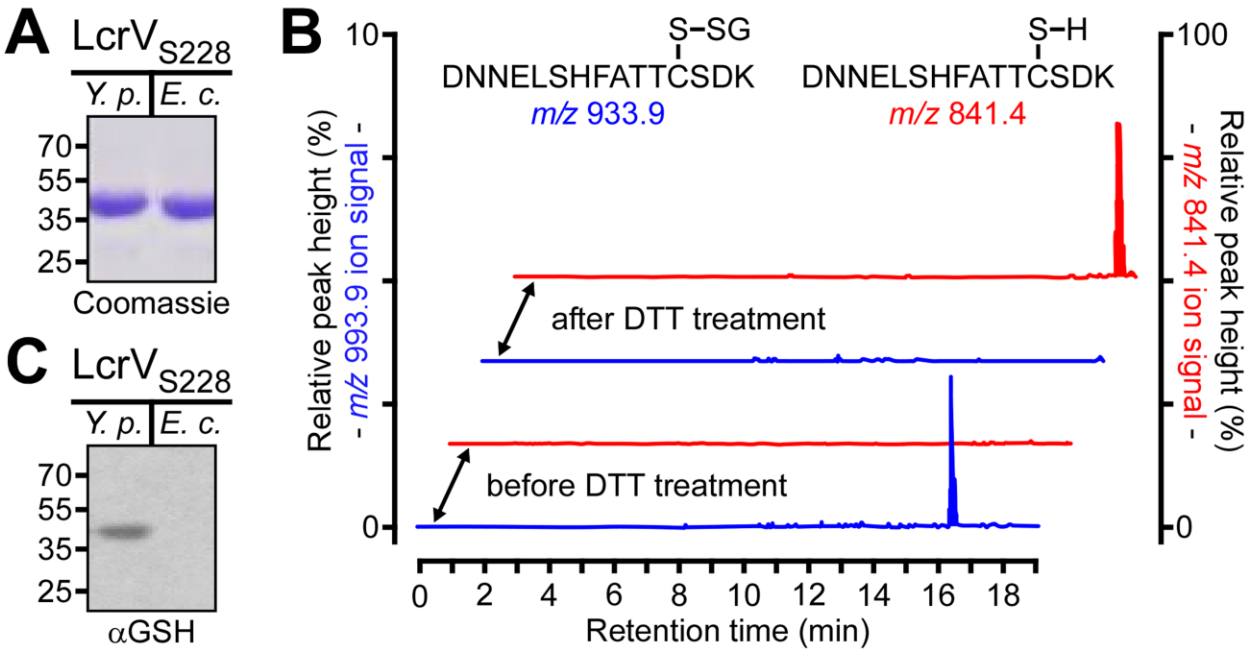

Figure 1. LcrV secreted by *Y. pestis* is glutathionylated at Cys^{273}. (*A*) Coomassie-stained SDS-PAGE of LcrV$_{S228}$ purified via Strep-Tactin affinity chromatography from either the culture supernatant of *Y. pestis* KLD29(pKG48) (*Y.p.*) or cell lysates of *E. coli* DH5α(pKG48) (*E.c.*). (*B*) Reconstructed ion traces for the unmodified (*m/z* 841.4) [(M + 2H)$^{2+}$ ion of 1,680.71] and glutathione-modified (*m/z* 993.9) [(M + 2H)$^{2+}$ ion of 1,985.79] tryptic peptides from the *Y. pestis* LcrV$_{S228}$ protein encompassing Cys^{273} before and after treatment with dithiothreitol (DTT). The chromatograms show the absence of the unmodified peptides and the presence of the glutathione-modified peptides before treatment and, following DTT treatment, the presence of the unmodified peptides and the absence of the glutathione-modified peptides. (*C*) LcrV$_{S228}$ purified from *Y. pestis* culture supernatants or *E. coli* extracts (rLcrV$_{S228}$) was analyzed by immunoblotting with glutathione-specific antiserum (αGSH).

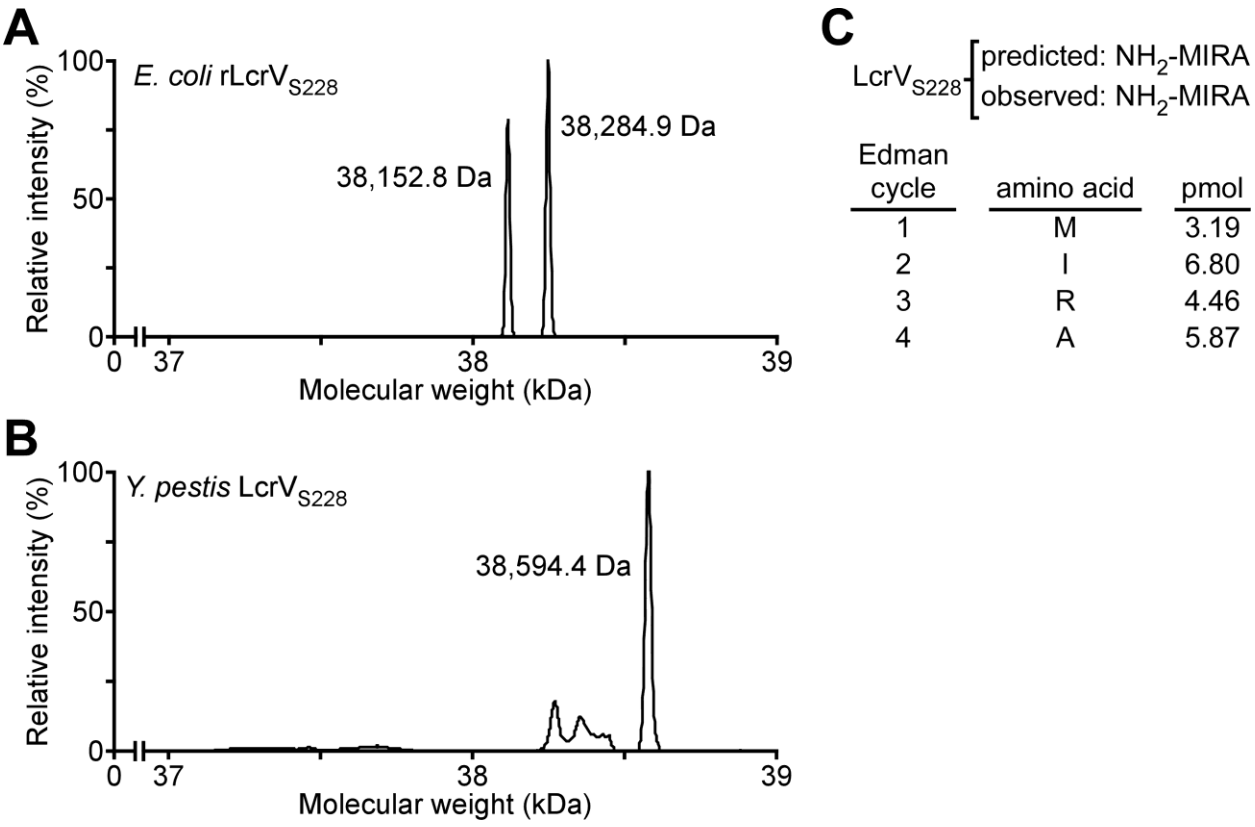

Edman cycle	amino acid	pmol
1	M	3.19
2	I	6.80
3	R	4.46
4	A	5.87

Figure 2. Mass determination and Edman sequencing of LcrV$_{S228}$. (*A* and *B*) Molecular mass spectra of (*A*) rLcrV$_{S228}$ purified from cell extracts of *E. coli* DH5α(pKG48) or (*B*) LcrV$_{S228}$ purified from culture supernatants of *Y. pestis* KLD29 Δ*lcrV*(pKG48) were reconstructed from the multiply charged ions recorded during combined liquid chromatography-electrospray ionization mass spectrometry (LC-ESI-MS). (*A*) The representative molecular mass spectrum of *E. coli* rLcrV$_{S228}$ reveals a predominate isoform with a measured mass of 38,284.9 ± 1.4 Da, which corresponds to the full-length LcrV$_{S228}$ protein, and a second isoform with a measured mass of 38,152.8 ± 1.5 Da, which corresponds to the LcrV$_{S228}$ protein lacking the initiator methionine residue. Data are means ± standard errors of the means (SEM) ($n = 9$). (*B*) A representative molecular mass spectrum of *Y. pestis* LcrV$_{S228}$ reveals a single predominate isoform with a measured mass of 38,594.4 ± 2.3 Da, which is 314.2 Da heavier than the calculated mass for

Figure 2 (*continued*)

full-length $LcrV_{S228}$. Data are means ± SEM ($n = 6$). (*C*) $LcrV_{S228}$ was purified from *Y. pestis* supernatants and subjected to Edman sequencing; the preponderant N-terminal amino acid released for each cycle (and its picomole abundance) is listed.

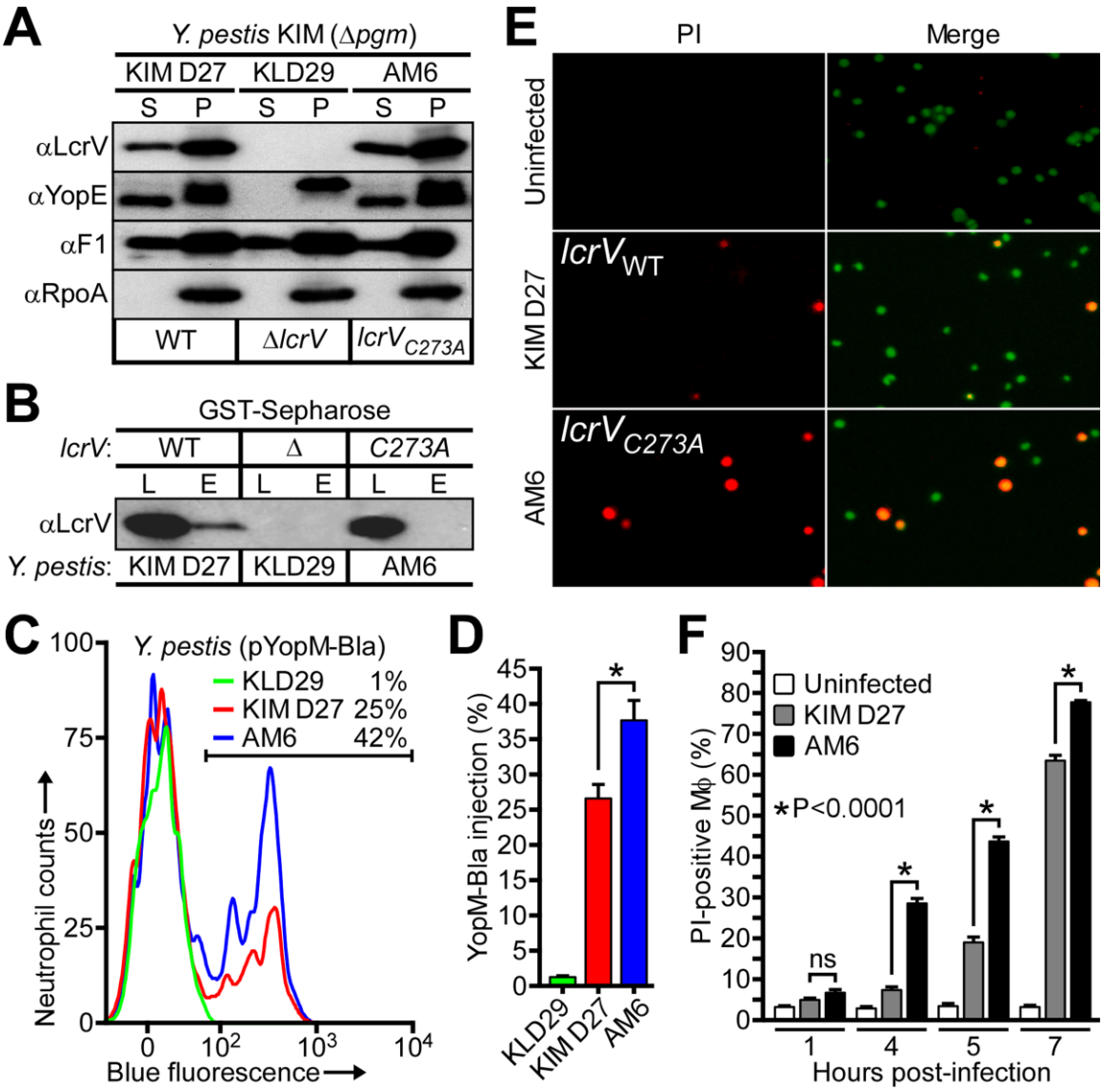

Figure 3. The *lcrV*$_{C273A}$ mutation abolishes LcrV glutathionylation and accelerates *Y. pestis*-mediated macrophage death. (*A*) *Y. pestis* KIM D27 *lcrV*, KLD29 Δ*lcrV*, and AM6 *lcrV*$_{C273A}$ were induced for type III secretion by growth at 37°C in M9-Casamino Acids (M9-Ca) minimal medium lacking exogenous calcium ions. Proteins in the supernatant (S) and bacterial pellet (P) were separated by centrifugation and identified by immunoblotting with rabbit antibodies specific for type III secretion substrates (LcrV and YopE), the secreted F1 pilus subunit (F1), and, as a fractionation control, cytoplasmic RNA polymerase subunit A (RpoA). (*B*) LcrV secreted by the

Figure 3 (*continued*)

indicated *Y. pestis* strains was assayed for glutathionylation by subjecting the culture supernatant to GST-Sepharose affinity chromatography. The load (L) and eluate (E) fractions were analyzed by immunoblotting with anti-LcrV. (*C* and *D*) Type III effector (YopM-Bla)-mediated cleavage of CCF2-AM-stained human polymorphonuclear leukocytes infected with *Y. pestis* KIM D27(pYopM-Bla), KLD29(pYopM-Bla), or AM6(pYopM-Bla) was analyzed via flow cytometry for blue fluorescence (YopM-Bla cleavage of CCF2-AM). (*C*) Representative histograms show the blue fluorescence traces of *Y. pestis*-infected neutrophils; the percentage of YopM-Bla-injected neutrophils (blue cells) is indicated above the gating scheme that was used to measure blue fluorescence above background. (*D*) Percentage of quantification of YopM-Bla-injected human neutrophils. Data are means ± SEM ($n = 3$). *, $P < 0.05$, by two-tailed unpaired Student's *t* test. (*E* and *F*) The kinetics of host cell death were examined by infecting murine J774.A1 macrophages with *Y. pestis* KIM D27 or AM6 and enumerating propidium iodide (PI)-positive cells. (*E*) Macrophages, either left uninfected or infected with *Y. pestis* KIM D27 or AM6, were stained with membrane-permeant (Hoechst [blue]) and membrane-impermeant (PI [red]) dyes and analyzed by fluorescence microscopy to determine *Y. pestis*-mediated macrophage death (PI positive, red, and Hoechst positive, magenta). (*F*) The kinetics of cell death were examined by quantifying PI-positive macrophages at timed intervals following *Y. pestis* infection. Data are means ± SEM ($n = 3$). *, $P < 0.0001$, and ns, not significant, by two-tailed unpaired Student's *t* test.

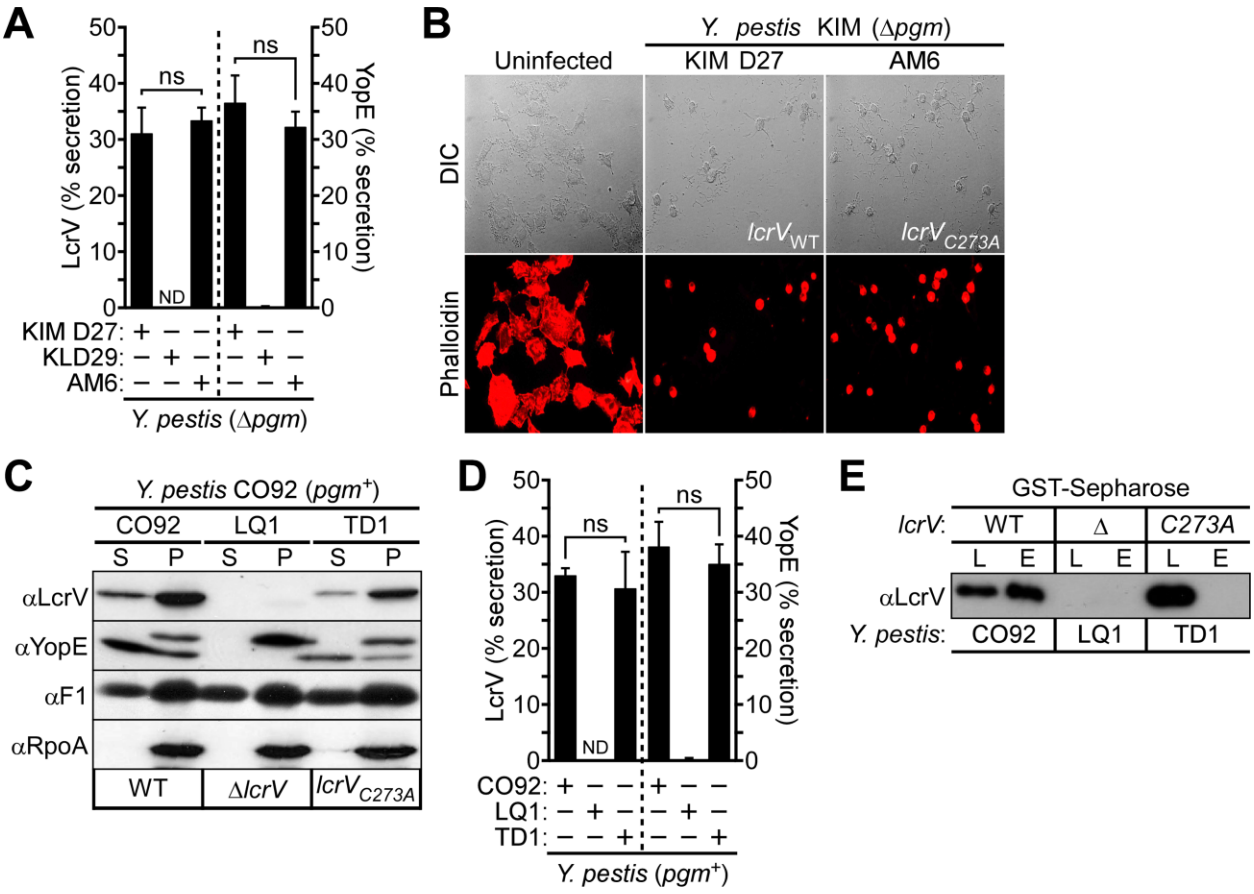

Figure 4. The codon substitution Cys^{273}Ala, which precludes LcrV glutathionylation, does not affect *Y. pestis* type III secretion of Yop effectors. (*A*) Densitometric quantification of LcrV and YopE secreted by *Y. pestis* KIM D27 (Δ*pgm lcrV*), KLD29 (Δ*pgm* Δ*lcrV*), and AM6 (Δ*pgm* $lcrV_{C273A}$) following growth at 37°C in M9-Ca minimal medium in the absence of exogenous calcium ions. The immunoreactive signal of each secreted protein (S) was normalized to its total abundance in the medium and pellet (S + P); the ratio of secreted protein to total protein, (S) / (S + P), is presented as a percent average. ND, no immunoreactive signal detected. (*B*) Compared to uninfected HeLa cells, infection by *Y. pestis* KIM D27 or AM6 causes actin cable rearrangements and cytotoxicity (cell rounding) as detected by differential interference contrast (DIC) or fluorescence microscopy of rhodamine-phalloidin-stained cells. (*C* and *D*) *Y. pestis*

Figure 4 (*continued*)

CO92 *pgm*$^+$ *lcrV*, LQ1 *pgm*$^+$ Δ*lcrV*, and TD1 *pgm*$^+$ *lcrV*$_{C273A}$ were induced for type III secretion by growth at 37°C in M9-Ca minimal medium with chelated calcium ions; secreted proteins (S) were separated from intact bacteria (pellet [P]) by centrifugation. (*C*) Representative immunoblot analysis was performed by probing fractions with antibodies specific for type III secretion substrates (LcrV and YopE), the secreted F1 pilus subunit (F1), and a cytoplasmic fractionation control (RpoA). (*D*) The percentage of secretion of LcrV and YopE was determined by densitometry. ND, no immunoreactive signal detected. (*E*) LcrV secreted by the indicated *Y. pestis* strains was assayed for glutathionylation by subjecting the culture supernatant to GST-Sepharose affinity chromatography. The load (L) and eluate (E) fractions were analyzed by immunoblotting with anti-LcrV. All data are means ± SEM ($n = 3$). ns, not significant by two-tailed unpaired Student's *t* test.

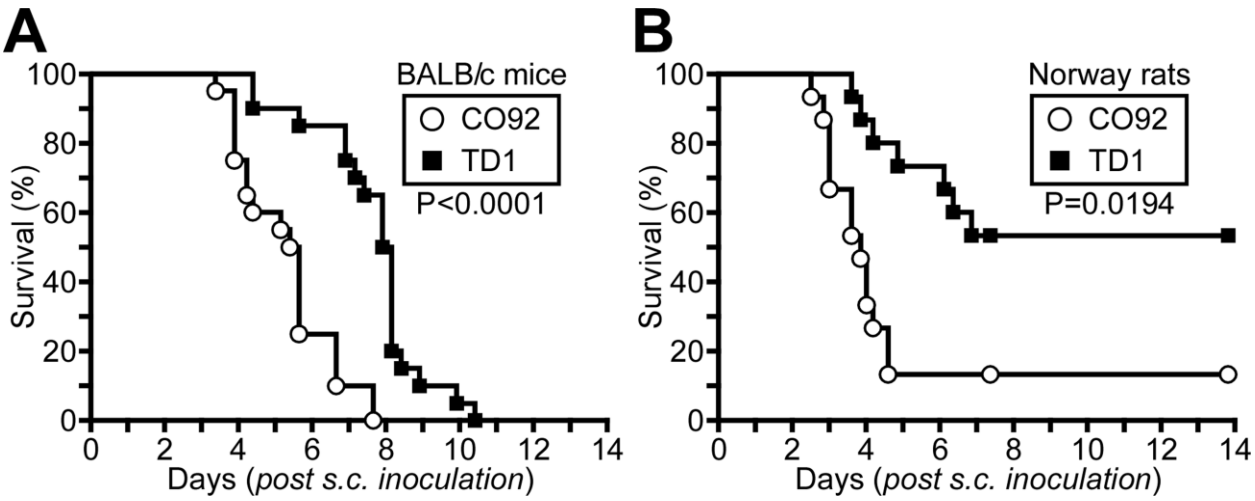

Figure 5. Glutathionylation of LcrV enhances bubonic plague pathogenesis. (*A*) Survival of cohorts of BALB/c mice ($n = 20$) infected via subcutaneous (s.c.) inoculation with 20 CFU of *Y. pestis* CO92 *lcrV* or *Y. pestis* TD1 $lcrV_{C273A}$. WT versus $lcrV_{C273A}$, $P < 0.0001$. (*B*) Survival of cohorts of Brown Norway rats ($n = 15$) infected via subcutaneous inoculation with 500 CFU of *Y. pestis* CO92 or TD1. WT versus $lcrV_{C273A}$, $P = 0.0194$. Statistical analysis was performed using the Gehan-Breslow-Wilcoxon test. Data are representative of two independent experiments.

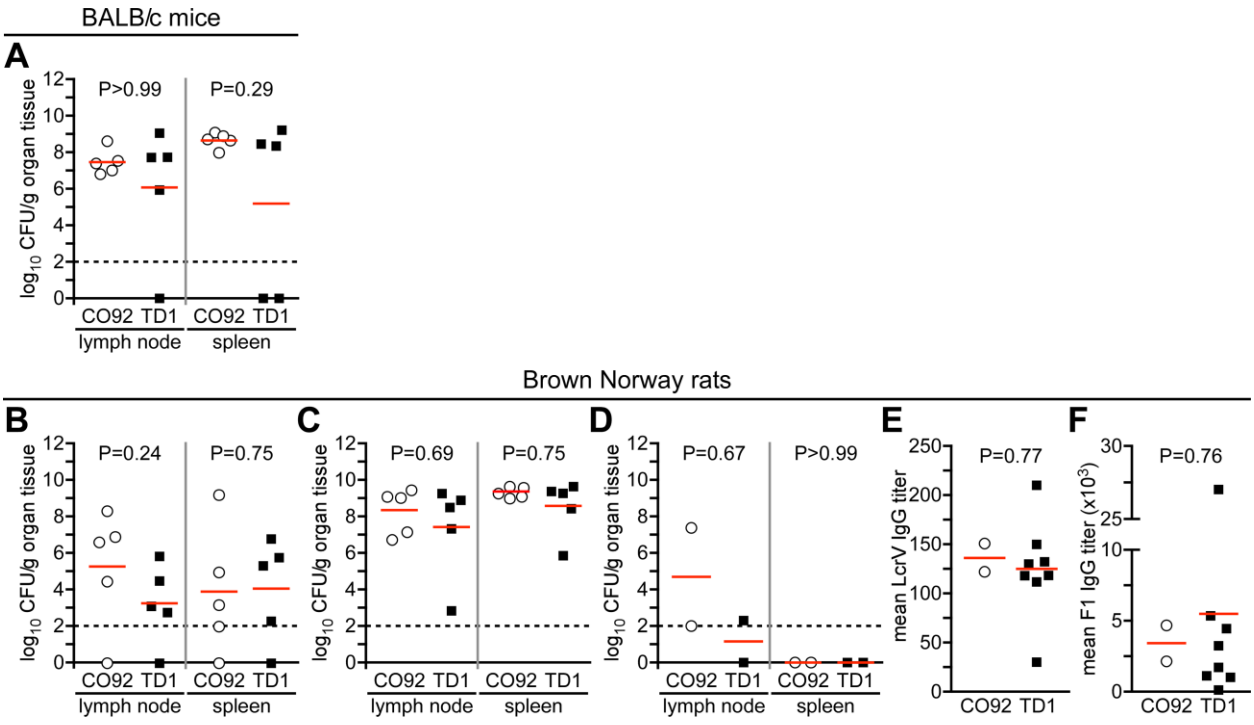

Figure 6. Kinetics of disease progression and host adaptive immune responses in bubonic plague-infected rodents. (*A*) BALB/c mice or (*B* to *F*) Brown Norway rats were infected by subcutaneous injection into the left inguinal fold with 20 CFU or 500 CFU, respectfully, of *Y. pestis* CO92 *pgm*$^+$ *lcrV* or *Y. pestis* TD1 *pgm*$^+$ *lcrV*$_{C273A}$. (*A*) Bacterial load in the regional lymph node and spleen of moribund BALB/c mice (n = 5) that were euthanized between 4 and 7 days postchallenge after exhibiting the symptoms of terminal illness. (*B*) Cohorts of Brown Norway rats (n = 5) were euthanized 72 h postchallenge to analyze the kinetics of bacterial replication in the regional lymph node as well as the kinetics of bacterial dissemination to the spleen. (*C*) Moribund rats (n = 5) that were euthanized between 4 and 7 days postchallenge were analyzed for disease progression by assessing the bacterial burden in the regional lymph node and spleen. (*D* to *F*) Bubonic plague-infected Brown Norway rats that survived for 14 days postchallenge were euthanized and necropsied. (*D*) Bacterial loads in the regional lymph node and spleen. (Note that

Figure 6 (*continued*)

since only two rats survived *Y. pestis* CO92 infection, necropsies were performed on two survivors—selected at random—of *Y. pestis* TD1 infection.) For rats surviving *Y. pestis* infection, serum IgG antibody titers for (*E*) LcrV or (*F*) capsular fraction F1 were quantified by ELISA. In panels *A* to *D*, the dotted lines represent the limit of detection, and red lines indicate geometric means. Statistical analysis was performed using the Mann-Whitney *U* test. In panels *E* and *F*, red lines indicate arithmetic means. Statistical analysis was performed using the two-tailed unpaired Student's *t* test. All data are representative of two independent experiments.

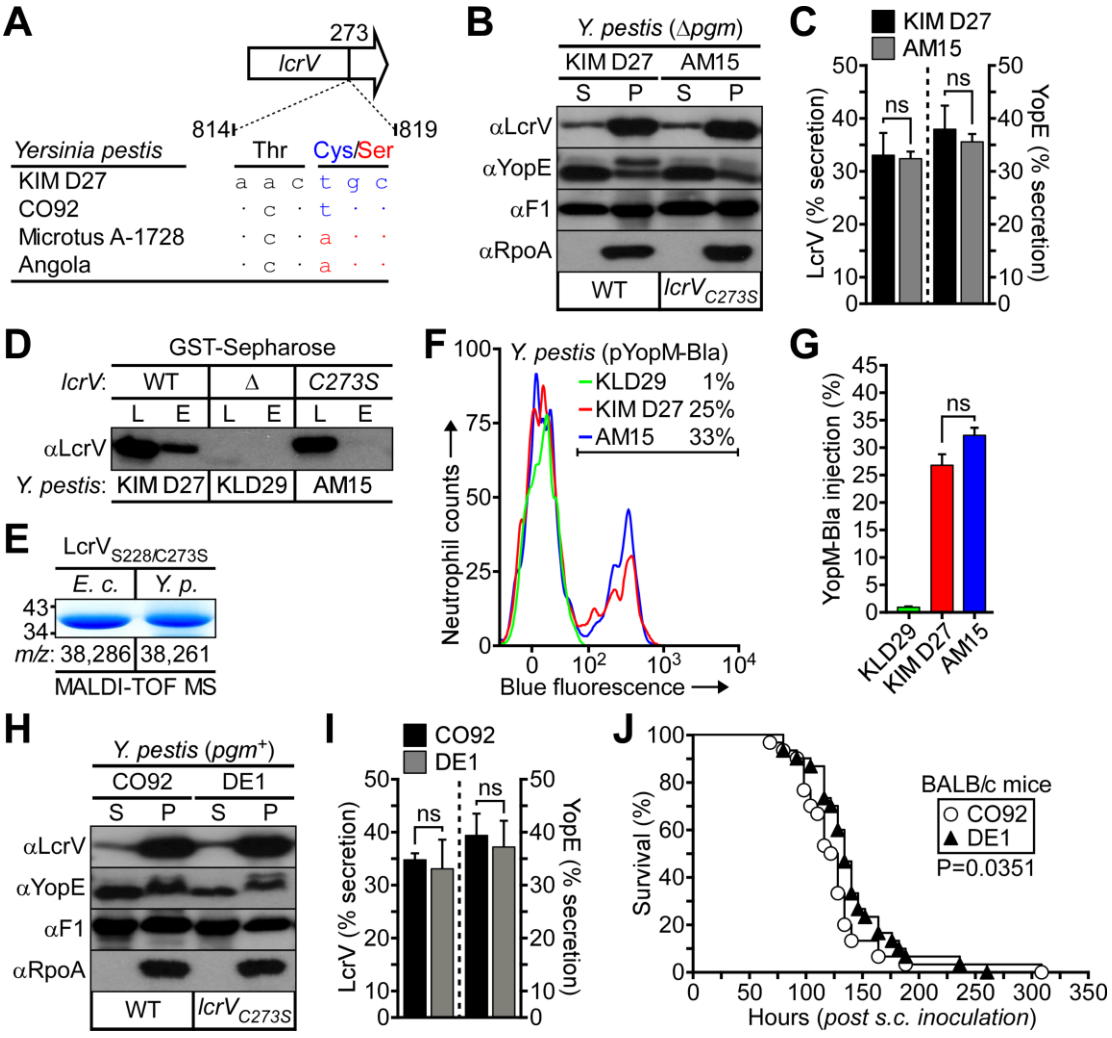

Figure 7. The codon substitution Cys^{273}Ser abolishes *Y. pestis* posttranslational modification of LcrV and attenuates virulence in a mouse model of bubonic plague. (*A*) *Y. pestis* isolates and nucleotide sequences at codons 272 to 273 (nucleotides 814 to 819 of *Y. pestis* CO92 *lcrV*) that impact codon 273 (Cys or Ser). (*B* and *C*) Following growth at 37°C in M9-Ca minimal medium lacking calcium ions, cultures of *Y. pestis* KIM D27 Δ*pgm lcrV* or AM15 Δ*pgm lcrV*$_{C273S}$ were fractionated and analyzed for type III secretion. (*B*) Representative immunoblot analysis was performed by probing supernatant (S) and pellet (P) fractions with the indicated rabbit antibodies. (*C*) Percentages of secretion of YopE and LcrV were determined by densitometric quantification

Figure 7 (*continued*)

of immunoreactive signals. (*D*) *Y. pestis* culture supernatants were subjected to GST-Sepharose affinity chromatography. The load (L) and eluate (E) fractions were immunoblotted with LcrV-specific antisera to assay for the secretion of glutathionylated LcrV. (*E*) *Y. pestis* KLD29 Δ*lcrV* and *E. coli* DH5α strains expressing $LcrV_{S228\ C273S}$ (pAM199) were propagated in LB broth at 37°C. LcrV was affinity purified from *Y. pestis* culture supernatants ($LcrV_{S228\ C273S}$) or *E. coli* lysates ($rLcrV_{S228\ C273S}$), visualized by Coomassie-stained SDS-PAGE, and analyzed by MALDI-TOF MS. The experimentally observed *m/z* of each $LcrV_{S228\ C273S}$ preparation is indicated. (*F* and *G*) Following infection with *Y. pestis* KIM D27(pYopM-Bla), KLD29(pYopM-Bla), or AM15(pYopM-Bla), human neutrophils were stained with CCF2-AM and analyzed by flow cytometry for blue fluorescence indicative of type III effector (YopM-Bla)-mediated cleavage of CCF2-AM. (*F*) Representative histograms show the blue fluorescence traces of *Y. pestis*-infected neutrophils; the percentage of YopM-Bla-injected neutrophils (blue cells) is indicated above the gating scheme that was used to measure blue fluorescence above background. (*G*) Percentage of quantification of YopM-Bla-injected human neutrophils. (*H* and *I*) *Y. pestis* CO92 pgm^+ *lcrV* and DE1 pgm^+ $lcrV_{C273S}$ were evaluated for type III secretion following growth at 37°C in M9-Ca minimal medium in the absence of exogenous calcium ions. (*H*) Representative immunoblot analysis of supernatant (S) and pellet (P) fractions. (*I*) Percentages of secretion of LcrV and YopE were determined by densitometry. (*J*) Survival of cohorts of BALB/c mice ($n = 15$) infected by subcutaneous injection into the left inguinal fold with 20 CFU of *Y. pestis* CO92 or DE1. The figure presents pooled data that were gathered from two independent experiments. For WT versus $lcrV_{C273S}$, $P = 0.0351$ by Gehan-Breslow-Wilcoxon test. In panels *C*, *G*, and *I*, data are means ± SEM ($n = 3$). ns, not significant by two-tailed unpaired Student's *t* test.

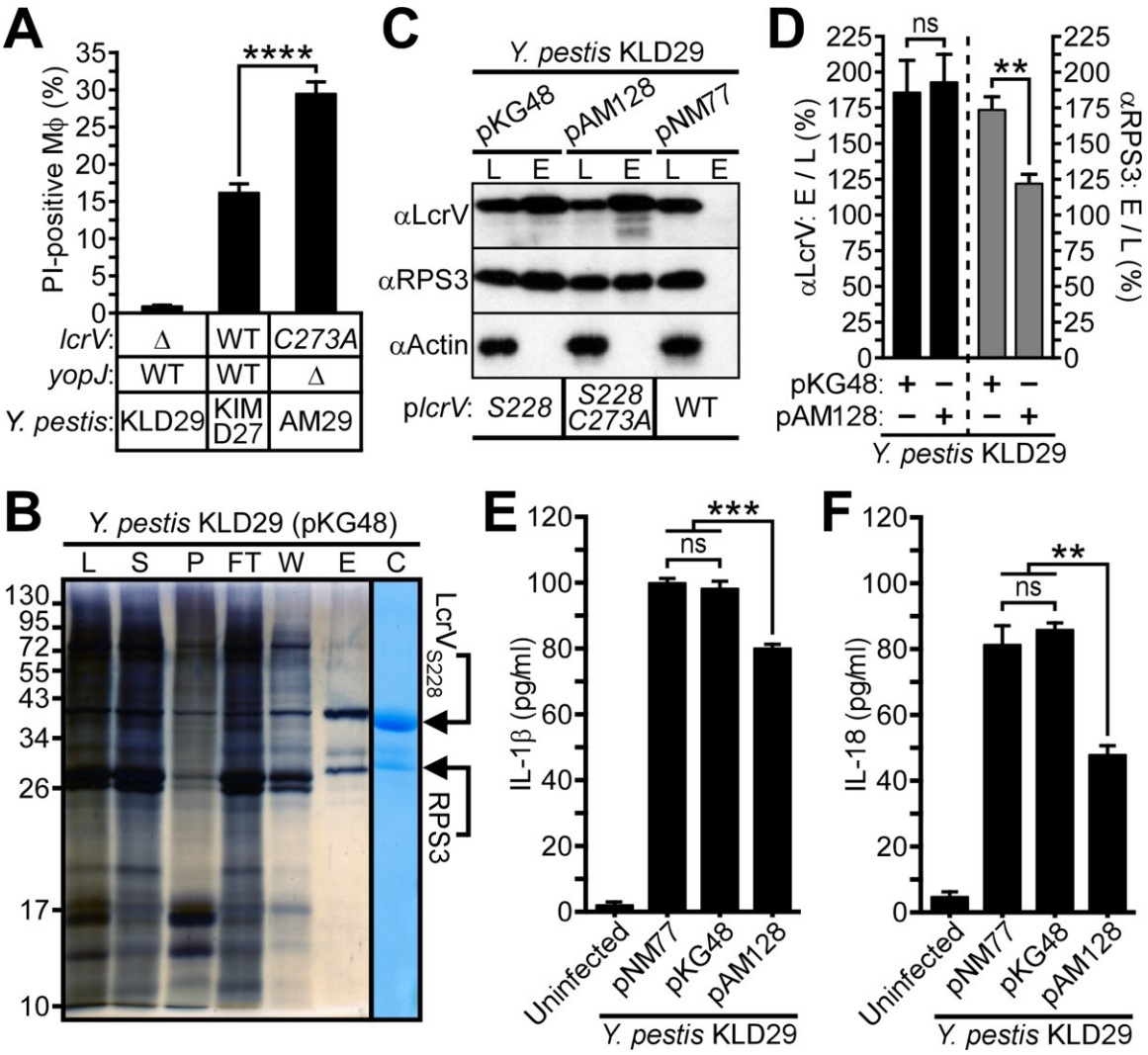

Figure 8. LcrV binds to macrophage RPS3 and modulates host inflammatory responses. (*A*) *Y. pestis*-mediated death of J774.A1 macrophages was assessed 3 h postinfection by propidium iodide staining. (*B*) *Y. pestis* KLD29 *lcrV*$_{S228}$(pKG48)-infected J774.A1 macrophages were subjected to Strep-Tactin affinity chromatography. The crude lysate (L), lysate supernatant (S), lysate pellet (P), flowthrough (FT), wash (W), and eluate (E) fractions were collected and analyzed by silver- and Coomassie-stained SDS-PAGE; bottom-up proteomics was used to identify the indicated protein bands as LcrV$_{S228}$ and macrophage ribosomal protein S3 (RPS3). (*C* and *D*) Immunoblotting of lysate (L) and eluate (E) fractions generated during Strep-Tactin affinity

Figure 8 (*continued*)

chromatography reveals variable association between LcrV variants and RPS3 in J774.A1 macrophages infected with *Y. pestis* KLD29 Δ*lcrV* expressing wild-type *lcrV* (pNM77), $lcrV_{S228}$ (pKG48), or $lcrV_{S228\ C273A}$ (pAM128). (*C*) Representative immunoblot analysis of LcrV and RPS3 purified from *Y. pestis*-infected macrophages; actin levels were used as a loading control. (*D*) Densitometric quantification of the interaction between $LcrV_{S228}$ and RPS3. Immunoreactive signals of Strep-Tactin-purified LcrV and RPS3 were normalized to the corresponding actin band; the ratio of eluate to lysate (E to L) is presented as a percent average. (*E* and *F*) Supernatants from J774.A1 macrophages, either left uninfected or infected with the indicated *Y. pestis* strains, were assayed by ELISA for (*E*) IL-1β or (*F*) IL-18. All data are means ± SEM ($n = 3$). **, $P < 0.01$, ***, $P < 0.001$, and ****, $P < 0.0001$, and ns, not significant. Statistical analysis was performed using the two-tailed unpaired Student's *t* test (panels *A* and *D*) or one-way analysis of variance (ANOVA) with Tukey's multiple-comparison posttest (panels *E* and *F*).

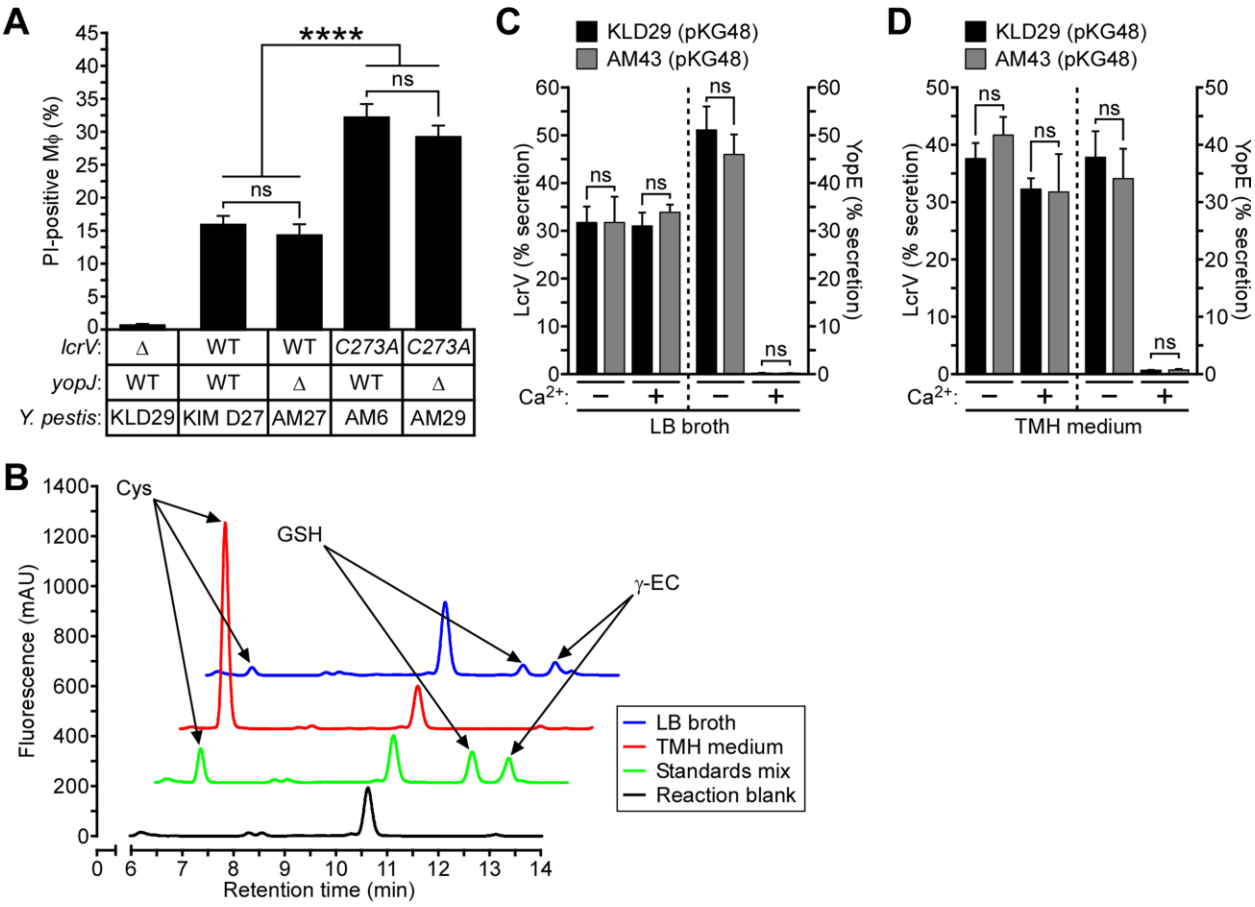

Figure 9. *yopJ* is dispensable for *lcrV*$_{C273A}$-mediated killing of *Y. pestis*-infected macrophages, and type III secretion is not impacted by loss of glutathione synthetase (*gshB*). (*A*) An in-frame deletion of *yopJ* was introduced by allelic exchange with wild-type *Y. pestis* KIM D27 and its *lcrV*$_{C273A}$ variant, *Y. pestis* AM6, to generate *Y. pestis* AM27 *lcrV* Δ*yopJ* and *Y. pestis* AM29 *lcrV*$_{C273A}$ Δ*yopJ*, respectively. Murine J774.A1 macrophages were infected for 3 h with the indicated *Y. pestis* strains, and macrophage cell death was quantified by enumerating propidium iodide (PI)-positive cells. (*B*) Partial HPLC chromatograms include a reaction blank that was used to identify peaks originating from the derivatization reaction in the absence of sample-derived thiols, a standard mixture containing 10 pmol of Cys, GSH, and γ-EC that was used to assign peak positions for the corresponding thiol-mBBr adducts on the basis of

Figure 9 (*continued*)

retention time, and sample runs for TMH medium and LB broth. (*C* and *D*) Densitometric quantification of $LcrV_{S228}$ and YopE secreted by *Y. pestis* KLD29 Δ*lcrV*(pKG48) and AM43 Δ*lcrV* Δ*gshB*(pKG48) following growth in the presence ($+Ca^{2+}$) or absence ($-Ca^{2+}$) of calcium ions at 37°C in (*C*) LB broth or (*D*) TMH medium. The immunoreactive signal of each secreted protein (S) was normalized to its total abundance in the medium and pellet (S + P); the ratio of secreted protein to total protein, (S) / (S + P), is presented as a percent average. All data are means ± SEM ($n = 3$). ****, $P < 0.0001$, and ns, not significant, by two-tailed unpaired Student's *t* test.

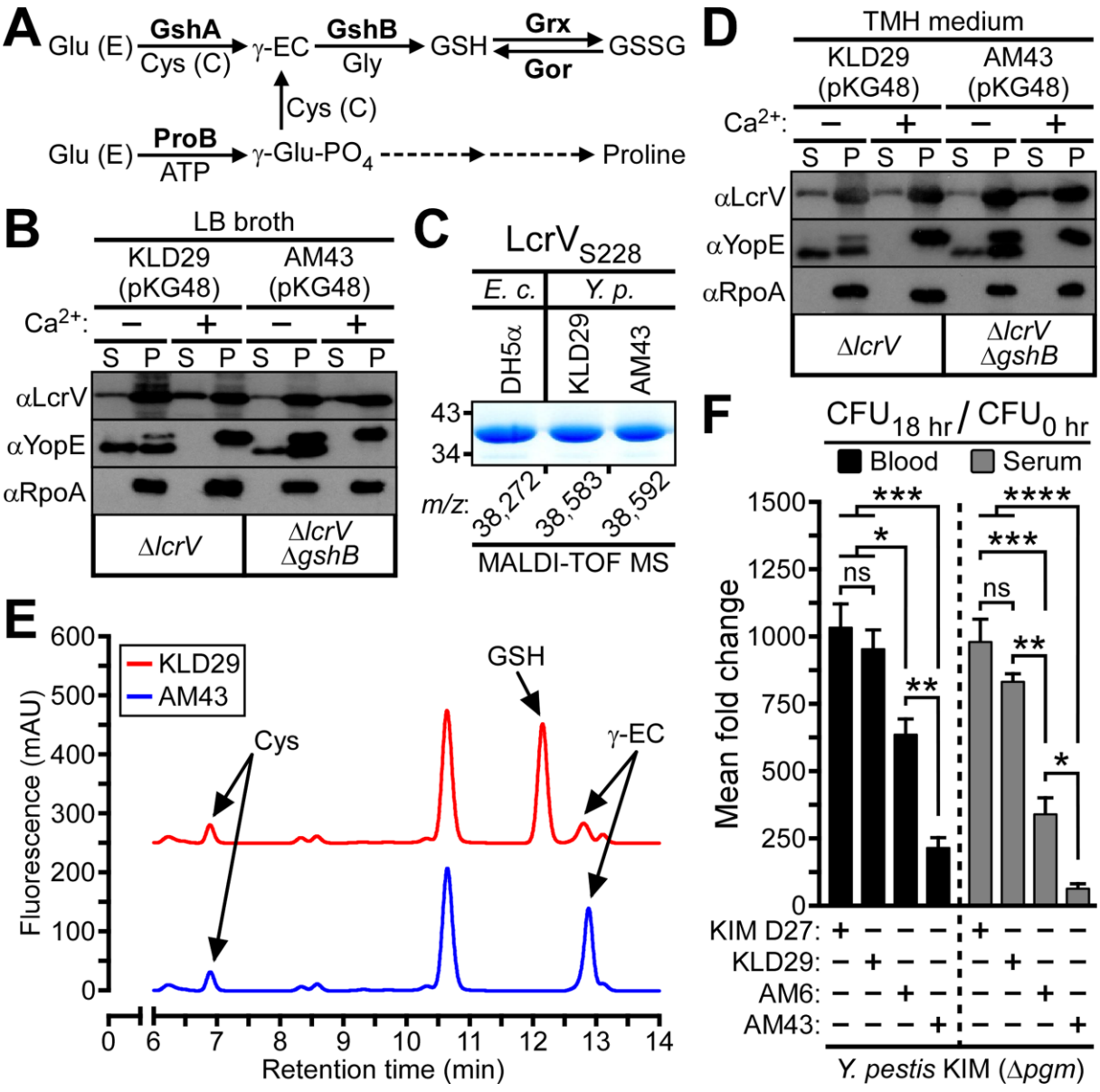

Figure 10. Extracellular glutathione modifies secreted LcrV and promotes *Y. pestis* survival in blood. (*A*) Pathways of glutathione biosynthesis in *E. coli*. Glu (E), glutamic acid; Cys (C), cysteine; GshA, γ-glutamylcysteine synthetase; GshB, glutathione synthetase; ProB, γ-glutamyl kinase; γ-EC, γ-glutamylcysteine; GSH, glutathione; GSSG, glutathione disulfide; Gor, glutathione reductase; Grx, glutaredoxin; γ-glutamyl-PO_4, γ-glutamyl phosphate. (*B*) *Y. pestis* KLD29 Δ*lcrV* $lcrV_{S228}$(pKG48) and AM43 Δ*lcrV* Δ*gshB* $lcrV_{S228}$(pKG48) were grown at 37°C in

Figure 10 (*continued*)

LB broth, in either the presence or absence of calcium ions (Ca^{2+}), and assayed for type III secretion by immunoblotting; proteins secreted into the supernatant (S) were separated from intact bacteria (P) by centrifugation. (*C*) *Y. pestis* and *E. coli* strains expressing $LcrV_{S228}$ (pKG48) were propagated in LB broth. LcrV was purified from *Y. pestis* supernatants ($LcrV_{S228}$) or *E. coli* extracts ($rLcrV_{S228}$), visualized by Coomassie-stained SDS-PAGE, and analyzed by MALDI-TOF MS to reveal the *m/z* of each $LcrV_{S228}$ purification sample. (*D*) *Y. pestis* strains were analyzed for calcium-regulated type III secretion in TMH medium. (*E*) Partial HPLC chromatograms of LMW thiol-mBBr derivatives extracted from *Y. pestis* cultures grown to the stationary phase in TMH medium. Peaks corresponding to Cys, GSH, and γ-EC were assigned on the basis of retention time by comparison to a chromatogram of thiol standards. (*F*) Approximately 10^5 CFU of *Y. pestis* KIM D27 *lcrV*, KLD29 Δ*lcrV*, AM6 $lcrV_{C273A}$, or AM43 Δ*lcrV* Δ*gshB* was inoculated into 4 ml of defibrinated sheep blood or heat-inactivated sheep serum. Culture aliquots were removed before and after 18 h of growth at 37°C and plated on LB agar to enumerate bacterial load. *Y. pestis* growth was calculated as the mean fold increase in bacteria at the time of inoculation ($CFU_{0\ h}$) to bacteria recovered after the 37°C incubation ($CFU_{18\ h}$). Data are means ± SEM ($n = 3$). *, $P < 0.05$, **, $P < 0.01$, ***, $P < 0.001$, and ****, $P < 0.0001$, and ns, not significant, by one-way ANOVA with Tukey's multiple-comparison posttest.

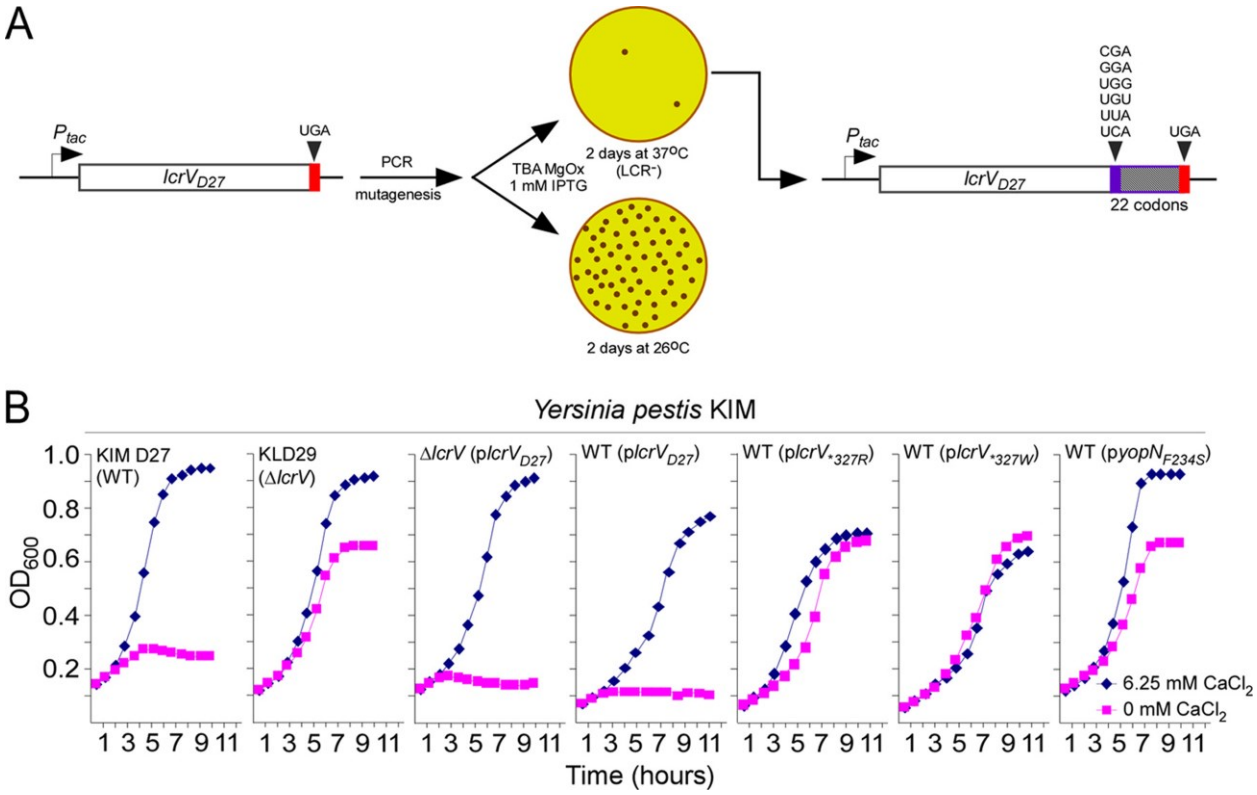

Figure A1. ***Yersinia pestis lcrV*** **mutants with the dominant negative low-calcium response (LCR⁻) phenotype.** (*A*) *lcrV*$_{D27}$ was subjected to PCR mutagenesis, cloned under the control of the pHSG576 *tac* promoter, and electroporated into *Y. pestis* strain KIM D27. Transformants were quantified after colony formation on TBA supplemented with magnesium oxalate (MgOx) at 26°C or 37°C, at the latter temperature with selection for dominant negative LCR⁻ mutants. Plasmids were isolated and again electroporated into *Y. pestis* strain KIM D27, growth of cells with the LCR⁻ phenotype was verified, and plasmids were sequenced, which identified 18 mutations with missense mutations in codon 327 (UGA). These mutations extend the *lcrV* open reading frame by 22 codons (GSKQGGSVSPFFYQYCEYLRP*). (*B*) *Y. pestis* strains KIM D27 (wild-type [WT] *lcrV*) or KLD29 (Δ*lcrV*) harboring either no plasmid or p*lcrV*$_{D27}$, p*lcrV*$_{*327W}$, and p*lcrV*$_{*327R}$ were cultured at 37°C in TMH medium supplemented with either 0 mM or 6.25 mM $CaCl_2$. Growth was

Figure A1 (*continued*)

recorded as an increase in the optical density at 600 nm (OD_{600}). p*yopN*$_{F234S}$, which has been reported to cause a dominant negative LCR$^-$ phenotype (Ferracci et al. 2005), was used as a control.

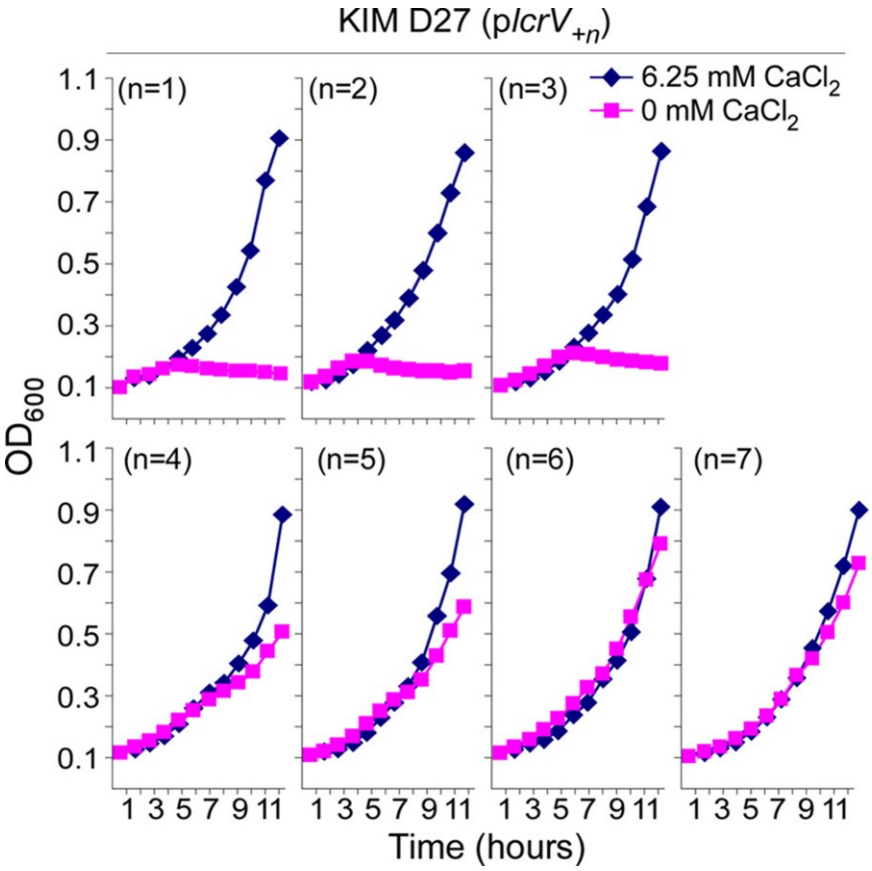

Figure A2. Short extensions at the C terminus of LcrV cause a dominant negative LCR$^-$ phenotype in *Y. pestis*. The open reading frame of *lcrV*$_{D27}$ was extended by single-codon insertions at position 327, immediately prior to the UGA stop codon. *Y. pestis* strain KIM D27 harboring p*lcrV*$_{+1}$, p*lcrV*$_{+2}$, p*lcrV*$_{+3}$, p*lcrV*$_{+4}$, p*lcrV*$_{+5}$, p*lcrV*$_{+6}$, or p*lcrV*$_{+7}$ was cultured at 37°C in TMH medium supplemented with either 0 mM or 6.25 mM $CaCl_2$. Growth was recorded as an increase in the OD_{600}.

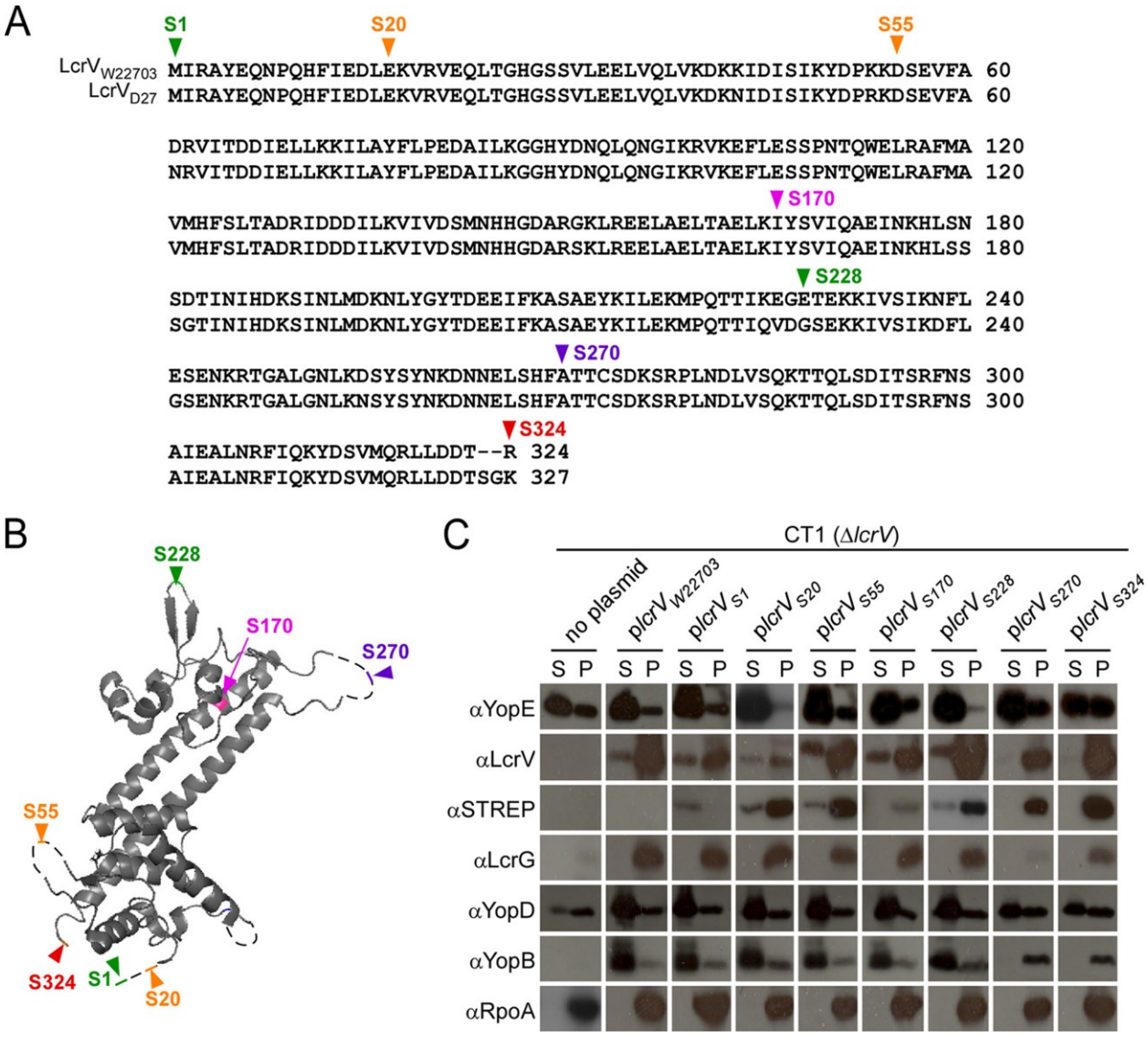

Figure A3. Strep tag insertions in LcrV. (*A*) Alignment of amino acid sequences derived from the *lcrV* gene of *Y. enterocolitica* strain W22703 ($LcrV_{W22703}$) or *Y. pestis* strain KIM D27 ($LcrV_{D27}$). LcrVs derived from *Y. enterocolitica* and *Y. pestis* were aligned. Arrowheads and S numbers identify the amino acids (codons) where the Strep tag (NH_2-WSHPQFEK-COOH) was inserted into $LcrV_{W22703}$. (*B*) Ribbon diagram illustrating the three-dimensional X-ray structure of LcrV (Derewenda et al. 2004) and the positions of the Strep tags. $LcrV_{S1}$ and $LcrV_{S228}$ (both green) displayed wild-type LcrV phenotypes in both *Y. enterocolitica* and *Y. pestis*. $LcrV_{S270}$ (purple) was

Figure A3 (*continued*)

nonfunctional, and $LcrV_{S324}$ (red) caused a dominant negative blockade of the type III pathway in both *Y. enterocolitica* and *Y. pestis*. $LcrV_{S20}$ and $LcrV_{S55}$ (both orange) caused a dominant negative blockade of type III secretion only in *Y. pestis* and not in *Y. enterocolitica*. Finally, $LcrV_{S170}$ (magenta) did not affect type III secretion *in vitro* but failed to promote effector translocation for both *Y. enterocolitica* and *Y. pestis*. (*C*) *Y. enterocolitica* CT1 (Δ*lcrV* variant of W22703) without plasmid or harboring p$lcrV_{W22703}$, p$lcrV_{S1}$, p$lcrV_{S20}$, p$lcrV_{S55}$, p$lcrV_{S170}$, p$lcrV_{S228}$, p$lcrV_{S270}$, or p$lcrV_{S324}$ was grown for 3 h at 37°C in TSB supplemented with 5 mM EGTA to chelate calcium and 1 mM IPTG to induce the expression of plasmid-borne *lcrV* alleles. *Yersinia* cultures were centrifuged, and the extracellular medium was removed with the supernatant (S) and separated from the bacterial sediment (pellet [P]). Proteins in both fractions were precipitated with trichloroacetic acid and analyzed by immunoblotting with rabbit antisera raised against YopE (αYopE), LcrV (αLcrV), YopB (αYopB), YopD (αYopD), LcrG (αLcrG), and RpoA (αRpoA) or a monoclonal antibody specific for the Strep tag (αSTREP).

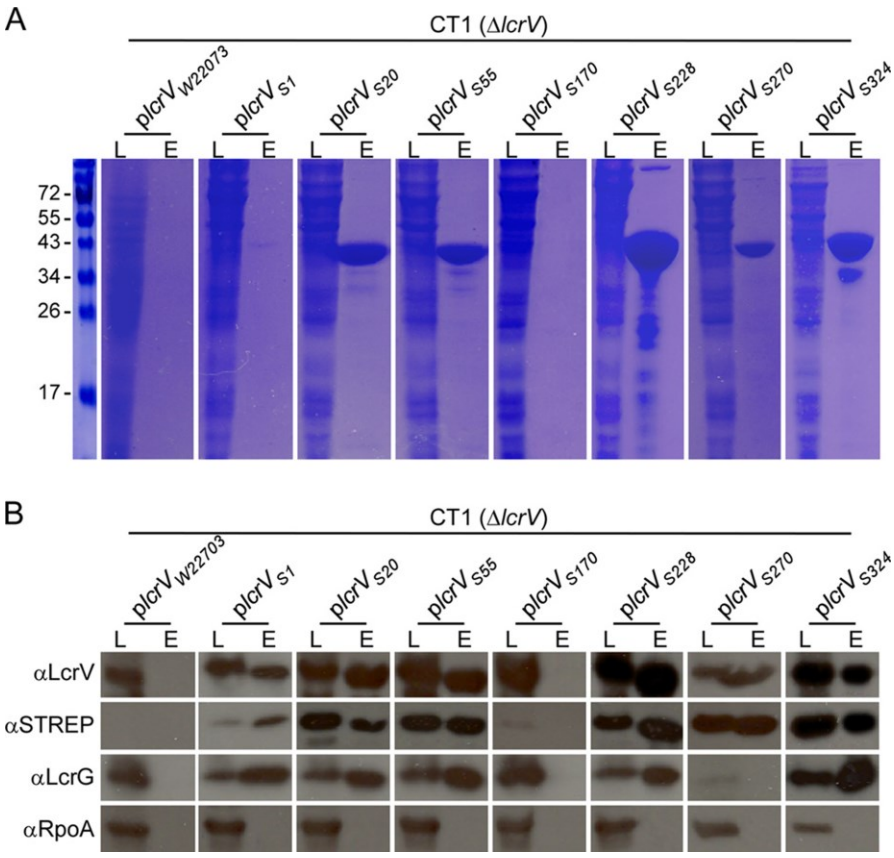

Figure A4. Affinity chromatography of Strep-tagged LcrV. (*A*) Cleared lysates of *Y. enterocolitica* CT1 (Δ*lcrV*) harboring p*lcrV*$_{W22703}$ or Strep-tagged LcrV (p*lcrV*$_{S1}$, p*lcrV*$_{S20}$, p*lcrV*$_{S55}$, p*lcrV*$_{S170}$, p*lcrV*$_{S228}$, p*lcrV*$_{S270}$, and p*lcrV*$_{S324}$) were derived from cultures grown for 3 h at 37°C in TSB supplemented with 5 mM EGTA to chelate calcium and 1 mM IPTG to induce the expression of plasmid-borne *lcrV* alleles. Cleared lysates (L) were subjected to affinity chromatography on Strep-Tactin resin and eluted with desthiobiotin (E). Proteins in both samples were analyzed by Coomassie blue-stained SDS-PAGE. The migratory positions were proteins with known molecular mass (in kDa, indicated on the left). (*B*) Samples were subjected to immunoblotting with rabbit antisera raised against LcrV (αLcrV), LcrG (αLcrG), and RpoA (αRpoA) or with monoclonal antibody against the Strep tag (αSTREP).

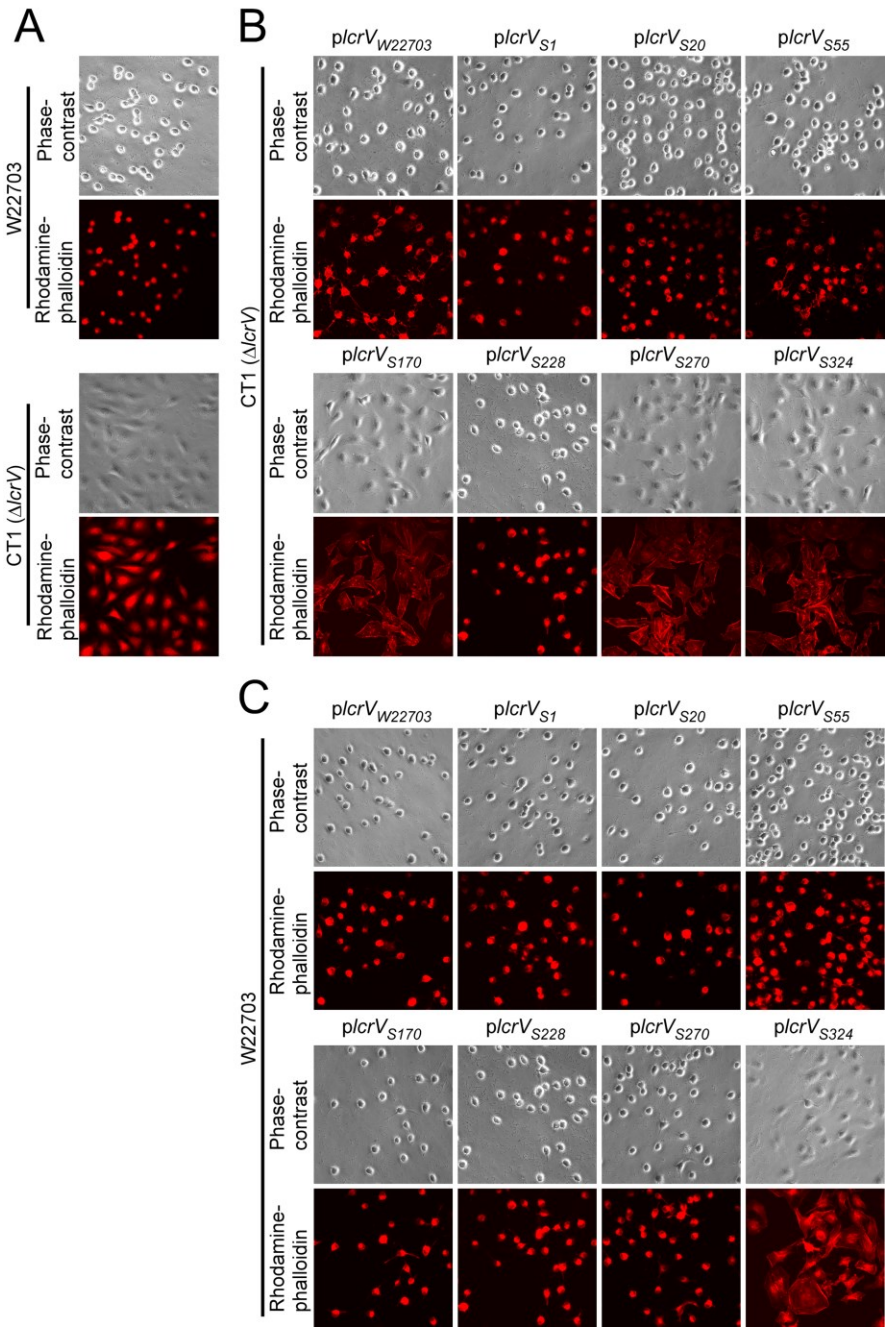

Figure A5. Strep-tagged LcrV and *Yersinia enterocolitica* effector translocation. (*A*) *Y. enterocolitica* strains W22703 (wild-type *lcrV*) and CT1 (Δ*lcrV*) were used to infect HeLa tissue culture cells for 3 h at an MOI of 10. Samples were fixed, stained with rhodamine-phalloidin, and imaged by fluorescence or phase-contrast microscopy to reveal actin cable rearrangements and

Figure A5 (*continued*)

cell rounding as a measure for effector translocation. (*B*) *Y. enterocolitica* CT1 strains harboring *lcrV* plasmids (p*lcrV*$_{W22703}$, p*lcrV*$_{S1}$, p*lcrV*$_{S20}$, p*lcrV*$_{S55}$, p*lcrV*$_{S170}$, p*lcrV*$_{S228}$, p*lcrV*$_{S270}$, and p*lcrV*$_{S324}$) were subjected to the same assay as described for panel *A*. (*C*) *Y. enterocolitica* W22703 strains harboring *lcrV* plasmids (p*lcrV*$_{W22703}$, p*lcrV*$_{S1}$, p*lcrV*$_{S20}$, p*lcrV*$_{S55}$, p*lcrV*$_{S170}$, p*lcrV*$_{S228}$, p*lcrV*$_{S270}$, and p*lcrV*$_{S324}$) were subjected to the same assay as described for panel *A*.

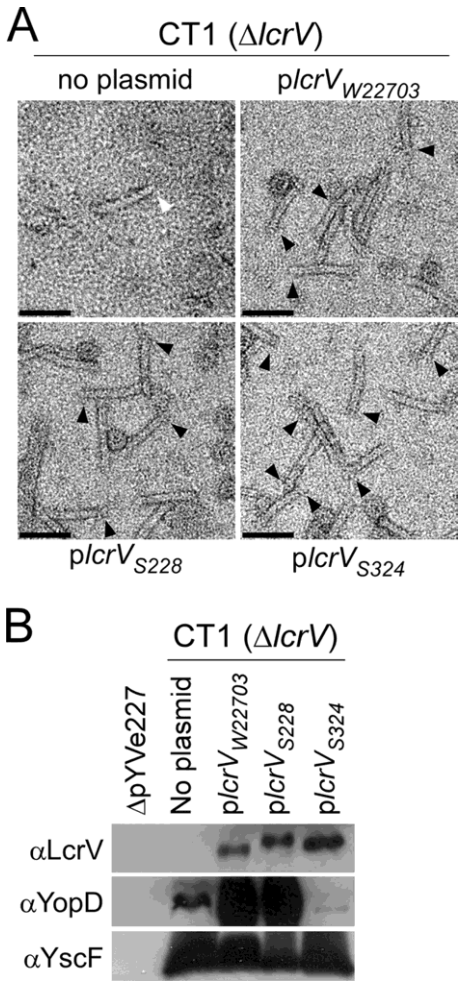

Figure A6. LcrV$_{S324}$ caps YscF needles that lack YopD. (*A*) Cultures of *Y. enterocolitica* CT1 (Δ*lcrV*) harboring p*lcrV*$_{W22703}$, p*lcrV*$_{S228}$, p*lcrV*$_{S324}$, or no plasmid were centrifuged, and the bacterial sediment was sheared to break off type III needle complexes. Bacteria were removed by slow-speed centrifugation, and the filtered supernatant was ultracentrifuged to sediment type III needle complexes, which were analyzed by transmission electron microscopy. The arrowheads identify LcrV caps of type III needle complexes. (*B*) *Y. enterocolitica* CT1 (Δ*lcrV*) and *Y. enterocolitica* ΔpYVe227 cultures were subjected to the isolation of type III needle complexes as described above. Samples were analyzed by immunoblotting with rabbit antisera raised against LcrV (αLcrV), YopD (αYopD), and YscF (αYscF).

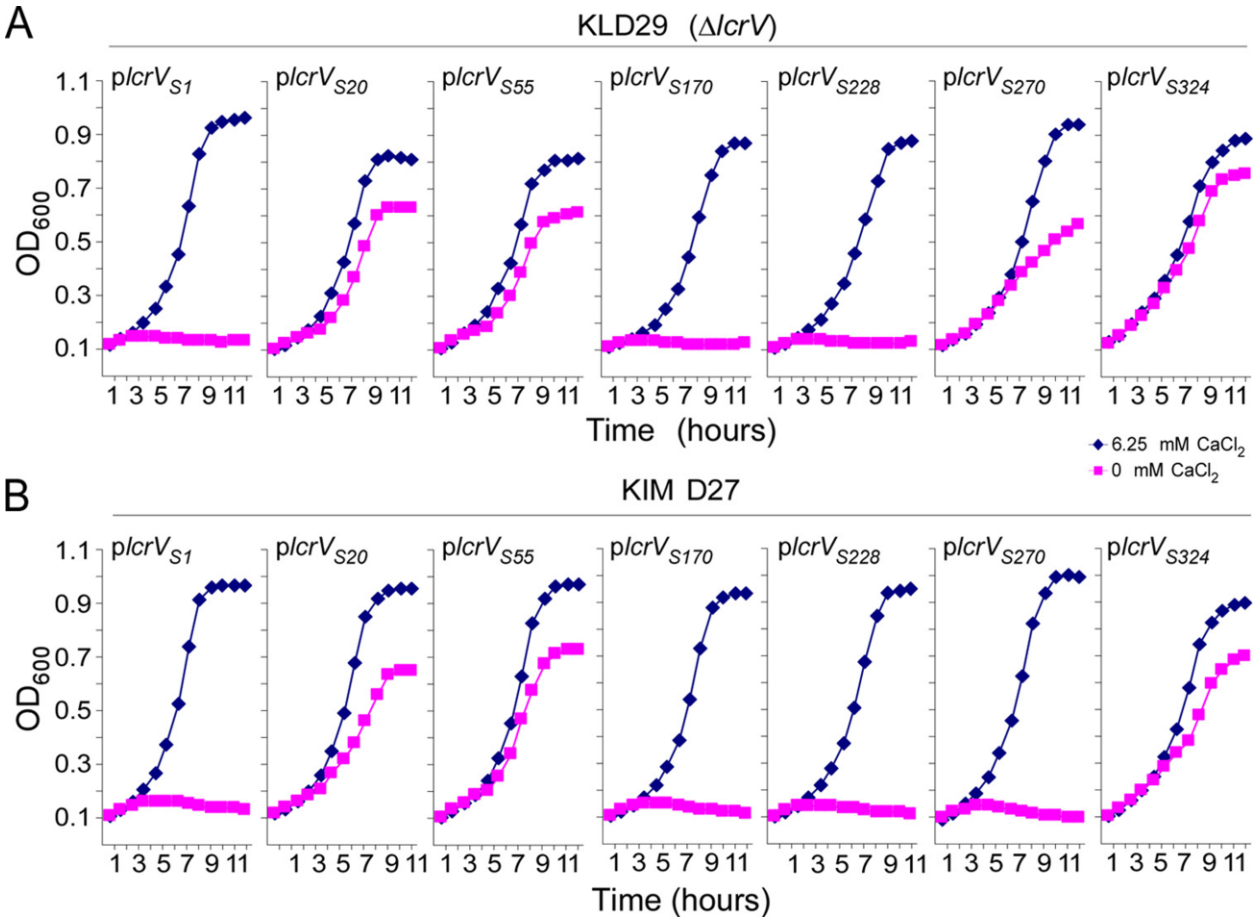

Figure A7. Strep-tagged LcrVs and their LCR phenotypes in *Yersinia pestis*. (*A*) *Y. pestis* KLD29 (Δ*lcrV*) expressing Strep-tagged LcrV (p*lcrV*$_{S1}$, p*lcrV*$_{S20}$, p*lcrV*$_{S55}$, p*lcrV*$_{S170}$, p*lcrV*$_{S228}$, p*lcrV*$_{S270}$, and p*lcrV*$_{S324}$) was cultured at 37°C in TMH medium supplemented with either 0 mM or 6.25 mM $CaCl_2$. Growth was recorded as an increase in the OD_{600}. (*B*) *Y. pestis* strain KIM D27 (wild-type *lcrV*) expressing Strep-tagged LcrV (p*lcrV*$_{S1}$, p*lcrV*$_{S20}$, p*lcrV*$_{S55}$, p*lcrV*$_{S170}$, p*lcrV*$_{S228}$, p*lcrV*$_{S270}$, and p*lcrV*$_{S324}$) was cultured at 37°C in TMH medium supplemented with either 0 mM or 6.25 mM $CaCl_2$. Growth was recorded as an increase in the OD_{600}.

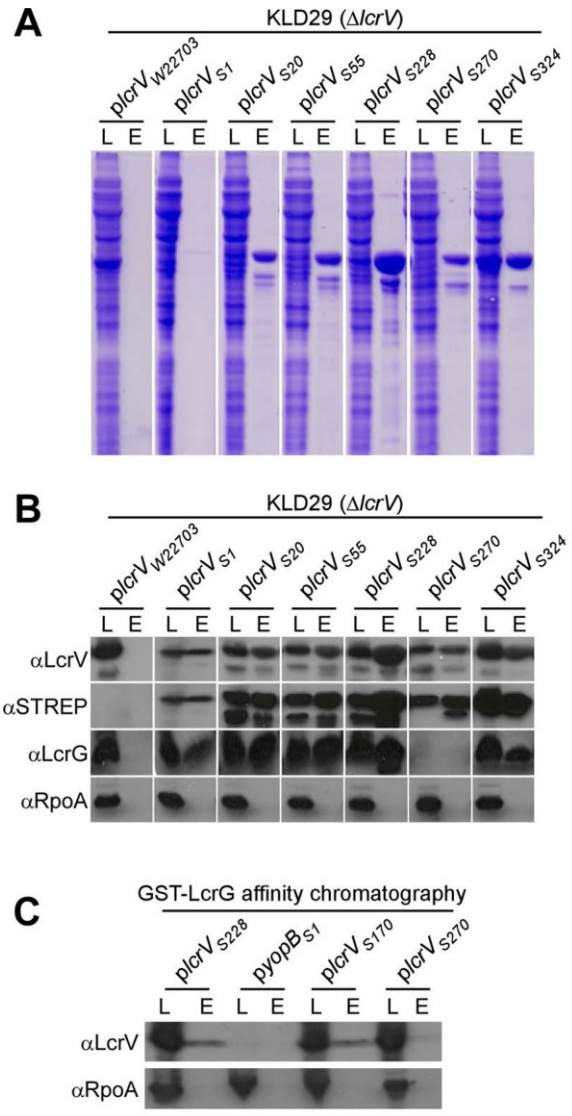

Figure A8. Affinity chromatography of Strep-tagged LcrV expressed in *Y. pestis*. (*A*) Cleared lysates of *Y. pestis* KLD29 (Δ*lcrV*) harboring p*lcrV*$_{W22703}$ or Strep-tagged LcrV (p*lcrV*$_{S1}$, p*lcrV*$_{S20}$, p*lcrV*$_{S55}$, p*lcrV*$_{S228}$, p*lcrV*$_{S270}$, and p*lcrV*$_{S324}$) were derived from cultures grown for 3 h at 37°C in TSB supplemented with 5 mM EGTA to chelate calcium and 1 mM IPTG to induce the expression of plasmid-borne *lcrV* alleles. Cleared lysates (L) were subjected to affinity chromatography on Strep-Tactin resin and eluted with desthiobiotin (E). Proteins in both samples were analyzed by Coomassie blue-stained SDS-PAGE. (*B*) Samples were subjected to immunoblotting with rabbit

Figure A8 (*continued*)

antisera raised against LcrV (αLcrV), LcrG (αLcrG), and RpoA (αRpoA) or with monoclonal antibody against the Strep tag (αSTREP). (*C*) GST-LcrG was purified from the cytoplasm of *E. coli* using affinity chromatography. Glutathione-Sepharose charged with GST-LcrG was dispensed in four aliquots and subjected to affinity chromatography of *Y. pestis* KLD29 (Δ*lcrV*) lysates with $LcrV_{S228}$, $LcrV_{S170}$, or $LcrV_{S270}$. The abundance of $LcrV_{S228}$, $LcrV_{S170}$, or $LcrV_{S270}$ in the *Y. pestis* lysate (L) and the eluate (E) of GST-LcrG affinity chromatography was detected by immunoblotting (αLcrV). GST-LcrG retained $LcrV_{S228}$ and $LcrV_{S170}$, but not $LcrV_{S270}$. As a control, *Y. pestis* KLD29 (Δ*lcrV*) lysate with YopB harboring a Strep tag at the N terminus ($YopB_{S1}$) did not lead to the retention of LcrV following GST-LcrG chromatography. Further, *Y. pestis* RpoA was not retained following GST-LcrG affinity chromatography (αRpoA).

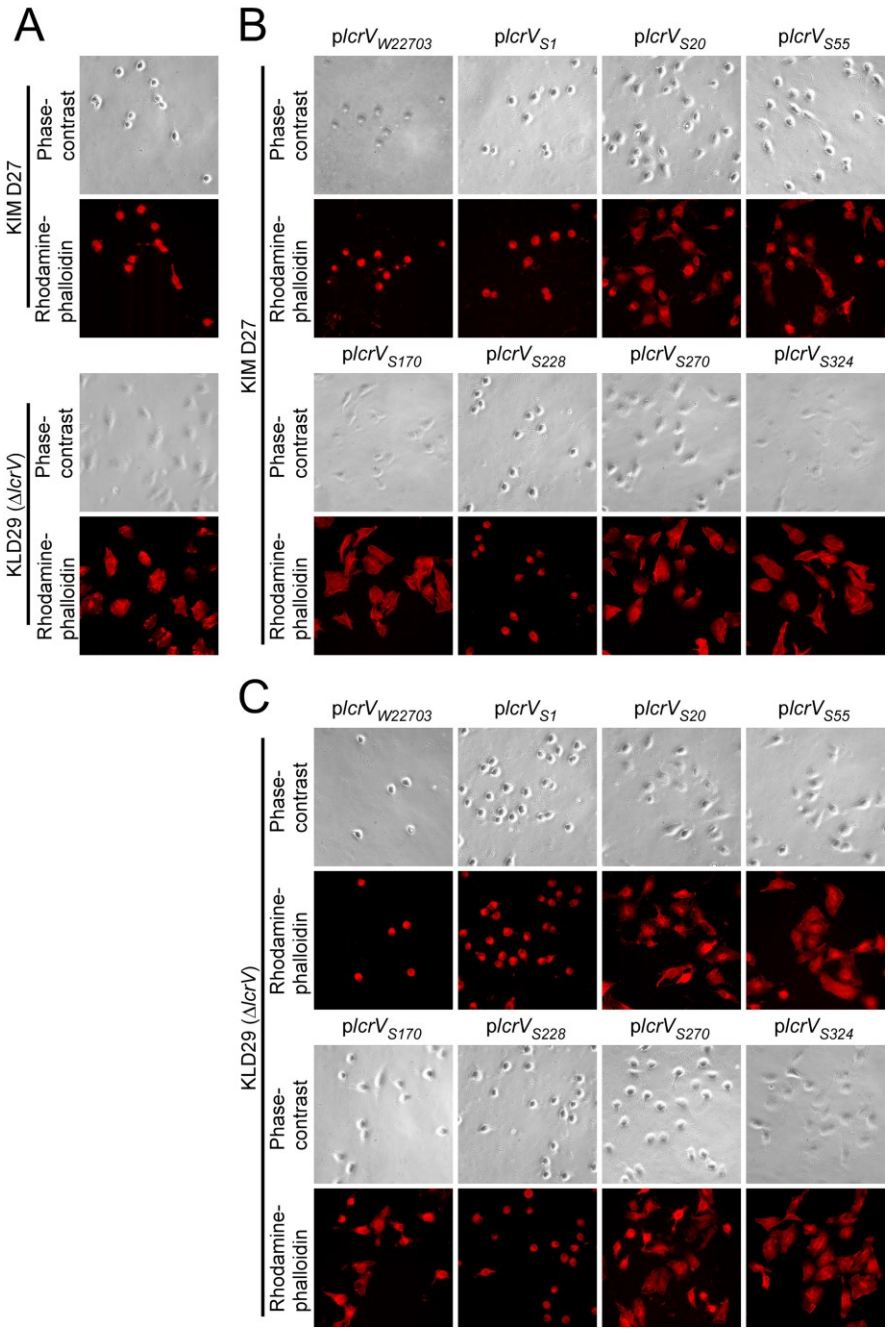

Figure A9. Strep-tagged LcrV and *Yersinia pestis* effector translocation. (*A*) *Y. pestis* strains KIM D27 (wild-type *lcrV*) and KLD29 (Δ*lcrV*) were used to infect HeLa tissue culture cells for 3 h at an MOI of 10. Samples were fixed, stained with rhodamine-phalloidin, and imaged by fluorescence or phase-contrast microscopy to reveal actin cable rearrangements and cell rounding

Figure A9 (*continued*)

as a measure for effector translocation. (*B*) *Y. pestis* KIM D27 strains harboring *lcrV* plasmids (p*lcrV*$_{W22703}$, p*lcrV*$_{S1}$, p*lcrV*$_{S20}$, p*lcrV*$_{S55}$, p*lcrV*$_{S170}$, p*lcrV*$_{S228}$, p*lcrV*$_{S270}$, and p*lcrV*$_{S324}$) were subjected to the same assay as described for panel *A*. (*C*) *Y. pestis* KLD29 strains harboring *lcrV* plasmids (p*lcrV*$_{W22703}$, p*lcrV*$_{S1}$, p*lcrV*$_{S20}$, p*lcrV*$_{S55}$, p*lcrV*$_{S170}$, p*lcrV*$_{S228}$, p*lcrV*$_{S270}$, and p*lcrV*$_{S324}$) were subjected to the same assay as described for panel *A*.

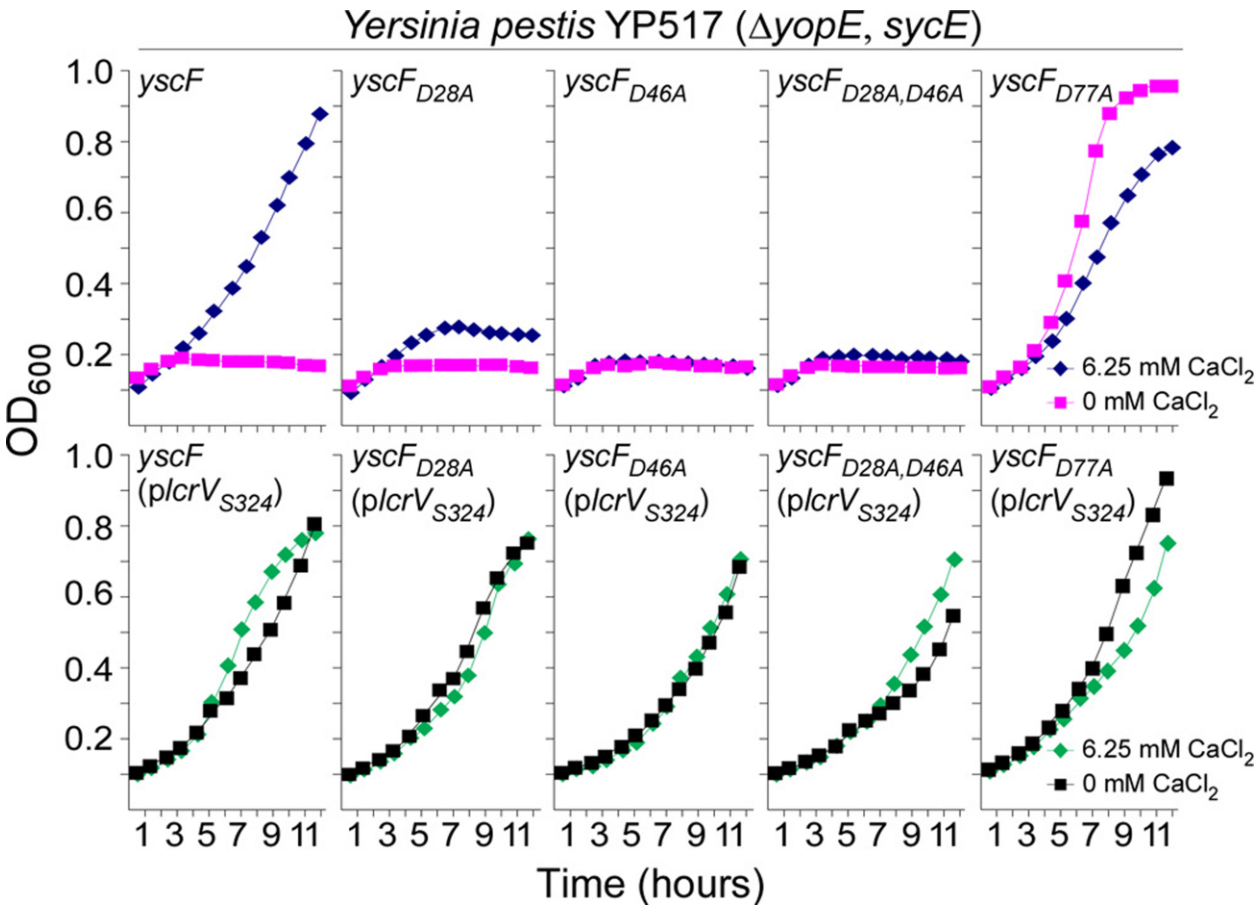

Figure A10. LcrV$_{S324}$ causes a dominant negative LCR$^-$ phenotype in *Y. pestis* harboring calcium-blind alleles *yscF$_{D28A}$* and/or *yscF$_{D46A}$*. *Y. pestis* YP517 (Δ*yopE*/*sycE*) harboring wild-type *yscF*, the calcium-blind alleles *yscF$_{D28A}$* and/or *yscF$_{D46A}$*, or the LCR$^-$ *yscF$_{D77A}$* allele were transformed with p*lcrV$_{S324}$*. Strains without (top panels) or with p*lcrV$_{S324}$* (bottom panels) were cultured at 37°C in TMH medium supplemented with either 0 mM or 6.25 mM $CaCl_2$. Growth was recorded as an increase in the OD_{600}.

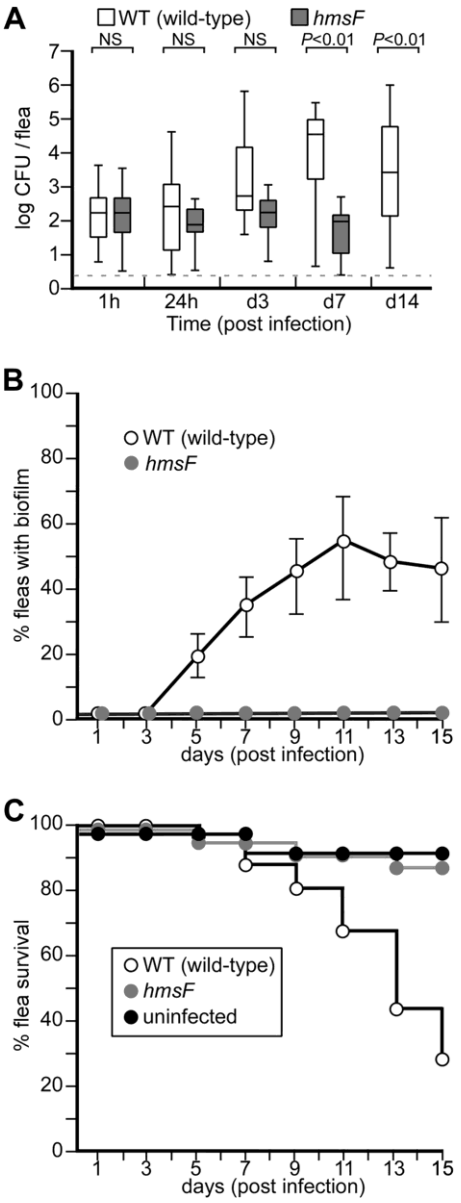

Figure B1. *Y. pestis* colonization of cat fleas requires the *hmsF* locus. (*A*) Cat fleas (n = 100) were infected by one-time feeding on defibrinated sheep's blood inoculated with 1×10^8 CFU wild-type *Y. pestis* CO92(ΔpCD1) or its *hmsF* mutant and were subsequently fed sterile blood. At various time intervals of hours (h) or days (d), the infected fleas were homogenized and plated on HIA, and CFU were enumerated. The box plot represents *Y. pestis* flea colonization data in log CFU, where the horizontal line denotes the mean and the whiskers indicate variability outside

Figure B1 (*continued*)

the upper and lower quartiles. The dashed line identifies the limit of detection. NS, not significant. (*B*) Infected-flea cohorts ($n = 100$) were monitored by dissection of the gut and microscopy to detect biofilm formation. Fleas with a visible mass spreading from the proventriculus into the midgut were scored positive. The data shown represent averages of five independent experiments. The error bars indicate standard deviations. (*C*) Survival of cat fleas ($n = 100$) that were either left uninfected or infected with wild-type or *hmsF* mutant *Y. pestis* CO92(ΔpCD1) and monitored for survival. The data are representative of more than five independent experiments.

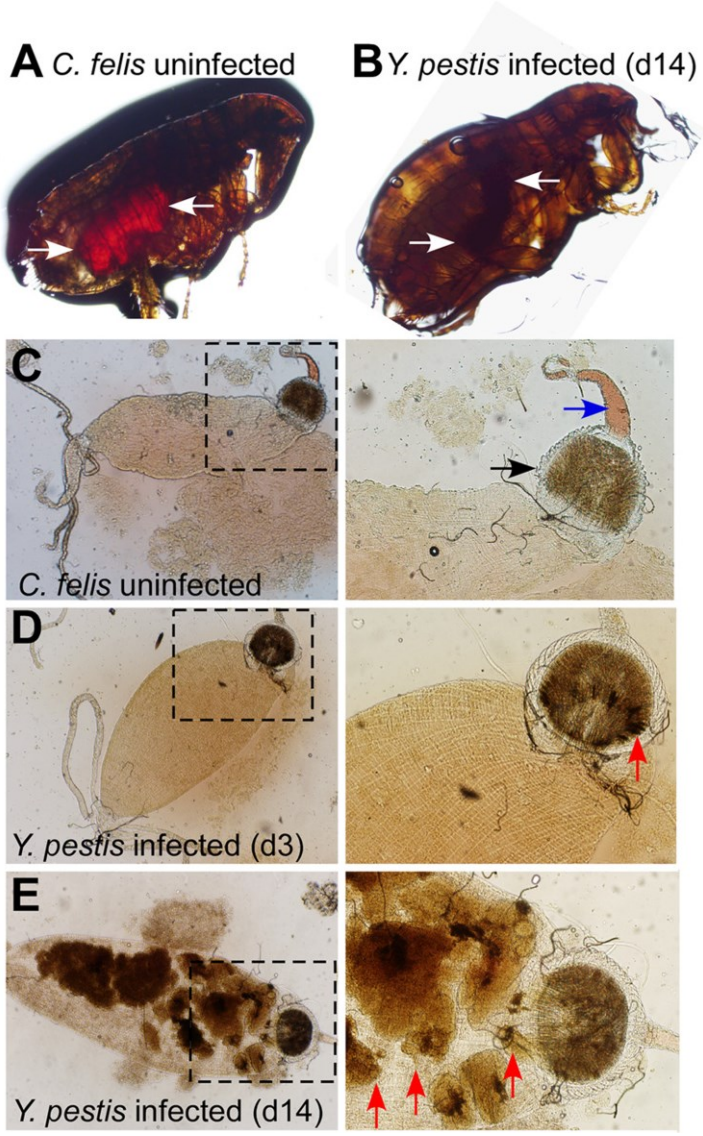

Figure B2. *Y. pestis* induced aggregates and gut blockade in cat fleas. (*A* and *B*) Micrographs of immobilized live adult uninfected (*A*) and *Y. pestis* CO92(ΔpCD1)-infected (*B*) cat fleas maintained in an artificial feeder for 14 days. Evidence of a recent blood meal is indicated by a red-stained midgut (arrows in panel *A*). In infected fleas, the digestive tract appears smaller and is filled with a dark mass extending from the proventriculus along the entire gut (arrows in panel *B*). (*C*) Gut of a dissected uninfected cat flea (boxed area magnified on the right) identifying the esophagus (blue arrow) and proventriculus (black arrow). (*D*) Gut of a dissected cat flea

Figure B2 (*continued*)

3 days (d3) after infection with *Y. pestis* CO92(ΔpCD1) (boxed area magnified on the right) identifying dark-pigmented material deposited in the proventriculus (red arrow). (*E*) Gut of a dissected cat flea 14 days after infection with *Y. pestis* CO92(ΔpCD1) (boxed area magnified on the right) identifying large amounts of dark-pigmented material in the proventriculus, midgut, and hindgut (red arrows). The images are representative of more than 50 analyzed cat fleas in each cohort.

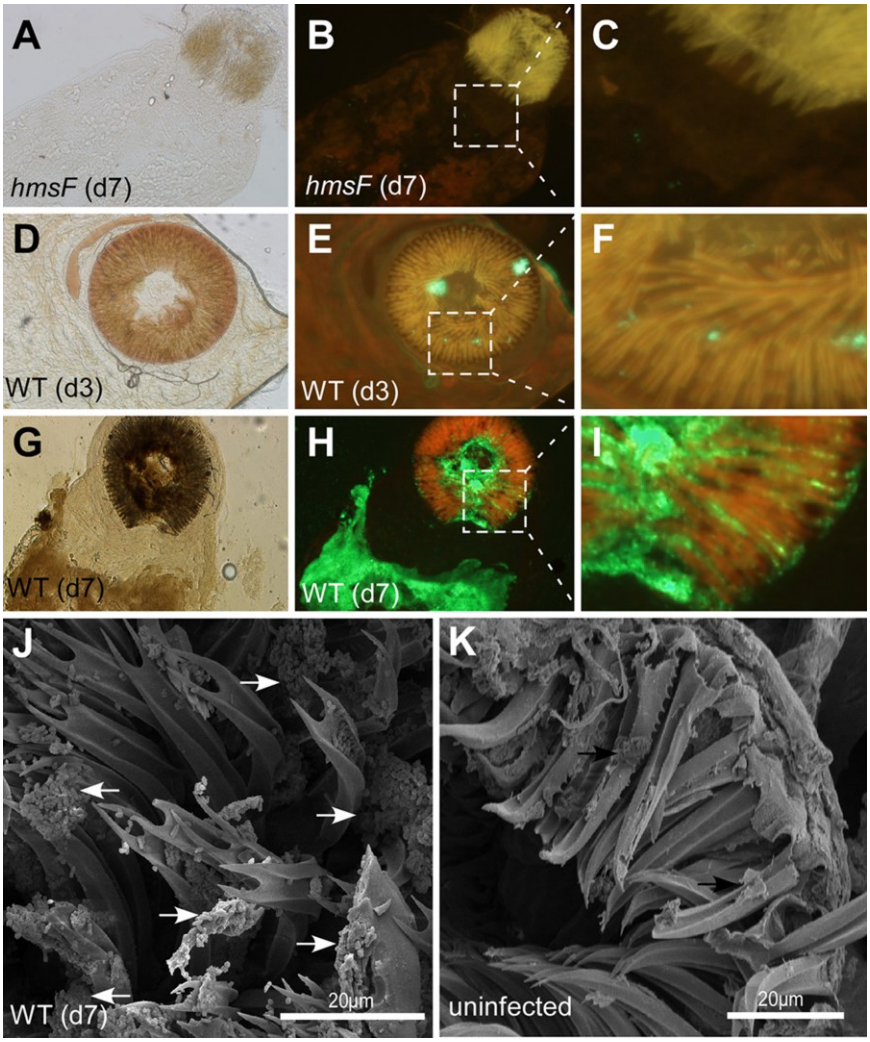

Figure B3. ***Y. pestis*** **forms biofilms in the proventriculus and in the gut of infected cat fleas.** (*A* to *C*) Representative bright-field (*A*) and fluorescence microscopy (*B*) images (the boxed area is magnified in panel *C*) of the dissected digestive tracts of fleas (n = 30) 7 days (d7) after infection with *hmsF* mutant *Y. pestis* CO92(ΔpCD1, pEGFP). The fluorescence images were acquired in red Texas Red (594-nm) and green GFP (488-nm) fluorescence channels and merged, which, due to autofluorescence, reveals the contours of the proventriculus as orange signals and GFP-expressing *Y. pestis* in green. (*D* to *F*) Representative bright-field (*D*) and fluorescence microscopy (*E*) images (the boxed area is magnified in panel *F*) of dissected digestive tracts of fleas (n = 30) 3 days after

Figure B3 (*continued*)

infection with wild-type *Y. pestis* CO92(ΔpCD1, pEGFP). Note the areas of green fluorescence (*F*) derived from GFP-expressing wild-type *Y. pestis* in the proventriculus. (*G* to *I*) Representative bright-field (*G*) and fluorescence microscopy (*H*) images (the boxed area is magnified in panel *I*) of dissected digestive tracts of fleas ($n = 30$) 7 days after infection with wild-type *Y. pestis* CO92(ΔpCD1, pEGFP). Note the massive biofilm of GFP-expressing *Y. pestis* in the midgut and proventriculus. (*J* and *K*) The dissected proventriculus of fleas infected with wild-type *Y. pestis* CO92(ΔpCD1) (*J*) or uninfected fleas (*K*) was fixed and viewed by scanning electron microscopy (SEM). The arrows indicate *Y. pestis* CO92(ΔpCD1) aggregates on the spines of the cat flea proventriculus.

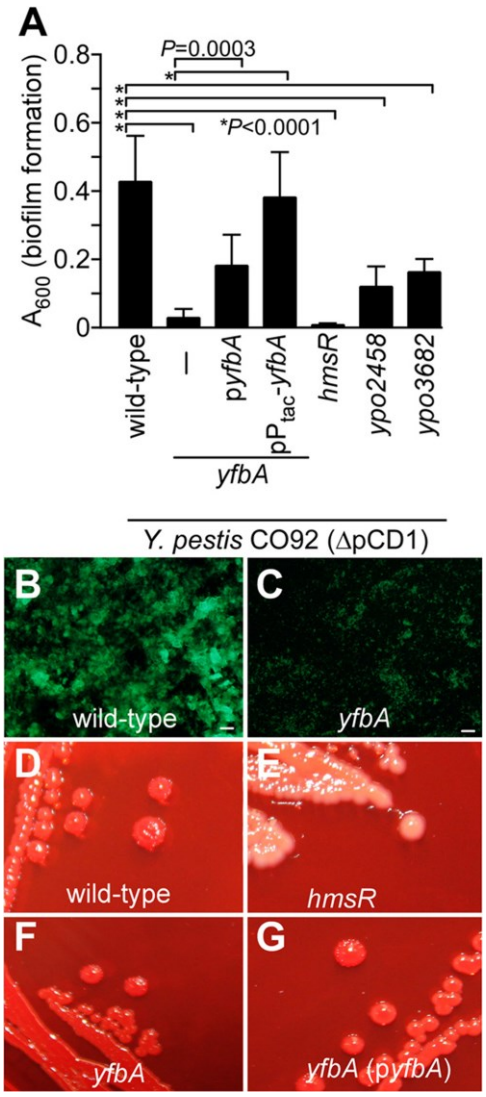

Figure B4. Three LysR-type transcriptional regulators contribute to *Y. pestis in vitro* biofilm formation. (*A*) A library of *Y. pestis* CO92(ΔpCD1) mutants with mini-Tn*5* insertional lesions was screened for *in vitro* biofilm defects by incubating static cultures for 24 h at 26°C and crystal violet staining. This approach identified variants with insertions in *ypo2150* (*yfbA*), *ypo2458*, and *ypo3682*, each of which encodes an LTTR. As a control, a *Y. pestis* mutant with an insertional lesion in *hmsR* was also defective for biofilm formation and plasmids p*yfbA* (*yfbA* under the control of its native promoter) and pP_{tac}-*yfbA* (*yfbA* under the control of the IPTG-inducible P_{tac} promoter)

Figure B4 (*continued*)

increased biofilm formation of the *yfbA* mutant. The data represent the means and standard errors of the means (SEM) from 10 independent experimental determinations. (*B* and *C*) Biofilm cultures of wild-type *Y. pestis* CO92(ΔpCD1) (*B*) and its *yfbA* mutant (*C*) were stained with Syto9, and fluorescence microcopy images were acquired (bars, 20 μm). (*D* and *E*) A Congo Red agar plate was inoculated with *Y. pestis* strains and incubated at 26°C for 48 h. The microscopy images reveal the PNAG (*hms*)-dependent Congo Red pigmentation phenotype of wild-type *Y. pestis* CO92(ΔpCD1) (*D*) compared to the nonpigmented staining phenotype of the *hmsR* mutant (*E*). (*F* and *G*) *Y. pestis* CO92(ΔpCD1) *yfbA* (*F*) and *yfbA*(p*yfbA*) (*G*) strains form pigmented colonies on Congo Red agar plates.

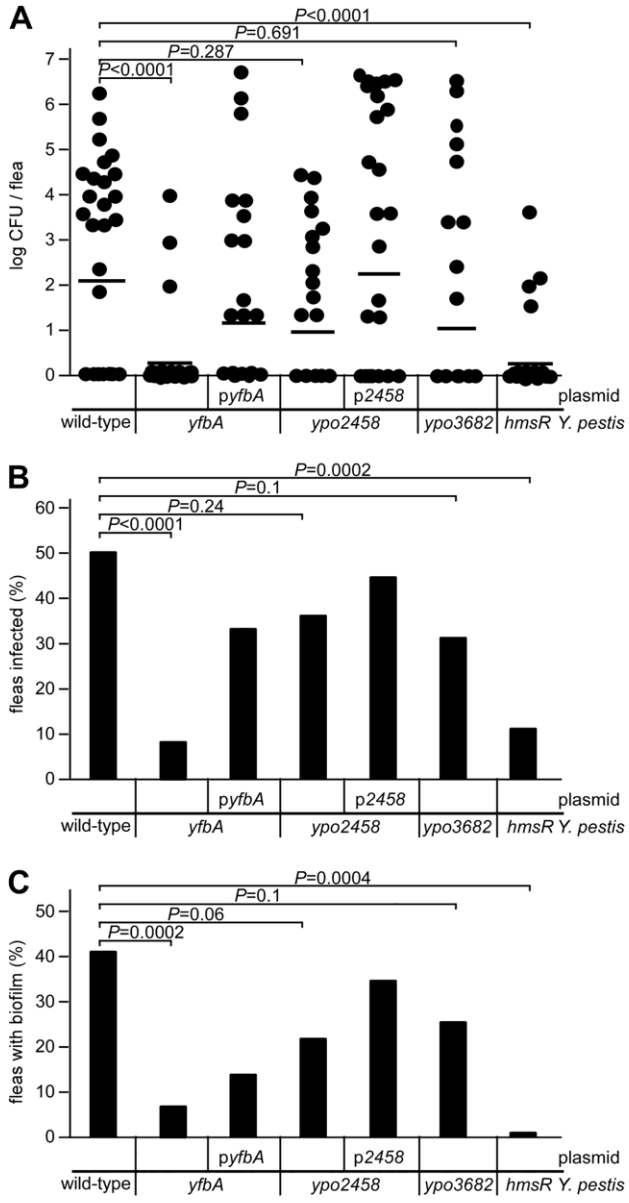

Figure B5. The *yfbA* gene is required for *Y. pestis* CO92(ΔpCD1) cat flea colonization and biofilm formation. (*A*) *Y. pestis* loads in the intestinal tracts of cat fleas ($n = 36$) infected for 14 days with wild-type or *yfbA*, *yfbA*(p*yfbA*), *ypo2458*, *ypo2458*(p*ypo2458*), *ypo3682*, or *hmsR* mutant strains. The horizontal bar indicates the nonparametric mean of each data set. Significance was calculated using the Mann-Whitney test for nonparametric distributions. (*B*) Percentages of fleas ($n = 36$) producing viable CFU 14 days after infection with wild-type or *yfbA*, *yfbA*(p*yfbA*),

Figure B5 (*continued*)

ypo2458, *ypo2458*(p*ypo2458*), *ypo3682*, or *hmsR* mutant *Y. pestis*. Significance was calculated using the Student *t* test. (*C*) Percentages of fleas harboring biofilm formation, indicative of gut blockage ($n = 20$ to 30), 14 days after infection with wild-type or *yfbA*, *yfbA*(p*yfbA*), *ypo2458*, *ypo2458*(p*ypo2458*), *ypo3682*, or *hmsR* mutant *Y. pestis*. The fleas were dissected in PBS. The proventriculus and midgut were removed and viewed at ×20 magnification using an Olympus IX81 microscope. The data are representative of two independent experiments. Significance was calculated with the Student *t* test.

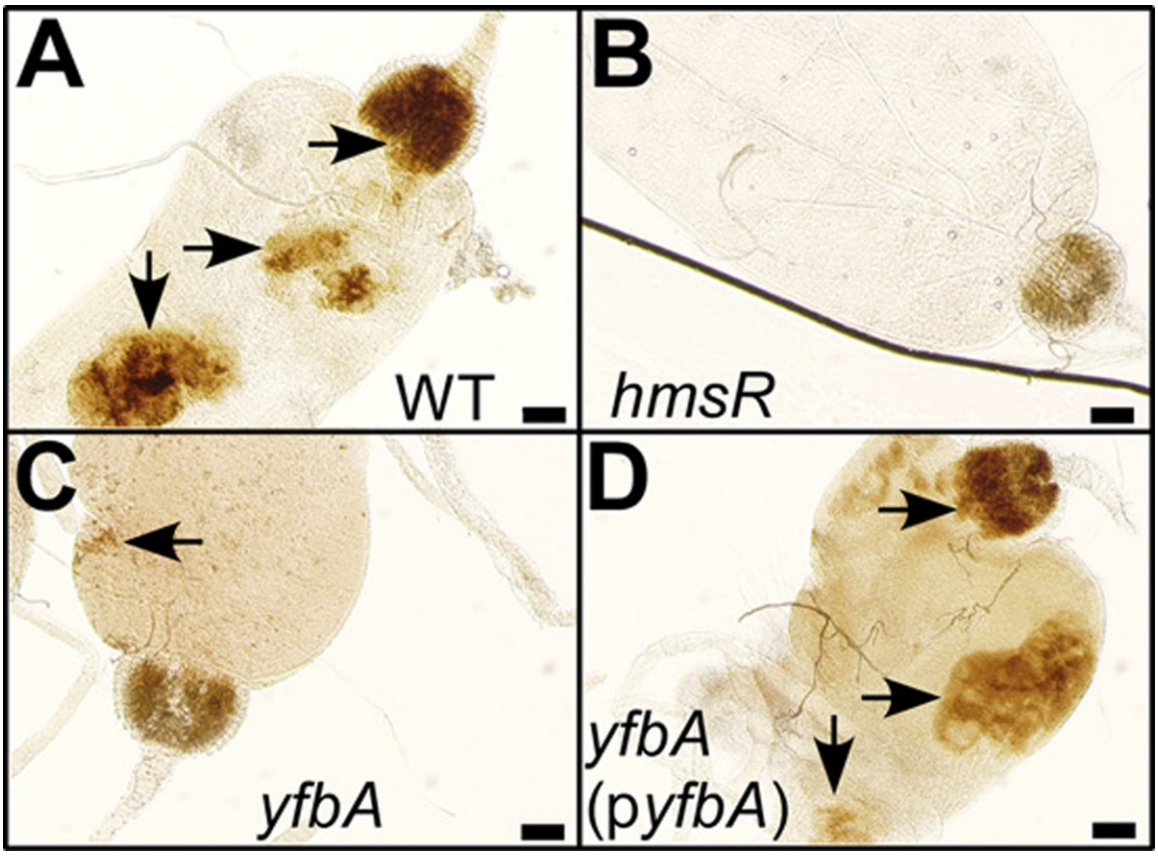

Figure B6. The *yfbA* gene is required for *Y. pestis* CO92(ΔpCD1) biofilm formation in cat fleas. Cat fleas ($n = 30$) were dissected, and their intestinal tracts were analyzed by bright-field microscopy 14 days (d14) after infection with either wild-type *Y. pestis* CO92(ΔpCD1) (WT) (*A*) or its *hmsR* (*B*), *yfbA* (*C*), or *yfbA*(p*yfbA*) (*D*) mutant strain. Representative images were acquired and inspected for biofilm formation (arrows). Bars denote 0.1 mm.

APPENDIX D

TABLES

Table 1. Summary of mass spectrometry analysis of tryptic peptides from *Y. pestis* $LcrV_{S228}$ and *E. coli* $rLcrV_{S228}$

	Molecular mass (Da)				
		$rLcrV_{S228}$		$LcrV_{S228}$	
$LcrV_{S228}$ peptide[a]	Calculated[b]	Observed[c]	Delta[d]	Observed[e]	Delta[f]
21-49[g]	3192.66	NF[h]	—	3193.37	−0.71
215-236	2612.98	NF	—	2612.18	0.80
1-20	2516.86	2516.18	0.68	NF	—
219-239	2473.74	2473.13	0.61	NF	—
19-40	2420.79	2420.38	0.41	2421.48	−0.69
117-137	2409.80	2409.68	0.12	2410.13	−0.33
21-42	2408.73	2409.68	−0.95	NF	—
316-334	2244.55	NF	—	2243.58	0.97
296-315	2237.45	NF	—	2238.02	−0.57
21-40	2165.47	2165.63	−0.16	2165.93	−0.46
219-236	2129.37	2129.33	0.04	2129.63	−0.26
101-116	1963.18	1963.28	−0.10	1963.58	−0.40
4-18	1861.00	1861.43	−0.43	1860.68	0.32
103-116	1735.87	NF	—	1736.48	−0.61
87-100	1599.73	1599.08	0.65	NF	—
117-130	1596.88	1596.28	0.60	1596.88	0.00
50-62	1596.72	NF	—	1596.88	−0.16
153-165	1514.74	1513.98	0.76	1514.78	−0.04
74-86	1505.82	1505.39	0.43	1506.78	−0.96
197-208	1491.62	1491.44	0.18	1491.89	−0.27
138-150	1450.59	1450.66	−0.07	1450.38	0.21
241-253	1449.67	1450.28	−0.61	1450.58	−0.91
87-99	1443.54	1443.89	−0.35	1444.38	−0.84
177-189	1408.53	1408.38	0.15	1408.78	−0.25
63-73	1286.53	1285.88	0.65	1286.68	−0.15
166-176	1277.48	1276.94	0.54	1277.39	0.09
285-295	1256.42	1255.94	0.48	1256.69	−0.27
155-165	1245.39	1244.99	0.40	1245.14	0.25
63-72	1157.65	1157.99	−0.34	1157.99	−0.34
306-315	1133.58	1133.99	−0.41	1134.14	−0.56
296-305	1120.57	1120.94	−0.37	1120.94	−0.37
54-62	1064.53	NF	—	1064.99	−0.46
246-254	1064.53	NF	—	1064.99	−0.46
41-49	1044.58	1044.74	−0.16	1044.89	−0.31
55-62	936.43	936.59	−0.16	936.74	−0.31
246-253	908.42	908.54	−0.12	908.99	−0.57
320-326	897.40	897.74	−0.34	897.74	−0.34
263-269	874.38	874.49	−0.11	874.79	−0.41
327-334	847.43	847.58	−0.15	847.79	−0.36

Table 1 (*continued*)

	Molecular mass (Da)				
		rLcrV$_{S228}$		LcrV$_{S228}$	
LcrV$_{S228}$ peptide[a]	Calculated[b]	Observed[c]	Delta[d]	Observed[e]	Delta[f]
131-137	830.44	830.54	−0.10	830.99	−0.55
190-196	819.42	819.59	−0.17	819.74	−0.32
43-49	801.46	801.59	−0.13	801.74	−0.28
255-262	772.44	772.79	−0.35	722.79	−0.35
240-245	686.47	686.84	−0.37	686.84	−0.37
209-214	667.32	668.30	−0.98	667.79	−0.47
241-245	558.37	558.59	−0.22	558.59	−0.22
50-53	549.25	549.59	−0.34	549.59	−0.34
316-319	534.32	534.59	−0.27	534.29	0.03
151-154	502.32	NF	—	501.59	0.73
215-218	501.32	501.29	0.03	501.59	−0.27
1-3	418.24	418.34	−0.10	418.34	−0.10
270-284	1681.75	1680.74	1.01	NF	—
270-284-GSH	1987.07	NF	—	1987.43	−0.36
270-284[i]	1680.70	1680.71	−0.0083	NF	—
270-284-GSH[i,j]	1985.79	NF	—	1985.79	−0.0002

[a,b] Peptide sequences derived from *in silico* tryptic cleavage of LcrV$_{S228}$ and their calculated masses.

[c,d] Observed mass of tryptic peptides derived from rLcrV$_{S228}$ that had been purified by affinity chromatography from cell lysates of *E. coli* DH5α(pKG48) and then identified by liquid chromatography-electrospray ionization mass spectrometry (LC-ESI-MS) and their delta with the predicted mass.

[e,f] Observed mass of tryptic peptides derived from LcrV$_{S228}$ that had been purified by affinity chromatography from culture supernatants of *Y. pestis* KLD29(pKG48) and then identified by LC-ESI-MS and their delta with the predicted mass.

[g] This data set was obtained with the Sciex API III^{+} instrument; the calculated masses are a mixture of monoisotopic and average depending on the resolution observed in the spectra unless otherwise indicated.

[h] NF = not found.

[i] These data were obtained with the Agilent QTOF instrument; the calculated masses are monoisotopic.

[j] 270-284-GSH = glutathionylated peptide 270-284.

Table 2. Tandem mass spectrometry of the 1,985.79-Da $LcrV_{S228}$ peptide

Residue	#	Calculated *m/z*	Found[a] *m/z*	Error (ppm)	+305.068159 calculated	Found *m/z*	Error (ppm)
					y ions		
D	15	—					
N	14	1566.6853	NF[b]	—	1871.753459[c]	NF	—
N	13	1452.6424	NF	—	1757.710559	1757.68243	16.00
E	12	1338.5994	NF	—	1643.667559	1643.66496	1.58
L	11	1209.5568	NF	—	1514.624959	1514.62361	0.89
S	10	1096.4728	NF	—	1401.540959	1401.53408	4.91
H	9	1009.4408	NF	—	1314.508959	1314.50293	4.59
F	8	872.3818	872.36486	−19.40	1177.449959	1177.44546	3.82
A	7	725.3134	NF	—	1030.381559	1030.37738	4.06
T	6	654.2763	NF	—	959.344459	959.34008	4.56
T	5	553.2286	NF	—	858.296759	858.29600	0.88
C	4	452.1810	NF	—	757.249159	757.25393	−6.30
S	3	349.1718	349.17224	1.30	654.239959	NF	—
D	2	262.1397	262.14044	2.80	567.207859	NF	—
K	1	147.1128	147.11296	1.10	452.180959	NF	—
					b ions		
D	1						
N	2	230.0771	230.07836	5.48	535.145259[d]	NF	—
N	3	344.1201	344.12084	2.15	649.188259	NF	—
E	4	473.1627	473.16257	−0.27	778.230859	NF	—
L	5	586.2467	586.24761	1.55	891.314859	NF	—
S	6	673.2788	673.27996	1.72	978.346959	NF	—
H	7	810.3377	810.33583	−2.31	1115.405859	NF	—
F	8	957.4061	957.40085	−5.48	1262.474259	NF	—
A	9	1028.4432	1028.44074	−2.39	1333.511359	NF	—
T	10	1129.4909	1129.48625	−4.12	1434.559059	NF	—
T	11	1230.5386	1230.52721	−9.26	1535.606759	NF	—
C	12	1333.5477	NF	—	1638.615859	NF	—
S	13	1420.5798	NF	—	1725.647959	NF	—
D	14	1535.6067	NF	—	1840.674859	NF	—
K	15	—					

[a] Collisionally induced dissociation of the 1,985.79-Da peptide in a tandem mass spectrometry experiment.

[b] NF = not found.

[c] y + 305.068159.

[d] b + 305.068159.

Table 3. Peptide mass fingerprinting by LC-MS/MS identifies macrophage RPS3 as a ligand of translocated LcrV

m/z				
Observed[a,b]	Calculated[c]	Δ[d]	Matching RPS3 peptide[e]	Residues
1024.5822	1024.5826	−0.0004	KFVADGIFK	10-18
896.4876	896.4876	0.0000	FVADGIFK	11-18
1092.5688	1092.5684	0.0004	AELNEFLTR	19-27
1423.6714	1423.6700	0.0014	ELAEDGYSGVEVR	28-40
1029.6315	1029.6303	0.0012	TEIIILATR	46-54
1156.7048	1156.7048	0.0000	IRELTAVVQK	66-75
1728.8584	1728.8592	−0.0008	RFGFPEGSVELYAEK	76-90
1572.7597	1572.7581	0.0016	FGFPEGSVELYAEK	77-90
1302.6839	1302.6834	0.0005	GLCAIAQAESLR	95-106
798.5195	798.5196	−0.0001	LLGGLAVR	109-116
2468.1941*	2468.1915	0.0026	FVDGLMIHSGDPVNYYVDTAVR	152-173
714.4507	714.4509	−0.0002	QGVLGIK	179-185
1143.5858	1143.5867	−0.0009	IMLPWDPSGK	188-197
1458.8314	1458.8315	−0.0001	KPLPDHVSIVEPK	202-214
2910.5853	2910.5823	0.0030	KPLPDHVSIVEPKDEILPTTPISEQK	202-227
1470.7697	1470.7686	0.0011	DEILPTTPISEQK	215-227
1573.8052*	1573.8043	0.0009	GGKPEPPAMPQPVPTA	228-243

[a] Peptide mass fingerprinting was performed by the Taplin Biological Mass Spectrometry Facility (Harvard Medical School) by bottom-up proteomics using microcapillary liquid chromatography–tandem mass spectrometry (LC-MS/MS).

[b] An asterisk (*) denotes that the observed ion was accompanied by a less intense ion with an increased *m/z* (+15.99); this accompanying ion was interpreted as an oxygen adduct of the parent ion resulting from oxidation of the peptide's single methionine residue.

[c] Monoisotopic *m/z* calculations were determined using Protein Prospector (http://prospector.ucsf.edu/prospector/mshome.htm).

[d] Observed *m/z* − Calculated *m/z*.

[e] SWISS-PROT database searches were used to identify matching peptides in the 40S ribosomal protein S3 (RPS3) of *Mus musculus* (http://www.uniprot.org/uniprot/P62908).

Table 4. MALDI-TOF MS analysis of $LcrV_{S228}$ and $LcrV_{S228\ C273S}$ purified from *Y. pestis* supernatants or *E. coli* extracts

Protein[a]	Strain[b]	Genotype	Molecular weight (Da)					Predicted structure
			Calculated[c] (±GSH)	Observed −DTT	Δ[d] $rLcrV_{S228}$	Δ[e] $LcrV_{S228}$	Observed[f] +DTT	
$rLcrV_{S228}$	*E. coli* DH5α (pKG48)	WT (p*lcrV*$_{S228}$)	38,280.22	38,271.66	−8.56	−313.88	38,281.05	[$LcrV_{S228}$]-SH
$LcrV_{S228}$	*Y. pestis* KLD29 (pKG48)	Δ*lcrV* (p*lcrV*$_{S228}$)	38,585.54	38,583.10	302.88	−2.44	38,282.55	[$LcrV_{S228}$]-GSH
$LcrV_{S228}$	*Y. pestis* AM43 (pKG48)	Δ*lcrV*, Δ*gshB* (p*lcrV*$_{S228}$)	—	38,592.16	311.94	6.62	38,281.27	[$LcrV_{S228}$]-GSH
$rLcrV_{S228\ C273S}$	*E. coli* DH5α (pAM199)	WT (p*lcrV*$_{S228\ C273S}$)	38,264.16	38,286.09	21.93	—	—	[$LcrV_{S228\ C273S}$]-SH
$LcrV_{S228\ C273S}$	*Y. pestis* KLD29 (pAM199)	Δ*lcrV* (p*lcrV*$_{S228\ C273S}$)	38,264.16	38,261.34	−2.82	—	—	[$LcrV_{S228\ C273S}$]-SH

[a] Purified LcrV was either left untreated (−DTT) or treated with dithiothreitol (+DTT), and then spotted undiluted with sinapinic acid onto a MALDI plate and analyzed by matrix-assisted laser desorption ionization–time of flight mass spectrometry (MALDI-TOF MS).

[b] All bacterial strains were propagated in LB broth during Strep-Tactin affinity purification experiments.

[c] Average molecular weights of non-glutathionylated $rLcrV_{S228}$ (38,280.22 Da) and glutathionylated $LcrV_{S228}$ (38,585.54 Da), as well as non-glutathionylated $rLcrV_{S228\ C273S}$ and $LcrV_{S228\ C273S}$ (38,264.16 Da), were calculated using Protein Prospector (http://prospector.ucsf.edu/prospector/mshome.htm).

[d] Observed molecular weight − Calculated molecular weight of $rLcrV_{S228}$ or $rLcrV_{S228\ C273S}$.

[e] Observed molecular weight − Calculated molecular weight of glutathionylated $LcrV_{S228}$.

[f] DTT treatment of *Y. pestis* $LcrV_{S228}$ collapsed the observed molecular weight to match that of *E. coli* $rLcrV_{S228}$.

Table 5. Bacterial strains and plasmids used in this study

Strains	Description
E. coli	
DH5α	*supE44* Δ*lacU169* (ϕ*80lacZ*Δ*M15*) *hsdR17 recA1 endA1 gyrA96 thi1 relA1*
S17-1	*thi pro recA*::RP4-2-Tc::Mu-Km::Tn*7 str* (λpir$^+$), *hsdR* mutant, *hsdM* mutant
Y. pestis KIM (Δ*pgm*)	
KIM D27	Wild-type isolate (Δ*pgm*, pCD1$^+$, pFra$^+$, pPCP1$^+$); also called KIM5
KLD29	Δ*lcrV*
AM6	$lcrV_{C273A}$
AM15	$lcrV_{C273S}$
AM27	Δ*yopJ*
AM29	$lcrV_{C273A}$, Δ*yopJ*
AM43	Δ*lcrV*, Δ*gshB*
Y. pestis CO92 (*pgm*$^+$)	
CO92	Wild-type isolate (*pgm*$^+$, pCD1$^+$, pFra$^+$, pPCP1$^+$)
LQ1	Δ*lcrV*
TD1	$lcrV_{C273A}$
DE1	$lcrV_{C273S}$

Plasmids	Description[a,b]
pLC28	Suicide vector, Cm^r
pCVD442	Suicide vector, Amp^r
pNM77	pHSG575 derivative, *tac* promoter fused to wild-type *lcrV*, Cm^r
pKG48	pNM77 derivative, *tac* promoter fused to $lcrV_{S228}$ (Strep tag inserted after LcrV residue 228), Cm^r
pAM128	pKG48 derivative, *tac* promoter fused to $lcrV_{S228\ C273A}$, Cm^r
pAM199	pKG48 derivative, *tac* promoter fused to $lcrV_{S228\ C273S}$, Cm^r
pYopM-Bla (pMM83)	pHSG576 derivative, native *yopM* promoter fused to *yopM-bla*, Cm^r
pGST-Bla (pMM91)	pHSG576 derivative, native *yopM* promoter fused to *gst-bla*, Cm^r
pAM105	pLC28 derivative, $lcrV_{C273A}$ allelic exchange construct for *Y. pestis* KIM D27, Cm^r
pCVD442-lcrV$_{C273A}$	pCVD442 derivative, $lcrV_{C273A}$ allelic exchange construct for *Y. pestis* CO92, Amp^r
pAM155	pCVD442 derivative, $lcrV_{C273S}$ allelic exchange construct, Amp^r
pAM178	pCVD442 derivative, *yopJ* deletion construct, Amp^r
pAM196	pCVD442 derivative, *gshB* deletion construct, Amp^r

[a] Chloramphenicol-resistant (Cm^r).

[b] Ampicillin-resistant (Amp^r).

Table 6. Primers used in this study

Primer name	Sequence (5′ → 3′)[a,b]
P140 for	CACTTTGCCACCACCgcgTCGGATAAGTCCAGG
P140 rev	CCTGGACTTATCCGAcgcGGTGGTGGCAAAGTG
P141 for	G**TCTAGA**GATATCGGCTTAACGCCTG
P141 rev	C**GGATCC**AACTAGCTTACCTAACTC
P142 for	AGC**GTCGAC**GATATCGGCTTAACGCCTG
P142 rev	AGC**GAGCTC**AACTAGCTTACCTAACTC
P190 for	CACTTTGCCACCACCaGCTCGGATAAGTCCA
P190 rev	TGGACTTATCCGAGCtGGTGGTGGCAAAGTG
P227 for	AAA**GAGCTC**CGGGAGCTATCTGATTTGCTTAG
P227 rev	AAA**AAGCTT**TTATTTATCCTTATTCAGGGAATTAACAGC
P228 for	AAA**AAGCTT**TGTATTTTGGAAATCTTGCTCCAG
P228 rev	AAA**GTCGAC**GGAACAGATGGTAATACTGTAACCGAAC
P296 for	AAA**GAGCTC**GGATTGAATGGGAACATGTGGTTC
P296 rev	AAA**GGATCC**TCTTTTCTCCTAGTGGGAAATGGGGT
P297 for	AAA**GGATCC**TACATAAAACGGGGTGTGGTGTT
P297 rev	AAA**GTCGAC**GCAACAGTCACTTTTGTCATGAGAA

[a] Boldface nucleotides indicate a restriction site.

[b] Lowercase nucleotides differ from the wild-type sequence and result in an amino acid substitution.

Table A1. Missense mutations in *lcrV* codon 327 block *Yersinia pestis* type III secretion

		% type III secretion ([S] / [S + P])[a]	
Y. pestis strain	Plasmid	YopE	LcrV
KIM D27 (wild type)	p*lcrV*$_{D27}$	36.6	28.3
KIM D27 (wild type)	p*lcrV*$_{*327R}$	1.3	12.6
KIM D27 (wild type)	p*lcrV*$_{*327W}$	1.2	10.3
KLD29 (Δ*lcrV*)	None	1.7	ND[b]
KLD29 (Δ*lcrV*)	p*lcrV*$_{D27}$	33.2	36.2

[a] Type III secretion of *Y. pestis* was measured after 3 h of growth in cultures that were grown in media with chelated calcium ions at 37°C. Following centrifugation, the extracellular medium was separated into the supernatant (S) and the bacterial pellet (P), and proteins in both fractions were precipitated with trichloroacetic acid and analyzed by immunoblotting with specific antibodies against the type III secretion substrates YopE and LcrV. Secretion was quantified by calculating the percent amount of secreted protein [S] derived from protein in both the medium and the pellet [S + P].

[b] ND, no immunoreactive signal detected.

Table A2. Insertions of the eight-codon Strep tag at various positions into *lcrV* and its effect on *Yersinia pestis* type III secretion of YopE or LcrV

	% type III secretion ([S] / [S + P])[a]			
	KIM D27 (wild type)		KLD29 (Δ*lcrV*)	
Plasmid	YopE	LcrV	YopE	LcrV
None	47.1	21.3	3.7	ND[b]
p*lcrV*$_{W22703}$	50.3	37.8	51.1	31.8
p*lcrV*$_{S1}$	52.3	25.8	60.8	24.1
p*lcrV*$_{S20}$	4.6	16.8	7.7	22.7
p*lcrV*$_{S55}$	4.1	15.8	13.2	21.9
p*lcrV*$_{S170}$	48.4	39.7	45.6	36.3
p*lcrV*$_{S228}$	49.2	38.9	63.4	37.6
p*lcrV*$_{S270}$	54.1	38.5	2.8	1.1

[a] Type III secretion of *Y. pestis* strains without or with *lcrV* plasmids was measured after 3 h of growth in cultures that were grown in media with chelated calcium ions at 37°C. Following centrifugation, the extracellular medium was separated into the supernatant (S) and the bacterial pellet (P), and proteins in both fractions were precipitated with trichloroacetic acid and analyzed by immunoblotting with specific antibodies against the type III secretion substrates YopE and LcrV. Secretion was quantified by calculating the percent amount of secreted protein [S] compared to protein in both the medium and the pellet [S + P].

[b] ND, no immunoreactive signal detected.

Table A3. LcrV$_{S324}$ blocks type III secretion of YopH in *Y. pestis* calcium-blind mutants with *yscF*$_{D28A}$ and *yscF*$_{D46A}$ mutations

	Y. pestis (Δ*yopE*/*sycE*) % type III secretion ([S] / [S + P])[a]			
	No plasmid		p*lcrV*$_{S324}$	
yscF allele	YopH	LcrV	YopH	LcrV
yscF	45.2	42.7	2.9	5.3
yscF$_{D28A}$	44.9	39.8	4.5	18.2
yscF$_{D46A}$	45.8	29.1	4.4	15.3
yscF$_{D28A,D46A}$	47.3	45.8	2.2	9.3
yscF$_{D77A}$	0.9	1.1	3.3	4.9

[a] Type III secretion of *Y. pestis* strains with or without p*lcrV*$_{S324}$ was measured after 3 h of growth in cultures that were grown in media with chelated calcium ions at 37°C. Following centrifugation, the extracellular medium was separated into the supernatant (S) and the bacterial pellet (P), and proteins in both fractions were precipitated with trichloroacetic acid and analyzed by immunoblotting with specific antibodies against the type III secretion substrates YopH and LcrV. Secretion was quantified by calculating the percent amount of secreted protein [S] compared to protein in both the medium and the pellet [S + P].

REFERENCES

Achtman, M., K. Zurth, G. Morelli, G. Torrea, A. Guiyoule, and E. Carniel. 1999. "*Yersinia pestis*, the Cause of Plague, Is a Recently Emerged Clone of *Yersinia pseudotuberculosis*." *Proceedings of the National Academy of Sciences of the United States of America* 96 (24): 14043–48. https://doi.org/10.1073/pnas.96.24.14043.

Allaoui, A., R. Schulte, and G. R. Cornelis. 1995. "Mutational Analysis of the *Yersinia enterocolitica virC* Operon: Characterization of *yscE*, *F*, *G*, *I*, *J*, *K* Required for Yop Secretion and *yscH* Encoding YopR." *Molecular Microbiology* 18 (2): 343–55. https://doi.org/10.1111/j.1365-2958.1995.mmi_18020343.x.

Altschul, S. F., W. Gish, W. Miller, E. W. Myers, and D. J. Lipman. 1990. "Basic Local Alignment Search Tool." *Journal of Molecular Biology* 215 (3): 403–10. https://doi.org /10.1016/S0022-2836(05)80360-2.

Anderson, D. M., N. A. Ciletti, H. Lee-Lewis, D. Elli, J. Segal, K. L. DeBord, K. A. Overheim, M. Tretiakova, R. R. Brubaker, and O. Schneewind. 2009. "Pneumonic Plague Pathogenesis and Immunity in Brown Norway Rats." *American Journal of Pathology* 174 (3): 910–21. https://doi.org/10.2353/ajpath.2009.071168.

Anderson, D. M., K. S. Ramamurthi, C. Tam, and O. Schneewind. 2002. "YopD and LcrH Regulate the Expression of *Yersinia enterocolitica* YopQ at a Post-Transcriptional Step and Bind to *yopQ* mRNA." *Journal of Bacteriology* 184 (5): 1287–95. https://doi.org /10.1128/JB.184.5.1287-1295.2002.

Anderson, D. M., and O. Schneewind. 1997. "A mRNA Signal for the Type III Secretion of Yop Proteins by *Yersinia enterocolitica*." *Science* 278 (5340): 1140–43. https://doi.org /10.1126/science.278.5340.1140.

Anderson, M. E. 1998. "Glutathione: An Overview of Biosynthesis and Modulation." *Chemico-Biological Interactions* 111–112: 1–14. https://doi.org/10.1016/S0009-2797(97)00146-4.

Andrews, G. P., D. G. Heath, G. W. Anderson, S. L. Welkos, and A. M. Friedlander. 1996. "Fraction 1 Capsular Antigen (F1) Purification from *Yersinia pestis* CO92 and from an *Escherichia coli* Recombinant Strain and Efficacy against Lethal Plague Challenge." *Infection and Immunity* 64 (6): 2180–87.

Anisimov, A. P., S. V. Dentovskaya, E. A. Panfertsev, T. E. Svetoch, P. K. Kopylov, B. W. Segelke, A. Zemla, M. V. Telepnev, and V. L. Motin. 2010. "Amino Acid and Structural Variability of *Yersinia pestis* LcrV Protein." *Infection, Genetics and Evolution* 10 (1): 137–45. https://doi.org/10.1016/j.meegid.2009.10.003.

Anisimov, A. P., L. E. Lindler, and G. B. Pier. 2004. “Intraspecific Diversity of *Yersinia pestis*.” *Clinical Microbiology Reviews* 17 (2): 434–64. https://doi.org/10.1128/CMR.17.2.434464.2004.

Antelmann, H., and J. D. Helmann. 2011. “Thiol-Based Redox Switches and Gene Regulation.” *Antioxidants & Redox Signaling* 14 (6): 1049–63. https://doi.org/10.1089/ars.2010.3400.

Bacot, A. W., and C. J. Martin. 1914. “LXVII. Observations on the Mechanism of the Transmission of Plague by Fleas.” *Journal of Hygiene* 13 (Supplement): 423–39.

Baker, E. E., H. Sommer, L. E. Foster, E. Meyer, and K. F. Meyer. 1952. “Studies on Immunization against Plague: I. The Isolation and Characterization of the Soluble Antigen of *Pasteurella pestis*.” *Journal of Immunology* 68 (2): 131–45.

Bazanova, L. P., and M. P. Maevskii. 1996. “The Duration of the Persistence of the Plague Microbe in the Body of the Flea *Citellophilus tesquorum altaicus*.” [In Russian.] *Meditsinskaya Parazitologiya i Parazitarnye Bolezni* 2: 45–48.

Benedictow, O. J. 2004. *The Black Death, 1346–1353: The Complete History*. Woodbridge, UK: Boydell Press.

Benner, G. E., G. P. Andrews, W. R. Byrne, S. D. Strachan, A. K. Sample, D. G. Heath, and A. M. Friedlander. 1999. “Immune Response to *Yersinia* Outer Proteins and Other *Yersinia pestis* Antigens after Experimental Plague Infection in Mice.” *Infection and Immunity* 67 (4): 1922–28.

Black, D. S., and J. B. Bliska. 1997. “Identification of $p130^{Cas}$ as a Substrate of *Yersinia* YopH (Yop51), a Bacterial Protein Tyrosine Phosphatase That Translocates into Mammalian Cells and Targets Focal Adhesions.” *EMBO Journal* 16 (10): 2730–44. https://doi.org/10.1093/emboj/16.10.2730.

Blaylock, B., B. J. Berube, and O. Schneewind. 2010. “YopR Impacts Type III Needle Polymerization in *Yersinia* Species.” *Molecular Microbiology* 75 (1): 221–29. https://doi.org/10.1111/j.1365-2958.2009.06988.x.

Blaylock, B., K. E. Riordan, D. M. Missiakas, and O. Schneewind. 2006. “Characterization of the *Yersinia enterocolitica* Type III Secretion ATPase YscN and Its Regulator, YscI.” *Journal of Bacteriology* 188 (10): 3525–34. https://doi.org/10.1128/JB.188.10.3525-3534.2006.

Blocker, A., N. Jouihri, E. Larquet, P. Gounon, F. Ebel, C. Parsot, P. Sansonetti, and A. Allaoui. 2001. “Structure and Composition of the *Shigella flexneri* ‘Needle Complex’, a Part of Its Type III Secreton.” *Molecular Microbiology* 39 (3): 652–63. https://doi.org/10.1046/j.1365-2958.2001.02200.x.

Blomfield, I. C., V. Vaughn, R. F. Rest, and B. I. Eisenstein. 1991. "Allelic Exchange in *Escherichia coli* Using the *Bacillus subtilis sacB* Gene and a Temperature-Sensitive pSC101 Replicon." *Molecular Microbiology* 5 (6): 1447–57. https://doi.org/10.1111/j.1365-2958.1991.tb00791.x.

Bobrov, A. G., O. Kirillina, D. A. Ryjenkov, C. M. Waters, P. A. Price, J. D. Fetherston, D. Mack, W. E. Goldman, M. Gomelsky, and R. D. Perry. 2011. "Systematic Analysis of Cyclic di-GMP Signalling Enzymes and Their Role in Biofilm Formation and Virulence in *Yersinia pestis*." *Molecular Microbiology* 79 (2): 533–51. https://doi.org/10.1111/j.1365-2958.2010.07470.x.

Bos, K. I., A. Herbig, J. Sahl, N. Waglechner, M. Fourment, S. A. Forrest, J. Klunk, V. J. Schuenemann, D. Poinar, M. Kuch, G. B. Golding, O. Dutour, P. Keim, D. M. Wagner, E. C. Holmes, J. Krause, and H. N. Poinar. 2016. "Eighteenth Century *Yersinia pestis* Genomes Reveal the Long-Term Persistence of an Historical Plague Focus." *eLife* 5: e12994. https://doi.org/10.7554/eLife.12994.

Bos, K. I., V. J. Schuenemann, G. B. Golding, H. A. Burbano, N. Waglechner, B. K. Coombes, J. B. McPhee, S. N. DeWitte, M. Meyer, S. Schmedes, J. Wood, D. J. Earn, D. A. Herring, P. Bauer, H. N. Poinar, and J. Krause. 2011. "A Draft Genome of *Yersinia pestis* from Victims of the Black Death." *Nature* 478 (7370): 506–10. https://doi.org/10.1038/nature10549.

Bos, K. I., P. Stevens, K. Nieselt, H. N. Poinar, S. N. DeWitte, and J. Krause. 2012. "*Yersinia pestis*: New Evidence for an Old Infection." *PLOS ONE* 7 (11): e49803. https://doi.org/10.1371/journal.pone.0049803.

Brandes, N., S. Schmitt, and U. Jakob. 2009. "Thiol-Based Redox Switches in Eukaryotic Proteins." *Antioxidants & Redox Signaling* 11 (5): 997–1014. https://doi.org/10.1089/ARS.2008.2285.

Broz, P., C. A. Mueller, S. A. Müller, A. Philippsen, I. Sorg, A. Engel, and G. R. Cornelis. 2007. "Function and Molecular Architecture of the *Yersinia* Injectisome Tip Complex." *Molecular Microbiology* 65 (5): 1311–20. https://doi.org/10.1111/j.13652958.2007.05871.x.

Brubaker, R. R. 1969. "Mutation Rate to Nonpigmentation in *Pasteurella pestis*." *Journal of Bacteriology* 98 (3): 1404–6.

———. 1991. "Factors Promoting Acute and Chronic Diseases Caused by *Yersiniae*." *Clinical Microbiology Reviews* 4 (3): 309–24. https://doi.org/10.1128/CMR.4.3.309.

Buhnerkempe, M. G., R. J. Eisen, B. Goodell, K. L. Gage, M. F. Antolin, and C. T. Webb. 2011. "Transmission Shifts Underlie Variability in Population Responses to *Yersinia pestis* Infection." *PLOS ONE* 6 (7): e22498. https://doi.org/10.1371/journal.pone.0022498.

Burrows, T. W. 1956. “An Antigen Determining Virulence in *Pasteurella pestis*.” *Nature* 177 (4505): 426–27. https://doi.org/10.1038/177426b0.

———. 1957. “Virulence of *Pasteurella pestis*.” *Nature* 179 (4572): 1246–47. https://doi.org/10.1038/1791246a0.

Chain, P. S., E. Carniel, F. W. Larimer, J. Lamerdin, P. O. Stoutland, W. M. Regala, A. M. Georgescu, L. M. Vergez, M. L. Land, V. L. Motin, R. R. Brubaker, J. Fowler, J. Hinnebusch, M. Marceau, C. Medigue, M. Simonet, V. Chenal-Francisque, B. Souza, D. Dacheux, J. M. Elliott, A. Derbise, L. J. Hauser, and E. Garcia. 2004. “Insights into the Evolution of *Yersinia pestis* through Whole-Genome Comparison with *Yersinia pseudotuberculosis*.” *Proceedings of the National Academy of Sciences of the United States of America* 101 (38): 13826–31. https://doi.org/10.1073/pnas.0401412101.

Chain, P. S., P. Hu, S. A. Malfatti, L. Radnedge, F. Larimer, L. M. Vergez, P. Worsham, M. C. Chu, and G. L. Andersen. 2006. “Complete Genome Sequence of *Yersinia pestis* Strains Antiqua and Nepal516: Evidence of Gene Reduction in an Emerging Pathogen.” *Journal of Bacteriology* 188 (12): 4453–63. https://doi.org/10.1128/JB.00124-06.

Chen, T. H., and K. F. Meyer. 1974. “Susceptibility and Antibody Response of *Rattus* Species to Experimental Plague.” *Journal of Infectious Diseases* 129 (Supplement 1): S62–71. https://doi.org/10.1093/infdis/129.Supplement_1.S62.

Cheng, L. W., D. M. Anderson, and O. Schneewind. 1997. “Two Independent Type III Secretion Mechanisms for YopE in *Yersinia enterocolitica*.” *Molecular Microbiology* 24 (4): 757–65. https://doi.org/10.1046/j.1365-2958.1997.3831750.x.

Cheng, L. W., and O. Schneewind. 2000. “Type III Machines of Gram-Negative Bacteria: Delivering the Goods.” *Trends in Microbiology* 8 (5): 214–20. https://doi.org/10.1016/S0966-842X(99)01665-0.

Chosewood, L. C. and D. E. Wilson, eds. 2009. *Biosafety in Microbiological and Biomedical Laboratories*, 5th ed. HHS Publication No. (CDC) 21-1112. Washington, DC: U.S. Department of Health and Human Services, Public Health Service, Centers for Disease Control and Prevention, National Institutes of Health. https://www.cdc.gov/biosafety/publications/bmbl5/bmbl.pdf.

Comer, J. E., D. E. Sturdevant, A. B. Carmody, K. Virtaneva, D. Gardner, D. Long, R. Rosenke, S. F. Porcella, and B. J. Hinnebusch. 2010. “Transcriptomic and Innate Immune Responses to *Yersinia pestis* in the Lymph Node during Bubonic Plague.” *Infection and Immunity* 78 (12): 5086–98. https://doi.org/10.1128/IAI.00256-10.

Cornelis, G. R. 2000. “Molecular and Cell Biology Aspects of Plague.” *Proceedings of the National Academy of Sciences of the United States of America* 97 (16): 8778–83. https://doi.org/10.1073/pnas.97.16.8778.

———. 2002. "*Yersinia* Type III Secretion: Send in the Effectors." *Journal of Cell Biology* 158 (3): 401–8. https://doi.org/10.1083/jcb.200205077.

———. 2006. "The Type III Secretion Injectisome." *Nature Reviews: Microbiology* 4 (11): 811–25. https://doi.org/10.1038/nrmicro1526.

Cornelis, G. R., T. Biot, C. Lambert de Rouvroit, T. Michiels, B. Mulder, C. Sluiters, M.-P. Sory, M. Van Bouchaute, and J.-C. Vanooteghem. 1989. "The *Yersinia yop* Regulon." *Molecular Microbiology* 3 (10): 1455–59. https://doi.org/10.1111/j.13652958.1989 .tb00129.x.

Cornelis, G. R., A. Boland, A. P. Boyd, C. Geuijen, M. Iriarte, C. Neyt, M.-P. Sory, and I. Stainier. 1998. "The Virulence Plasmid of *Yersinia*, an Antihost Genome." *Microbiology and Molecular Biology Reviews* 62 (4): 1315–52.

Cornelis, G. R., and C. Colson. 1975. "Restriction of DNA in *Yersinia enterocolitica* Detected by Recipient Ability for a Derepressed R Factor from *Escherichia coli*." *Journal of General Microbiology* 87 (2): 285–91. https://doi.org/10.1099/00221287-87-2-285.

Cornelis, G. R., J.-C. Vanooteghem, and C. Sluiters. 1987. "Transcription of the *yop* Regulon from *Y. enterocolitica* Requires Trans Acting pYV and Chromosomal Genes." *Microbial Pathogenesis* 2 (5): 367–79. https://doi.org/10.1016/0882-4010(87)90078-7.

Cornelius, C. A., L. E. Quenee, D. Elli, N. A. Ciletti, and O. Schneewind. 2009. "*Yersinia pestis* IS*1541* Transposition Provides for Escape from Plague Immunity." *Infection and Immunity* 77 (5): 1807–16. https://doi.org/10.1128/IAI.01162-08.

Cornelius, C. A., L. E. Quenee, K. A. Overheim, F. Koster, T. L. Brasel, D. Elli, N. A. Ciletti, and O. Schneewind. 2008. "Immunization with Recombinant V10 Protects Cynomolgus Macaques from Lethal Pneumonic Plague." *Infection and Immunity* 76 (12): 5588–97. https://doi.org/10.1128/IAI.00699-08.

Dalle-Donne, I., R. Rossi, G. Colombo, D. Giustarini, and A. Milzani. 2009. "Protein *S*-Glutathionylation: A Regulatory Device from Bacteria to Humans." *Trends in Biochemical Sciences* 34 (2): 85–96. https://doi.org/10.1016/j.tibs.2008.11.002.

Dalle-Donne, I., R. Rossi, D. Giustarini, R. Colombo, and A. Milzani. 2007. "S-Glutathionylation in Protein Redox Regulation." *Free Radical Biology and Medicine* 43 (6): 883–98. https://doi.org/10.1016/j.freeradbiomed.2007.06.014.

Darby, C., S. L. Ananth, L. Tan, and B. J. Hinnebusch. 2005. "Identification of g*mhA*, a *Yersinia pestis* Gene Required for Flea Blockage, by Using a *Caenorhabditis elegans* Biofilm System." *Infection and Immunity* 73 (11): 7236–42. https://doi.org/10.1128/IAI.73.11 .7236-7242.2005.

Davis, S., M. Begon, L. De Bruyn, V. S. Ageyev, N. L. Klassovskiy, S. B. Pole, H. Viljugrein, N. C. Stenseth, and H. Leirs. 2004. "Predictive Thresholds for Plague in Kazakhstan." *Science* 304 (5671): 736–38. https://doi.org/10.1126/science.1095854.

Deane, J. E., P. Abrusci, S. Johnson, and S. M. Lea. 2010. "Timing Is Everything: The Regulation of Type III Secretion." *Cellular and Molecular Life Sciences* 67 (7): 1065–75. https://doi.org/10.1007/s00018-009-0230-0.

DeBord, K. L., D. M. Anderson, M. M. Marketon, K. A. Overheim, R. W. DePaolo, N. A. Ciletti, B. Jabri, and O. Schneewind. 2006. "Immunogenicity and Protective Immunity against Bubonic Plague and Pneumonic Plague by Immunization of Mice with the Recombinant V10 Antigen, a Variant of LcrV." *Infection and Immunity* 74 (8): 4910–14. https://doi.org/10.1128/IAI.01860-05.

DeBord, K. L., V. T. Lee, and O. Schneewind. 2001. "On the Role of LcrG and LcrV during the Type III Targeting of Effector Yops by *Yersinia enterocolitica*." *Journal of Bacteriology* 183 (15): 4588–98. https://doi.org/10.1128/JB.183.15.4588-4598.2001.

De Lay, N., D. J. Schu, and S. Gottesman. 2013. "Bacterial Small RNA-Based Negative Regulation: Hfq and Its Accomplices." *Journal of Biological Chemistry* 288 (12): 7996–8003. https://doi.org/10.1074/jbc.R112.441386.

de Lorenzo, V., L. Eltis, B. Kessler, and K. N. Timmis. 1993. "Analysis of *Pseudomonas* Gene Products Using *lacI*^{q}/P*trp-lac* Plasmids and Transposons That Confer Conditional Phenotypes." *Gene* 123 (1): 17–24. https://doi.org/10.1016/0378-1119(93)90533-9.

DePaolo, R. W., F. Tang, I. Kim, M. Han, N. Levin, N. Ciletti, A. Lin, D. M. Anderson, O. Schneewind, and B. Jabri. 2008. "Toll-Like Receptor 6 Drives Differentiation of Tolerogenic Dendritic Cells and Contributes to LcrV-Mediated Plague Pathogenesis." *Cell Host Microbe* 4 (4): 350–61. https://doi.org/10.1016/j.chom.2008.09.004.

Derewenda, U., A. Mateja, Y. Devedjiev, K. M. Routzahn, A. G. Evdokimov, Z. S. Derewenda, and D. S. Waugh. 2004. "The Structure of *Yersinia pestis* V-Antigen, an Essential Virulence Factor and Mediator of Immunity against Plague." *Structure* 12 (2): 301–6. https://doi.org/10.1016/j.str.2004.01.010.

Diepold, A., M. Amstutz, S. Abel, I. Sorg, U. Jenal, and G. R. Cornelis. 2010. "Deciphering the Assembly of the *Yersinia* Type III Secretion Injectisome." *EMBO Journal* 29 (11): 1928–40. https://doi.org/10.1038/emboj.2010.84.

Diepold, A., U. Wiesand, M. Amstutz, and G. R. Cornelis. 2012. "Assembly of the *Yersinia* Injectisome: The Missing Pieces." *Molecular Microbiology* 85 (5): 878–92. https://doi.org/10.1111/j.1365-2958.2012.08146.x.

Diepold, A., U. Wiesand, and G. R. Cornelis. 2011. "The Assembly of the Export Apparatus (YscR,S,T,U,V) of the *Yersinia* Type III Secretion Apparatus Occurs Independently of Other Structural Components and Involves the Formation of an YscV Oligomer." *Molecular Microbiology* 82 (2): 502–14. https://doi.org/10.1111/j.1365-2958.2011.07830.x.

Doll, J. M., P. S. Zeitz, P. Ettestad, A. L. Bucholtz, T. Davis, and K. L. Gage. 1994. "Cat-Transmitted Fatal Pneumonic Plague in a Person Who Traveled from Colorado to Arizona." *American Journal of Tropical Medicine and Hygiene* 51 (1): 109–14. https://doi.org/10.4269/ajtmh.1994.51.109.

Donnenberg, M. S., and J. B. Kaper. 1991. "Construction of an *eae* Deletion Mutant of Enteropathogenic *Escherichia coli* by Using a Positive-Selection Suicide Vector." *Infection and Immunity* 59 (12): 4310–17.

Douglas, J. R., and C. M Wheeler. 1943. "Sylvatic Plague Studies: II. The Fate of *Pasteurella pestis* in the Flea." *Journal of Infectious Diseases* 72 (1): 18–30. https://doi.org/10.1093/infdis/72.1.18.

Du, Y., R. Rosqvist, and Å. Forsberg. 2002. "Role of Fraction 1 Antigen of *Yersinia pestis* in Inhibition of Phagocytosis." *Infection and Immunity* 70 (3): 1453–60. https://doi.org/10.1128/IAI.70.3.1453-1460.2002.

Eisen, R. J., S. W. Bearden, A. P. Wilder, J. A. Montenieri, M. F. Antolin, and K. L. Gage. 2006. "Early-Phase Transmission of *Yersinia pestis* by Unblocked Fleas as a Mechanism Explaining Rapidly Spreading Plague Epizootics." *Proceedings of the National Academy of Sciences of the United States of America* 103 (42): 15380–85. https://doi.org/10.1073/pnas.0606831103.

Eisen, R. J., J. N. Borchert, J. L. Holmes, G. Amatre, K. Van Wyk, R. E. Enscore, N. Babi, L. A. Atiku, A. P. Wilder, S. M. Vetter, S. W. Bearden, J. A. Montenieri, and K. L. Gage. 2008. "Early-Phase Transmission of *Yersinia pestis* by Cat Fleas (*Ctenocephalides felis*) and Their Potential Role as Vectors in a Plague-Endemic Region of Uganda." *American Journal of Tropical Medicine and Hygiene* 78 (6): 949–56.

Eisen, R. J., and K. L. Gage. 2012. "Transmission of Flea-Borne Zoonotic Agents." *Annual Review of Entomology* 57: 61–82. https://doi.org/10.1146/annurev-ento-120710-100717.

Erickson, D. L., C. O. Jarrett, J. A. Callison, E. R. Fischer, and B. J. Hinnebusch. 2008. "Loss of a Biofilm-Inhibiting Glycosyl Hydrolase during the Emergence of *Yersinia pestis*." *Journal of Bacteriology* 190 (24): 8163–70. https://doi.org/10.1128/JB.01181-08.

Erickson, D. L., C. O. Jarrett, B. W. Wren, and B. J. Hinnebusch. 2006. "Serotype Differences and Lack of Biofilm Formation Characterize *Yersinia pseudotuberculosis* Infection of the *Xenopsylla cheopis* Flea Vector of *Yersinia pestis*." *Journal of Bacteriology* 188 (3): 1113–19. https://doi.org/10.1128/JB.188.3.1113-1119.2006.

Erickson, D. L., N. R. Waterfield, V. Vadyvaloo, D. Long, E. R. Fischer, R. Ffrench-Constant, and B. J. Hinnebusch. 2007. "Acute Oral Toxicity of *Yersinia pseudotuberculosis* to Fleas: Implications for the Evolution of Vector-Borne Transmission of Plague." *Cellular Microbiology* 9 (11): 2658–66. https://doi.org/10.1111/j.1462-5822.2007.00986.x.

Fahey, R. C. 2013. "Glutathione Analogs in Prokaryotes." *Biochimica et Biophysica Acta* 1830 (5): 3182–98. https://doi.org/10.1016/j.bbagen.2012.10.006.

Ferracci, F., F. D. Schubot, D. S. Waugh, and G. V. Plano. 2005. "Selection and Characterization of *Yersinia pestis* YopN Mutants That Constitutively Block Yop Secretion." *Molecular Microbiology* 57 (4): 970–87. https://doi.org/10.1111/j.1365-2958.2005.04738.x.

Forman, S., A. G. Bobrov, O. Kirillina, S. K. Craig, J. Abney, J. D. Fetherston, and R. D. Perry. 2006. "Identification of Critical Amino Acid Residues in the Plague Biofilm Hms Proteins." *Microbiology* 152 (11): 3399–410. https://doi.org/10.1099/mic.0.29224-0.

Frank, K. M., O. Schneewind, and W. J. Shieh. 2011. "Investigation of a Researcher's Death Due to Septicemic Plague." *New England Journal of Medicine* 364 (26): 2563–64. https://doi.org/10.1056/NEJMc1010939.

Freitag, N. E., G. C. Port, and M. D. Miner. 2009. "*Listeria monocytogenes*—from Saprophyte to Intracellular Pathogen." *Nature Reviews: Microbiology* 7 (9): 623–28. https://doi.org /10.1038/nrmicro2171.

Friedlander, A. M., S. L. Welkos, P. L. Worsham, G. P. Andrews, D. G. Heath, G. W. Anderson, M. L. Pitt, J. Estep, and K. Davis. 1995. "Relationship between Virulence and Immunity as Revealed in Recent Studies of the F1 Capsule of *Yersinia pestis*." *Clinical Infectious Diseases* 21 (Supplement 2): S178–181. https://doi.org/10.1093/clinids/21 .Supplement_2.S178.

Gage, K. L., D. T. Dennis, K. A. Orloski, P. Ettestad, T. L. Brown, P. J. Reynolds, W. J. Pape, C. L. Fritz, L. G. Carter, and J. D. Stein. 2000. "Cases of Cat-Associated Human Plague in the Western US, 1977–1998." *Clinical Infectious Diseases* 30 (6): 893–900. https://doi.org/10.1086/313804.

Gage, K. L., and M. Y. Kosoy. 2005. "Natural History of Plague: Perspectives from More Than a Century of Research." *Annual Review of Entomology* 50: 505–28. https://doi.org/10.1146 /annurev.ento.50.071803.130337.

Galán, J. E., and A. Collmer. 1999. "Type III Secretion Machines: Bacterial Devices for Protein Delivery into Host Cells." *Science* 284 (5418): 1322–28. https://doi.org/10.1126/science .284.5418.1322.

Galán, J. E., and H. Wolf-Watz. 2006. "Protein Delivery into Eukaryotic Cells by Type III Secretion Machines." *Nature* 444 (7119): 567–73. https://doi.org/10.1038/nature05272.

Gao, X., and P. R. Hardwidge. 2011. “Ribosomal Protein S3: A Multifunctional Target of Attaching/Effacing Bacterial Pathogens.” *Frontiers in Microbiology* 2: 137. https://doi.org/10.3389/fmicb.2011.00137.

Gao, X.-H., M. Bedhomme, D. Veyel, M. Zaffagnini, and S. D. Lemaire. 2009. “Methods for Analysis of Protein Glutathionylation and Their Application to Photosynthetic Organisms.” *Molecular Plant* 2 (2): 218–35. https://doi.org/10.1093/mp/ssn072.

Gerke, C., A. Kraft, R. Sussmuth, O. Schweitzer, and F. Götz. 1998. “Characterization of the *N*-Acetylglucosaminyltransferase Activity Involved in the Biosynthesis of the *Staphylococcus epidermidis* Polysaccharide Intercellular Adhesin.” *Journal of Biological Chemistry* 273 (29): 18586–93. https://doi.org/10.1074/jbc.273.29.18586.

Ghezzi, P. 2005. “Regulation of Protein Function by Glutathionylation.” *Free Radical Research* 39 (6): 573–80. https://doi.org/10.1080/10715760500072172.

———. 2013. “Protein Glutathionylation in Health and Disease.” *Biochimica et Biophysica Acta* 1830 (5): 3165–72. https://doi.org/10.1016/j.bbagen.2013.02.009.

Girard, G. 1955. “Plague.” *Annual Review of Microbiology* 9: 253–76. https://doi.org/10.1146/annurev.mi.09.100155.001345.

Girard, G., and J. Robic. 1942. “L’état actuel de la peste à Madagascar et la prophylaxie vaccinale par le virus-vaccin.” *Bulletin de la Société de Pathologie Exotique* 35: 42–49.

Goguen, J. D., J. Yother, and S. C. Straley. 1984. “Genetic Analysis of the Low Calcium Response in *Yersinia pestis* Mu d1(Ap *lac*) Insertion Mutants.” *Journal of Bacteriology* 160 (3): 842–48.

Gonzalez, R. J., E. H. Weening, M. C. Lane, and V. L. Miller. 2015. “Comparison of Models for Bubonic Plague Reveals Unique Pathogen Adaptations to the Dermis.” *Infection and Immunity* 83 (7): 2855–61. https://doi.org/10.1128/IAI.00140-15.

Gopal, S., I. Borovok, A. Ofer, M. Yanku, G. Cohen, W. Goebel, J. Kreft, and Y. Aharonowitz. 2005. “A Multidomain Fusion Protein in *Listeria monocytogenes* Catalyzes the Two Primary Activities for Glutathione Biosynthesis.” *Journal of Bacteriology* 187 (11): 3839–47. https://doi.org/10.1128/JB.187.11.3839-3847.2005.

Gould, L. H., J. Pape, P. Ettestad, K. S. Griffith, and P. S. Mead. 2008. “Dog-Associated Risk Factors for Human Plague.” *Zoonoses and Public Health* 55 (8–10): 448–54. https://doi.org/10.1111/j.1863-2378.2008.01132.x.

Graham, C. B., J. N. Borchert, W. C. Black, L. A. Atiku, J. T. Mpanga, K. A. Boegler, S. M. Moore, K. L. Gage, and R. J. Eisen. 2013. “Blood Meal Identification in Off-Host Cat Fleas (*Ctenocephalides felis*) from a Plague-Endemic Region of Uganda.” *American Journal of Tropical Medicine and Hygiene* 88 (2): 381–89. https://doi.org/10.4269/ajtmh.2012.12-0532.

Gray, M. J., W. Y. Wholey, and U. Jakob. 2013. "Bacterial Responses to Reactive Chlorine Species." *Annual Review of Microbiology* 67: 141–60. https://doi.org/10.1146/annurev-micro-102912-142520.

Håkansson, S., T. Bergman, J.-C. Vanooteghem, G. R. Cornelis, and H. Wolf-Watz. 1993. "YopB and YopD Constitute a Novel Class of *Yersinia* Yop Proteins." *Infection and Immunity* 61 (1): 71–80.

Håkansson, S., K. Schesser, C. Persson, E. E. Galyov, R. Rosqvist, F. Homblé, and H. Wolf-Watz. 1996. "The YopB Protein of *Yersinia pseudotuberculosis* Is Essential for the Translocation of Yop Effector Proteins across the Target Cell Plasma Membrane and Displays a Contact-Dependent Membrane Disrupting Activity." *EMBO Journal* 15 (21): 5812–23.

Hamad, M. A., and M. L. Nilles. 2007. "Structure-Function Analysis of the C-Terminal Domain of LcrV from *Yersinia pestis*." *Journal of Bacteriology* 189 (18): 6734–39. https://doi.org/10.1128/JB.00539-07.

Hanahan, D. 1983. "Studies on Transformation of *Escherichia coli* with Plasmids." *Journal of Molecular Biology* 166 (4): 557–80. https://doi.org/10.1016/S0022-2836(83)80284-8.

Harper, K. 2017. *The Fate of Rome: Climate, Disease, & the End of an Empire*. Princeton: Princeton University Press.

Henikoff, S., G. W. Haughn, J. M. Calvo, and J. C. Wallace. 1988. "A Large Family of Bacterial Activator Proteins." *Proceedings of the National Academy of Sciences of the United States of America* 85 (18): 6602–6. https://doi.org/10.1073/pnas.85.18.6602.

Higuchi, K. 1970. "An Improved Chemically Defined Culture Medium for Strain L Mouse Cells Based on Growth Responses to Graded Levels of Nutrients Including Iron and Zinc Ions." *Journal of Cellular Physiology* 75 (1): 65–72. https://doi.org/10.1002/jcp.1040750108.

Hinnebusch, B. J. 2003. "Transmission Factors: *Yersinia pestis* Genes Required to Infect the Flea Vector of Plague." *Advances in Experimental Medicine and Biology* 529: 55–62. https://doi.org/10.1007/0-306-48416-1_11.

———. 2012. "Biofilm-Dependent and Biofilm-Independent Mechanisms of Transmission of *Yersinia pestis* by Fleas." *Advances in Experimental Medicine and Biology* 954: 237–43. https://doi.org/10.1007/978-1-4614-3561-7_30.

Hinnebusch, B. J., E. R. Fischer, and T. G. Schwan. 1998. "Evaluation of the Role of the *Yersinia pestis* Plasminogen Activator and Other Plasmid-Encoded Factors in Temperature-Dependent Blockage of the Flea." *Journal of Infectious Diseases* 178 (5): 1406–15. https://doi.org/10.1086/314456.

Hinnebusch, B. J., A. E. Rudolph, P. Cherepanov, J. E. Dixon, T. G. Schwan, and Å. Forsberg. 2002. "Role of *Yersinia* Murine Toxin in Survival of *Yersinia pestis* in the Midgut of the Flea Vector." *Science* 296 (5568): 733–35. https://doi.org/10.1126/science.1069972.

Hodgson, A., E. M. Wier, K. Fu, X. Sun, H. Yu, W. Zheng, H. P. Sham, K. Johnson, S. Bailey, B. A. Vallance, and F. Wan. 2015. "Metalloprotease NleC Suppresses Host NF-κB/Inflammatory Responses by Cleaving p65 and Interfering with the p65/RPS3 Interaction." *PLOS Pathogens* 11 (3): e1004705. https://doi.org/10.1371/journal.ppat.1004705.

Hoe, N. P., and J. D. Goguen. 1993. "Temperature Sensing in *Yersinia pestis*: Translation of the LcrF Activator Protein Is Thermally Regulated." *Journal of Bacteriology* 175 (24): 7901–9. https://doi.org/10.1128/jb.175.24.7901-7909.1993.

Hoiczyk, E., and G. Blobel. 2001. "Polymerization of a Single Protein of the Pathogen *Yersinia enterocolitica* into Needles Punctures Eukaryotic Cells." *Proceedings of the National Academy of Sciences of the United States of America* 98 (8): 4669–74. https://doi.org/10.1073/pnas.071065798.

Hondorp, E. R., and R. G. Matthews. 2004. "Oxidative Stress Inactivates Cobalamin-Independent Methionine Synthase (MetE) in *Escherichia coli*." *PLOS Biology* 2 (11): e336. https://doi.org/10.1371/journal.pbio.0020336.

Hopkins, F. G. 1921. "On an Autoxidisable Constituent of the Cell." *Biochemical Journal* 15 (2): 286–305. https://doi.org/10.1042/bj0150286.

Hueck, C. J. 1998. "Type III Protein Secretion Systems in Bacterial Pathogens of Animals and Plants." *Microbiology and Molecular Biology Reviews* 62 (2): 379–433.

Hwang, C., H. F. Lodish, and A. J. Sinskey. 1995. "Measurement of Glutathione Redox State in Cytosol and Secretory Pathway of Cultured Cells." *Methods in Enzymology* 251: 212–21. https://doi.org/10.1016/0076-6879(95)51123-7.

Inglesby, T. V., D. T. Dennis, D. A. Henderson, J. G. Bartlett, M. S. Ascher, E. Eitzen, A. D. Fine, A. M. Friedlander, J. Hauer, J. F. Koerner, M. Layton, J. McDade, M. T. Osterholm, T. O'Toole, G. Parker, T. M. Perl, P. K. Russell, M. Schoch-Spana, and K. Tonat. 2000. "Plague as a Biological Weapon: Medical and Public Health Management." *Journal of the American Medical Association* 283 (17): 2281–90. https://doi.org/10.1001/jama.283.17.2281.

Inglesby, T. V., R. Grossman, and T. O'Toole. 2001. "A Plague on Your City: Observations from TOPOFF." *Clinical Infectious Diseases* 32 (3): 436–45. https://doi.org/10.1086/318513.

Ivanov, M. I., B. L. Noel, R. Rampersaud, P. Mena, J. L. Benach, and J. B. Bliska. 2008. "Vaccination of Mice with a Yop Translocon Complex Elicits Antibodies That Are Protective against Infection with F1^{-} *Yersinia pestis*." *Infection and Immunity* 76 (11): 5181–90. https://doi.org/10.1128/IAI.00189-08.

Jackson, M. W., and G. V. Plano. 2000. "Interactions between Type III Secretion Apparatus Components from *Yersinia pestis* Detected Using the Yeast Two-Hybrid System." *FEMS Microbiology Letters* 186 (1): 85–90. https://doi.org/10.1111/j.1574-6968.2000.tb09086.x.

Janowiak, B. E., and O. W. Griffith. 2005. "Glutathione Synthesis in *Streptococcus agalactiae*: One Protein Accounts for γ-Glutamylcysteine Synthetase and Glutathione Synthetase Activities." *Journal of Biological Chemistry* 280 (12): 11829–39. https://doi.org/10.1074/jbc.M414326200.

Jarrett, C. O., E. Deak, K. E. Isherwood, P. C. F. Oyston, E. R. Fischer, A. R. Whitney, S. D. Kobayashi, F. R. DeLeo, and B. J. Hinnebusch. 2004. "Transmission of *Yersinia pestis* from an Infectious Biofilm in the Flea Vector." *Journal of Infectious Diseases* 190 (4): 783–92. https://doi.org/10.1086/422695.

Journet, L., C. Agrain, P. Broz, and G. R. Cornelis. 2003. "The Needle Length of Bacterial Injectisomes Is Determined by a Molecular Ruler." *Science* 302 (5651): 1757–60. https://doi.org/10.1126/science.1091422.

Kearse, M., R. Moir, A. Wilson, S. Stones-Havas, M. Cheung, S. Sturrock, S. Buxton, A. Cooper, S. Markowitz, C. Duran, T. Thierer, B. Ashton, P. Meintjes, and A. Drummond. 2012. "Geneious Basic: An Integrated and Extendable Desktop Software Platform for the Organization and Analysis of Sequence Data." *Bioinformatics* 28 (12): 1647–49. https://doi.org/10.1093/bioinformatics/bts199.

Kilonzo, B. S., T. J. Mbise, D. C. Mwalimu, and L. Kindamba. 2006. "Observations on the Endemicity of Plague in Karatu and Ngorongoro, Northern Tanzania." *Tanzania Health Research Bulletin* 8 (1): 1–6. https://doi.org/10.4314/thrb.v8i1.14262.

Kim, S. O., K. Merchant, R. Nudelman, W. F. Beyer, T. Keng, J. Deangelo, A. Hausladen, and J. S. Stamler. 2002. "OxyR: A Molecular Code for Redox-Related Signaling." *Cell* 109 (3): 383–96. https://doi.org/10.1016/S0092-8674(02)00723-7.

Kimbrough, T. G., and S. I. Miller. 2000. "Contribution of *Salmonella typhimurium* Type III Secretion Components to Needle Complex Formation." *Proceedings of the National Academy of Sciences of the United States of America* 97 (20): 11008–13. https://doi.org/10.1073/pnas.200209497.

Kirillina, O., J. D. Fetherston, A. G. Bobrov, J. Abney, and R. D. Perry. 2004. "HmsP, a Putative Phosphodiesterase, and HmsT, a Putative Diguanylate Cyclase, Control Hms-Dependent Biofilm Formation in *Yersinia pestis*." *Molecular Microbiology* 54 (1): 75–88. https://doi.org/10.1111/j.1365-2958.2004.04253.x.

Klatt, P., and S. Lamas. 2000. “Regulation of Protein Function by S-Glutathiolation in Response to Oxidative and Nitrosative Stress.” *European Journal of Biochemistry* 267 (16): 4928–44. https://doi.org/10.1046/j.1432-1327.2000.01601.x.

Koo, J. T., T. M. Alleyne, C. A. Schiano, N. Jafari, and W. W. Lathem. 2011. “Global Discovery of Small RNAs in *Yersinia pseudotuberculosis* Identifies *Yersinia*-Specific Small, Noncoding RNAs Required for Virulence.” *Proceedings of the National Academy of Sciences of the United States of America* 108 (37): E709–717. https://doi.org/10.1073/pnas.1101655108.

Koster, M., W. Bitter, H. de Cock, A. Allaoui, G. R. Cornelis, and J. Tommassen. 1997. “The Outer Membrane Component, YscC, of the Yop Secretion Machinery of *Yersinia enterocolitica* Forms a Ring-Shaped Multimeric Complex.” *Molecular Microbiology* 26 (4): 789–97. https://doi.org/10.1046/j.1365-2958.1997.6141981.x.

Kupferberg, L. L., and K. Higuchi. 1958. “Role of Calcium Ions in the Stimulation of Growth of Virulent Strains of *Pasteurella pestis*.” *Journal of Bacteriology* 76 (1): 120–21.

LaRock, C. N., and B. T. Cookson. 2012. “The *Yersinia* Virulence Effector YopM Binds Caspase-1 to Arrest Inflammasome Assembly and Processing.” *Cell Host Microbe* 12 (6): 799–805. https://doi.org/10.1016/j.chom.2012.10.020.

Lee, C. A. 1997. “Type III Secretion Systems: Machines to Deliver Bacterial Proteins into Eukaryotic Cells?” *Trends in Microbiology* 5 (4): 148–56. https://doi.org/10.1016/S0966-842X(97)01029-9.

Lee, P. C., C. M. Stopford, A. G. Svenson, and A. Rietsch. 2010. “Control of Effector Export by the *Pseudomonas aeruginosa* Type III Secretion Proteins PcrG and PcrV.” *Molecular Microbiology* 75 (4): 924–41. https://doi.org/10.1111/j.1365-2958.2009.07027.x.

Lee, V. T., S. K. Mazmanian, and O. Schneewind. 2001. “A Program of *Yersinia enterocolitica* Type III Secretion Reactions Is Triggered by Specific Host Signals.” *Journal of Bacteriology* 183 (17): 4970–78. https://doi.org/10.1128/JB.183.17.4970-4978.2001.

Lee, V. T., and O. Schneewind. 1999. “Type III Secretion Machines and the Pathogenesis of Enteric Infections Caused by *Yersinia* and *Salmonella* Spp.” *Immunological Reviews* 168 (1): 241–55. https://doi.org/10.1111/j.1600-065X.1999.tb01296.x.

Lee, V. T., C. Tam, and O. Schneewind. 2000. “LcrV, a Substrate for *Yersinia enterocolitica* Type III Secretion, Is Required for Toxin Targeting into the Cytosol of HeLa Cells.” *Journal of Biological Chemistry* 275 (47): 36869–75. https://doi.org/10.1074/jbc.M002467200.

Lemaître, N., F. Sebbane, D. Long, and B. J. Hinnebusch. 2006. "*Yersinia pestis* YopJ Suppresses Tumor Necrosis Factor Alpha Induction and Contributes to Apoptosis of Immune Cells in the Lymph Node but Is Not Required for Virulence in a Rat Model of Bubonic Plague." *Infection and Immunity* 74 (9): 5126–31. https://doi.org/10.1128/IAI.00219-06.

Ligon, B. L. 2006. "Plague: A Review of Its History and Potential as a Biological Weapon." *Seminars in Pediatric Infectious Diseases* 17 (3): 161–70. https://doi.org/10.1053/j.spid.2006.07.002.

Ligtenberg, K. G., N. C. Miller, A. Mitchell, G. V. Plano, and O. Schneewind. 2013. "LcrV Mutants That Abolish *Yersinia* Type III Injectisome Function." *Journal of Bacteriology* 195 (4): 777–87. https://doi.org/10.1128/JB.02021-12.

Lillig, C. H., A. Potamitou, J. D. Schwenn, A. Vlamis-Gardikas, and A. Holmgren. 2003. "Redox Regulation of 3′-Phosphoadenylylsulfate Reductase from *Escherichia coli* by Glutathione and Glutaredoxins." *Journal of Biological Chemistry* 278 (25): 22325–30. https://doi.org/10.1074/jbc.M302304200.

Little, L. K. 2007. "Life and Afterlife of the First Plague Pandemic." In *Plague and the End of Antiquity: The Pandemic of 541–750*, edited by L. K. Little, 3–32. New York: Cambridge University Press.

Loi, V. V., M. Rossius, and H. Antelmann. 2015. "Redox Regulation by Reversible Protein *S*-Thiolation in Bacteria." *Frontiers in Microbiology* 6: 187. https://doi.org/10.3389/fmicb.2015.00187.

Luebke, J. L., and D. P. Giedroc. 2015. "Cysteine Sulfur Chemistry in Transcriptional Regulators at the Host–Bacterial Pathogen Interface." *Biochemistry* 54 (21): 3235–49. https://doi.org/10.1021/acs.biochem.5b00085.

Maddocks, S. E., and P. C. F. Oyston. 2008. "Structure and Function of the LysR-Type Transcriptional Regulator (LTTR) Family Proteins." *Microbiology* 154 (12): 3609–23. https://doi.org/10.1099/mic.0.2008/022772-0.

Marketon, M. M., R. W. DePaolo, K. L. DeBord, B. Jabri, and O. Schneewind. 2005. "Plague Bacteria Target Immune Cells during Infection." *Science* 309 (5741): 1739–41. https://doi.org/10.1126/science.1114580.

Marlovits, T. C., T. Kubori, M. Lara-Tejero, D. Thomas, V. M. Unger, and J. E. Galán. 2006. "Assembly of the Inner Rod Determines Needle Length in the Type III Secretion Injectisome." *Nature* 441 (7093): 637–40. https://doi.org/10.1038/nature04822.

Marlovits, T. C., T. Kubori, A. Sukhan, D. R. Thomas, J. E. Galán, and V. M. Unger. 2004. "Structural Insights into the Assembly of the Type III Secretion Needle Complex." *Science* 306 (5698): 1040–42. https://doi.org/10.1126/science.1102610.

Masip, L., K. Veeravalli, and G. Georgiou. 2006. “The Many Faces of Glutathione in Bacteria.” *Antioxidants & Redox Signaling* 8 (5–6): 753–62. https://doi.org/10.1089/ars.2006.8.753.

Matson, J. S., and M. L. Nilles. 2001. “LcrG-LcrV Interaction Is Required for Control of Yops Secretion in *Yersinia pestis*.” *Journal of Bacteriology* 183 (17): 5082–91. https://doi.org/10.1128/JB.183.17.5082-5091.2001.

Matteï, P.-J., E. Faudry, V. Job, T. Izoré, I. Attree, and A. Dessen. 2011. “Membrane Targeting and Pore Formation by the Type III Secretion System Translocon.” *FEBS Journal* 278 (3): 414–26. https://doi.org/10.1111/j.1742-4658.2010.07974.x.

Meister, A. 1995. “Glutathione Biosynthesis and Its Inhibition.” *Methods in Enzymology* 252: 26–30. https://doi.org/10.1016/0076-6879(95)52005-8.

Meyer, K. F. 1970. “Effectiveness of Live or Killed Plague Vaccines in Man.” *Bulletin of the World Health Organization* 42 (5): 653–66.

Michiels, T., J.-C. Vanooteghem, C. Lambert de Rouvroit, B. China, A. Gustin, P. Boudry, and G. R. Cornelis. 1991. “Analysis of *virC*, an Operon Involved in the Secretion of Yop Proteins by *Yersinia enterocolitica*.” *Journal of Bacteriology* 173 (16): 4994–5009. https://doi.org/10.1128/jb.173.16.4994-5009.1991.

Michiels, T., P. Wattiau, R. Brasseur, J.-M. Ruysschaert, and G. R. Cornelis. 1990. “Secretion of Yop Proteins by *Yersiniae*.” *Infection and Immunity* 58 (9): 2840–49.

Miller, N. C., L. E. Quenee, D. Elli, N. A. Ciletti, and O. Schneewind. 2012. “Polymorphisms in the *lcrV* Gene of *Yersinia enterocolitica* and Their Effect on Plague Protective Immunity.” *Infection and Immunity* 80 (4): 1572–82. https://doi.org/10.1128/IAI.05637-11.

Minato, Y., A. Ghosh, W. J. Faulkner, E. J. Lind, S. S. Bartra, G. V. Plano, C. O. Jarrett, B. J. Hinnebusch, J. Winogrodzki, P. Dibrov, and C. C. Häse. 2013. “Na^+/H^+ Antiport Is Essential for *Yersinia pestis* Virulence.” *Infection and Immunity* 81 (9): 3163–72. https://doi.org/10.1128/IAI.00071-13.

Minocha, R., W. C. Shortle, S. L. Long, and S. C. Minocha. 1994. “A Rapid and Reliable Procedure for Extraction of Cellular Polyamines and Inorganic Ions from Plant Tissues.” *Journal of Plant Growth Regulation* 13 (4): 187–93. https://doi.org/10.1007/BF00226036.

Minocha, R., P. Thangavel, O. P. Dhankher, and S. Long. 2008. “Separation and Quantification of Monothiols and Phytochelatins from a Wide Variety of Cell Cultures and Tissues of Trees and Other Plants Using High Performance Liquid Chromatography.” *Journal of Chromatography A* 1207 (1–2): 72–83. https://doi.org/10.1016/j.chroma.2008.08.023.

Mitchell, A., C. Tam, D. Elli, T. Charlton, P. Osei-Owusu, F. Fazlollahi, K. F. Faull, and O. Schneewind. 2017. "Glutathionylation of *Yersinia pestis* LcrV and Its Effects on Plague Pathogenesis." *mBio* 8 (3): e0064-17. https://doi.org/10.1128/mBio.00646-17.

Morelli, G., Y. Song, C. J. Mazzoni, M. Eppinger, P. Roumagnac, D. M. Wagner, M. Feldkamp, B. Kusecek, A. J. Vogler, Y. Li, Y. Cui, N. R. Thomson, T. Jombart, R. Leblois, P. Lichtner, L. Rahalison, J. M. Petersen, F. Balloux, P. Keim, T. Wirth, J. Ravel, R. Yang, E. Carniel, and M. Achtman. 2010. "*Yersinia pestis* Genome Sequencing Identifies Patterns of Global Phylogenetic Diversity." *Nature Genetics* 42 (12): 1140–43. https://doi.org/10.1038/ng.705.

Mota, L. J., L. Journet, I. Sorg, C. Agrain, and G. R. Cornelis. 2005. "Bacterial Injectisomes: Needle Length Does Matter." *Science* 307 (5713): 1278. https://doi.org/10.1126 /science.1107679.

Mueller, C. A., P. Broz, and G. R. Cornelis. 2008. "The Type III Secretion System Tip Complex and Translocon." *Molecular Microbiology* 68 (5): 1085–95. https://doi.org/10.1111 /j.1365-2958.2008.06237.x.

Mueller, C. A., P. Broz, S. A. Müller, P. Ringler, F. Erne-Brand, I. Sorg, M. Kuhn, A. Engel, and G. R. Cornelis. 2005. "The V-Antigen of *Yersinia* Forms a Distinct Structure at the Tip of Injectisome Needles." *Science* 310 (5748): 674–76. https://doi.org/10.1126/science .1118476.

Mukherjee, S., G. Keitany, Y. Li, Y. Wang, H. L. Ball, E. J. Goldsmith, and K. Orth. 2006. "*Yersinia* YopJ Acetylates and Inhibits Kinase Activation by Blocking Phosphorylation." *Science* 312 (5777): 1211–14. https://doi.org/10.1126/science.1126867.

Nakajima, R., and R. R. Brubaker. 1993. "Association between Virulence of *Yersinia pestis* and Suppression of Gamma Interferon and Tumor Necrosis Factor Alpha." *Infection and Immunity* 61 (1): 23–31.

Nakajima, R., V. L. Motin, and R. R. Brubaker. 1995. "Suppression of Cytokines in Mice by Protein A-V Antigen Fusion Peptide and Restoration of Synthesis by Active Immunization." *Infection and Immunity* 63 (8): 3021–29.

Nilles, M. L., K. A. Fields, and S. C. Straley. 1998. "The V Antigen of *Yersinia pestis* Regulates Yop Vectorial Targeting as well as Yop Secretion through Effects on YopB and LcrG." *Journal of Bacteriology* 180 (13): 3410–20.

Nilles, M. L., A. W. Williams, E. Skryzpek, and S. C. Straley. 1997. "*Yersinia pestis* LcrV Forms a Stable Complex with LcrG and May Have a Secretion-Related Regulatory Role in the Low-Ca^{2+} Response." *Journal of Bacteriology* 179 (4): 1307–16. https://doi.org /10.1128/jb.179.4.1307-1316.1997.

Noden, B. H., S. Radulovic, J. A. Higgins, and A. F. Azad. 1998. “Molecular Identification of *Rickettsia typhi* and *R. felis* in Co-Infected *Ctenocephalides felis* (Siphonaptera: Pulicidae).” *Journal of Medical Entomology* 35 (4): 410–14. https://doi.org/10.1093/jmedent/35.4.410.

Olsson, J., P. J. Edqvist, J. E. Bröms, Å. Forsberg, H. Wolf-Watz, and M. S. Francis. 2004. “The YopD Translocator of *Yersinia pseudotuberculosis* Is a Multifunctional Protein Comprised of Discrete Domains.” *Journal of Bacteriology* 186 (13): 4110–23. https://doi.org/10.1128/JB.186.13.4110-4123.2004.

Orloski, K. A., and M. Eidson. 1995. “*Yersinia pestis* Infection in Three Dogs.” *Journal of the American Veterinary Medical Association* 207 (3): 316–18.

Overheim, K. A., R. W. DePaolo, K. L. DeBord, E. M. Morrin, D. M. Anderson, N. M. Green, R. R. Brubaker, B. Jabri, and O. Schneewind. 2005. “LcrV Plague Vaccine with Altered Immunomodulatory Properties.” *Infection and Immunity* 73 (8): 5152–59. https://doi.org/10.1128/IAI.73.8.5152-5159.2005.

Parkhill, J., B. W. Wren, N. R. Thomson, R. W. Titball, M. T. G. Holden, M. B. Prentice, M. Sebaihia, K. D. James, C. Churcher, K. L. Mungall, S. Baker, D. Basham, S. D. Bentley, K. Brooks, A. M. Cerdeño-Tárraga, T. Chillingworth, A. Cronin, R. M. Davies, P. Davis, G. Dougan, T. Feltwell, N. Hamlin, S. Holroyd, K. Jagels, A. V. Karlyshev, S. Leather, S. Moule, P. C. F. Oyston, M. Quail, K. Rutherford, M. Simmonds, J. Skelton, K. Stevens, S. Whitehead, and B. G. Barrell. 2001. “Genome Sequence of *Yersinia pestis*, the Causative Agent of Plague.” *Nature* 413 (6855): 523–27. https://doi.org/10.1038/35097083.

Pechous, R. D., V. Sivaraman, P. A. Price, N. M. Stasulli, and W. E. Goldman. 2013. “Early Host Cell Targets of *Yersinia pestis* during Primary Pneumonic Plague.” *PLOS Pathogens* 9 (10): e1003679. https://doi.org/10.1371/journal.ppat.1003679.

Pechous, R. D., V. Sivaraman, N. M. Stasulli, and W. E. Goldman. 2016. “Pneumonic Plague: The Darker Side of *Yersinia pestis*.” *Trends in Microbiology* 24 (3): 190–97. https://doi.org/10.1016/j.tim.2015.11.008.

Perry, R. D., and J. D. Fetherston. 1997. “*Yersinia pestis*—Etiologic Agent of Plague.” *Clinical Microbiology Reviews* 10 (1): 35–66.

Perry, R. D., P. A. Harmon, W. S. Bowmer, and S. C. Straley. 1986. “A Low-Ca^{2+} Response Operon Encodes the V Antigen of *Yersinia pestis*.” *Infection and Immunity* 54 (2): 428–34.

Perry, R. D., M. L. Pendrak, and P. Schuetze. 1990. “Identification and Cloning of a Hemin Storage Locus Involved in the Pigmentation Phenotype of *Yersinia pestis*.” *Journal of Bacteriology* 172 (10): 5929–37. https://doi.org/10.1128/jb.172.10.5929-5937.1990.

Pettersson, J., A. Holmström, J. Hill, S. Leary, E. Frithz-Lindsten, A. von Euler-Matell, E. Carlsson, R. Titball, Å. Forsberg, and H. Wolf-Watz. 1999. "The V-Antigen of *Yersinia* Is Surface Exposed before Target Cell Contact and Involved in Virulence Protein Translocation." *Molecular Microbiology* 32 (5): 961–76. https://doi.org/10.1046/j.1365-2958.1999.01408.x.

Pollack, C., S. C. Straley, and M. S. Klempner. 1986. "Probing the Phagolysosomal Environment of Human Macrophages with a Ca^{2+}-Responsive Operon Fusion in *Yersinia pestis*." *Nature* 322 (6082): 834–36. https://doi.org/10.1038/322834a0.

Pollitzer, R. 1951. "Plague Studies: I. A Summary of the History and a Survey of the Present Distribution of the Disease." *Bulletin of the World Health Organization* 4 (4): 475–533.

Portman, J. L., Q. Huang, M. L. Reniere, A. T. Iavarone, and D. A. Portnoy. 2017. "Activity of the Pore-Forming Virulence Factor Listeriolysin O Is Reversibly Inhibited by Naturally Occurring S-Glutathionylation." *Infection and Immunity* 85 (4): e00959-16. https://doi.org/10.1128/IAI.00959-16.

Potter, A. J., C. Trappetti, and J. C. Paton. 2012. "*Streptococcus pneumoniae* Uses Glutathione to Defend against Oxidative Stress and Metal Ion Toxicity." *Journal of Bacteriology* 194 (22): 6248–54. https://doi.org/10.1128/JB.01393-12.

Prentice, M. B., and L. Rahalison. 2007. "Plague." *Lancet* 369 (9568): 1196–207. https://doi.org/10.1016/S0140-6736(07)60566-2.

Quastel, J. H., C. P. Stewart, and H. E. Tunnicliffe. 1923. "On Glutathione: IV. Constitution." *Biochemical Journal* 17 (4–5): 586–92. https://doi.org/10.1042/bj0170586.

Quenee, L. E., B. J. Berube, J. Segal, D. Elli, N. A. Ciletti, D. M. Anderson, and O. Schneewind. 2010. "Amino Acid Residues 196–225 of LcrV Represent a Plague Protective Epitope." *Vaccine* 28 (7): 1870–76. https://doi.org/10.1016/j.vaccine.2009.11.076.

Quenee, L. E., N. A. Ciletti, D. Elli, T. Hermanas, and O. Schneewind. 2011. "Prevention of Pneumonic Plague in Mice, Rats, Guinea Pigs and Non-Human Primates with Clinical Grade rV10, rV10-2 or F1-V Vaccines." *Vaccine* 29 (38): 6572–83. https://doi.org/10.1016/j.vaccine.2011.06.119.

Quenee, L. E., C. A. Cornelius, N. A. Ciletti, D. Elli, and O. Schneewind. 2008. "*Yersinia pestis caf1* Variants and the Limits of Plague Vaccine Protection." *Infection and Immunity* 76 (5): 2025–36. https://doi.org/10.1128/IAI.00105-08.

Quenee, L. E., T. Hermanas, N. Ciletti, H. Louvel, N. C. Miller, D. Elli, B. Blaylock, A. Mitchell, J. Schroeder, T. Krausz, J. Kanabrocki, and O. Schneewind. 2012. "Hereditary Hemochromatosis Restores the Virulence of Plague Vaccine Strains." *Journal of Infectious Diseases* 206 (7): 1050–58. https://doi.org/10.1093/infdis/jis433.

Quenee, L. E., and O. Schneewind. 2009. “Plague Vaccines and the Molecular Basis of Immunity against *Yersinia pestis*.” *Human Vaccines* 5 (12): 817–23. https://doi.org /10.4161/hv.9866.

Rall, T. W., and A. L. Lehninger. 1952. “Glutathione Reductase of Animal Tissues.” *Journal of Biological Chemistry* 194 (1): 119–30.

Ramamurthi, K. S., and O. Schneewind. 2002. “Type III Protein Secretion in *Yersinia* Species.” *Annual Review of Cell and Developmental Biology* 18 (1): 107–33. https://doi.org /10.1146/annurev.cellbio.18.012502.105912.

Rebeil, R., C. O. Jarrett, J. D. Driver, R. K. Ernst, P. C. F. Oyston, and B. J. Hinnebusch. 2013. “Induction of the *Yersinia pestis* PhoP-PhoQ Regulatory System in the Flea and Its Role in Producing a Transmissible Infection.” *Journal of Bacteriology* 195 (9): 1920–30. https://doi.org/10.1128/JB.02000-12.

Rempe, K. A., A. K. Hinz, and V. Vadyvaloo. 2012. “Hfq Regulates Biofilm Gut Blockage That Facilitates Flea-Borne Transmission of *Yersinia pestis*.” *Journal of Bacteriology* 194 (8): 2036–40. https://doi.org/10.1128/JB.06568-11.

Reniere, M. L., A. T. Whiteley, K. L. Hamilton, S. M. John, P. Lauer, R. G. Brennan, and D. A. Portnoy. 2015. “Glutathione Activates Virulence Gene Expression of an Intracellular Pathogen.” *Nature* 517 (7533): 170–73. https://doi.org/10.1038/nature14029.

Rijstenbil, J. W., and J. A. Wijnholds. 1996. “HPLC Analysis of Nonprotein Thiols in Planktonic Diatoms: Pool Size, Redox State and Response to Copper and Cadmium Exposure.” *Marine Biology* 127 (1): 45–54. https://doi.org/10.1007/bf00993642.

Riordan, K. E., and O. Schneewind. 2008. “YscU Cleavage and the Assembly of *Yersinia* Type III Secretion Machine Complexes.” *Molecular Microbiology* 68 (6): 1485–501. https://doi.org/10.1111/j.1365-2958.2008.06247.x.

Rosqvist, R., I. Bölin, and H. Wolf-Watz. 1988. “Inhibition of Phagocytosis in *Yersinia pseudotuberculosis*: A Virulence Plasmid-Encoded Ability Involving the Yop2b Protein.” *Infection and Immunity* 56 (8): 2139–43.

Rosqvist, R., K.-E. Magnusson, and H. Wolf-Watz. 1994. “Target Cell Contact Triggers Expression and Polarized Transfer of *Yersinia* YopE Cytotoxin into Mammalian Cells.” *EMBO Journal* 13 (4): 964–72. https://doi.org/10.1002/j.1460-2075.1994.tb06341.x.

Ross, J. A., and G. V. Plano. 2011. “A C-Terminal Region of *Yersinia pestis* YscD Binds the Outer Membrane Secretin YscC.” *Journal of Bacteriology* 193 (9): 2276–89. https://doi.org/10.1128/JB.01137-10.

Russell, P., S. M. Eley, S. E. Hibbs, R. J. Manchee, A. J. Stagg, and R. W. Titball. 1995. "A Comparison of Plague Vaccine, USP and EV76 Vaccine Induced Protection against *Yersinia pestis* in a Murine Model." *Vaccine* 13 (16): 1551–56. https://doi.org/10.1016/0264-410X(95)00090-N.

Salkeld, D. J., and P. Stapp. 2006. "Seroprevalence Rates and Transmission of Plague (*Yersinia pestis*) in Mammalian Carnivores." *Vector-Borne and Zoonotic Diseases* 6 (3): 231–39. https://doi.org/10.1089/vbz.2006.6.231.

Sato, H., and D. W. Frank. 2011. "Multi-Functional Characterisitics of the *Pseudomonas aeruginosa* Type III Needle-Tip Protein, PcrV; Comparison to Orthologs in Other Gram-Negative Bacteria." *Frontiers in Microbiology* 2: 142. https://doi.org/10.3389/fmicb.2011.00142.

Sato, H., M. L. Hunt, J. J. Weiner, A. T. Hansen, and D. W. Frank. 2011. "Modified Needle-Tip PcrV Proteins Reveal Distinct Phenotypes Relevant to the Control of Type III Secretion and Intoxication by *Pseudomonas aeruginosa*." *PLOS ONE* 6 (3): e18356. https://doi.org/10.1371/journal.pone.0018356.

Sawa, T., H. Katoh, and H. Yasumoto. 2014. "V-Antigen Homologs in Pathogenic Gram-Negative Bacteria." *Microbiology and Immunology* 58 (5): 267–85. https://doi.org/10.1111/1348-0421.12147.

Schnupf, P., and D. A. Portnoy. 2007. "Listeriolysin O: A Phagosome-Specific Lysin." *Microbes and Infection* 9 (10): 1176–87. https://doi.org/10.1016/j.micinf.2007.05.005.

Schrag, S. J., and P. Wiener. 1995. "Emerging Infectious Disease: What Are the Relative Roles of Ecology and Evolution?" *Trends in Ecology & Evolution* 10 (8): 319–24. https://doi.org/10.1016/S0169-5347(00)89118-1.

Schwiesow, L., H. Lam, P. Dersch, and V. Auerbuch. 2015. "*Yersinia* Type III Secretion System Master Regulator LcrF." *Journal of Bacteriology* 198 (4): 604–14. https://doi.org/10.1128/JB.00686-15.

Sebbane, F., D. Gardner, D. Long, B. B. Gowen, and B. J. Hinnebusch. 2005. "Kinetics of Disease Progression and Host Response in a Rat Model of Bubonic Plague." *American Journal of Pathology* 166 (5): 1427–39. https://doi.org/10.1016/S0002-9440(10)62360-7.

Sebbane, F., C. Jarrett, D. Gardner, D. Long, and B. J. Hinnebusch. 2009. "The *Yersinia pestis* c*af1M1A1* Fimbrial Capsule Operon Promotes Transmission by Flea Bite in a Mouse Model of Bubonic Plague." *Infection and Immunity* 77 (3): 1222–29. https://doi.org/10.1128/IAI.00950-08.

Sebbane, F., N. Lemaître, D. E. Sturdevant, R. Rebeil, K. Virtaneva, S. F. Porcella, and B. J. Hinnebusch. 2006. "Adaptive Response of *Yersinia pestis* to Extracellular Effectors of Innate Immunity during Bubonic Plague." *Proceedings of the National Academy of Sciences of the United States of America* 103 (31): 11766–71. https://doi.org/10.1073/pnas.0601182103.

Seifert, L., I. Wiechmann, M. Harbeck, A. Thomas, G. Grupe, M. Projahn, H. C. Scholz, and J. M. Riehm. 2016. "Genotyping *Yersinia pestis* in Historical Plague: Evidence for Long-Term Persistence of *Y. pestis* in Europe from the 14th to the 17th Century." *PLOS ONE* 11 (1): e0145194. https://doi.org/10.1371/journal.pone.0145194.

Simond, P.-L. 1898. "La propagation de la peste." *Annales de l'Institute Pasteur* 12: 625–87.

Skryzpek, E., and S. C. Straley. 1993. "LcrG, a Secreted Protein Involved in Negative Regulation of the Low-Calcium Response in *Yersinia pestis*." *Journal of Bacteriology* 175 (11): 3520–28. https://doi.org/10.1128/jb.175.11.3520-3528.1993.

———. 1995. "Differential Effects of Deletions in *lcrV* on Secretion of V Antigen, Regulation of the Low-Ca^{2+} Response, and Virulence of *Yersinia pestis*." *Journal of Bacteriology* 177 (9): 2530–42. https://doi.org/10.1128/jb.177.9.2530-2542.1995.

Slack, P. 1989. "The Black Death Past and Present. 2. Some Historical Problems." *Transactions of the Royal Society of Tropical Medicine and Hygiene* 83 (4): 461–63. https://doi.org/10.1016/0035-9203(89)90247-2.

Sneller, F. E. C., L. M. van Heerwaarden, P. L. M. Koevoets, R. Vooijs, H. Schat, and J. A. C. Verkleij. 2000. "Derivatization of Phytochelatins from *Silene vulgaris*, Induced Upon Exposure to Arsenate and Cadmium: Comparison of Derivatization with Ellman's Reagent and Monobromobimane." *Journal of Agricultural and Food Chemistry* 48 (9): 4014–19. https://doi.org/10.1021/jf9903105.

Sodeinde, O. A., Y. V. B. K. Subrahmanyam, K. Stark, T. Quan, Y. Bao, and J. D. Goguen. 1992. "A Surface Protease and the Invasive Character of Plague." *Science* 258 (5084): 1004–7. https://doi.org/10.1126/science.1439793.

Song, M., M. Husain, J. Jones-Carson, L. Liu, C. A. Henard, and A. Vázquez-Torres. 2013. "Low-Molecular-Weight Thiol-Dependent Antioxidant and Antinitrosative Defences in *Salmonella* Pathogenesis." *Molecular Microbiology* 87 (3): 609–22. https://doi.org/10.1111/mmi.12119.

Sorg, I., S. Wagner, M. Amstutz, S. A. Müller, P. Broz, Y. Lussi, A. Engel, and G. R. Cornelis. 2007. "YscU Recognizes Translocators as Export Substrates of the *Yersinia* Injectisome." *EMBO Journal* 26 (12): 3015–24. https://doi.org/10.1038/sj.emboj.7601731.

Sorg, J. A., B. Blaylock, and O. Schneewind. 2006. “Secretion Signal Recognition by YscN, the *Yersinia* Type III Secretion ATPase.” *Proceedings of the National Academy of Sciences of the United States of America* 103 (44): 16490–95. https://doi.org/10.1073/pnas.0605974103.

Sorg, J. A., N. C. Miller, and O. Schneewind. 2005. “Substrate Recognition of Type III Secretion Machines—Testing the RNA Signal Hypothesis.” *Cellular Microbiology* 7 (9): 1217–25. https://doi.org/10.1111/j.1462-5822.2005.00563.x.

Stainier, I., S. Bleves, C. Josenhans, L. Karmani, C. Kerbourch, I. Lambermont, S. Tötemeyer, A. Boyd, and G. R. Cornelis. 2000. “YscP, a *Yersinia* Protein Required for Yop Secretion That Is Surface Exposed, and Released in Low Ca^{2+}.” *Molecular Microbiology* 37 (5): 1005–18. https://doi.org/10.1046/j.1365-2958.2000.02026.x.

Stenseth, N. C., B. B. Atshabar, M. Begon, S. R. Belmain, E. Bertherat, E. Carniel, K. L. Gage, H. Leirs, and L. Rahalison. 2008. “Plague: Past, Present, and Future.” *PLOS Medicine* 5 (1): e3. https://doi.org/10.1371/journal.pmed.0050003.

Sun, Y.-C., X.-P. Guo, B. J. Hinnebusch, and C. Darby. 2012. “The *Yersinia pestis* Rcs Phosphorelay Inhibits Biofilm Formation by Repressing Transcription of the Diguanylate Cyclase Gene *hmsT*.” *Journal of Bacteriology* 194 (8): 2020–26. https://doi.org/10.1128/JB.06243-11.

Sun, Y.-C., B. J. Hinnebusch, and C. Darby. 2008. “Experimental Evidence for Negative Selection in the Evolution of a *Yersinia pestis* Pseudogene.” *Proceedings of the National Academy of Sciences of the United States of America* 105 (23): 8097–101. https://doi.org/10.1073/pnas.0803525105.

Sun, Y.-C., A. Koumoutsi, C. Jarrett, K. Lawrence, F. C. Gherardini, C. Darby, and B. J. Hinnebusch. 2011. “Differential Control of *Yersinia pestis* Biofilm Formation *In Vitro* and in the Flea Vector by Two c-di-GMP Diguanylate Cyclases.” *PLOS ONE* 6 (4): e19267. https://doi.org/10.1371/journal.pone.0019267.

Takeshita, S., M. Sato, M. Toba, W. Masahashi, and T. Hashimoto-Gotoh. 1987. “High-Copy-Number and Low-Copy-Number Plasmid Vectors for *lacZα*-Complementation and Chloramphenicol- or Kanamycin-Resistance Selection.” *Gene* 61 (1): 63–74. https://doi.org/10.1016/0378-1119(87)90365-9.

Tam, C., O. Demke, T. Hermanas, A. Mitchell, A. P. A. Hendrickx, and O. Schneewind. 2014. “YfbA, a *Yersinia pestis* Regulator Required for Colonization and Biofilm Formation in the Gut of Cat Fleas.” *Journal of Bacteriology* 196 (6): 1165–73. https://doi.org/10.1128/JB.01187-13.

Torruellas, J., M. W. Jackson, J. W. Pennock, and G. V. Plano. 2005. “The *Yersinia pestis* Type III Secretion Needle Plays a Role in the Regulation of Yop Secretion.” *Molecular Microbiology* 57 (6): 1719–33. https://doi.org/10.1111/j.1365-2958.2005.04790.x.

Tweten, R. K., E. M. Hotze, and K. R. Wade. 2015. "The Unique Molecular Choreography of Giant Pore Formation by the Cholesterol-Dependent Cytolysins of Gram-Positive Bacteria." *Annual Review of Microbiology* 69: 323–40. https://doi.org/10.1146/annurev-micro-091014-104233.

Vadyvaloo, V., C. Jarrett, D. E. Sturdevant, F. Sebbane, and B. J. Hinnebusch. 2010. "Transit through the Flea Vector Induces a Pretransmission Innate Immunity Resistance Phenotype in *Yersinia pestis*." *PLOS Pathogens* 6 (2): e1000783. https://doi.org/10.1371/journal.ppat.1000783.

Van Laer, K., C. J. Hamilton, and J. Messens. 2013. "Low-Molecular-Weight Thiols in Thiol–Disulfide Exchange." *Antioxidants & Redox Signaling* 18 (13): 1642–53. https://doi.org/10.1089/ars.2012.4964.

Veeravalli, K., D. Boyd, B. L. Iverson, J. Beckwith, and G. Georgiou. 2011. "Laboratory Evolution of Glutathione Biosynthesis Reveals Natural Compensatory Pathways." *Nature Chemical Biology* 7 (2): 101–5. https://doi.org/10.1038/nchembio.499.

Vergauwen, B., J. Elegheert, A. Dansercoer, B. Devreese, and S. N. Savvides. 2010. "Glutathione Import in *Haemophilus influenzae* Rd Is Primed by the Periplasmic Heme-Binding Protein HbpA." *Proceedings of the National Academy of Sciences of the United States of America* 107 (30): 13270–75. https://doi.org/10.1073/pnas.1005198107.

Vergauwen, B., K. Verstraete, D. B. Senadheera, A. Dansercoer, D. G. Cvitkovitch, E. Guédon, and S. N. Savvides. 2013. "Molecular and Structural Basis of Glutathione Import in Gram-Positive Bacteria via GshT and the Cystine ABC Importer TcyBC of *Streptococcus mutans*." *Molecular Microbiology* 89 (2): 288–303. https://doi.org/10.1111/mmi.12274.

Vetter, S. M., R. J. Eisen, A. M. Schotthoefer, J. A. Montenieri, J. L. Holmes, A. G. Bobrov, S. W. Bearden, R. D. Perry, and K. L. Gage. 2010. "Biofilm Formation Is Not Required for Early-Phase Transmission of *Yersinia pestis*." *Microbiology* 156 (7): 2216–25. https://doi.org/10.1099/mic.0.037952-0.

Wade, S. E., and J. R. Georgi. 1988. "Survival and Reproduction of Artificially Fed Cat Fleas, *Ctenocephalides felis* Bouché (Siphonaptera: Pulicidae)." *Journal of Medical Entomology* 25 (3): 186–90. https://doi.org/10.1093/jmedent/25.3.186.

Wan, F., A. Weaver, X. Gao, M. Bern, P. R. Hardwidge, and M. J. Lenardo. 2011. "IKKβ Phosphorylation Regulates RPS3 Nuclear Translocation and NF-κB Function during Infection with *Escherichia coli* Strain O157:H7." *Nature Immunology* 12 (4): 335–43. https://doi.org/10.1038/ni.2007.

Webb, C. T., C. P. Brooks, K. L. Gage, and M. F. Antolin. 2006. "Classic Flea-Borne Transmission Does Not Drive Plague Epizootics in Prairie Dogs." *Proceedings of the National Academy of Sciences of the United States of America* 103 (16): 6236–41. https://doi.org/10.1073/pnas.0510090103.

Wheeler, C. M., and J. R. Douglas. 1945. “Sylvatic Plague Studies: V. The Determination of Vector Efficiency.” *Journal of Infectious Diseases* 77 (1): 1–12. https://doi.org/10.1093/infdis/77.1.1

Williamson, E. D., P. M. Vesey, K. J. Gillhespy, S. M. Eley, M. Green, and R. W. Titball. 1999. “An IgG1 Titre to the F1 and V Antigens Correlates with Protection against Plague in the Mouse Model.” *Clinical and Experimental Immunology* 116 (1): 107–14. https://doi.org/10.1046/j.1365-2249.1999.00859.x.

Winter, C. C., W. B. Cherry, and M. D. Moody. 1960. “An Unusual Strain of *Pasteurella pestis* Isolated from a Fatal Human Case of Plague.” *Bulletin of the World Health Organization* 23 (2–3): 408–9.

Wood, S. E., J. Jin, and S. A. Lloyd. 2008. “YscP and YscU Switch the Substrate Specificity of the *Yersinia* Type III Secretion System by Regulating Export of the Inner Rod Protein YscI.” *Journal of Bacteriology* 190 (12): 4252–62. https://doi.org/10.1128/JB.00328-08.

Yersin, A. 1894. “La peste bubonique à Hong-Kong.” Annales de l’Institute Pasteur 2: 428–30.

Yin, J.-X., A. Geater, V. Chongsuvivatwong, X.-Q. Dong, C.-H. Du, and Y.-H. Zhong. 2011. “Predictors for Abundance of Host Flea and Floor Flea in Households of Villages with Endemic Commensal Rodent Plague, Yunnan Province, China.” *PLOS Neglected Tropical Diseases* 5 (3): e997. https://doi.org/10.1371/journal.pntd.0000997.

Yip, C. K., T. G. Kimbrough, H. B. Felise, M. Vuckovic, N. A. Thomas, R. A. Pfuetzner, E. A. Frey, B. B. Finlay, S. I. Miller, and N. C. J. Strynadka. 2005. “Structural Characterization of the Molecular Platform for Type III Secretion System Assembly.” *Nature* 435 (7042): 702–7. https://doi.org/10.1038/nature03554.

Yother, J., T. W. Chamness, and J. D. Goguen. 1986. “Temperature-Controlled Plasmid Regulon Associated with Low Calcium Response in *Yersinia pestis*.” *Journal of Bacteriology* 165 (2): 443–47. https://doi.org/10.1128/jb.165.2.443-447.1986.

Yother, J., and J. D. Goguen. 1985. “Isolation and Characterization of Ca^{2+}-Blind Mutants of *Yersinia pestis*.” *Journal of Bacteriology* 164 (2): 704–11.

Zavialov, A. V., J. Berglund, A. F. Pudney, L. J. Fooks, T. M. Ibrahim, S. MacIntyre, and S. D. Knight. 2003. “Structure and Biogenesis of the Capsular F1 Antigen from *Yersinia pestis*: Preserved Folding Energy Drives Fiber Formation.” *Cell* 113 (5): 587–96. https://doi.org/10.1016/S0092-8674(03)00351-9.

Zheng, Y., S. Lilo, I. E. Brodsky, Y. Zhang, R. Medzhitov, K. B. Marcu, and J. B. Bliska. 2011. “A *Yersinia* Effector with Enhanced Inhibitory Activity on the NF-κB Pathway Activates the NLRP3/ASC/Caspase-1 Inflammasome in Macrophages.” *PLOS Pathogens* 7 (4): e1002026. https://doi.org/10.1371/journal.ppat.1002026.

Zhou, D., Z. Tong, Y. Song, Y. Han, D. Pei, X. Pang, J. Zhai, M. Li, B. Cui, Z. Qi, L. Jin, R. Dai, Z. Du, J. Wang, Z. Guo, J. Wang, P. Huang, and R. Yang. 2004. "Genetics of Metabolic Variations between *Yersinia pestis* Biovars and the Proposal of a New Biovar, Microtus." *Journal of Bacteriology* 186 (15): 5147–52. https://doi.org/10.1128/JB.186.15.5147-5152.2004.